PNL-7600 Pt. 1
UC-408

17

Pacific Northwest Laboratory Annual Report for 1990 to the DOE Office of Energy Research

Part 1: Biomedical Sciences
June 1991

Prepared for the U.S. Department of Energy
under Contract DE-AC06-76RLO 1830

Pacific Northwest Laboratory
Operated by Battelle Memorial Institute
for the U.S. Department of Energy

Battelle

DISCLAIMER

PACIFIC NORTHWEST LABORATORY
operated by
BATTELLE MEMORIAL INSTITUTE
for the
UNITED STATES DEPARTMENT OF ENERGY
under Contract DE-AC06-76RLO 1830

Printed in the United States of America

Available to DOE and DOE contractors from the Office of Scientific and Technical Information, P.O. Box 62, Oak Ridge, TN 37831; prices available from (615) 576-8401. FTS 626-8401.

Available to the public from the National Technical Information Service, U.S. Department of Commerce, 5285 Port Royal Rd., Springfield, VA 22161.

PNL-7600, Pt. 1
UC-408

Pacific Northwest Laboratory Annual Report for 1990 to the DOE Office of Energy Research

Part 1: Biomedical Sciences

J. F. Park and Staff

June 1991

Prepared for
the U.S. Department of Energy
under Contract DE-AC06-76RLO 1830

Pacific Northwest Laboratory
Richland, Washington 99352

Preface

This 1990 Annual Report from Pacific Northwest Laboratory (PNL) to the U.S. Department of Energy (DOE) describes research in environment, safety, and health conducted during fiscal year 1990. The report again consists of five parts, each in a separate volume.

The five parts of the report are oriented to particular segments of the PNL program. Parts 1 to 4 report on research performed for the DOE Office of Health and Environmental Research in the Office of Energy Research. Part 5 reports progress on all research performed for the Assistant Secretary for Environment, Safety, and Health. In some instances, the volumes report on research funded by other DOE components or by other governmental entities under interagency agreements. Each part consists of project reports authored by scientists from several PNL research departments, reflecting the multidisciplinary nature of the research effort.

The parts of the 1990 Annual Report are:

Part 1: Biomedical Sciences			
	Program Manager:	J. F. Park	J. F. Park, Report Coordinator S. A. Kreml, Editor
Part 2: Environmental Sciences			
	Program Manager:	R. E. Wildung	M. G. Hefty, Report Coordinator D. A. Perez, Editor K. K. Chase, Text Processor
Part 3: Atmospheric Sciences			
	Program Manager:	C. E. Elderkin	C. E. Elderkin, Report Coordinator E. L. Owczarski, Editor
Part 4: Physical Sciences			
	Program Manager:	L. H. Toburen	L. H. Toburen, Report Coordinator K. A. Parnell, Editor
Part 5: Environment, Safety, Health, and Quality Assurance			
	Program Managers:	L. G. Faust R. V. Moraski J. M. Selby	D. K. Hilliard, Report Coordinator and Editor

Activities of the scientists whose work is described in this annual report are broader in scope than the articles indicate. PNL staff have responded to numerous requests from DOE during the year for planning, for service on various task groups, and for special assistance.

Credit for this annual report goes to the many scientists who performed the research and wrote the individual project reports, to the program managers who directed the research and coordinated the technical progress reports, to the editors who edited the individual project reports and assembled the five parts, and to Ray Baalman, editor in chief, who directed the total effort.

T. S. Tenforde
Health and Environmental
Research Program Office

Previous reports in this series:

Annual Report for:

1951	HW-25021, HW-25709
1952	HW-27814, HW-28636
1953	HW-30437, HW-30464
1954	HW-30306, HW-33128, HW-35905, HW-35917
1955	HW-39558, HW-41315, HW-41500
1956	HW-47500
1957	HW-53500
1958	HW-59500
1959	HW-63824, HW-65500
1960	HW-69500, HW-70050
1961	HW-72500, HW-73337
1962	HW-76000, HW-77609
1963	HW-80500, HW-81746
1964	BNWL-122
1965	BNWL-280, BNWL 235, Vol. 1-4; BNWL-361
1966	BNWL-480, Vol. 1; BNWL-481, Vol. 2, Pt. 1-4
1967	BNWL-714, Vol. 1; BNWL-715, Vol. 2, Pt. 1-4
1968	BNWL-1050, Vol. 1;, Pt. 1-2; BNWL-1051, Vol. 2, Pt. 1-3
1969	BNWL-1306, Vol. 1;, Pt. 1-2; BNWL-1307, Vol. 2, Pt. 1-3
1970	BNWL-1550, Vol, 1;, Pt. 1-2; BNWL-1551, Vol. 2, Pt. 1-2
1971	BNWL-1650, Vol. 1;, Pt. 1-2; BNWL-1651, Vol. 2, Pt. 1-2
1972	BNWL-1750, Vol. 1;, Pt. 1-2; BNWL-1751, Vol. 2, Pt. 1-2
1973	BNWL-1850, Pt. 1-4
1974	BNWL-1950, Pt. 1-4
1975	BNWL-2000, Pt. 1-4
1976	BNWL-2100, Pt. 1-5
1977	PNL-2500, Pt. 1-5
1978	PNL-2850, Pt. 1-5
1979	PNL-3300, Pt. 1-5
1980	PNL-3700, Pt. 1-5
1981	PNL-4100, Pt. 1-5
1982	PNL-4600, Pt. 1-5
1983	PNL-5000, Pt. 1-5
1984	PNL-5500, Pt. 1-5
1985	PNL-5750, Pt. 1-5
1986	PNL-6100, Pt. 1-5
1987	PNL-6500, Pt. 1-5
1988	PNL-6800, Pt. 1-5
1989	PNL-7200, Pt. 1-5

Foreword

This report summarizes progress on OHER human health, biological, and general life sciences research programs conducted at PNL in FY 1990. The research develops the knowledge and scientific principles necessary to identify, understand, and anticipate the long-term health consequences of energy-related radiation and chemicals. Our continuing emphasis is to decrease the uncertainty of health risk estimates from existing and developing energy-related technologies through an increased understanding of how radiation and chemicals cause biological damage.

The sequence of this report of PNL research reflects the OHER programmatic structure. The first section, on human health research, concerns epidemiological and statistical studies for assessing health risks. The next section contains reports of biological research in laboratory animals and in vitro cell systems, including research with radionuclides and chemicals. The general life sciences research section reports research conducted for the OHER human genome research program.

Human Health Research

The section on human health research reports the status of epidemiological studies, including occupational studies of workers at the Hanford site, a study of the occurrence of cancer around the Tatum Salt Dome Test Site, and epidemiological, longitudinal, and experimental studies of the possible role of iron in sensitivity to radiation injury.

The Hanford data were analyzed with adjustments for socioeconomic status, the database was expanded to include more detail on both dosimetry and job histories, and a technical report was completed on dosimetry practices from 1944 to 1989. Cancer risk of pooled data from mortality studies of workers at the Hanford Site, Oak Ridge National Laboratory, and Rocky Flats Weapons Plant were analyzed, taking into account the patterns of risk identified in the BEIR V report models based on high dose data, primarily the atomic bomb survivor data. Computer simulations were conducted to evaluate the adequacy of asymptotic approximations. Plans for pooled analyses of data from nuclear workers in the United States, the United Kingdom, and Canada focused on sources of bias and uncertainty in dose estimates across countries and facilities to determine procedures for adjusting doses.

The first phase of the Tatum Salt Dome Test Site study was completed. This phase has shown that there does not appear to be an excess of cancer deaths or evidence of a cluster of cancers associated with the test site.

In cellular studies of the possible role of iron in sensitivity to radiation injury, in vitro experiments with Chinese hamster ovary cells showed that nontoxic increases in the iron content of the growth medium can greatly increase sensitivity of these cells to killing by radiation. These results may have important implications for the association of body iron stores with subsequent cancer risk observed in epidemiology studies.

Biological Research

The section on biological research reports results from experimental animal dose-effect relationship studies with inhaled radionuclides. Life-span studies in beagles with inhaled $^{239}Pu(NO_3)_4$ were in the 13th postexposure year. The last dogs in the $^{239}PuO_2$ and $^{238}PuO_2$ studies died in FY 1990. The primary plutonium-exposure-related causes of death were lung cancer for inhaled $^{239}PuO_2$ and lung and bone cancer for inhaled $^{238}PuO_2$ and $^{239}Pu(NO_3)_4$. The lung tumor risk resulting from a given cumulative radiation dose to the lungs from $^{239}PuO_2$ was higher than from a similar dose from $^{238}PuO_2$. The extrapolated lifetime risk at 1 rad was estimated to be 7 per 10^6 for $^{239}PuO_2$ and 1 per 10^6 for $^{238}PuO_2$.

Other plutonium-exposure-related effects include sclerosis of the tracheobronchial lymph nodes, lymphopenia, focal radiation pneumonitis, focal dystrophic osteolytic lesions in bone, adenomatous hyperplasia of the liver, serum chemistry indicative of liver damage, and intrahepatic bile duct tumors. In the project "National Radiobiology Archives," information from these life-span studies in beagles and from beagle radiation studies from other DOE laboratories will be stored in a computerized database with selected research documents and tissues for future research and analyses.

Dose-effect-relationship studies on inhaled $^{239}PuO_2$ in rats are in progress to obtain lung tumor incidence data at lifetime lung doses of 0.07 to 20 Gy. Thus far, the lung cancer dose-response curve is best fitted by a quadratic function and a "practical" threshold of 1-2 Gy; maximum lung cancer incidence was at 8 Gy. Increased cell proliferation of type 2 alveolar epithelium may account for much of the carcinogenicity and the possible existence of a practical threshold similar to that seen with nongenotoxic chemicals. The incidence of brain tumors in plutonium-exposed rats (1.4%) was about twice that seen in controls.

Rats exposed by inhalation to radon and decay products are under study to determine the influence of dose, dose rate, and cigarette smoke on lung cancer incidence. Analyses of histopathological data for 100-WL (working-level) exposure rates showed that lung tumor incidence was elevated compared to that of controls at cumulative exposures comparable to those found in houses, that is, 40 WLM (working-level months). Histopathological examination of sacrificed rats at 25, 52, and 78 weeks from start of exposure to 100 WL and 320 WLM on an initiation-promotion-initiation study showed no lung tumors at 25 weeks. At 52 and 78 weeks, those with a 320-WLM continuous exposure had increased lung tumor incidence compared to those with split exposure with or without cigarette smoke. The results suggest that cigarette smoke ameliorates radon-progeny-induced lung tumors; however, preneoplastic lung lesions were more prevalent and severe in rats exposed to smoke after radon-progeny exposure than before radon-progeny exposure.

A DOE interlaboratory comparison of survival-response data on Chinese hamster ovary cells exposed to radon and radon progeny revealed a D_0 value of about a 64-cGy dose to the cell nucleus. Analysis of radon-induced mutations at the CHO-HGPRT locus after 76-cGy alpha doses to the nucleus showed predominantly deletion-type events (48%), with 24% showing no change from the parental line and 28% showing rearrangements of the Southern blot bonding patterns. In contrast, spontaneous mutants exhibited 11% deletion-type events and 89% showed no change. Methods for calculating the radiation dose to cell nuclei from radon and decay products have been developed for our in vitro cell exposures. Comparison of the calculated and measured values showed good agreement over a wide range of energy.

In our Dosimetry of Radon Progeny project, we developed a comprehensive model, with a committee of the National Research Council/National Academy of Sciences, to examine the extrapolation of risk estimates developed from studies of underground miners to the general population exposed to radon in the home environment. On the basis of bronchial doses to basal and secretory cells averaged for exposures in the home relative to miners, the overall value of the extrapolation was 0.62. To provide a simpler technique to characterize exposure to unattached radon progeny in laboratory research and in domestic or occupational settings, we developed an Unattached Radon Progeny Size-Spectrometer to measure the concentration and unattached fraction of potential alpha energy in air and also the activity-size distribution of the unattached progeny.

Studies to examine the role of oncogenes, growth factors, and their receptors in radiation-induced lung cancer use tumor tissue from the animal studies previously described. Using immunocytochemical assays of formalin-fixed, paraffin-embedded lung tissue, we have demonstrated abnormally high expression of epidermal growth factor receptor, epidermal growth factor, transforming growth factor-α, and bombesin in radon-induced rat lung tumors, mainly associated with epidermoid carcinomas. We have preliminary evidence of K-*ras* activation in radon-induced rat lung tumors and observed an altered 12th codon in one tumor. Chemical agents usually activate *ras* genes by causing specific and reproducible single-point

mutations in the 12th, 13th, 59th, or 61st codons. In plutonium-induced dog lung tumors examined thus far, the N-*ras* 2nd-exon sequences are identical with the normal canine sequence. In the 1st exon, only one tumor had altered sequences. We have found K-*ras* 1st-exon lesions in four chronic myeloproliferative (CMP) tumors and H-*ras* mutations in two of four CMP tumors from dogs exposed to gamma radiation at Argonne National Laboratory. A study of mutations of tumor suppressor genes, retinoblastoma susceptibility (Rb) and p53, as targets in radiation carcinogenesis was begun because large deletions are a major component of genetic damage by ionizing radiation, because these genes are defective in human osteosarcoma and lung cancer, and because plutonium caused lung and bone tumors in experimental animals.

In our chemical-related biological research, we are evaluating transcriptional processes in benzo[a]-pyrene diol-expoxide-modified DNA to understand the influence of DNA adducts on gene regulation. Distinct transcriptional breakpoints with adducted DNA were present, suggesting that the adducted molecule prevented progress of the polymerase along the DNA template. As the level of modification increased, the polymerase inhibition increased, so that at high levels the adducts may prevent initiation of transcription. The interaction between damage induced by radiation and by metals, organic solvents, and fibers is being studied. Multiplicative interactions were demonstrated with beryllium and x-rays for chromosome aberrations. No interaction between gamma rays and silicon carbide fibers or hexone was demonstrated using micronuclei as an endpoint.

In our fetal and juvenile radiation research, we continued to examine correlates between the physicochemical and biological factors that may be involved in fetoplacental radionuclide disposition. We found that fetoplacental radionuclide disposition displays a good general correlation to values of fractional absorption from the gastrointestinal tract. Radon progeny were restricted in their transfer to the fetus; the major dose to the fetus came from radon that crossed the placenta and from its decay products. In mechanistic studies of prenatal irradiation teratogenesis, immunocytochemical alterations of extracellular matrix by in vitro radiation effects on limb buds or blastocyst development showed fibronectin staining was decreased after 1 Gy.

General Life Sciences Research

PNL is developing a computer information system to graphically display and manipulate the vast amounts of information about the human genome. The user interface, named GnomeView, provides researchers with graphical representations of chromosomes, genetic and physical maps, and DNA sequences on a SUN workstation. It accesses database centers such as GENBANK as primary information sources. Unique features include the ability to provide genetic information in easily understandable color graphics, allowing the user to create hybrid or new maps.

J. E. Schmaltz, a detailee to OHER's Human Genome Research program, provided computer science expertise to the computational analysis and database components of the Human Genome Task Group. He participated in review, coordination, and liaison of the informatics components of this multidisciplinary program.

PNL biomedical research is an interdisciplinary effort requiring scientific contributions from many research departments at PNL. Personnel in the Life Sciences Center are the principal contributors to this report.

Requests for reprints from the list of publications will be honored while supplies are available.

Contents

Preface iii

Foreword v

Human Health Research

Statistical Health Effects Studies, *E. S. Gilbert* 1
Tatum Dome Cancer Incidence Study, *L. E. Sever* 7
Iron Stores and Risk of Cancer, *R. G. Stevens* 9

Biological Research

Inhaled Plutonium Oxide in Dogs, *J. F. Park* 13
Inhaled Plutonium Nitrate in Dogs, *G. E. Dagle* 25
National Radiobiology Archives, *C. R. Watson* 33
Low-Level $^{239}PuO_2$ Life-Span Studies, *C. L. Sanders* 39
Inhalation Hazards to Uranium Miners, *F. T. Cross* 45
Mechanisms of Radon Injury, *F. T. Cross* 51
Dosimetry of Radon Progeny, *A. C. James* 55
Aerosol Technology Development, *A. C. James* 65
Growth Factors in Radiation Carcinogenesis, *F. C. Leung* 71
Oncogenes in Radiation-Induced Carcinogenesis, *M. E. Frazier/G. L. Stiegler* 79
Mutation of DNA Targets, *R. P. Schneider* 85
Molecular Events During Tumor Initiation, *D. L. Springer* 91
Genotoxicity of Inhaled Energy Effluents, *A. L. Brooks* 97
Fetal and Juvenile Radiotoxicity, *M. R. Sikov* 103

General Life Sciences Research

GnomeView II: A Graphical Interface to the Human Genome, *R. J. Douthart* 109
Synthesis of Human Genome Information, *J. E. Schmaltz* 113

Appendix: Dose-Effect Studies with Inhaled Plutonium in Beagles 117

Publications and Presentations

Publications 133
Presentations 143

Author Index 153
Distribution Distr.1

Human
Health
Research

Statistical Health Effects Studies

Principal Investigator: *E. S. Gilbert*

Other Investigators: *J. A. Buchanan, J. J. Fix, and N. A. Holter*

The overall objective of this project is to increase understanding of health risks resulting from low-level chronic exposure by providing methodology and analyses for a direct assessment of these risks. Analyses of data on workers exposed occupationally to low levels of radiation, which are a major component of this project, have included analyses of data at the Hanford Site in southeastern Washington State and of pooled data from three DOE facilities. Efforts in the past year have included refining of previous analyses, conducting computer simulations to evaluate certain statistical techniques used in the analyses of these data, contributing to national and international pooling of data, completing a document describing Hanford historical external dosimetry data, participating in plans for DOE's Comprehensive Epidemiological Data Resource (CEDR), and developing updated and more detailed data on Hanford workers to meet the needs of both pooled analyses and CEDR.

The BEIR V Model Applied to the Pooled U.S. Data

Data from the three studies included in U.S. pooled analyses [Hanford Site, Oak Ridge National Laboratory (ORNL), and Rocky Flats Weapons Plant] have been analyzed, taking into account the patterns of risk identified in the recent BEIR V report. The BEIR V report provided models for estimating low-level radiation risks that incorporated dependencies on sex, age at exposure, and time since exposure. The models were based on analyses of high dose data, primarily the atomic bomb survivor data. Because it is expected that the BEIR V models will play a major role in radiation risk assessment in the next few years, it is of interest to evaluate the consistency of its predictions using data on workers exposed to low-level external radiation.

The combined U.S. data have been analyzed by expressing estimates and confidence limits as multiples of the risks expected under the BEIR V model. This approach yielded negative risk estimates, but upper confidence limits indicated that data were consistent with the BEIR V predictions. The upper confidence limit for leukemia was slightly higher than the BEIR V linear-quadratic prediction, and the upper confidence limit for all cancer except leukemia was about twice the BEIR V prediction.

It is also of interest to consider the number of radiation-induced cancers that would be predicted by the BEIR V models. Analyses of data from Hanford, ORNL, and Rocky Flats included 42 leukemia deaths. The BEIR V leukemia model would predict that 2.7 of these deaths were radiation induced. For all cancers other than leukemia, 985 deaths were included, and BEIR V models would predict that 9.2 of these deaths were radiation induced. The leukemia prediction was based on a linear-quadratic model, while the prediction for other cancers was based on a linear model. BEIR V recommended reducing the linear estimates by a factor between 2 and 10 for doses received at low dose rates, but a correction was not included in the foregoing predictions.

Analyses of Hanford Data with Adjustment for Socioeconomic Status

Analyses of worker data have been based primarily on internal comparisons by level of radiation exposure. A possible source of bias in this comparison is that those workers performing jobs involving radiation exposure may have different socioeconomic characteristics than workers performing other jobs. As part of the international combined analyses, we have used job category data for Hanford workers to assign social class in a way that is fairly comparable to the definition used in worker studies in the United Kingdom.

Most Hanford workers with higher radiation exposures were classified as skilled and semi-skilled manual workers, social classes III-M and IV, respectively. Workers in social classes III-NM (primarily clerical workers), and workers in social class V (unskilled workers), generally had very little radiation exposure, while workers in social classes I and II (professional, technical, and managerial workers) had intermediate exposures.

The relationship of both noncancer and cancer mortality with social class was examined. Noncancer mortality was found to be strongly related to social class, but cancer mortality did not show as strong a relationship. Nevertheless, we performed an analysis of radiation exposure and mortality that included stratification on social class, obtaining, for all cancer except leukemia, both a slightly lower estimate and a slightly lower upper confidence limit than in analysis without such stratification.

Computer Simulations to Evaluate the Adequacy of Asymptotic Approximations

Statistical procedures used to analyze nuclear worker data are generally based on the assumption that certain statistics are reasonably well approximated by normal distributions. Because the dose distributions in these studies are highly skewed, and because the number of deaths from some diseases of interest may be small (leukemia, for example), the normal approximations may not be adequate. To address this issue, computer simulations have been conducted to assess the validity of specific results in the U.S. pooled analyses and also the general behavior of certain statistical procedures as both sample size and the size of the true effect are varied.

Specifically, the asymptotic upper confidence limits for the excess relative risk (β) estimate for leukemia based on the U.S. pooled analyses (Gilbert et al. 1989) have been evaluated; results are shown in Table 1. The first line in Table 1 shows the one-sided 95% upper confidence limits for β, expressed as a percent increase per 10 mSv, that were obtained from the asymptotic approximation based on the score statistic. To obtain the results shown in the second line, 5000 samples were generated under the assumption that the true β was equal to the approximate upper confidence limit in line 1, and the actual confidence level was estimated. In all cases, the actual confidence levels differed significantly from 95%, and, with the exception of Rocky Flats, exceeded 95%. However, the approximations were reasonably good considering that some of the sample sizes were very small and the dose distributions very skewed. To obtain the results in the third line of Table 1, the simulation process was repeated until a value of β was found that yielded a confidence level that was consistent with a one-sided 95% level. With the exception of Rocky Flats, the actual upper confidence limits were lower than the asymptotic approximations.

Additional simulations were conducted to investigate the result of varying both the number of deaths and the size of the true excess relative risk β. The exposure distribution was taken to be the average of the exposure distributions from the risk sets associated with the 42 leukemia deaths included in the combined nuclear worker analyses. The results in Table 2 are relevant for evaluating the behavior of the score statistic and the likelihood ratio statistic for testing the null hypothesis that the excess relative risk was equal to zero ($\beta = 0$). Table 2 shows the percentage of times that the null hypothesis would be rejected using a one-sided test with the alpha level set equal to 5% and 1% for several sample sizes. The results indicate that, with smaller sample sizes, the score statistic rejects the null hypothesis too often, but that the likelihood ratio test performs very well, even with a sample size as small as 10. The score statistic, rather than the likelihood ratio statistic, has generally been used in analyzing nuclear worker data. These results indicate that the likelihood ratio test would be a better choice, or, alternatively, the score statistic should be supplemented with computer simulations.

Additional simulations based on the assumption of positive values for β indicated that problems can occur with the asymptotic approximations provided by both the score test and the likelihood ratio statistic. The simulations also indicated that there was little to differentiate the two approaches in terms of power or precision in estimation, provided the approximation difficulty was handled appropriately.

TABLE 1. Upper One-Sided 95% Confidence Limits for the Leukemia Excess Relative Risk (β) Based on the Score Statistic

	Hanford	ORNL	Rocky Flats	Combined
Upper limits based on asymptotic approximation[(a)]	4.8%	14%	52%	3.4%
Estimated actual confidence level[(b)]	95.8%	95.5%	93.6%	96.0%
Upper limits based on computer simulations[(c)]	4.3%	12%	60%	2.8%
Number of deaths	27	11	4	42

(a) Upper limits (based on two-sided 90% limits) obtained from asymptotic normal approximation.
(b) Percent of 5000 samples for which the calculated statistic was less than -1.645.
(c) For 95% of the 5000 samples generated at the indicated limit, the calculated statistic exceeded the comparable statistic based on the actual cases.

TABLE 2. Simulations Conducted with $\beta = 0.0$ (Right-Hand Tail)[(a)]

Number of Deaths	Score Statistic 5%	Score Statistic 1%	Likelihood Ratio Statistic 5%	Likelihood Ratio Statistic 1%
10	8.7	3.8	5.0	1.2
20	7.4	2.9	4.4	0.8
50	6.7	2.2	4.5	0.8
100	6.2	2.0	4.7	1.0
500	5.7	1.7	4.9	1.1

(a) Entries indicate percent of 5000 samples in which test statistic exceeded upper 5% (1%) nominal level obtained from the asymptotic approximation (one-tailed test).

Pooling of Data from the United States, United Kingdom, and Canada

Plans for international combined analyses of nuclear worker studies in the United States, United Kingdom, and Canada are proceeding with the International Agency for Research on Cancer (IARC) serving as the coordinating agency. A subcommittee of the working group (consisting of representatives from all studies) has met three times, with PNL providing representation for the U.S. studies.

Dosimetry has been a major focus of these meetings. At the most recent meeting, held in March 1990, several sources of bias and uncertainty in dose estimates were discussed to evaluate possible differences across countries and facilities and to determine procedures for adjusting doses to obtain estimates of deep dose and of organ dose. Sources of uncertainty considered included missing records, use of high thresholds, calibration of dosimeters in air rather than on a phantom, wearing position of the dosimeter, and conversion from exposure to deep dose. Problems with dose assessment from neutron radiation or internal deposition of radionuclides were also addressed.

For the purpose of estimating the risk per unit of dose, the committee decided to focus on workers who received radiation exposure primarily from photon radiation of energy greater than about 100 keV. Workers with potential for substantial dose from low-energy photons, neutrons, or internal depositions would be flagged in the data supplied to IARC, and would be excluded from some analyses; these workers comprise only a very small proportion of the workers included in the international studies.

Preliminary data on workers at the Hanford Site, ORNL, and Rocky Flats Weapons Plant have been provided to IARC. The final data for Hanford workers, including all variables indicated in the protocol for the international combined analyses, will be provided by the end of 1990. It is expected that data from other countries will also be provided by this time.

External Dosimetry for Hanford Site Workers

To make the best use of available epidemiologic data in assessing risks from exposure to low-level radiation, it is important that the methods used to assess and record personnel dose be understood. It is particularly important to evaluate comparability of recorded dose over time and among workers

performing different types of work. In addition, recent efforts to combine data from several nuclear worker studies, both within the United States and internationally, make it necessary to evaluate the comparability of dose estimates across studies.

An extensive technical report documenting historical dosimetry practices at the Hanford Site has been completed. This report provides a historical review of the equipment, dosimetry techniques, and calibration protocols used at Hanford to measure and record personnel dose from the inception of Hanford operations in 1944 through 1989. An evaluation of the capability of each dosimeter to accurately estimate the dose to personnel included comparison of the recorded dose to the 1-cm-depth dose in tissue (i.e., deep dose) for six different facility types considered to represent Hanford operations. The evaluation was based on (1) review of extensive historical documentation, (2) results of a laboratory intercomparison of all Hanford film dosimeters during 1989, (3) results from performance testing of the Hanford thermoluminescent dosimeter during 1989, and (4) the professional judgment of the authors based on dosimetry experience during nearly five decades of Hanford operations.

For exposure to higher energy (>100-keV) photon fields, which comprise most personnel exposure in Hanford facilities, the difference between the recorded whole-body dose and the actual deep dose was estimated to be about ±50% for the two-element film dosimeter (used from 1944 through 1956), ±30% for the multi-element film dosimeter (used from 1957 through 1971), and ±20% for the TLD (used from 1972 through 1989). Greater differences were estimated for facilities in which complex mixtures of beta and photon radiation or neutron radiation were present.

The evaluation identified one group, who worked in the plutonium finishing facility, for whom doses were probably seriously underestimated before 1972. This underestimation occurred because earlier film badge dosimeters (used before 1972) did not adequately measure neutron dose, and the two-element dosimeter (used before 1957) did not measure dose from low energy x-rays. These personnel comprise a very small percentage of the total employed at Hanford since 1944.

Comprehensive Epidemiologic Data Resource (CEDR)

PNL has participated in the DOE's Comprehensive Epidemiologic Data Resource (CEDR) Steering Committee and in the CEDR Information Systems Working Group. The CEDR program was established to develop a public-use data set containing worker demographics, work histories, radiation and chemical exposures, medical information, vital statistics, and other health-related data on workers at DOE facilities. Four meetings of the CEDR Steering Committee were held and a CEDR Program Plan developed. In addition, presentations were made to the National Academy of Sciences Advisory Committee, established to provide guidance on the establishment and control of data included in CEDR. Hanford data (without cause-of-death information) and the MOX software package were provided to be part of the initial version of CEDR.

Hanford data were also provided to Dr. Alice Stewart in response to a request by the Three Mile Island Fund. These data included the analysis file, a detailed occupational history file, and seven additional files including detailed information on both external and internal dosimetry. None of the files included personal identifiers.

Expansion of the Hanford Site Database

Efforts to develop an updated and expanded database continue. An analysis file meeting the specifications of the IARC protocol has been completed and includes more detail on both dosimetry and job histories than our previous analysis file. Creating this file required linking occupational histories received from the Hanford Environmental Health Foundation (HEHF), several dosimetry files received from PNL's Health Physics Department, and our previous analysis file. Because HEHF and dosimetry files are maintained independently, discrepancies in Social Security numbers, names, birth dates, and hire and termination dates are common occurrences. An important aspect of creating the analysis file is performing edits within and between files, resolving discrepancies, and keeping track of changes in files and reasons for discrepancies. In addition, a special procedure was developed for transforming the occupational history file to a more manageable and useful form.

Reference Cited

Gilbert, E. S., S. A. Fry, L. A. Wiggs, G. L. Voelz, D. L. Cragle, and G. R. Petersen. 1989. Analyses of combined mortality data on workers at the Hanford Site, Oak Ridge National Laboratory, and Rocky Flats Nuclear Weapons Plant. *Radiat. Res.* 120:19-35.

Tatum Dome Cancer Incidence Study

Principal Investigator: *L. E. Sever*

The U.S. Department of Energy (DOE) was asked to study the occurrence of cancers in the area around the Tatum Salt Dome Test Site in Lamar County, Mississippi. A two-phased approach is being employed, and the first phase has been completed. This phase has shown that the numbers of cancer deaths or types of cancers in the area around Tatum Dome are not different than expected. That is, there does not appear to be an excess of cancer deaths or evidence of a cluster of cancers associated with the test site. There are, however, limitations to studying only information on deaths. In cooperation with the Mississippi State Department of Health, a second phase therefore is underway. The essential question to be answered in Phase II is this: Is there an excess number of cancers, particularly types of cancer known to be associated with radiation exposure, near the Tatum Dome site?

At the request of Mississippi Senator Trent Lott, the DOE, through Pacific Northwest Laboratory, has begun a study of the occurrence of cancers in the area around the Tatum Salt Dome Test Site, Lamar County, Mississippi. Citizens from the area had expressed concern that the rates of cancer around Tatum Dome are too high and are related to the nuclear tests conducted at the site in the 1960s. In 1989, community representatives presented a petition to Senator Lott requesting a cancer study. They also gave Senator Lott lists of persons whom they believed had died of cancer and of living persons in the area with cancer. Senator Lott's office supplied these lists to the DOE with his request that the DOE thoroughly investigate the question of whether cancer risks are increased in the area around Tatum Dome.

As Phase I of the cancer study, three types of data regarding cancer deaths in the area were used: (1) available cancer mortality statistics for Lamar County and the State of Mississippi; (2) death certificates for the cancer deaths reported by the community; and (3) death certificate-reported cancer deaths for Lamar County. On the basis of cancer mortality statistics, Lamar County death rates from cancer are not significantly higher than the state rates in Mississippi (Table 1). Copies of the death certificates were requested for the people on the list provided to the DOE by Senator Lott's office. The distribution of types of cancer did not differ from that of Lamar County as a whole (Table 2); that is, there was not a cluster of any type of cancer associated with Tatum Dome.

TABLE 1. Cancer Mortality Rate[(a)] for All Cancers Combined

Date(s)	Geographical Location	Rate[(a)]	Data Source
1980-1989	Lamar County	186.2	Mississippi State Department of Health
1980-1989	Mississippi	178.9	Mississippi State Department of Health
1986	United States	194.7	National Center for Health Statistics

(a) Deaths per 100,000 population.

TABLE 2. Numbers of Cancer Deaths from Death Certificates

	1980-1988	
Diagnosis	"Tatum Dome"[(a)]	Lamar County[(b)]
Nasopharynx	2	3
Esophagus	1	5
Stomach	1	7
Liver	1	5
Larynx	1	3
Lung	7	103
Breast	1	18
Brain	1	5
Multiple myeloma	1	8
Total	16	160

(a) Based on list of cancer deaths provided by Senator Trent Lott's office.
(b) Based on Mississippi State Department of Health report.

In addition to the death certificates, a listing of cancer deaths from Lamar County was obtained from the Mississippi State Department of Health. To compare the deaths from specific types of cancers in the area around the Tatum Dome Site with a part of Lamar County at a distance from the test site, the 1980-1988 cancer deaths were identified for Lumberton and Purvis, which includes the majority of residents near the Tatum Dome site, and two towns geographically distant for comparison. The numbers of deaths for each of 10 types of cancer for the area around the dome were compared to the numbers of deaths expected based on rates from the comparison towns. The numbers of deaths for Lumberton and Purvis from specific types of cancers did not differ from the numbers expected (Table 3).

TABLE 3. Deaths (1980-1988) from Selected Cancer Types

	Lumberton and Purvis	
	Observed	Expected[(a)]
Esophagus	3	5
Stomach	5	4
Liver	2	4
Larynx	2	1
Lung	77	57
Breast	10	18
Brain	2	5
Multiple myeloma	7	5
Non-Hodgkin's lymphoma	5	8
Leukemia	8	13
Total	120	120

(a) Expected on basis of distribution of cancer deaths for Hattiesburg and Sumrall.

In summary, on the basis of the Phase I review of death information, the numbers of cancer deaths or types of cancers in the area around Tatum Dome are not different than expected. That is, there does not appear to be an excess of cancer deaths or evidence of a cluster of cancers associated with the test site. Because there are limitations to studying only information on deaths, a second phase of the cancer study is under way in cooperation with the Mississippi State Department of Health.

The results of Phase I of the cancer study and the plans for Phase II were described as part of four community meetings held in August 1990. At meetings held in the towns of Baxterville, Columbia, Purvis, and Lumberton, citizens and media representatives were given an opportunity to ask questions about the study.

In Phase II, which is currently under way, the number of cancers of selected types occurring in Lamar County will be determined and evaluated to determine if certain types of cancer are found more frequently around Tatum Dome. The Phase II study will include not only persons who died of cancer, but also persons with cancer who survived. The approach currently used in Phase II is to attempt to identify all persons with selected types of cancers in Lamar County between 1980 and 1990. People with cancers will be identified using hospital records, death certificates, and other sources. Once the cancer cases have been identified, the location of their residence will be mapped relative to the Tatum Dome Site, and the distribution around the site will be compared with the rest of Lamar County. The essential question to be answered is: Is there an excess number of cancers, particularly types of cancer known to be associated with radiation exposure, near the Tatum Dome Site?

Collection of information regarding cancer cases in Lamar County is now under way. Completion of the study, with a report to the community on the findings, is expected in the autumn of 1991.

Iron Stores and Risk of Cancer

Principal Investigator: *R. G. Stevens*

Other Investigators: *J. M. Nelson*

Collaborators: *K. Neriishi, Radiation Effects Research Foundation, Hiroshima, Japan; B. Graubard, W. Blot, and C. Land, National Cancer Institute, Bethesda, Maryland*

This research program is studying the effect of body iron stores on the long-term risk of cancer and on the prognosis after cancer diagnosis, and the possible modifying effect of iron stores on risk of radiation-induced tumor formation. During this year, hypotheses to be tested have continued to be formulated and will be tested in the National Health and Nutrition Examination Survey (NHANES) and other data sets. In addition, preliminary laboratory experiments have been conducted that complement epidemiological analyses. Evidence from in vitro experiments with Chinese hamster ovary (CHO) cells shows that nontoxic increases in the iron content of the growth medium can greatly increase sensitivity of these cells to killing by radiation. These results, which will be explored further in the laboratory, may have important implications for human susceptibility to injury from radiation exposure.

Mechanisms

There are two general mechanisms by which iron may increase risk of cancer or affect radiation-induced transformation. First, excess intracellular iron may increase the ambient concentration of oxygen radicals, leading to depletion of cellular reserves of reducing agents. Increased oxidative stress may thus render the cell more sensitive to the radicals produced by ionizing radiation. Excess intracellular iron may also increase the effective range of radicals produced by radiation. Second, iron may be a limiting nutrient to the growth and replication of a transformed cell in the human body, and high iron stores thus may increase the likelihood that a transformed cell will survive to become a clinically apparent neoplasm (Stevens and Kalkwarf 1990).

If body iron stores affect sensitivity to radiation injury, this effect has important implications for second malignant neoplasms arising from radiation therapy, diagnostic radiation exposure, occupational radiation and residential radon exposures, and exposure of astronauts and airline crews to cosmic radiation. In these instances, relative capacity of the host to scavenge oxygen radicals may influence cancer risk associated with radiation exposure, and this capacity may be closely related to iron metabolism. Nutritional antioxidants have received much attention in this regard, but the "oxidant" iron has received very little.

The association of body iron stores and of serum albumin level with subsequent cancer risk in men seen in the epidemiological studies done to date are intriguing findings. In a chapter for a book to be published by the Environmental Health Institute, Stevens and Neriishi (in press) examined in detail the possible role of iron in radiation injury and the role of oxygen radicals in the relationship. A chapter for another book (Stevens and Blumberg, in press) reported possible mechanisms for an effect of albumin and considered informative studies that might be pursued.

Experimental Studies

Cellular studies of the possible role of iron in sensitivity to radiation injury have begun in collaboration with J. M. Nelson. A study by Whiting et al. (1981) in which ferritin added to growth medium increased chromosome damage to Chinese hamster ovary (CHO) cells was used as a guide to execute a study of survival after irradiation. The first experiment was designed to

determine the toxicity of ferritin. The results showed that ferritin is toxic at concentrations greater than 100 μg/ml. Apoferritin (iron-free) is not toxic, even at concentrations in excess of 1000 μg/ml.

In the next experiment, two sets of plates were made at ferritin concentrations of 0 (control), 0.5, 2, 8, and 32 μg/ml. Twelve plates were made at each ferritin concentration in each of the two sets for a total of 120 plates. One set (60 plates, 12 at each ferritin concentration) was exposed to 4 Gy of x rays; the other set was not. Plated cells were allowed to grow for 2 weeks in an incubator at 37°C, and colonies were counted. The irradiated control plates contained 0.50 times the number of colonies of the unirradiated control plates; that is, exposure to 4 Gy of x rays killed ~50% of the cells. Under the hypothesis that ferritin killing is independent of x-ray killing, the ratio of each set of irradiated plates at a given ferritin concentration to their respective unirradiated plates should be 0.50. Ratios greater than 0.50 would suggest radioprotection, and lower ratios would suggest radiosensitization. At concentrations of 0.5, 2, and 8 μg/ml, the ratios were 0.45, 0.47, and 0.44, respectively; that is, virtually no interactive effect of ferritin with radiation was observed. However, at a ferritin concentration of 32 μg/ml the ratio was only 0.14. In addition, the unirradiated plates with 32 μg/ml ferritin had nearly the same number of colonies as the unirradiated control plates. Taken together, these results indicate that 32 μg/ml ferritin is not at all toxic yet is effectively radiosensitizing to CHO cells.

In the next experiment, 0, 16, 32, 64, and 128 μg/ml ferritin were used as the five exposure levels. The ratio of the irradiated control plates to the unirradiated control plates was 0.71 in this experiment; that is, exposure to 4 Gy of x rays killed ~30% of the cells. The respective ratios for each ferritin level were 0.59, 0.30, 0.15, and 0.33, respectively. No killing was observed in the unirradiated plates at ferritin concentrations of 16 and 32 μg/ml. At 64 μg/ml ferritin, there was 40% killing, and at 128 μg/ml there was 99% killing. These results confirmed the radiosensitizing effect of 32 μg/ml ferritin. In addition, this experiment showed that higher levels of ferritin that were toxic in themselves also increased the killing efficiency of radiation.

Normal serum contains ~10 μg/ml iron, primarily bound to transferrin. The growth medium for CHO cells contains 10% fetal calf serum and thus ~1 μg/ml iron. Because ferritin is ~19% iron by weight, 32 μg/ml ferritin represents ~6 μg/ml iron. Thus, an approximate sevenfold increase in the iron concentration of the growth medium of CHO cells is not toxic, but is dramatically radiosensitizing. Although ferritin added at 32 μg/ml increases the iron content of standard CHO growth medium sevenfold, it represents less than a twofold increase in iron concentration to cells growing in blood in whole animals.

There are many possible implications of these results for human exposure to radiation. If generation of oxygen radicals by excess iron accounts for the results, then there may also be implications for exposure to toxic chemicals.

Future Plans

The prominence of iron in human physiology and the high iron content of the Western diet emphasize the importance of pursuing further research on the possible role of iron in risk of cancer and in risk of radiation-induced transformation. Thus, the experimental program will be expanded, and the molecular mechanisms whereby ferritin sensitizes CHO cells to radiation injury will be investigated.

Analyses of iron status and of serum albumin and cancer risk in the NHANES I population will be expanded in scope and detail. A new followup of the original population has yielded several hundred more cancer cases. These data will allow for a more detailed consideration of possible interactions of iron and albumin with each other and with other factors. It will also increase the power of the study for examining these effects in women.

References Cited

Stevens, R. G., and B. S. Blumberg. Serum albumin and risk of cancer. In: *Nutrition and Cancer Prevention: Investigating the Role of Macronutrients,* M. S. Micozzi and T. Moon, eds. Marcel Dekker, New York (in press).

Stevens, R. G., and D. R. Kalkwarf. 1990. Iron, radiation, and cancer. *Environ. Health Perspect.* 87:291-300.

Stevens, R. G., and K. Neriishi. Iron and oxidative damage in human cancer. In: *Mechanisms and Consequences of Oxidative Damage,* A. Bloom and L. Spatz, eds. Oxford University Press, New York (in press).

Whiting, R. F., L. Wei, and H. F. Stich. 1981. Chromosome-damaging activity of ferritin and its relation to chelation and reduction of iron. *Cancer Res.* 41:1628-1636.

Biological
Research

Inhaled Plutonium Oxide in Dogs

Principal Investigator: *J. F. Park*

Other Investigators: *R. L. Buschbom, G. E. Dagle, K. M. Gideon, E. S. Gilbert, G. J. Powers, H. A. Ragan, C. O. Romsos, C. R. Watson, R. E. Weller, and E. L. Wierman*

Technical Assistance: *R. F. Flores, B. B. Kimsey, B. G. Moore, R. P. Schumacher, and M. J. Steele*

This project is concerned with long-term experiments to determine the life-span dose-effect relationships of inhaled $^{239}PuO_2$ or $^{238}PuO_2$ in beagles. The data will be used to estimate the health effects of inhaled transuranics. Beagle dogs given a single exposure to $^{239}PuO_2$ or $^{238}PuO_2$ aerosols to obtain dose-level groups with initial lung burdens (ILB) approximately 1, 8, 40, 150, 700, and 2800 times the maximum permissible lung dose for a plutonium worker have been observed for life-span dose-effect relationships; all the dogs have now died. Increased incidence of lung tumors was observed in the four highest dose-level groups exposed to $^{239}PuO_2$. Increased incidence of lung and/or bone tumors was observed in the five highest dose-level groups exposed to $^{238}PuO_2$. The lung tumor risk resulting from a given cumulative radiation dose to the lungs from $^{239}PuO_2$ was significantly higher than from a similar dose from $^{238}PuO_2$. The extrapolated lifetime risk at 1 rad was estimated to be 7 per 10^6 for $^{239}PuO_2$ and 1 per 10^6 for $^{238}PuO_2$. Chronic lymphopenia, occurring 0.5 to 2 years after exposure, was the earliest observed effect after inhalation of either $^{239}PuO_2$ or $^{238}PuO_2$ in the four highest dose-level groups that had ILB ≥80 nCi. Other plutonium-exposure-related effects include sclerosis of the tracheobronchial lymph nodes, focal radiation pneumonitis, adenomatous hyperplasia of the liver, increased serum glutamic pyruvic transaminase, and dystrophic osteolytic lesions in the skeleton.

To determine the life-span dose-effect relationships of inhaled plutonium, 18-month-old beagle dogs were exposed to aerosols of $^{239}PuO_2$ (mean AMAD, 2.3 μm; mean GSD, 1.9), prepared by calcining the oxalate at 750°C for 2 hours; or to $^{238}PuO_2$ (mean AMAD, 1.8 μm; mean GSD, 1.9), prepared by calcining the oxalate at 700°C and subjecting the product to $H_2{}^{16}O$ steam in argon exchange at 800°C for 96 hours. This material, referred to as pure plutonium oxide, is used as fuel in space-nuclear-power systems.

One hundred thirty dogs exposed to $^{239}PuO_2$ in 1970 and 1971 were selected for long-term studies; 14 were sacrificed to obtain plutonium distribution and pathology data and 116 were assigned to life-span dose-effect studies (Table 1). The 116 dogs exposed to $^{238}PuO_2$ in 1973 and 1974 were selected for life-span dose-effect studies (Table 2), and 21 additional dogs were exposed for periodic sacrifice. The Appendix (which follows Part 1 of this Annual Report) shows the status of the dogs in these experiments. The *Pacific Northwest Laboratory Annual Report for 1989 to the Office of Energy Research (Part 1)*

TABLE 1. Life-Span Dose-Effect Studies with Inhaled $^{239}PuO_2$ in Beagles[a]

Dose-Level Group	Number of Dogs		Initial Lung Deposition[b]	
	Male	Female	nCi[c]	nCi/g Lung[c]
Control	10	10	0	0
1	12	12	3.5±1.3	0.029±0.011
2	10	11	22±4	0.18±0.04
3	10	10	79±14	0.66±0.13
4	11	11	300±62	2.4±0.4
5	10	11	1100±170	9.3±1.4
6	3	5	5800±3300	50±22
	66	70		

(a) Exposed in 1970 and 1971.
(b) Estimated from external thorax counts at 14 and 30 days after exposure and estimated lung weights (0.011 x body weight).
(c) Mean ± 95% confidence intervals around means.

summarized the results of the $^{239}PuO_2$ study. For this year (1990) we summarized the results of the $^{238}PuO_2$ study and compared lung cancer risks estimates from the two studies.

TABLE 2. Life-Span Dose-Effect Studies with Inhaled $^{238}PuO_2$ in Beagles[a]

Dose-Level Group	Number of Dogs		Initial Lung Deposition[b]	
	Male	Female	nCi[c]	nCi/g Lung[c]
Control	10	100	0	
1	10	10	2.3±0.8	0.016±0.007
2	11	10	18±3	0.15±0.03
3	12	10	77±11	0.56±0.07
4	10	10	350±81	2.6±0.5
5	10	10	1300±270	10±1.9
6	7	6	5200±1400	43±12
	70	66		

(a) Exposed in 1973 and 1974.
(b) Estimated from external thorax counts at 14 and 30 days after exposure and estimated lung weights (0.011 x body weight).
(c) Mean ± 95% confidence intervals around means.

Table 3 shows the primary causes of death and the distribution of ^{238}Pu in the tissues of these animals as percent of final body burden. Figure 1 shows the ^{238}Pu tissue distribution as percent of initial lung burden (ILB) for all dogs for which tissue radiochemical analyses are complete. The ILB for those dogs for which radiochemical analysis of excreta were not complete were estimated from external thorax counts at 14 and 30 days after exposure. For dogs whose analyses were complete, ILB were estimated from the summation of the tissue burdens of plutonium, plus the plutonium excreted, minus plutonium excreted in the feces during the first 3 days after exposure. The latter was assumed to be deposited in the upper respiratory tract.

Uptake and retention functions were fitted to the organ burden data. Based on the premise that the organ burdens were interrelated, the uptake and retention function for all organs was fitted simultaneously instead of fitting isolated functions for each organ. The organs were treated as compartments of a single system, with transfer rates specifying the total amount, leaving a compartment per unit time and the fractional distribution of that amount among the other compartments. The transfer rates assumed that plutonium moved through the body in a single pass. The material initially deposited in the lung was either excreted or moved to some other organ, from which it was excreted. It was assumed that there were no feedback loops in the system. Organ systems included lung, thoracic lymph nodes, liver, skeleton, and all other tissues. The functions were estimated using weighted, nonlinear least squares. The weights were estimated by biweighting procedures that give the more extreme data values very little weight.

Table 4 summarizes, by dose-level group, mortality and lesions associated with death through 16 years after exposure to $^{238}PuO_2$; all the dogs have died. Mean survival time was decreased in the two highest dose-level groups compared to the other groups. Of the 116 exposed dogs euthanized, 33 were killed because of bone tumors, 10 because of lung tumors, and 1 because of radiation pneumonitis. Thirteen of the dogs that had bone tumors also had lung tumors. Five dogs with lung tumors were euthanized for other causes; also, 1 control dog was euthanized because of a lung tumor. Of 33 dogs with bone tumors, 31 had osteosarcomas; 1 dose-level Group 1 dog (989F) had a fibrosarcoma in the ilium, and 1 dose-level Group 4 dog (1103F) had a fibrosarcoma in a vertebra. None of the control dogs had bone tumors. All the exposed dogs with osteosarcomas were in dose-level Groups 4, 5, and 6. Lung tumors were observed in all dose-level groups. Of the 31 osteosarcomas, 13 were in vertebrae, 2 in femora, 4 in ribs, 3 in scapulae, 5 in the pelvis, 1 in the tibia, 1 in the sternum, 1 in the sacrum, and 1 in the humerus.

One dose-level Group 3 dog died of hepatocellular carcinoma; one dose-level 1 and one dose-level 3 dog died of hemangiosarcomas in the liver. Three dose-level 4 dogs, one dose-level 3 dog, one dose-level 2 dog, and one control dog had bile duct carcinomas or adenomas as incidental observations at necropsy not related to the cause of death. Three exposed dogs with incidental liver tumors also had lung or bone tumors, and two were euthanized for other causes. The one control dog with liver tumors was also euthanized for other causes.

TABLE 3. Tissue Distribution of Plutonium in Beagles After Inhalation of $^{238}PuO_2$

Dog Number	Time After Exposure, months	Final Body Burden, μCi	Percent of Final Body Burden					Cause of Death
			Lungs	Thoracic Lymph Nodes[a]	Abdominal Lymph Nodes[b]	Liver	Skeleton	
1032M	0.25	0.150	97	0.34	0.20	1.7	0.16	Sacrifice
921F	1	0.0044	93	0.65	0.04	0.38	2.1	Sacrifice
930F	1	0.052	99	0.63	0.01	0.07	0.35	Sacrifice
931F	1	0.347	96	1.9	0.01	0.05	0.36	Sacrifice
929F	2	0.017	91	7.5	0.002	0.26	0.58	Sacrifice
932F	2	0.382	96	2.5	0.01	0.18	0.39	Sacrifice
923F	2	0.0023	88	9.4	0.03	0.09	0.44	Sacrifice
925M	3	0.0064	91	4.1	0.04	0.04	1.2	Sacrifice
926M	3	0.078	87	11	0.23	0.65	1.1	Sacrifice
934M	3	0.902	92	4.8	1.7	0.45	0.95	Sacrifice
1318M	12	0.030	45	27	0.08	10	15	Sacrifice
1319M	12	0.077	41	26	0.03	11	20	Sacrifice
1214M	13	0.014	52	9.2	0.32	6.2	16	Sacrifice
1310M	25	0.026	19	36	0.08	15	28	Sacrifice
1317M	25	0.041	20	33	0.16	17	26	Sacrifice
1315M	25	0.047	22	31	0.04	17	28	Sacrifice
1191F	35	0.658	26	32	0.13	18	22	Pneumonia
1215M	36	0.011	21	43	0.17	13	21	Sacrifice
1311M	37	0.036	13	31	0.22	21	32	Sacrifice
994F	42	5.024	17	45	0.50	18	18	Addison's disease
970F	48	0.0022	20	34	0.36	16	24	Sacrifice
1312M	49	0.035	6.8	29	0.26	25	35	Sacrifice
1143M	49	6.331	11	43	2.0	15	22	Bone tumor, lung tumor
1025M	50	10.033	16	27	7.1	24	23	Lung tumor
1064M	51	8.427	13	48	1.9	15	20	Bone tumor, lung tumor
1175F	52	3.641	14	31	0.08	25	26	Lung tumor
1079M	56	2.182	9.8	40	4.3	13	25	Addison's disease
1096F	59	1.204	4.3	22	2.7	36	24	Addison's disease
1189M	60	0.044	8.9	25	0.16	37	25	Sacrifice
1115F	61	1.534	5.0	32	2.3	26	33	Bone tumor
1162F	61	3.663	12	32	5.9	21	25	Bone tumor, Addison's disease
1009M	62	4.360	15	25	2.4	31	23	Lung tumor
974F	64	1.465	5.1	24	5.9	33	29	Bone tumor
1092M	65	1.515	2.1	26	9.1	29	30	Bone tumor
975F	66	3.749	11	30	2.1	28	25	Bone tumor, lung tumor
1042F	69	1.494	4.7	25	2.9	32	33	Bone tumor, lung tumor
1037M	69	2.417	7.1	27	7.8	28	27	Bone tumor
1027M	70	2.546	3.8	15	7.0	40	31	Bone tumor, lung tumor
1006F	72	2.826	7.5	30	3.4	29	26	Bone tumor, lung tumor
1057M	72	1.748	3.0	35	2.2	33	24	Bone tumor
1082M	78	0.0083	2.4	20	0.31	40	34	Paralysis
1081M	80	0.361	4.6	15	0.48	47	29	Hemangiosarcoma (heart)
1058F	80	1.000	2.0	18	4.4	31	41	Bone tumor, adrenal tumor
1002M	84	1.786	2.9	31	2.0	31	28	Bone tumor, lung tumor
1109F	86	0.885	0.93	23	4.0	34	35	Bone tumor, Addison's disease, lung tumor
1218F	86	0.678	2.7	23	4.1	42	25	Bone tumor
1071M	91	1.088	5.4	28	3.4	27	33	Bone tumor, lung tumor
1063M	94	0.00060	3.4	15	1.3	22	43	Brain tumor, heart tumor
1160F	95	0.956	1.6	21	0.91	43	30	Bone tumor, lung tumor
960M	95	0.036	4.0	21	0.49	33	39	Malignant lymphoma

(a) Includes tracheobronchial, mediastinal, and sternal lymph nodes.
(b) Includes hepatic, splenic, and mesenteric lymph nodes.

TABLE 3. Continued

Dog Number	Time After Exposure, months	Final Body Burden, μCi	Percent of Final Body Burden					Cause of Death
			Lungs	Thoracic Lymph Nodes[a]	Abdominal Lymph Nodes[b]	Liver	Skeleton	
1040M	96	0.059	3.0	17	0.96	40	35	Parathyroid adenoma
1140M	97	0.504	3.8	18	7.7	37	30	Bone tumor
989F	99	0.0017	5.1	11	1.2	22	29	Bone tumor (fibrosarcoma)
1211M	99	0.895	1.3	29	4.7	39	23	Bone tumor
1173M	99	0.462	2.0	33	7.5	21	33	Bone tumor
1043F	103	0.037	3.5	16	0.57	33	42	Empyema, pituitary tumor, Cushing's disease
1192F	109	0.345	2.4	7.3	4.6	36	46	Bone tumor
1178M	110	0.594	0.86	17	2.0	33	42	Bone tumor, lung tumor
1047M	115	0.241	1.4	7.8	11	28	48	Herniated vertebral disc
1106F	117	0.0029	1.3	16	1.8	9.9	57	Adrenal carcinoma
1103F	118	0.232	0.76	18	3.1	45	32	Bone tumor, lung tumor
1188M	119	0.0089	0.71	2.5	0.94	68	24	Metastatic lung tumor
1066M	121	0.035	1.1	4.4	0.52	57	32	Malignant lymphoma
1069F	121	0.0022	9.1	2.1	1.6	51	34	Malignant lymphoma
1030F	122	0.160	1.5	15	1.1	22	56	Pneumonia
951M	122	0.0023	3.3	8.9	0.77	47	35	Anesthesia
1229M	123	0.0060	0.94	11	0.73	35	49	Pneumonia
1072M	124	0.079	0.65	4.1	1.6	57	34	Radiation pneumonitis
1157M	124	0.294	0.55	3.5	3.7	41	44	Bone tumor
971F	125	0.0095	1.7	5.5	0.44	49	41	Hemangiosarcoma (spleen)
1078F	125	0.025	0.98	9.6	0.60	46	41	Meningioma
952F	125	0.106	1.0	4.4	2.1	39	48	Bone tumor
1059F	126	0.050	4.2	7.4	0.99	45	39	Malignant lymphoma
991F	126	0.058	1.8	14	0.81	36	41	Urinary bladder tumor
1070M	126	0.011	1.9	9.5	0.70	51	34	Round cell sarcoma (kidney)
1166M	128	0.354	1.8	11	1.6	47	35	Malignant lymphoma
983M	132	0.274	1.5	5.9	2.9	47	37	Adrenal tumor, pituitary tumor
1035F	132	0.172	2.8	10	1.9	19	53	Bone tumor, Cushing's disease
1031F	134	0.025	1.9	13	0.97	17	65	Pneumonia
1190F	134	0.033	0.84	4.4	1.2	49	41	Lung tumor
1062M	135	0.270	0.63	2.6	3.9	46	44	Bone tumor, lung tumor
1177M	136	0.142	0.77	5.0	0.89	36	53	Bone tumor
959M	138	0.0025	3.4	14	0.62	33	48	Liver abscess
992F	139	0.264	0.73	8.0	2.7	42	42	Bone tumor
1194F	140	0.0014	0.67	10	9.0	20	56	Malignant lymphoma
1105F	140	0.00074	0.62	5.6	0.70	44	45	Malignant lymphoma
1193F	141	0.0037	0.58	9.2	1.0	37	48	Immune hemolytic anemia
973F	142	0.127	3.7	7.0	1.8	44	39	Bone tumor
1060F	142	0.011	0.61	10	0.68	39	47	Pneumonia
1114M	143	0.272	0.51	7.4	2.9	39	47	Bone tumor, bile duct carcinoma
1222M	143	0.0051	8.5	4.0	0.82	36	47	Malignant mesothelioma (mediastinal)
1053F	143	0.061	1.9	5.0	0.83	45	41	Cushing's disease
1176M	145	0.051	0.39	5.9	0.90	52	38	Hemangioma (spleen)
1309M	146	0.019	1.4	4.8	0.96	46	44	Hemangiosarcoma (liver)
1230M	150	0.0027	0.34	12	1.2	41	41	Hemangiosarcoma (liver)
1198M	151	0.156	0.52	2.4	4.5	59	30	Acute pneumonia, lung tumor
1219F	152	0.020	0.76	8.4	0.97	34	50	Chronic nephropathy
1220F	152	0.136	0.74	7.7	1.1	38	48	Malignant lymphoma, Addison's disease
1165M	152	0.042	0.66	7.8	1.6	47	39	Acute pneumonia

(a) Includes tracheobronchial, mediastinal, and sternal lymph nodes.
(b) Includes hepatic, splenic, and mesenteric lymph nodes.

TABLE 3. Continued

Dog Number	Time After Exposure, months	Final Body Burden, μCi	Percent of Final Body Burden					Cause of Death
			Lungs	Thoracic Lymph Nodes[a]	Abdominal Lymph Nodes[b]	Liver	Skeleton	
1008M	153	0.00049	1.4	13	0.57	34	47	Fibrosarcoma (spleen)
1033M	154	0.0042	0.93	5.3	0.84	19	70	Lung tumor
1026M	154	0.072	0.99	4.2	0.46	51	40	Hepatic dysplasia
1065F	154	0.0035	0.72	8.9	0.69	27	60	Malignant lymphoma, lung tumor
1216M	156	0.0096	2.5	6.9	1.4	49	37	Malignant lymphoma
982M	157	0.067	1.5	4.2	0.79	52	37	Pneumonia, thyroid carcinoma
999F	157	0.0045	0.53	8.3	0.66	40	46	Nasal sarcoma, lung tumor
972F	159	0.024	1.4	9.5	1.1	40	47	Allergic bronchitis
998M	159	0.0010	1.4	13	0.56	46	35	Lung tumor
1050F	159	0.0075	0.57	7.3	1.3	39	48	Lung tumor
997M	160	0.112	5.7	8.9	0.85	42	40	Lung tumor
1056M	160	0.060	0.58	2.1	1.5	37	56	Pneumonia, thyroid carcinoma
1195M	161	0.099	0.57	2.1	1.0	52	43	Chronic nephropathy, bile duct adenoma
1091F	161	0.078	2.9	5.1	3.3	28	54	Thyroid carcinoma
1039M	162	0.00079	0.71	5.8	0.50	54	36	Heart failure
993F	162	0.0052	0.39	9.6	1.0	26	59	Malignant lymphoma
1108F	164	0.027	0.85	6.2	0.78	37	50	Posterior paralysis
1316M	165	0.026	1.2	3.1	0.61	53	39	Posterior paralysis
1090F	167	0.0054	0.39	3.6	0.74	43	49	Heart failure
955M	169	0.0084	2.3	5.4	0.45	36	53	Lung tumor, bile duct adenoma
1003M	170	0.00031	1.1	11	0.85	40	42	Transition cell carcinoma (urinary bladder)
1095F	170	0.00066	0.67	2.9	0.88	50	42	Chronic nephropathy
1036F	170	0.0061	0.57	4.1	0.80	40	50	Malignant melanoma (oral)
1004M	171	0.072	1.5	9.9	1.2	48	36	Malignant lymphoma, lung tumor, cholangiosarcoma
1212F	172	0.022	1.1	8.8	1.1	34	51	Hepatocellular carcinoma
1055M	172	0.00073	0.87	9.5	1.2	47	39	Malignant melanoma (oral)
1221F	173	0.016	0.80	7.7	0.71	22	64	Malignant lymphoma, cholangiosarcoma
1207F	174	0.012	0.76	2.7	0.45	62	32	Herniated vertebral disc
1158M	175	0.029	0.54	2.7	0.54	60	33	Nasal carcinoma
1046M	178	0.0091	1.7	4.7	0.65	46	43	Lung tumor
1196F	178	0.0078	0.71	4.5	0.58	45	46	Salivary squamous carcinoma, lung tumor
1000F	179	0.018	0.55	3.5	0.61	54	39	Transitional cell carcinoma (urinary bladder)
1204M	180	0.0038	0.56	7.4	0.53	34	53	Transitional cell carcinoma (uretha)
1023F	182	0.000039	2.6	1.9	1.9	28	49	Pneumonia
1089F	183	0.016	0.55	3.7	1.6	35	54	Chronic nephropathy
1044F	186	0.00086	0.57	3.6	0.54	46	42	Epilepsy
981M	193	0.0088	0.37	2.8	0.63	35	55	Chronic nephropathy
1084M	195	0.0039	0.55	3.4	1.7	41	47	Malignant lymphoma, heart

(a) Includes tracheobronchial, mediastinal, and sternal lymph nodes.
(b) Includes hepatic, splenic, and mesenteric lymph nodes.

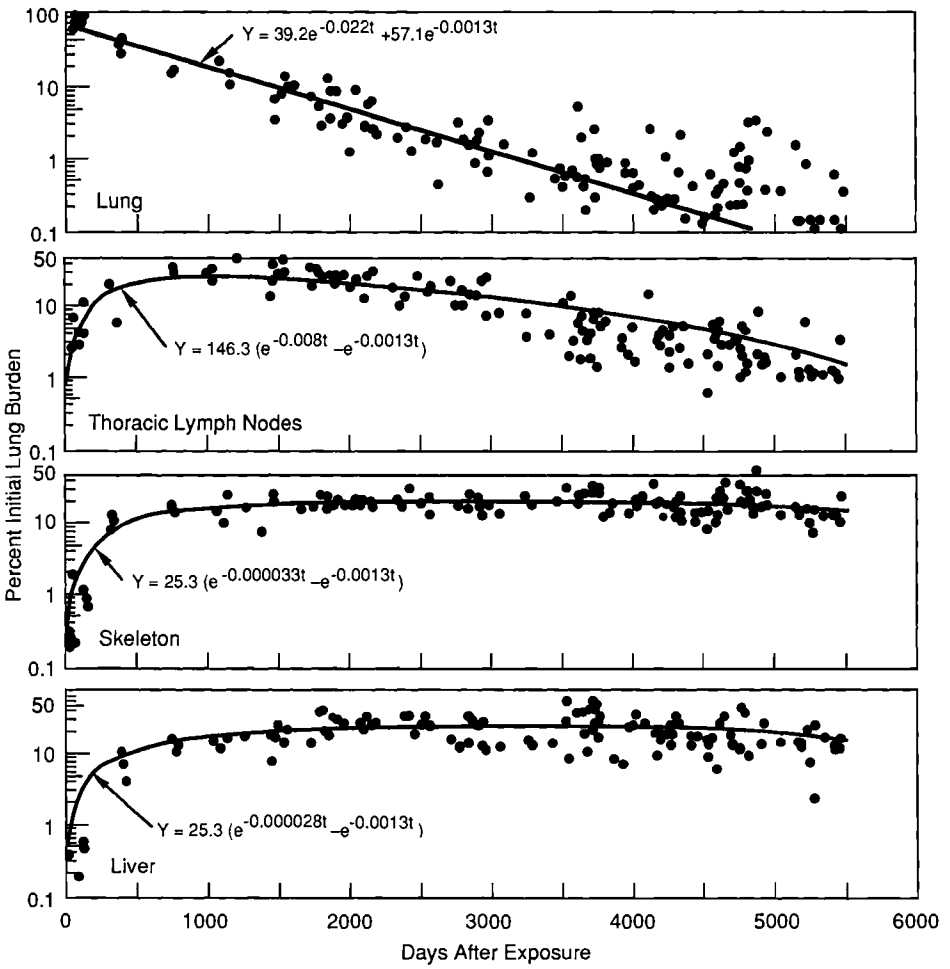

FIGURE 1. Plutonium in Dogs After Inhalation of $^{238}PuO_2$. Points represent data from individual dogs. Uptake and retention curves and functions were based on dogs in which initial lung burdens were estimated from the final plutonium body burden, plus the plutonium excreted, minus that excreted in the feces during first 3 days after exposure or from external thorax counts at 14 and 30 days after exposure.

During the 3 to 16 years after exposure, 62 exposed dogs died or were euthanized as a result of causes presently thought to be unrelated to plutonium exposure; 32 died of various neoplastic diseases, and 30 of various other causes. One control dog was euthanized because of lung tumors, 1 of incidental liver tumors, 11 of various neoplastic diseases, and 7 of various other causes.

The lung tumors were classified as bronchioloalveolar carcinomas in 16 dogs, bronchioloalveolar adenoma in 1 dog, adenocarcinoma in 5 dogs, adenosquamous carcinoma in 4 dogs and epidermoid carcinoma in 1 dog. In 1 dog, three lung tumor types were observed: bronchioloalveolar, adenocarcinoma, and fibrosarcoma. Metastases were observed in the lungs; thoracic, hepatic, mesenteric, and axillary lymph nodes; vertebra; esophagus; stomach; liver; and adrenal of 1 dog with bronchioloalveolar carcinoma. Metastases were observed in the lungs; thoracic, hepatic, and splenic lymph nodes; trachea; esophagus; mediastinum; thyroid; diaphragm; and hearts of 2 dogs with pulmonary adenocarcinoma. One dog with adenosquamous carcinoma had metastases to the lung, thoracic lymph nodes, and heart. The dog with epidermoid carcinoma had metastases to the lungs, thoracic lymph nodes, and diaphragm. The lung tumor in the control dog was an adenocarcinoma with metastases to the thoracic lymph nodes. Bone tumor metastases were found in the

TABLE 4. Summary of Lesions in Dogs Euthanized During the 16-Year Period After Inhalation of $^{238}PuO_2$

	Dose Group						
	6	5	4	3	2	1	Control
Number of Dogs/Group	13	20	20	22	21	20	20
Number of Dead Dogs/Group	13	20	20	22	21	20	20
Mean Survival Post Exposure, years	5	7	12	12	13	12	13
Condition[(a)]							
Bone tumor	2	11	4			1	
Lung tumor	3		1	1	3	1	1
Lung tumor, bile duct adenoma					1		
Bone and lung tumor	6	4	2				
Bone tumor, bile duct carcinoma			1				
Bone tumor, Addison's disease	1						
Bone and lung tumor, Addison's disease		1					
Salivary squamous carcinoma, lung tumor					1		
Nasal sarcoma, lung tumor					1		
Nasal carcinoma				1			1
Pneumonia, lung tumor			1				
Malignant lymphoma, lung tumor, cholangiocarcinoma				1			
Malignant lymphoma, lung tumor					1		
Malignant lymphoma, cholangiosarcoma			1				
Malignant lymphoma			1	3	2	4	4
Malignant lymphoma, Addison's disease			1				
Hemangioma (spleen)			1				
Hemangiosarcoma (heart, omentum, spleen)			1		1		2
Fibrosarcoma (spleen)						1	
Hemangiosarcoma (liver)				1		1	
Hepatocellular carcinoma				1			
Urinary bladder/urethra tumor			1	1		2	2
Urethra tumor, bile duct adenoma							1
Pituitary tumor, Cushing's disease			1	1			1
Pituitary tumor							1
Pneumonia, thyroid carcinoma				2			
Thyroid carcinoma			1				
Malignant melanoma (oral)					1	1	
Malignant mesothelioma					1		
Brain and heart tumor						1	
Brain tumor					1		
Parathyroid adenoma				1			
Adrenal carcinoma						1	
Round cell sarcoma (kidney)					1		
Adrenal and pituitary tumors			1				
Lung tumor, metastatic					1		
Pneumonia		1	1	2	2	1	1
Pulmonary interstitial fibrosis							1
Allergic bronchitis				1			
Radiation pneumonitis				1			
Renal amyloidosis, splenic hemangioma							1
Chronic nephropathy				2	1	1	2
Chronic nephropathy, bile duct adenoma			1				
Addison's disease	1	2					
Posterior paralysis				2			
Herniated vertebral disk		1			1		
Spinal cord degeneration					1		
Cervical disc disease							1
Liver abscess						1	
Hepatic dysplasia				1			
Heart failure					1	1	
Immune hemolytic anemia						1	
Pyometra							1
Epilepsy						1	
Anesthesia						1	

(a) Number of dogs with lesion associated with death.

lungs of 6 dogs; in 3 dogs, the bone tumor metastasized to lungs, thoracic lymph nodes, liver, spleen, and heart; in 1 dog, the bone tumor metastasized to the iliac lymph nodes; and in 1 dog, the bone tumor metastasized to the lungs, pleura, diaphragm and heart. The 6 dogs with Addison's disease, which were in dose-level Groups 4, 5, and 6, had adrenal cortical atrophy.

In addition to the lesions associated with the cause of death, lesions in the lungs of the dose-level Groups 4, 5, and 6 dogs included focal alveolar histocytosis, alveolitis, alveolar epithelial cell hyperplasia, alveolar emphysema, pleural fibrosis, and interstitial fibrosis. Numerous alpha stars were observed, mainly in foci of fibrosis, and single alpha tracks were scattered throughout sections in foci of alveolar histocytosis and in alveolar septa. Sclerosing lymphadenopathy in the tracheobronchial and mediastinal lymph nodes was associated with high concentrations of plutonium observed as alpha stars in dose-level Groups 3, 4, 5, and 6. Similar but less severe lesions were seen in the hepatic lymph nodes. In dose-level Groups 5 and 6, there were extensive alterations in bone, including multiple areas of focal atrophy of bone; endosteal, trabecular, and peritrabecular bone fibrosis; and osteolysis of cortical, endosteal, and trabecular bone. One dog had lesions of secondary hypertrophic osteoarthropathy.

Radioactivity in the bone was present as single tracks, generally scattered throughout the bone, cartilage, and bone marrow. The liver contained foci of hepatocellular fatty change, where small clusters of single tracks were seen. There was also mild, focal, nodular hyperplasia of hepatocytes in dose-level Groups 3, 4, 5, and 6. Elevated serum glutamic pyruvic transaminase (GPT) levels, suggestive of liver damage, were observed in dose-level Groups 3, 4, 5, and 6 dogs.

Dose-related lymphopenia was observed in groups with mean lung $^{238}PuO_2$ deposition of 77 nCi or more (Figure 2). Through 126 months after exposure, mean lymphocyte values were significantly lower ($p < 0.05$) for dose-level Groups 4 and 5 than for the control group. Lymphocyte values in the $^{238}PuO_2$-exposed dogs tended to increase after reaching a minimum, and mean lymphocyte concentrations in Group 3 dogs were not significantly different from values of control dogs 86 to 94 months after exposure. Lymphocyte values in the two lowest exposure groups (2.3 and 18 nCi) were not different from control values. A dose-related reduction in total leukocytes was evident, primarily because of lymphopenia, except in Groups 5 and 6, in which neutropenia was also observed. Through 118 months after exposure, mean leukocyte and neutrophil values were significantly lower ($p < 0.05$) for dose-level Group 5 than for the control group. No difference in monocyte values was seen in relation to dose levels. A significant and progressive reduction in eosinophils was evident only in dose-level Group 6 dogs following $^{238}PuO_2$ inhalation. No chronic effects have been observed in red cell parameters. By 14 years after exposure, too few dogs were alive for meaningful dose-group comparisons.

Lymphopenia, the earliest observed effect after inhalation of either $^{239}PuO_2$ or $^{238}PuO_2$, occurred after deposition of ~80 nCi plutonium in the lungs. On a concentration basis, the 80-nCi dose level is about 40 times the 16-nCi maximum permissible human lung deposition, based on 0.3 rem/week to the lung. Lymphopenia is thought to be related to the plutonium content of the tracheobronchial lymph nodes. Dose-level groups with initial lung burdens of ~80 nCi had lymphocyte counts less than those of controls by 12 months after exposure when the cumulative average lymph node doses were ~320 rad. Because of continuing transfer of plutonium to the lymph nodes, the dose rate at this time had increased to 620 rad per year.

In serum chemistry assays of $^{238}PuO_2$ dogs performed more than 120 months after exposure, alkaline phosphatase (ALP) and GPT values were higher than those of the control group only in dose-level Groups 3, 4, and 5 dogs (Figure 3). For individual dogs, these elevations were biphasic with an early increase followed by a return to control values; a later effect was characterized by persistent increasing elevations of both ALP and GPT. Calculation of the cumulative average radiation dose to mean time after exposure when serum chemistry values were first observed to be different from controls for dose-level 3, 4, and 5 dogs revealed a mean dose to liver of about 20, 75, and 200 rad respectively, for the late effect. At this time the dose rate was -2, ~10, and ~60 rad per year, respectively. Elevations in GPT were consistent with liver histopathological findings and radiochemical analyses indicating $^{238}PuO_2$

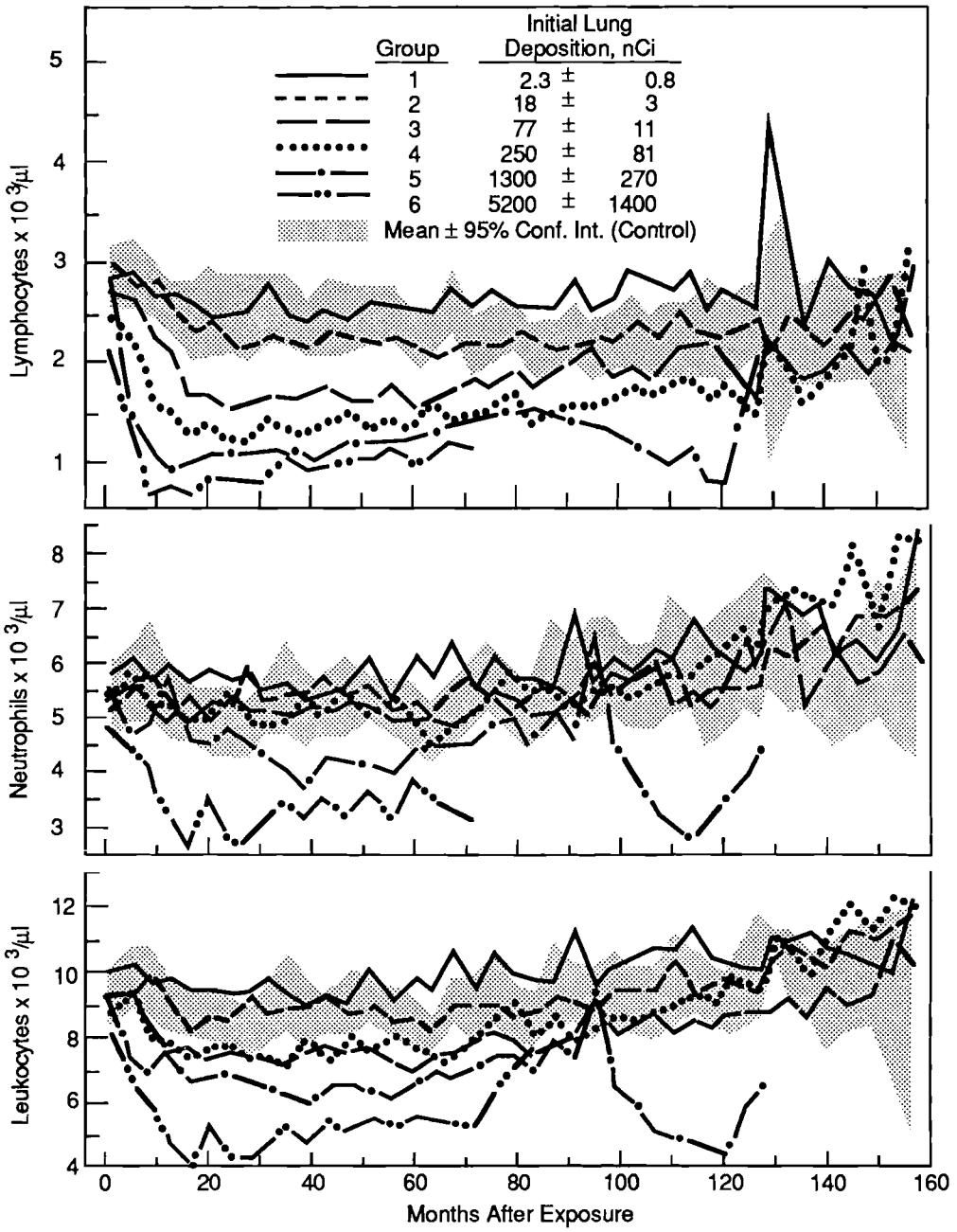

FIGURE 2. Mean Leukocyte, Neutrophil, and Lymphocyte Values in Dogs After Inhalation of $^{238}PuO_2$

translocation to the liver. Determination of gamma glutanyl transpeptidase concentrations and sulfobromophthalien sodium retention confirmed the presence of hepatic injury without functional impairment in dogs with chronically elevated GPT values. Alkaline phosphatase elevations occurred in some dogs with primary bone tumors and in others in which the increase was attributable to the liver (by heat inactivation of ALP) as the source of the largest portion of the ALP.

Cumulative radiation doses to death were estimated for the lungs of the ^{239}Pu dogs and the lungs and skeletons of the ^{238}Pu dogs (Table 5).

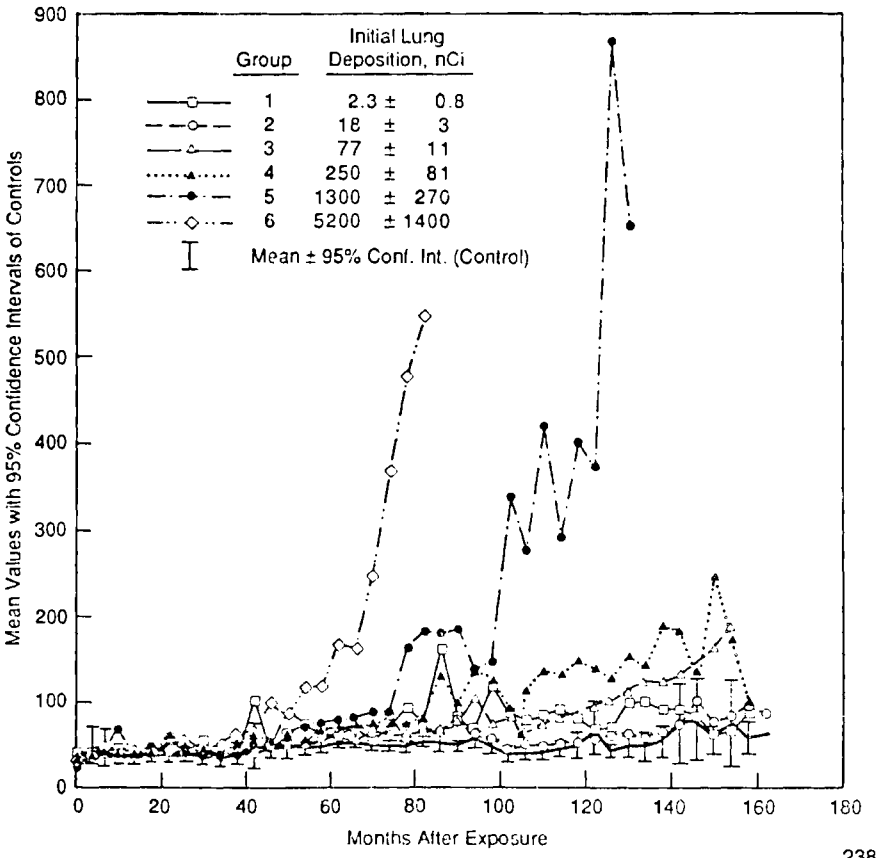

FIGURE 3. Serum Glutamic Pyruvic Transaminase Values (μ/L) in Dogs After Inhalation of $^{238}PuO_2$

TABLE 5. Estimates of Cumulative Radiation Doses to Lungs (^{239}Pu-Exposed) or Lungs and Skeletons (^{238}Pu-Exposed) of Dogs with Lung and/or Bone Tumors After Inhalation Exposure

	Dose-Level Group	Number of Dogs with Tumors	Survival Time Post Exposure, months	Cumulative Dose to Organ, rad
$^{239}PuO_2$ - Lung Tumors	6	1	69	7400[a]
	5	20	37 - 115	1700 - 4000
	4	16	93 - 177	500 - 1500
	3	10	98 - 183	150 - 480
	2	4	166 - 191	30 - 120
	1	1	182	4
$^{238}PuO_2$ - Lung Tumors	6	9	49 - 84	2100 - 8900[a]
	5	5	70 - 110	1200 - 2600
	4	4	118 - 160	190 - 440
	3	2	134 - 171	70 - 100
	2	7	154 - 178	7 - 33
	1	1	159	2
$^{238}PuO_2$ - Bone Tumors	6	9	49 - 84	170 - 470[b]
	5	16	61 - 132	80 - 230
	4	7	118 - 143	40 - 110
	3	0	0	---
	2	0	0	---
	1	1	99	<1

(a) Dose to lungs.
(b) Dose to skeleton.

For the dose calculations, mean plutonium concentration in the entire lung and skeleton was used. Exponential growth constants for 43 primary lung tumors were calculated in 30 dogs using sequential thoracic radiographs. The purpose was to determine if the time of tumor onset could be extrapolated from the growth constant and used to refine dose calculation. A wide range of doubling times (6-287 days) was observed. The exponential growth constants were not significantly dependent on tumor type, sex, age at time of diagnosis, initial lung deposition, or isotope. Extrapolations of time to tumor onset showed wide variation, indicating that such calculations cannot be used to reliably predict the onset of malignant growth in most cases.

A goal of this research is to increase understanding of health risk resulting from exposure to inhaled plutonium, with particular attention to lung cancer risks. Although no adequate data are available in humans exposed to plutonium for predicting lung cancer risk, data on humans exposed to other forms of irradiation are available, and include, for example, the Japanese atomic bomb survivor data and data from several studies of miners exposed to radon and radon progeny. In choosing methods for analyzing the data from these dogs, an important consideration is that results be in a form that can be readily compared with results of analyses of relevant human epidemiology data.

Analyses of human epidemiological data have generally modeled the hazard, or age-specific risk, as a function of dose and other factors. The model that has been most commonly used is a relative risk regression model in which hazard is a linear-quadratic function of risk and in which the baseline risks have been handled nonparametrically by introducing separate coefficients for each age group or, more generally, for each stratum. For analyses of the dog data, we used a similar model but substituted a Weibull function for separate baseline coefficients. This substitution was made primarily because baseline risk in dogs is more uncertain than in humans; thus, it is often desirable to present risk in absolute rather than relative terms as allowed by the Weibull model:

$$h(a, Da) = (\alpha + 1)\, a^{\alpha}(\Theta + \beta_1 D_a + \beta_2 D_a^{2})$$

where a is age, D_a is cumulative lung dose at age a, Θ is the baseline risk, and h is the hazard, or age-specific risk. In addition to continuous linear-quadratic functions, separate coefficients were fitted for each of five dose groups (<10, 10-50, 50-100, 100-2000, and >2000 rad).

The data were well fitted by a pure quadratic model with different coefficients for $^{239}PuO_2$ and $^{238}PuO_2$. Figure 4 shows both the fitted pure quadratic functions and the separate coefficients by dose group. Linear models were strongly rejected, and a linear-quadratic function did not improve the fit over a pure quadratic one. The risk resulting from a given cumulative dose from $^{239}PuO_2$ was significantly higher ($p < 0.001$) than from a similar dose from $^{238}PuO_2$. The extrapolated lifetime risk at 1 rad was estimated to be 7 per 10^6 for $^{239}PuO_2$ and 1 per 10^6 for $^{238}PuO_2$. For comparison, the lifetime risk at 1 rad for uranium miners in BEIR IV was 700 per 10^6. It is important to note that radiation dose estimates used for these analyses were based on current estimates of ILB and clearance rates, which require further analyses.

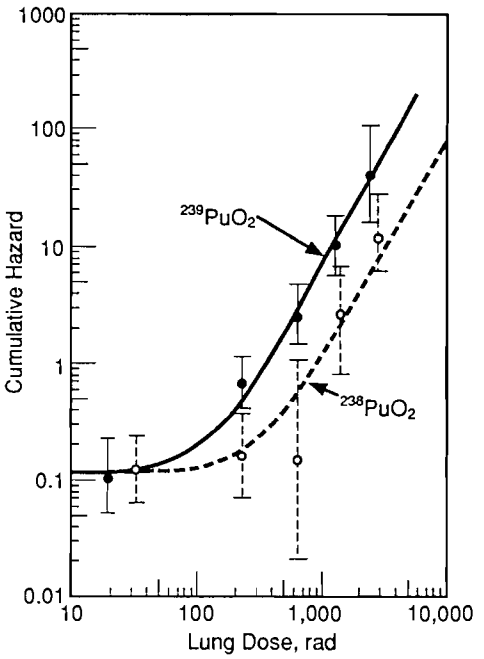

FIGURE 4. Lung Cancer Risk (Mean ± 95% Confidence Interval) for Inhaled Plutonium and Fitted Pure Quadratic Dose-Response Functions

Inhaled Plutonium Nitrate in Dogs

Principal Investigator: *G. E. Dagle*

Other Investigators: *R. R. Adee, R. L. Buschbom, K. M. Gideon, E. S. Gilbert, G. J. Powers, H. A. Ragan, C. O. Romsos, C. R. Watson, R. E. Weller, and E. L. Wierman*

Technical Assistance: *J. P. Bramson, K. H. Debban, R. F. Flores, B. B. Kimsey, B. G. Moore, D. L. Redetzke, R. P. Schumacher, and M. J. Steele*

The major objective of this project is to determine dose-effect relationships of inhaled plutonium nitrate in dogs to aid in predicting health effects of accidental exposure in man. For life-span dose-effect studies, beagle dogs were given a single inhalation exposure to $^{239}Pu(NO_3)_4$ in 1976 and 1977. The skeleton is generally considered the critical tissue with inhaled soluble plutonium that translocates to bone surfaces. Thus far, 13 years after exposure, 28 of 77 exposed dogs had bone tumors, 30 had lung tumors, and 7 had intrahepatic bile duct tumors.

The skeleton is generally considered the critical tissue after inhalation of "soluble" plutonium (e.g., plutonium nitrate), on the assumption that the plutonium will be rapidly translocated from the respiratory system to the skeleton. In several rodent studies, however, inhalation of "soluble" plutonium has resulted primarily in lung tumors. Skeletal tumors were seen less often, perhaps because they were not expressed within the short life span of the rodents. Therefore, beagle dogs were chosen for this study to compare relative risks with those from intravenously injected radionuclides in beagles at the University of Utah, inhalation studies with beta-, gamma-, and alpha-emitting radionuclides at the Inhalation Toxicology Research Institute (Lovelace), and external irradiation at the University of California (Davis) and at Argonne National Laboratory. More specifically, this study can be compared with inhaled $^{239}PuO_2$ and $^{238}PuO_2$ studies in beagle dogs at PNL (see *Inhaled Plutonium Oxide in Dogs*, this volume).

Six dose groups (105 dogs) were exposed, in 1976 and 1977, to aerosols of $^{239}Pu(NO_3)_4$ for life-span observations (Table 1). In addition, 20 dogs were exposed to nitric acid aerosols as vehicle controls; 25 dogs were exposed to aerosols of $^{239}Pu(NO_3)_4$ for periodic sacrifice to obtain plutonium distribution and pathogenesis data in developing lesions; 7 dogs were selected as controls for periodic sacrifice; and 20 dogs were selected as untreated controls for life-span observations. The Appendix (at the end of this volume of the *Annual Report*) shows the current status of each dog on these experiments.

TABLE 1. Life-Span Dose-Effect Studies with Inhaled $^{239}Pu(NO_3)_4$ in Beagles[a]

Dose-Level Group	Number of Dogs		Initial Lung Deposition[b]	
	Male	Female	nCi[c]	nCi/g Lung[c]
Control	10	10	0	0
Vehicle	10	10	0	0
1	10	10	2±2	0.02±0.02
2	10	10	8±4	0.06±0.04
3	10	10	56±17	0.5±0.2
4	10	10	295±67	2±0.8
5	10	10	1709±639	14±6
6	3	2	5445±1841	47±17

(a) Exposed in 1976 and 1977.
(b) Estimated from external thoracic counts at 2 weeks post exposure and estimated lung weights (0.011 x body weight).
(c) Mean ± standard deviation.

The average amount of plutonium in the lungs decreased to approximately 1% of the final body burden in dogs surviving 5 years or more (Table 2).

More than 90% of the burden translocated to the liver and skeleton; only about 1% translocated to thoracic and abdominal lymph nodes. This was in contrast to dogs that inhaled $^{239}PuO_2$; in these dogs, ~50% of the final body burden was present in thoracic lymph nodes, but only about 2% in the skeleton at 10 to 11 years after exposure.

The earliest observed biological effect was on the hematopoietic system: lymphopenia occurred at the two highest dose levels at 4 weeks after exposure to $^{239}Pu(NO_3)_4$. Total leukocyte concentrations were reduced significantly in the two highest dose groups, that is, Group 5 (mean initial alveolar deposition, ~1700 nCi) and Group 6 (~5500 nCi).

The reduction in white cells in Groups 5 and 6 resulted from an effect on most leukocyte types (neutrophils, lymphocytes, monocytes, and eosinophils). This is in contrast to the effects of both $^{239}PuO_2$ and $^{238}PuO_2$, which significantly depressed lymphocyte concentrations in groups with initial lung burdens of approximately 80 nCi or more. The lymphopenia at lower dose levels of plutonium oxides may be related to the more extensive translocation of plutonium oxide to the tracheobronchial lymph nodes and subsequent higher dosage levels to lymphocytes circulating through those lymph nodes. The results of these continuing evaluations are shown in Figure 1.

Serum enzyme assays have been performed throughout the postexposure period in an attempt to identify specific damage to liver or bone by plutonium translocated from the lung. Evaluation of these data has revealed a biphasic elevation of serum alkaline phosphatase (ALP) and serum glutamic pyruvic transaminase (GPT) in individual dogs. There was an early increase followed by a return to control values and then a late effect characterized by persistent, increased elevations of both ALP and GPT. Calculation of the cumulative average radiation dose to mean time after exposure, when serum chemistry values were first observed to be different from controls for dose-level Group 5 dogs, revealed a mean dose to liver of 280 rad for the late effect, which occurred 4.1 years post exposure. At this time, the dose rate was 60 to 70 rads per year. GPT and ALP values in dose-level Groups 3 and 4 were significantly higher ($p \leq 0.05$) than those for the control group (Figures 2 and 3).

Table 3 summarizes, by dose-level group, the mortality and lesions associated with deaths through 13 years after exposure to $^{239}Pu(NO_3)_4$. All five dogs at the highest dose level (Group 6) died from radiation pneumonitis 14 to 41 months after exposure. Histopathological examination of the lungs of these dogs revealed interstitial fibrosis, alveolar epithelial hyperplasia, increased numbers of alveolar macrophages, occasional small emphysematous cavities and, at times, very small nodules of squamous metaplasia at the termini of respiratory bronchioles. One dog at the highest dose level had a small bronchioloalveolar carcinoma as well as radiation pneumonitis.

All the dogs in dose-level Group 5 died or were euthanized 34 to 92 months after plutonium exposures. The principal cause of death at this exposure level was osteosarcoma, which occurred in 17 of 20 dogs; several had more than one site. The sites of the osteosarcomas were lumbar vertebrae (4 dogs), cervical vertebrae (3 dogs), thoracic vertebrae (2 dogs), humerus (5 dogs), pelvis (2 dogs), facial bones (2 dogs), ribs (2 dogs), and nasal turbinates (1 dog). Metastases to distal sites occurred in 6 dogs; these dogs also had radiation osteosis, generally characterized by peritrabecular fibrosis.

Other deaths in dose-level Group 5 were caused by radiation pneumonitis (two dogs) and multiple lung tumors (one dog). The multiple lung tumors, in different lobes, were papillary adenocarcinomas, combined epidermoid and adenocarcinoma, and bronchioloalveolar carcinoma; metastases were present in the tracheobronchial lymph nodes.

Malignant but nonfatal lung tumors were also present in nine dogs from dose-level Group 5 that died from osteosarcomas and in one dog that died from radiation pneumonitis. Typically, these arose subpleurally, proximal to areas of interstitial fibrosis or small cavities communicating with bronchioles. They consisted of bronchioloalveolar carcinomas

TABLE 2. Tissue Distribution of Plutonium in Beagles After Inhalation of $^{239}Pu(NO_3)_4$

Dog Number	Time After Exposure, months[a]	Final Body Burden, μCi	Percent of Final Body Burden					Cause of Death
			Lungs	Thoracic Lymph Nodes[b]	Abdominal Lymph Nodes[c]	Liver	Skeleton	
1359M	0.1	0.080	90.50	0.15	0.06	2.46	3.20	Sacrifice
1375F	0.1	0.073	89.61	0.14	0.01	0.97	4.68	Sacrifice
1407F	0.1	0.092	51.87	0.41	0.13	10.99	18.70	Sacrifice
1389M	0.5	0.053	24.07	0.38	0.08	41.28	26.21	Sacrifice
1390M	0.5	0.051	24.62	0.32	0.11	20.05	44.45	Sacrifice
1445F	0.5	0.057	26.42	0.32	0.11	21.28	44.73	Sacrifice
1329F	1	0.485	70.05	0.16	0.04	8.28	18.79	Sacrifice
1346M	1	0.902	76.81	0.32	0.03	10.45	10.30	Sacrifice
1347F	1	0.699	71.71	0.36	0.08	9.33	14.09	Sacrifice
1336M	1	0.032	71.38	0.22	0.05	5.72	19.73	Sacrifice
1341F	1	0.022	64.43	0.29	0.10	12.92	18.63	Sacrifice
1344F	1	0.052	58.68	0.25	0.04	21.87	16.09	Sacrifice
1335M	1	0.003	19.52	0.07	0.06	6.68	25.04	Sacrifice
1339F	1	0.001	19.08	0.13	0.08	20.92	45.47	Sacrifice
1351M	1	0.002	40.68	1.22	0.09	17.09	28.89	Sacrifice
1522F	3	0.059	54.68	0.57	0.10	11.52	28.24	Sacrifice
1529F	3	0.049	51.68	0.40	0.07	18.48	23.74	Sacrifice
1539M	3	0.072	52.45	0.31	0.05	18.58	25.03	Sacrifice
1564F	12	0.037	18.00	1.27	0.11	33.53	42.63	Sacrifice
1571F	12	0.053	22.37	1.47	0.11	28.76	42.91	Sacrifice
1588M	12	0.053	13.14	0.40	0.12	35.85	46.18	Sacrifice
1424M	14	4.625	33.10	1.43	0.16	26.49	36.88	Radiation pneumonitis
1517F	16	4.025	18.99	0.94	0.18	29.51	47.88	Radiation pneumonitis
1510F	17	4.048	22.00	1.15	0.05	20.71	52.00	Radiation pneumonitis
1420M	25	1.616	16.51	0.86	0.20	7.77	70.06	Radiation pneumonitis
1471M	34	1.375	9.25	0.73	0.12	26.92	58.34	Radiation pneumonitis
1518M	42	1.880	6.87	0.24	0.07	21.34	67.51	Radiation pneumonitis, lung tumor
1512M	42	2.136	4.31	0.60	0.08	49.93	42.66	Bone tumor
1508M	43	1.730	3.24	0.62	0.08	41.53	52.70	Bone tumor
1459F	51	1.567	4.40	0.15	0.12	30.86	61.41	Radiation pneumonitis, lung tumor
1492F	52	1.202	2.81	0.20	0.17	27.02	66.38	Bone tumor
1485F	54	1.052	0.82	0.35	0.07	31.13	63.94	Bone tumor
1502F	55	3.113	0.80	0.39	0.09	33.33	62.51	Bone tumor, lung tumor
1387F	55	0.167	1.41	0.22	0.12	45.48	49.10	Bone tumor
1429M	59	1.159	4.14	0.35	0.10	37.06	54.70	Bone tumor, lung tumor
1598F	60	0.058	0.90	0.14	0.17	24.44	31.62	Sacrifice
1576M	60	0.065	1.54	0.36	0.13	46.23	39.15	Sacrifice
1605F	60	0.025	1.87	0.11	0.12	52.32	39.37	Sacrifice
1646F	60	0.806	0.72	0.20	0.40	46.92	48.42	Bone tumor
1619F	62	1.361	0.55	0.59	0.13	37.87	58.63	Bone tumor
1589F	63	0.029	0.68	0.04	0.13	46.43	50.32	Sacrifice
1636M	66	0.634	1.21	0.27	0.52	53.97	39.09	Bone tumor
1652F	68	0.658	1.46	0.23	0.29	50.47	44.32	Bone tumor, lung tumor
1498F	69	0.845	0.59	0.32	0.13	26.63	53.37	Bone tumor, lung tumor
1659F	69	0.736	1.14	0.34	0.40	38.90	55.89	Bone tumor
1640M	76	0.177	4.01	0.64	0.63	54.41	36.59	Lung tumor
1419M	76	0.873	0.69	0.28	0.39	44.06	50.70	Bone tumor, lung tumor
1660M	82	0.854	0.76	0.53	0.53	37.51	56.17	Bone tumor, lung tumor
1621M	84	0.840	0.94	0.56	0.29	40.87	54.55	Bone tumor, lung tumor
1655M	88	0.505	1.05	0.22	0.93	41.83	52.14	Lung tumor, Bone tumor
1501M	92	0.002	1.62	0.50	0.79	38.05	48.41	Thyroid tumor
1648M	92	0.639	1.12	0.25	0.73	42.83	50.61	Bone tumor, lung tumor
1641M	92	0.869	0.78	0.24	0.48	45.72	48.89	Lung tumor

TABLE 2. Continued

Dog Number	Time After Exposure, months[a]	Final Body Burden, μCi	Percent of Final Body Burden					Cause of Death
			Lungs	Thoracic Lymph Nodes[b]	Abdominal Lymph Nodes[c]	Liver	Skeleton	
1408F	93	0.181	0.60	0.19	0.37	49.47	45.52	Bone tumor
1404M	93	0.217	0.82	0.28	0.72	46.24	48.62	Pleuritis
1470F	95	0.001	1.11	0.48	0.34	43.21	50.23	Meningioma
1489F	98	0.002	1.23	0.73	0.70	41.36	48.52	Esophageal tumor
1565F	101	0.001	0.77	1.55	0.87	43.62	44.09	Hemangiosarcoma
1385M	101	0.362	0.62	0.51	0.42	46.38	49.36	Bone tumor, lung tumor
1364M	102	0.370	1.13	0.32	0.40	49.46	46.17	Lung tumor
1503F	103	0.007	0.37	0.64	0.25	60.15	35.37	Thyroid tumor
1645F	105	0.182	0.73	0.41	0.46	55.96	40.70	Lung tumor
1587M	106	0.027	0.65	0.74	0.51	20.11	74.97	Hemangiosarcoma, lung tumor
1534M	106	0.201	0.96	0.43	0.49	50.78	43.95	Congestive heart failure
1521F	106	0.146	0.88	0.34	0.36	51.77	44.41	Bone tumor, lung tumor
1599F	106	0.007	0.69	0.54	0.48	34.04	60.60	Adrenal tumor
1413F	109	0.026	1.16	0.39	0.51	58.06	37.78	Malignant lymphoma
1391M	111	0.004	1.21	0.34	0.47	50.40	45.49	Thyroid tumor, lung tumor
1581M	111	0.002	0.52	0.95	0.31	38.21	56.46	Hemangiosarcoma
1602M	111	0.006	1.95	1.29	0.97	42.80	46.45	Epilepsy
1428F	114	0.230	0.72	0.62	0.56	35.16	60.14	Bone tumor, lung tumor
1386M	116	0.028	1.59	0.26	0.82	56.40	38.62	Hemangiosarcoma
1568M	116	0.034	0.93	0.50	0.54	42.27	52.10	Pneumonia
1590F	119	0.003	0.48	0.35	1.00	59.61	31.23	Mammary tumor
1530F	122	0.017	0.89	0.77	0.84	42.50	50.30	Bone tumor, lung tumor
1570F	122	0.001	0.34	0.91	0.42	30.80	63.13	Stomach tumor
1535F	122	0.145	0.62	0.67	0.74	19.27	73.73	Bone tumor, lung tumor
1446F	123	0.165	0.40	0.56	0.63	27.06	67.94	Pyometra, liver tumor
1540M	124	0.037	0.61	0.45	0.38	39.21	55.37	Lung tumor
1414F	126	0.121	1.29	0.42	0.54	44.44	49.50	Bone, lung, and liver tumors
1569F	126	0.031	0.53	0.42	0.31	50.23	45.17	Lung tumor
1575M	128	0.004	0.43	0.54	0.51	55.53	37.17	Prostate tumor
1456F	132	0.041	0.33	0.60	0.49	41.34	52.74	Pneumonia
1637M	132	0.105	1.22	0.64	0.31	45.50	49.64	Lung tumor
1607M	135	0.001	0.53	1.80	0.44	37.49	55.95	Liver tumor
1363M	135	0.046	0.51	0.69	0.44	55.62	40.23	Pneumonia, adrenal/liver tumor
1582F	136	0.034	0.64	0.69	4.82	31.22	57.87	Mammary tumor, liver tumor
1380M	136	0.041	0.57	0.70	0.82	34.11	58.90	Pneumonia
1618F	140	0.134	0.38	0.23	1.05	38.34	56.67	Bone tumor
1439F	143	0.033	0.41	0.69	0.75	25.65	68.09	Malignant lymphoma
1379M	144	0.202	0.56	0.72	0.85	25.30	67.38	Liver, lung, and bone tumors

(a) Radioanalysis not completed in dogs that died more than 144 months after exposure.
(b) Includes tracheobronchial, mediastinal, and sternal lymph nodes.
(c) Includes hepatic, splenic, and mesenteric lymph nodes.

in four dogs; papillary adenocarcinomas in two dogs; both bronchioloalveolar carcinoma and papillary adenocarcinoma in one dog; both papillary and tubular adenocarcinomas in one dog; a combined epidermoid and adenocarcinoma in one dog; and a bronchioloalveolar carcinoma, a papillary adenocarcinoma, and a mixed lung tumor in one dog. No metastases of these lung tumors were observed.

In dose-level Group 4, 19 dogs have now died, 54 to 156 months after plutonium exposure. The causes of death, probably related to plutonium exposure, included bone tumors (9 dogs), lung tumors (5 dogs), a delayed-onset radiation pneumonitis (1 dog), and a bile duct carcinoma (1 dog). Intrahepatic bile duct tumors were present in the livers of 4 additional dogs that died of other causes. Nonfatal lung tumors were present in

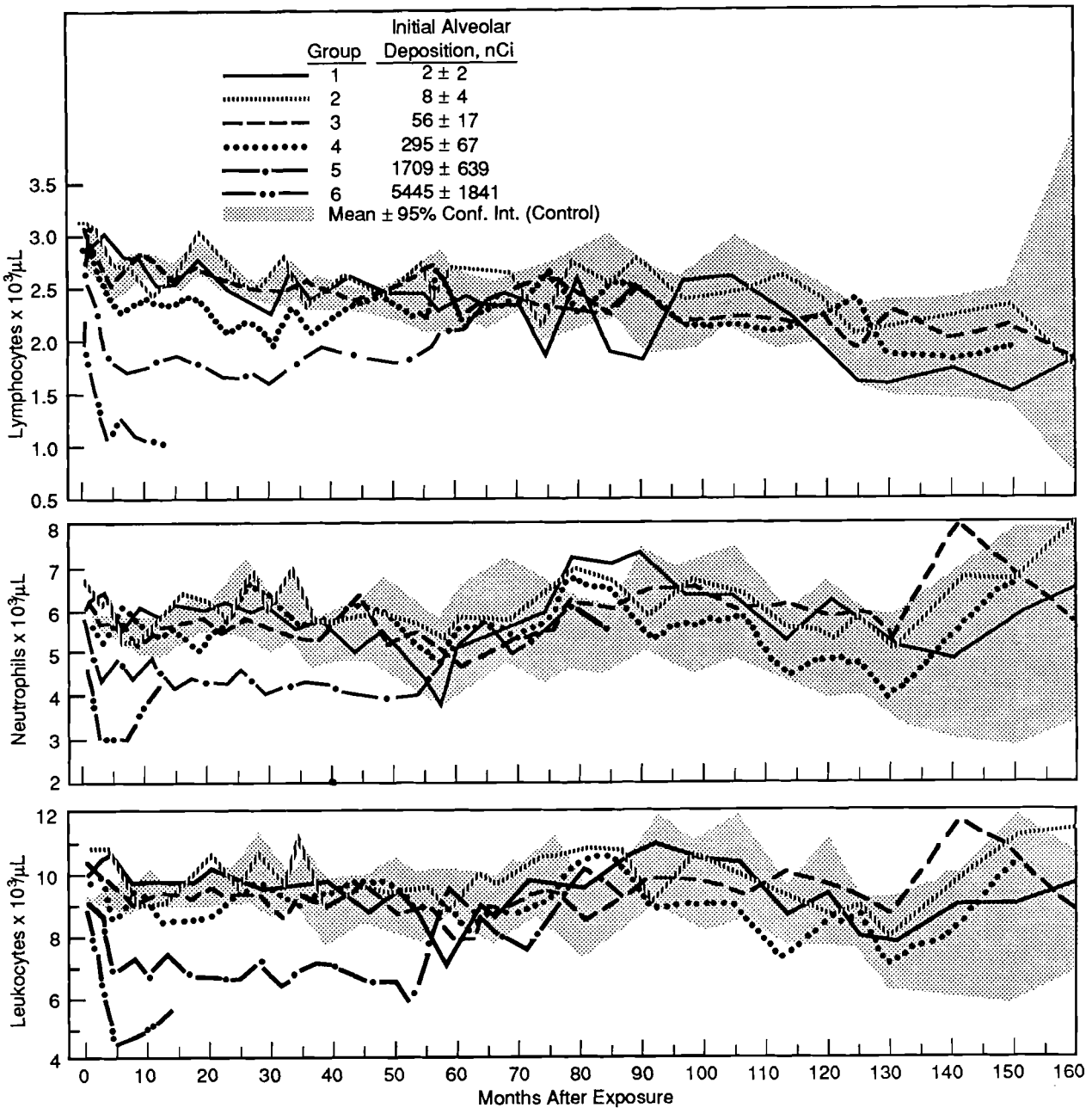

FIGURE 1. Mean Leukocyte, Neutrophil, and Lymphocyte Values in Dogs After Inhalation of $^{239}Pu(NO_3)_4$

8 dogs that died of other causes. Suppurative pleuritis, pyometra, and congestive heart failure occurred, respectively, in 3 dogs and were considered not related to plutonium exposure.

In dose-level Group 3, two dogs have died of lung tumors. Lung tumors were present in each of three dogs that died of a bone tumor, a thyroid tumor, and a hemangiosarcoma. Two additional dogs had bile duct tumors. This is the lowest exposure level with a mortality rate or incidence of lesions significantly different from that of control groups; a hepatocellular carcinoma, of uncertain relationship to plutonium exposure, occurred in one dog from dose-level Group 1.

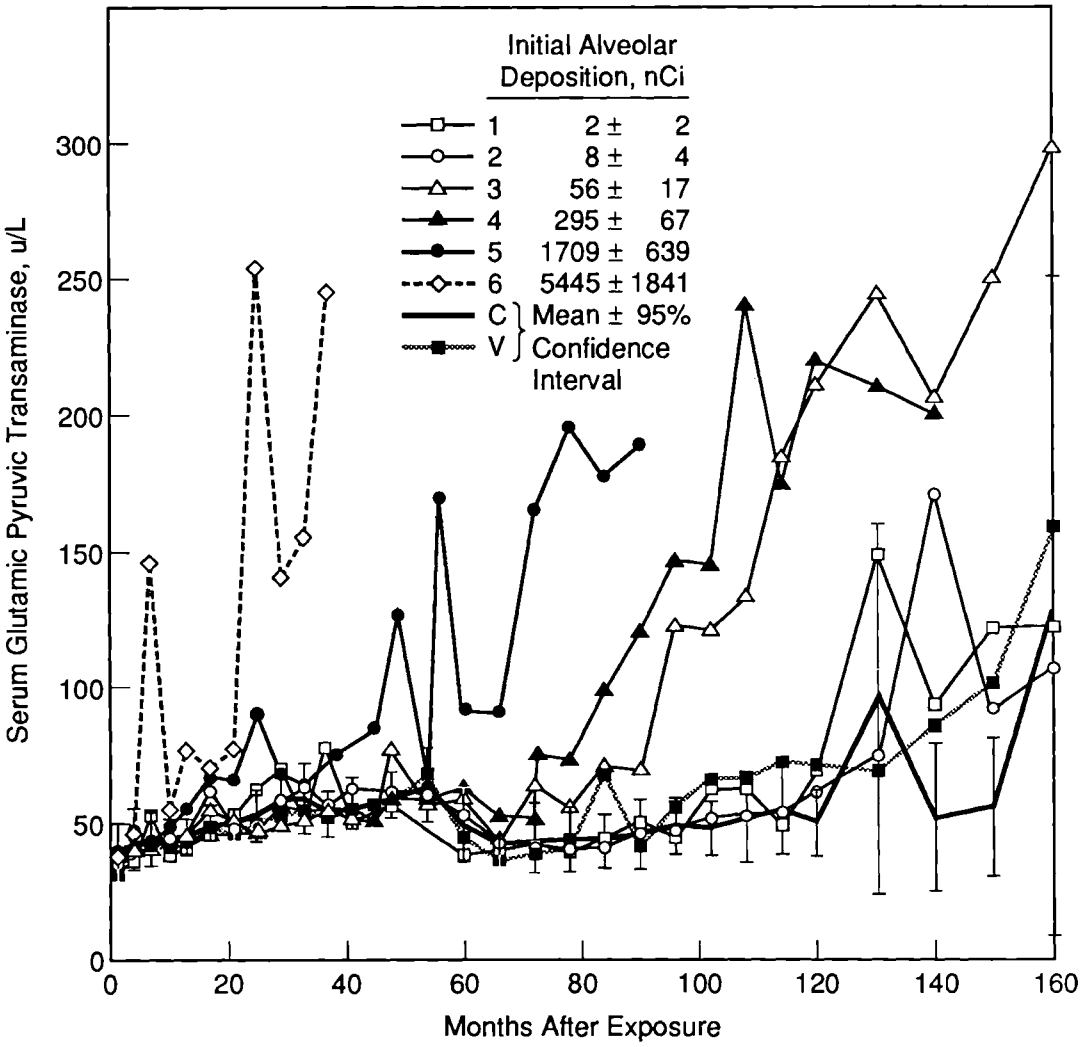

FIGURE 2. Serum Glutamic Pyruvic Transaminase (GPT) in Dogs After Inhalation of $^{239}Pu(NO_3)_4$

Although the skeleton is generally considered the critical tissue after inhalation of soluble plutonium, and 28 of 77 exposed dogs have died with bone tumors by 13 years after exposure, it should be noted that 30 of these 77 exposed dogs also had lung tumors. We have calculated that lung cancer risks for these dogs, based on estimated cumulative dose to the lung, are approximately 12 times higher for $^{239}Pu(NO_3)_4$ than for inhaled $^{239}PuO_2$ and 50 times higher than for inhaled $^{238}PuO_2$. Further, intrahepatic bile duct tumors have now occurred in 7 dogs.

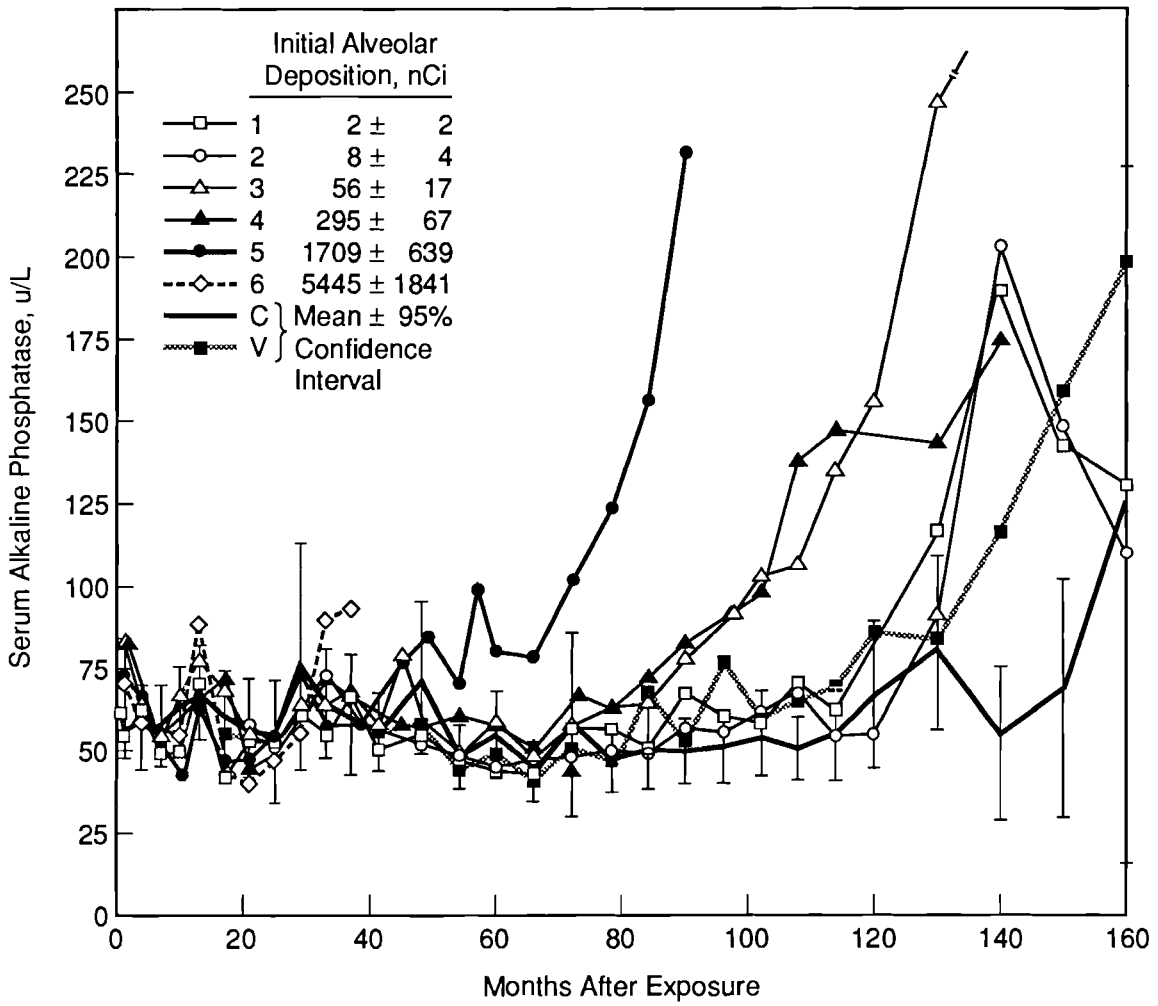

FIGURE 3. Serum Alkaline Phosphatase (ALP) in Dogs After Inhalation of $^{239}Pu(NO_3)_4$

TABLE 3. Lesions in Beagle Dogs 13 Years After Inhalation of $^{239}Pu(NO_3)_4$

	Dose Group							
	6	5	4	3	2	1	Vehicle	Control
Number of Dogs/Group	5	20	20	20	20	20	20	20
Number of Dead Dogs/Group	5	20	19	14	8	11	11	13
Condition[(a)]								
Radiation pneumonitis	4	1						
Radiation pneumonitis and lung tumor	1	1	1					
Bone tumor		8	3					
Bone and lung tumor		9	4	1				
Bone, lung, and liver tumor			2					
Lung tumor		1	4	2				
Liver, lung, and bone tumor			1					
Lung and liver tumor			1					
Hemangiosarcoma and lung tumor				1				
Thyroid and lung tumor				1				
Pyometra and liver tumor			1					
Pneumonia, adrenal and liver tumor				1				
Mammary and liver tumor				1				
Liver tumor						1		
Pneumonia or pleuritis			1	3		1		3
Lymphoma				2	1		4	
Thyroid tumor					2	2		2
Meningeal tumor						1		
Status epilepticus					1			1
Congestive heart failure			1					
Hemangiosarcoma				1		2		
Adrenal tumor					1			1
Esophageal/stomach tumor						2		
Intervertebral disc protrusion							2	1
Mammary tumor					2		1	
Cerebral hemorrhage								1
Prostate tumor					1			1
Pyometra								1
Mastocytoma							1	
Splenic tumor								1
Endocarditis								1
Nephropathy				1		1	2	
Malignant melanoma						1	1	

(a) Number of dogs with lesions associated with death.

National Radiobiology Archives

Principal Investigator: *C. R. Watson*

Other Investigators: *M. T. Karagianes, S. K. Smith, L. M. Lindgren, J. C. Prather, D. N. Rommereim, L. G. Smith, and R. C. Thompson*

The National Radiobiology Archives is a comprehensive effort to gather, organize, and catalog data, tissues, and documents related to radiobiology studies. This will provide future researchers with materials for analysis by advanced molecular biology techniques and with information for statistical analysis to compare results of these and other studies. The project concentrated initially on three tasks associated with studies of beagle dogs exposed to ionizing radiation at five DOE laboratories: (1) implementing an interlaboratory computerized **information system** containing a summarized dose-and-effects database with results for each of more than 5000 life-span-observation dogs, a collection inventory database, and a bibliographic database; (2) establishing a **document archives** of research materials such as logbooks, clinical notes, radiographic films, and pathologists' observations; and (3) establishing a **specimen archives** for research materials such as biopsy and necropsy tissue samples or histopathology blocks and slides. The databases were designed and have been populated with records from three laboratories. Tissue specimens and histopathology blocks from more than 1000 dogs have been received from the University of California at Davis. A collaborative effort was initiated for the analysis of ^{137}Cs studies with Argonne National Laboratory and the Inhalation Toxicology Research Institute.

Since the initiation of the Manhattan project, many investigations have been conducted into the biological effects of ionizing radiation. The focus of these studies has been on understanding the degree of risk and the nature of human health effects. When the acute effects of relatively large doses had been characterized, attention shifted to the relationship between low doses and cancer. This led to initiation of life-span studies of experimental animals in several DOE-supported laboratories. As these studies are completed, the National Radiobiology Archives (NRA) provides integration and preservation of this unique body of information and materials and encourages and facilitates its continued use.

Beagle Studies

Nearly 40 years ago, the U.S. Atomic Energy Commission made a far-reaching commitment to conduct life-span radiation effect studies in a relatively long-lived animal, the beagle dog, at five laboratories. As a consequence, a group of closely related experiments are now coming to fruition. These life-span studies, conducted at the University of Utah (U of Utah), the University of California at Davis (UC Davis), Argonne National Laboratory (ANL), Pacific Northwest Laboratory (PNL), and the Inhalation Toxicology Research Institute (ITRI), are the initial focus of Archives activities. These experiments are listed in Table 1, showing the NRA study code, the time period over which the exposures were conducted, the nature of the exposures, and the number of dogs held for life-span observation.

Three tasks are associated with integrating and preserving information from these studies. The computerized **information system** provides electronic access to summary data on each dog, the document and specimen collection catalogs, and bibliographic citations; the **document archives** houses and preserves nonbiological materials; and the **specimen archives** houses and preserves biological materials. This year, we report significant progress toward implementing the databases and establishing the specimen archives. Procedures were developed for cataloging the written materials in the document archives. Documents will be shipped to the NRA as studies are completed; this year, the documents were still in active use in the laboratories.

TABLE 1. Major Life-Span Studies Being Incorporated into the National Radiobiology Archives

NRA Study ID	Date of Exposures	Type of Exposure	Exposure Mode	Number of Life-Span Dogs
U-01[(a)]	1952-1974	^{239}Pu	IV injection	285
U-02	1953-1970	^{226}Ra	IV injection	164
U-03	1954-1963	^{228}Ra	IV injection	89
U-04	1954-1963	^{228}Th	IV injection	94
U-05	1955-1966	^{90}Sr	IV injection	99
U-06	1966-1975	^{241}Am	IV injection	117
U-07	1971-1974	^{249}Cf	IV injection	36
U-08	1971-1973	^{252}Cf	IV injection	35
U-09	1972-1978	^{239}Pu	IV injection (juvenile)	75
U-10	1973	^{253}Es	IV injection	5
U-11	1975-1978	^{239}Pu	IV injection (aged)	34
U-12	1975-1978	^{226}Ra	IV injection (juvenile)	53
U-13	1975-1980	^{226}Ra	IV injection (aged)	33
U-14	1977-1979	^{224}Ra	IV injection (multiple)	128
D-01	1952-1958	X ray	Whole body (fractionated)	360
D-02	1961-1969	^{90}Sr	Ingested (in utero to 540 days)	483
D-03	1964-1969	^{90}Sr	IV injection	45
D-04	1964-1969	^{226}Ra	IV injection (multiple)	335
A-01	1956	^{90}Sr	Transplacental	53
A-02	1957	^{90}Sr	SC injection (multiple, various ages)	98
A-03	1960-1964	^{144}Ce	IV injection	49
A-04	1961-1963	^{137}Cs	IV injection	65
A-05	1968-1978	Gamma ray	Whole body (continuous to death)	311
A-06	1968-1977	Gamma ray	WB (continuous to predetermined dose)	343
P-01	1959-1962	$^{239}PuO_2$	Inhalation	35
P-02	1967	$^{238}PuO_2$	Inhalation	22
P-03	1970-1972	$^{239}PuO_2$	Inhalation	136
P-04	1972-1975	$^{238}PuO_2$	Inhalation	136
P-05	1975-1977	$^{239}Pu(NO_3)_4$	Inhalation	148
I-01	1965-1967	$^{90}SrCl_2$	Inhalation	63
I-02	1966-1967	$^{144}CeCl_3$	Inhalation	70
I-03	1966-1967	$^{91}YCl_3$	Inhalation	54
I-04	1967-1971	^{144}Ce (FAP)[(b)]	Inhalation	126
I-05	1968-1969	$^{137}CsCl$	IV injection	66
I-06	1969-1971	^{90}Y (FAP)	Inhalation	101
I-07	1970-1971	^{91}Y (FAP)	Inhalation	108
I-08	1970-1974	^{90}Sr (FAP)	Inhalation	124
I-09	1972-1976	^{144}Ce (FAP)	Inhalation (juvenile)	54
I-10	1972-1975	^{144}Ce (FAP)	Inhalation (aged)	54
I-11	1972-1975	^{144}Ce (FAP)	Inhalation (multiple)	36
I-12	1973-1976	$^{238}PuO_2$	Inhalation (3.0 μm)	84
I-13	1974-1976	$^{238}PuO_2$	Inhalation (1.5 μm)	84
I-14	1977-1979	$^{239}PuO_2$	Inhalation (0.75 μm)	60
I-15	1977-1979	$^{239}PuO_2$	Inhalation (1.5 μm)	108
I-16	1977-1979	$^{239}PuO_2$	Inhalation (3.0 μm)	83
I-17	1977-1978	$^{239}PuO_2$	Inhalation (multiple, 0.75 μm)	72
I-18	1979-1983	$^{239}PuO_2$	Inhalation (juvenile, 1.5 μm)	108
I-19	1979-1982	$^{239}PuO_2$	Inhalation (aged, 1.5 μm)	60
Total:	1952-1983			5381

(a) Laboratory Codes: A, ANL; D, University of California at Davis; I, ITRI; P, PNL; U, University of Utah.
(b) FAP: radionuclide was adsorbed to an insoluble fused aluminosilicate vector aerosol.

Advisory Committee

The NRA is guided by an advisory committee (NRAAC) consisting of four external advisors:

Stephen A. Benjamin, Colorado State University: Dog Studies
J. A. Louis Dubeau, University of Southern California: Molecular Biology
Kenneth L. Jackson, University of Washington: Radiobiology
Philip R. Watson, Oregon State University: Databases

and eight participating advisors:

Bruce B. Boecker, Inhalation Toxicology Research Institute
Thomas E. Fritz, Argonne National Laboratory
Ronald L. Kathren, Hanford Environmental Health Foundation
Scott C. Miller, University of Utah
James F. Park, Pacific Northwest Laboratory
Otto G. Raabe, University of California at Davis
Robert G. Thomas, U.S. Department of Energy
Roy C. Thompson, Pacific Northwest Laboratory.

The NRAAC met in May 1990 to recommend policies and set priorities. An orderly process for nominating and determining materials to be included in the Archives on a study-by-study basis was established. The next advisory committee meeting will focus on the University of Utah studies. Future activities of the NRAAC include sponsorship of a workshop on current and future research uses of archived tissue specimens.

Information System

Computer database technology is essential to integrating this broad and diverse collection of information. The NRA is developing several interrelated databases, each of which follows the relational model. There are three major databases: the dose-effects summary, the collection inventory, and the bibliography. These systems are being developed on two hardware platforms, the DEC VAX configuration at ANL and the IBM PC systems at PNL. We are also using two database management software products, Oracle on the VAX and PC, and Paradox on the PC. We will evaluate these two approaches and select one within the next year.

The computerized summary database contains the dose to and the effect on each significant tissue in each dog. It has six major tables:

LAB	- describing each laboratory
STUDY	- describing each study (as shown in Table 1)
GROUP	- describing groups of animals within each study
ANIMAL	- summarizing each animal
TEFFECT	- effect (and diagnosis dates) observed in significant tissue category
TDOSE	- dose to each significant tissue category at diagnosis dates in TEFFECT.

The summary database also includes laboratory-specific supporting tables for information such as serial hematological determinations or clinical observations. Animals included in the database are classified as primary if they were included in the tables of life-span animals in the Appendix (pp. 126-221) of Roy C. Thompson's book, *Life-Span Effects of Ionizing Radiation in the Beagle Dog*. Incomplete records are also included for animals assigned to ancillary groups such as dosimetry, toxicology, special study, or breeding. Sufficient information is available for these ancillary animals to permit genealogical analysis of an entire colony. Progress toward populating the summary database is shown in Table 2.

The collection inventory database contains information about each of the bar code labels affixed to materials (or containers of materials) in the NRA collections. The database defines the materials and also tracks the location of items to allow rapid retrieval.

The bibliographic database uses the same bar code label system to identify reference materials. Location information about the materials is stored in the collection inventory database, while a complete bibliographic citation is stored in the bibliography system.

Document Archives

The research document archives collects the detailed research findings associated with each study. These include handwritten "raw" data such as exposure logbooks, clinical notes, laboratory

TABLE 2. Progress Toward Populating the Summary Database

NRA Study ID	Status of NRA Database Tables[a]						
	LAB	STUDY	GROUP	ANIMAL	TEFFECT	TDOSE	LAB SPECIFIC
U-01[b] to U-14	F	C	C	P			
D-01	F	C	C				
D-02, D-03, D-04	F	C	C	P			
A-01, A-02, A-03	F	C	C	P			
A-04	F	C	C	C	C		C
A-05, A-06	F	C	C	P			
P-01, P-02	F	C	C	P			
P-03, P-04, P-05	F	C	C	C			
I-01 to I-19	F	C	C				
Number of Records:							
Primary	5	48	364	1,609			
Total	5	58	417	12,917			

(a) Status Codes:
F, Final; database records are complete and reviewed by PI.
C, Complete; database records are complete, all significant fields have complete information.
P, Partial; database records are partially complete, some fields have no information.
(b) Laboratory Codes: U, University of Utah; D, University of California at Davis; A, ANL; P, PNL; I, ITRI.

analysis forms, hematological profiles, and animal care observations. A significant class of research document from these studies is photographic film - autoradiographs, radiographs, and photographs. "Summarized" data, usually reduced to computer files or publication reprints, are also included. Each document (or document container such as a folder) is given a bar-coded accession number label and stored in a controlled environment. This material is cataloged in the bibliographic database for rapid selection and retrieval.

The first contribution to the document archives is the extensive collection of supportive documentation that provided the basis for *Radioactivity and Health, A History*, by J. Newell Stannard. The initial portion of these documents was received and accessioned this year. The UC Davis clinical and radiographic records will be shipped to the Archives at the conclusion of their contract with DOE. Documents such as clinical records, radiographs, photographs, autoradiography preparations (as well as specimens such as organs, histology blocks, slides), at the U of Utah were accessioned in 1990; these materials will reside in Utah pending completion of the studies.

Specimen Archives

The biological specimen archives contains collected research materials such as tissues preserved in formalin or alcohol, tissue samples embedded in paraffin or plastic for histopathological analysis, microscope slides, and radiographic films. Many of these materials are radioactive and are associated with hazardous materials such as formalin, alcohol, or paraffin. An existing 1200-ft^2 cinder block building, 331-G, has been renovated as the repository of these specimens. It contains a specimen manipulation laboratory and storage bays with an automatic fire suppression system.

Materials nominated for inclusion in the document and/or specimen archives must be reviewed by the NRAAC. The first such review committee met at the UC Davis in December 1988 and recommended acceptance of materials related to three life-span, internal-emitter studies (shown in Table 1 as D-02, D-03, D-04). Specimens from a fourth study (D-01), involving external radiation, were deemed of insufficient scientific interest to warrant inclusion in the Archives. The first

contributions to the specimen archives were moved from UC Davis to PNL in 1990.

Supervision of the packing, shipment, receipt, and unpacking of the specimens was the major activity of the specimen archives task this year. Three types of material were shipped, including more than 2,600 plastic bags of biopsy and necropsy specimens associated with 1,024 animals, about 55,000 histopathology blocks and a few hundred slides, and 49 alcohol-filled, 1-gallon jars containing representative bones harvested from frozen skeletons.

Materials are nominated for donation to the Archives by an institution which recognizes that specific completed studies are worthy of consideration for inclusion in the Archives. The University of Utah is in the process of completing final analysis of several studies in which all the dogs are dead. In anticipation of moving selected materials to the NRA in the near future, we collaborated with the University of Utah staff to accession, characterize, and physically organize materials from these studies.

This year, 1457 bar-code-readable labels were affixed to storage containers at the University of Utah. Information about the location and contents of the containers is available in the NRA inventory database. These data will be used by the NRAAC in its deliberations about which University of Utah materials should be included in the Archives.

Progress toward establishment of the specimen archives is summarized as follows, with plans for the coming fiscal year in boldface type:

ANL — ^{137}Cs study (A-04) was accessioned in 1990. **^{137}Cs specimens will be loaned to ITRI in 1991, and the ^{144}Ce study (A-03) accessioning will be completed.**

UC Davis — Reviewed by NRAAC in 1988; three studies were selected. These were organized, harvested, and packed in 1989. Selected specimens from D-02, D-03, and D-04 were moved to PNL in 1990; presently in storage. **Specimens will be organized and accessioned at PNL in 1991.**

ITRI — No actions are planned until 1992.

PNL — **Specimens will be accessioned and organized for donation to NRA in 1991.**

U of Utah — Blocks, slides, radiographs, and clinical records were accessioned in 1990; 1457 bar-code-readable labels affixed to containers. **Accessioning of tissue specimens and review by NRAAC scheduled for 1991; specimens from selected studies may be shipped to NRA.**

Collaborations with Participating Laboratories

The cooperation of participating institutions and investigators is essential to achieve the goals of the NRA project. Collaboration has been excellent with the five institutions conducting life-span beagle studies. The NRA staff has been welcomed on several site visits, collaborative projects were initiated, and these laboratories' directors serve on the NRAAC.

This year, three NRA collaborations were active. NRA participated in the transfer of specimens from UC Davis by providing onsite supervision and accessioning of the packing as well as transportation to PNL; UC Davis completed specimen preparation and packing. NRA also participated in accessioning of specimens at the University of Utah. The NRA encourages analysis of studies that examine previous information from a new prospective by applying different analytical approaches or by combining results of studies performed at different institutions. This year we collaborated with ANL and ITRI on such an activity. One of the ITRI studies (I-05) involved animals injected with ^{137}CsCl solution in 1968-1969. A related study (A-04) was performed at ANL in 1961-1963.

Authors of reports on the ITRI study wanted to compare their results with those from ANL. NRA collaborated with ANL staff to achieve two goals. First, the tissue specimens, research records, dosimetry calculations, and other materials were accessioned and packaged and are ready to be sent to ITRI to aid in the compilation of the paper

comparing the two studies. Second, the electronic database at ANL was probed for information about the study, and subfiles were sent to the NRA database and the scientists at ANL and ITRI.

Future Activities

Detailed radionuclide metabolic studies in more than 150 primates have been conducted at Lawrence Berkeley Laboratory (LBL) and other institutions since the 1940s. Sera and excreta specimens were collected for periods of a few minutes to several years after injection. Informal discussions between the NRA staff and the LBL staff were initiated for donation of the primate materials to the NRA. Many radiobiology studies involved rodents. Many of these studies were large, and access to unsummarized, unpublished data from them is limited. As the NRA project matures, selected rodent studies will be considered for inclusion in the NRA summary database.

References Cited

Thompson, R. C. 1989. *Life-Span Effects of Ionizing Radiation in the Beagle Dog: A Summary Account of Four Decades of Research by the U.S. Department of Energy and Its Predecessor Agencies.* PNL-6822, Pacific Northwest Laboratory, Richland, Washington.

Stannard, N. J. 1988. *Radioactivity and Health: A History*, R. W. Baalman, ed. DOE/RL/10830-T59 (DE88013791), Office of Scientific and Technical Information, Springfield, Virginia.

Low-Level $^{239}PuO_2$ Life-Span Studies

Principal Investigator: *C. L. Sanders*

Other Investigators: *K. E. Lauhala and J. A. Mahaffey*

A total of 3192 female Wistar, 198 male Wistar, 192 female Long-Evans, and 200 female Fischer-344 rats were either sham exposed to, or given a single inhalation of, $^{239}PuO_2$. Rats are being examined during their life span for spatial-temporal dose-distribution patterns and for lung tumor formation. Significant life-span shortening was seen only at lung doses >8 Gy. The dose-response curve for all lung tumors continues to be best fitted by a quadratic function and a "practical" threshold of 1-2 Gy; maximum lung tumor incidence is seen at about 8 Gy. Similar quadratic fits were also seen with predominant individual tumor types, squamous carcinoma and adenocarcinoma. Differences in lung tumor incidences between Fischer-344 and Long-Evans rats may be attributed to a faster lung clearance of PuO_2 in Long-Evans rats. Increased cell proliferation of type 2 alveolar epithelium may account for much of the carcinogenicity of inhaled plutonium in the lung and the possible existence of a practical threshold response similar to that seen with nongenotoxic chemicals. The incidence of brain tumors in plutonium-exposed Wistar rats was about twice that seen in sham-control rats for both males and females ($p = 0.09$); the predominant tumor type was astrocytoma.

This project is one of only a few that will provide lung cancer risk data from an animal model at radiation doses as low as those received by nuclear workers, using a sufficient number of animals in control and low-dose groups to estimate tumor risk. The accurate determination of lung dose for each animal and the large numbers of animals in control and low-dose groups provide new information for decreasing the uncertainty of carcinogenic risk estimate in the lung. Quantitative light and scanning electron microscopic autoradiography, cell kinetic studies, and evaluation of the pathological evolution of pulmonary carcinoma are providing new insights into the radiation dose received by "target" cells of the lung and their progression to tumors.

Our objectives are to (1) describe the relationship between lung dose and lung tumor incidence; (2) identify target cells for lung tumor formation; (3) quantify the dose to target cells; and (4) describe the progression of target cells to tumor cells.

Lung Tumors in Female Wistar Rats

A total of 3192 young-adult, female, specific-pathogen-free (SPF) rats were used in the initial life-span study: 2134 were exposed to $^{239}PuO_2$ at initial lung burdens (ILB) ranging from 0.25 to about 180 nCi; 1058 were sham-exposed controls. Histopathological analyses have been completed on 2238 of 3192 female Wistar rats, including 731 sham-exposed controls and 1507 exposed animals. To date, only nine lung tumors have been found in 1251 rats with lung doses >0 to <1 Gy, of which four are benign adenomas (malignant tumor incidence of 0.52%), while four lung tumors have been found in 731 sham-exposed rats (malignant tumor incidence of 0.55%). At a lung dose >1 Gy, the incidence of lung tumors rapidly increases with a maximum tumor incidence of about 75% being seen at a lung dose of 8 Gy (Table 1). Significant life-span shortening was found at lung doses >8 Gy (Figure 1). These data indicate the presence of a possible "practical" threshold dose of about 1 Gy for lung tumor formation; below this threshold, lung tumors are much less likely to be seen. The evolution of squamous cell carcinoma from normal bronchiolar or alveolar epithelium involves a stepwise series of cellular changes, each dependent on the preceding step for further expression. Data from our life-span study with inhaled $^{239}PuO_2$ suggest that ^{239}Pu may act as a promoter of pulmonary carcinogenesis, particularly at lung doses >1 Gy, such that aggregation of particles leads to a sequence of inflammation, fibrosis, and epithelial

TABLE 1. Lung Tumor Incidences in Female Wistar Rats Following Inhalation of $^{239}PuO_2$

Dose to Lung, Gy[a]	Number of rats[b]	Survival Time After Exposure, days[a]	Incidence of Lung Tumors, %				
			Squamous Carcinoma	Adeno-carcinoma	Sarcoma[c]	Other Tumors[d]	Total
21.4 ± 1.3	9 (9)	398 ± 135	33.3	11.1	22.2	0	66.7
18.5 ± 0.97	11 (11)	484 ± 109	54.5	18.2	0	0	72.7
15.6 ± 0.82	14 (14)	482 ± 168	35.7	14.3	7.1	7.1	64.3
13.0 ± 0.55	16 (16)	586 ± 129	62.5	18.8	18.8	0	100
11.5 ± 0.25	15 (15)	592 ± 186	40.0	20.0	13.3	0	73.3
10.0 ± 0.51	16 (16)	541 ± 245	43.8	12.5	6.3	0	62.5
7.94 ± 0.47	20 (20)	647 ± 150	60.0	10.0	0	5.0	75.0
5.93 ± 0.63	17 (17)	680 ± 188	23.5	11.8	17.6	5.9	58.8
4.48 ± 0.23	17 (17)	705 ± 176	0	29.4	5.9	0	35.3
3.40 ± 0.28	29 (29)	656 ± 230	10.3	10.3	0	3.4	24.1
2.56 ± 0.24	35 (35)	685 ± 199	5.1	5.1	0	2.6	12.8
1.40 ± 0.32	37 (37)	653 ± 199	5.4	0	0	0	5.4
0.89 ± 0.05	39 (39)	699 ± 191	0	0	0	2.6	2.6
0.68 ± 0.06	63 (60)	695 ± 196	0	0	0	0	0
0.49 ± 0.06	60 (58)	662 ± 163	0	0	1.7	3.5	5.2
0.28 ± 0.05	140 (138)	702 ± 143	0.7	0	0	0.7	1.4
0.13 ± 0.03	373 (247)	736 ± 161	0	0	0	0.4	0.4
0.07 ± 0.02	1211 (729)	699 ± 189	0	0.1	0	0.1	0.3
0.005[e]	1058 (731)	737 ± 159	0	0.3	0.1	0.1	0.5

(a) Mean ± standard deviation.
(b) Number of rats with completed histopathology is given in parentheses.
(c) Hemangiosarcoma, fibrosarcoma, carcinosarcoma.
(d) Adenoma, mesothelioma.
(e) Estimated background lung dose.

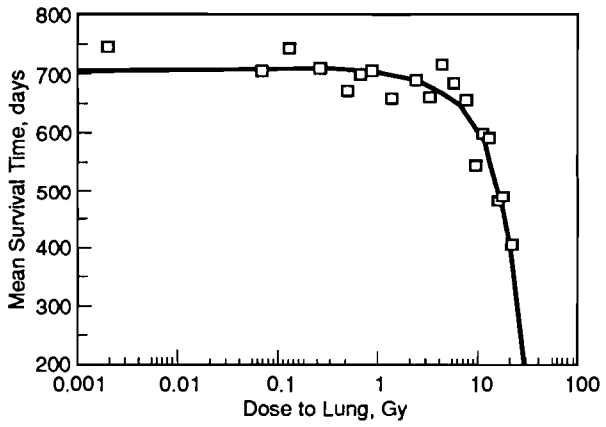

FIGURE 1. Median Survival Time for Female Wistar Rats Following Inhalation of $^{239}PuO_2$

metaplasia preceding carcinoma formation. Current data indicate a clear threshold dose of 1 Gy for squamous carcinoma formation.

The dose-response relationship for all tumor types, as well as for adenocarcinoma and squamous carcinoma tumor types, continues to be well fitted by a quadratic function (Figures 2 through 4). We suggest that the lower dose range of the quadratic curve (<1 Gy) represents primarily initiation events, while the much steeper, higher dose portion of the curve (>1 Gy) represents mostly promotion events caused by plutonium particle aggregation, resulting in the progressive expression of carcinogenesis. These dose-response relationships are similar to those reported for several other carcinogens. In the cases of urinary bladder carcinogenesis following sodium saccharin or melamine administration and nasal cavity carcinogenesis following formaldehyde inhalation, both in rats, a threshold response was observed with tumors entirely attributable to increases in stem cell populations without influencing the probability of initiation or transformation (Cohen and Ellwein 1990). Similar epigenetic responses have also been seen for squamous cell carcinoma induction

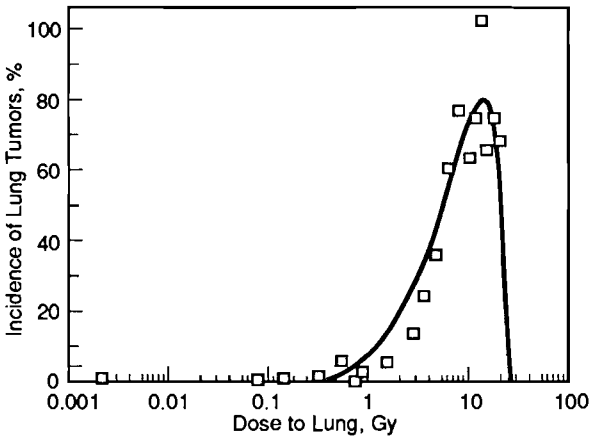

FIGURE 2. Incidence of Lung Tumors in Female Wistar Rats Exposed to $^{239}PuO_2$. Data were fitted by quadratic polynomial equation.

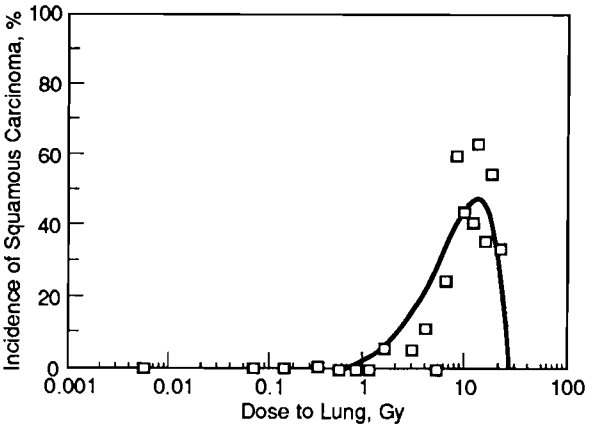

FIGURE 4. Incidence of Pulmonary Squamous Carcinoma in Female Wistar Rats Exposed to $^{239}PuO_2$. Data were fitted by quadratic polynomial equation.

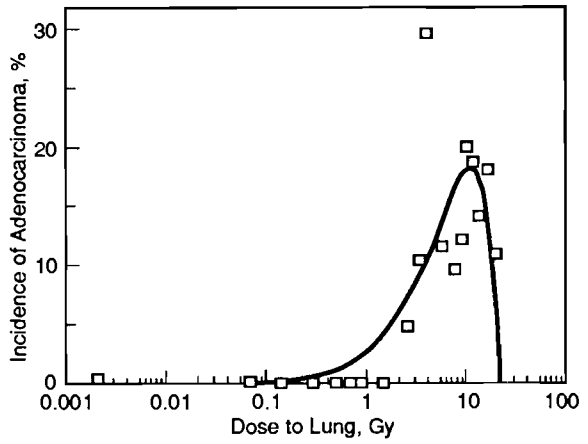

FIGURE 3. Incidence of Pulmonary Adenocarcinoma in Female Wistar Rats Exposed to $^{239}PuO_2$. Data were fitted by quadratic polynomial equation.

in rat lung following inhalation of nongenotoxic dusts such as titanium dioxide, coal dust, quartz, and volcanic ash.

Lung Tumor Progression

Damage and death of type 1 alveolar epithelial cells promote proliferative renewal of type 2 alveolar epithelial cells. Type 2 cells are the possible progenitor cells of most pulmonary carcinomas seen in the rat after inhalation of $^{239}PuO_2$. They receive a disproportionately larger share of alpha dose because of their location and proliferative reaction to damage. Morphological evidence indicates that type 2 alveolar epithelium may become ciliated and differentiate into bronchiolar-like epithelial cells (Figure 5). If so, ciliated bronchiolar-like cells in alveolar bronchiolization lesions may not arrive from migrating terminal epithelial cells but be derived from alveolar epithelium. Thus, the alveoli would be the target for most adenocarcinomas and squamous carcinomas. Small focal areas of squamous differentiation are seen in regions of intense alveolar fibrosis, which lead to squamous carcinoma. It is probable that the pulmonary carcinogenesis response is a result of both genotoxic damage and nongenotoxic damage, the latter of which would be expected to have a no-effect threshold above which cytotoxicity to type 2 alveolar cells becomes apparent. Substantial cytotoxicity and increased cell proliferation were not observed below a threshold dose of about 1 Gy.

Influence of Strain and Sex on Tumor Response

Male Wistar and female Fischer-344 and Long-Evans rats appear to exhibit similar lung tumor incidences at a lung dose of about 1 Gy, with Fischer-344 rats showing the highest incidence (Table 2). Lung tumor incidence in sham-exposed control Fischer-344 rats was also the highest of all strains and sexes. The incidence of lung tumors at

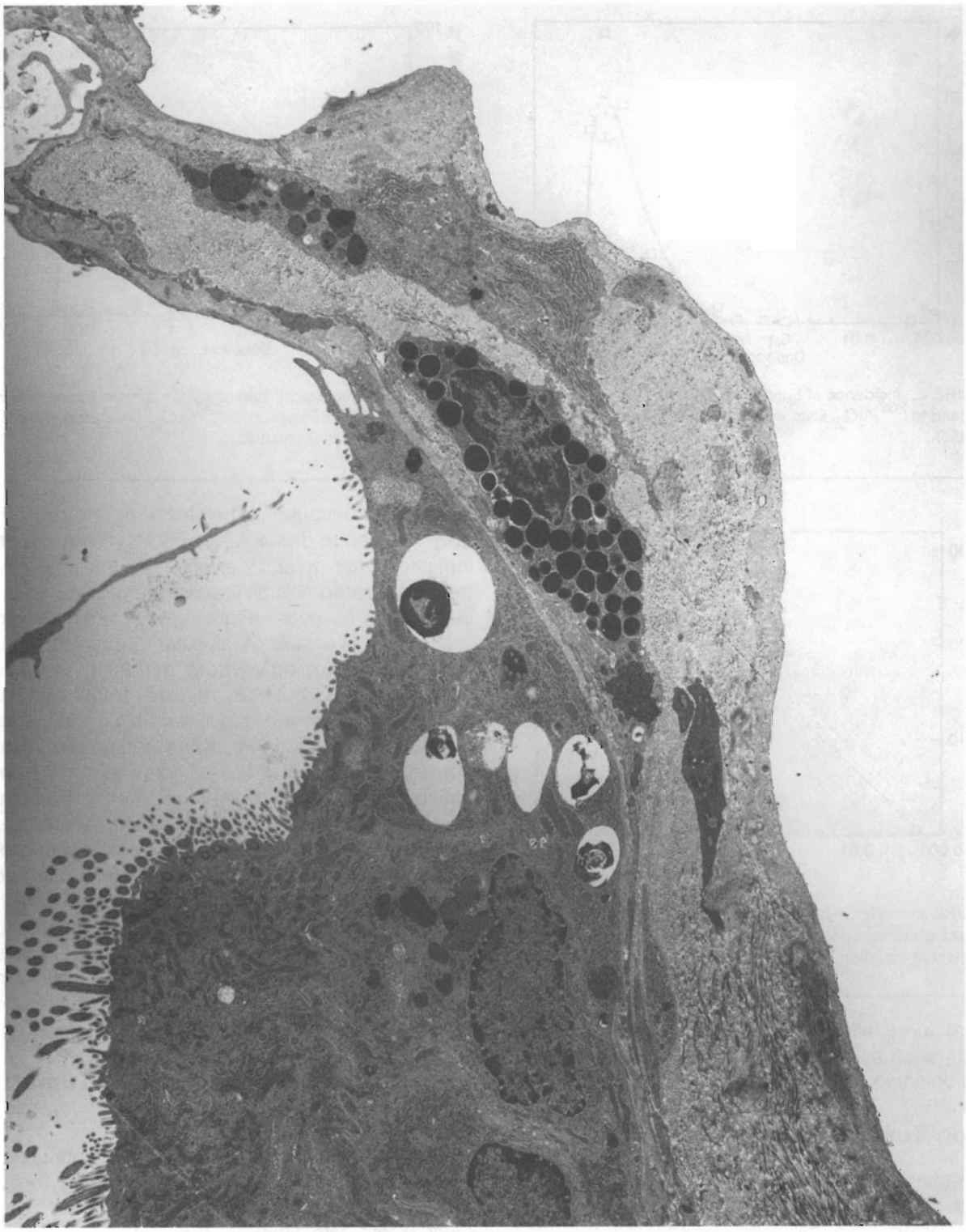

FIGURE 5. Transformation of Type 2 Alveolar Epithelium into Ciliated Bronchiolar Epithelium on Surface of Fibrotic Alveolar Wall

TABLE 2. Estimate of Lung Tumor Incidence by Gross Observation of the Lung in Rats Following Inhalation of $^{239}PuO_2$

Strain	Sex	Dose, Gy	Numbers of Rats	Numbers of Lung Tumors	Lung Tumors, %
Wistar	F	0	554	4	0.7
		<1.0	918	8	0.9
		>1.0	235	108	46.0
		>5.0	118	89	75.4
Wistar	M	0	60	0	0
		<1. 0	45	2	4.4
		>1.0	93	35	37.6
		>5.0	60	32	53.3
Fischer	F	0	60	1	1.7
		<1.0	79	11	13.9
		>5.0	60	41	68.3
Long-Evans	F	0	60	0	0
		<1.0	71	4	5.6
		>5.0	60	21	35.0

high doses was least in Long-Evans rats. These dose calculations assumed the same lung clearance curve for all rats. Quantitative autoradiography was carried out on the left lobe of each strain and sex of rats. Mean radiation doses to the lung at death were similar (about 10 Gy), using the same lung clearance curve to calculate dose. However, bronchiolar submucosal alpha-track concentration and the formation of large plutonium aggregates were substantially less in female Long-Evans rats than in Fischer-344 rats. Likewise, the incidence of lung tumors was only 35% in the Long-Evans strain but 68% in the Fischer-344 strain. An increased clearance of inhaled $^{239}PuO_2$ in the Long-Evans strain as compared to the Fischer-344 strain is the most likely explanation on the basis of studies by Ferin and Morehouse (1980) with inhaled titanium dioxide in the two strains (Figure 6). Thus, the mean lung dose in the lung of Long-Evans rats was probably significantly less than in Fischer-344 rats.

Brain Tumors

Brain tumors in man are associated with exposure to ionizing radiation. Increased incidences of brain tumors are seen in children irradiated for tinea capitis, diagnostic dental procedures, and primary head and neck tumors. Most studies indicate excess tumors at >1 Gy of cumulative exposure. Among plutonium and other nuclear workers, four studies have shown an excess in brain tumors, particularly for astrocytoma of the brain. Historically, untreated rats have a low incidence of brain tumors, about 1%. Astrocytoma followed by meningioma are the most prevalent brain tumor types found in rats. Previous life-span studies with inhaled plutonium in rats have not included microscopic examination of the brain.

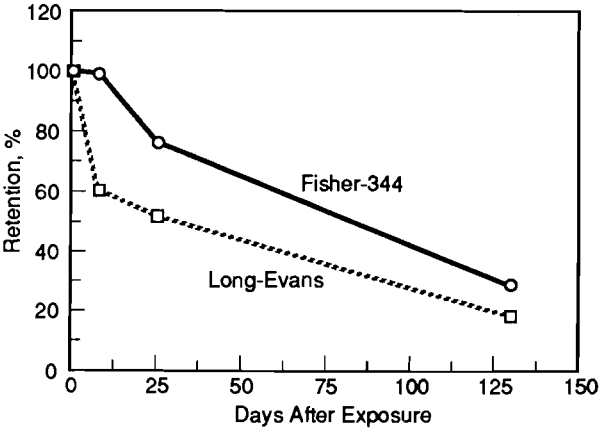

FIGURE 6. Lung Clearance of Inhaled Titanium Dioxide in Fisher-344 and Long-Evans Rats (Ferin and Morehouse 1980)

Among female Wistar rats, 6 brain tumors were found in 1058 control animals (incidence, 0.57%) and 24 brain tumors in 2134 exposed rats (incidence, 1.13%), at a level of significance of $p = 0.09$. Astrocytoma (21 rats) was the predominant tumor type (Figure 7), followed by meningioma (6 rats). Tumor types were similarly distributed among control and plutonium-exposed rats. Eighteen of 30 brain tumors were found in rats older than 2 years. Life spans for control and exposed rats with brain tumors were 829 ± 84 days and 781 ± 173 days, respectively. Five of 6 brain tumors in control rats and 12 of 24 brain tumors in plutonium-exposed rats were considered fatal. The incidence of brain tumors in male Wistar rats were 3.3% (2/60) in controls and 5.1% (7/138) in plutonium-exposed rats. The incidence of brain tumors in both control and treated males was significantly greater than the incidences in respective female groups. In summary, both sexes of the Wistar strain show an increase in brain tumors in animals exposed to inhaled plutonium, although the increase is not significant at the $p < 0.05$ level (Table 3).

TABLE 3. Brain Tumors in Wistar Rats with Both Sexes Combined

Treatment	Number of Rats	Incidence, %	
		Total	Astrocytoma
Control	1118	0.72	0.45
Pu-Exposed	2272	1.36	1.01

References Cited

Cohen, S. M., and L. B. Ellwein. 1990. Cell proliferation in carcinogenesis. *Science* 249:1007-1011.

Ferin, J., and B. Morehouse. 1980. Lung clearance of particles in two strains of rats. *Exp. Lung Res.* 1:251-257.

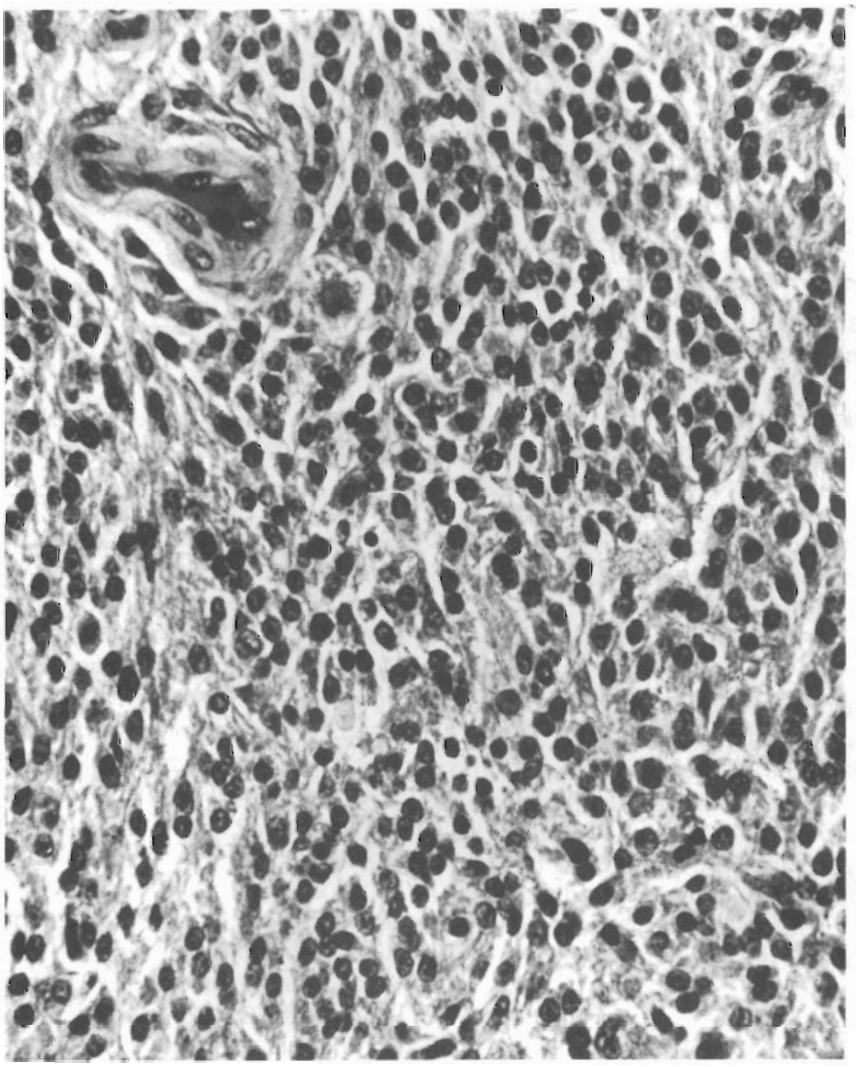

FIGURE 7. Astrocytoma of Brain in Female Rat Exposed to Plutonium

Inhalation Hazards to Uranium Miners

Principal Investigator: *F. T. Cross*

Other Investigators: *R. L. Buschbom, G. E. Dagle, K. M. Gideon, R. A. Gies, and E. S. Gilbert*

Technical Assistance: *C. R. Petty*

Using experimental animals, we are investigating levels of air contaminants that produce respiratory system disease in radon-exposed populations. Lung cancer incidence and deaths from degenerative lung disease are significantly elevated among uranium miners, but the cause-effect relationships for these diseases are based on inadequate epidemiological data. This project identifies agents or combinations of agents (both chemical and radiological), and their exposure levels, that produce respiratory tract lesions, including respiratory epithelial carcinoma, pneumoconiosis, and emphysema. Histopathological examination was continued on 8000 Series (radon-, radon-progeny-, and uranium ore-dust-exposed) life-span animals and completed on 11,000 Series (radon-, radon-progeny-, uranium ore-dust-, and cigarette-smoke-exposed) serial-sacrifice animals. Data on 8000 Series animals continue to show that the risk of lung tumors continues to decrease in proportion to the decrease in cumulative radon-progeny exposure and remains elevated at exposures comparable to those found in houses. Data on 11,000 Series animals continue to suggest that cigarette smoke ameliorates radon-progeny-induced lung tumors; however, adenomatosis (considered to be a preneoplastic lung lesion) is more prevalent and severe in rats exposed to smoke after radon-progeny exposure than before radon-progeny exposure. Finally, the validity of the dosimetric approach for estimating risks of plutonium exposures from radon exposures was examined.

Rat Exposure Protocols

The 6000 Series (1000-working level; WL) and 7000 Series (100-WL) experiments (Table 1) are designed to develop the relationships between response and exposure to radon progeny (at two rates of exposure) and carnotite uranium ore dust. The 8000 Series (100-WL) experiments (Table 2) are designed to extend the exposure-response relationships to cumulative exposure levels comparable to current conditions in the mines and to lifetime environmental exposures. The 9000 Series experiments (Table 3) continue the "low-dose" studies at exposure rates comparable to former occupational working levels (10 WL). They will help to further evaluate the hypothesis that the tumor probability per working-level month (WLM) exposure increases with decreasing exposure rate. In addition, concurrent exposure to varying levels of uranium ore dust tests the hypothesis that irritants (both specific and nonspecific) act synergistically with radiation exposures. The exposures of 6000, 7000, and 8000 Series animals are completed. Exposures of 9000 Series animals have been temporarily discontinued, ceasing with the 80-WLM and 15 mg/m^3 ore-dust exposures, pending analyses of existing data. Exposures of rats to uranium ore dust alone (10,000 Series experiments; Table 4) are completed.

The ore-dust studies address recent experimental data in rats (as well as human epidemiological data) linking silica exposures to lung cancer. Because the silica content of the ore dust in the animal studies exceeds 60%, this potential link in the response to combined ore-dust and radon-progeny exposures needs to be clarified. Exposures of rats to radon progeny, uranium ore dust, and cigarette-smoke mixtures [initiation-promotion-initiation (IPI; 11,000 Series) experiments; see *Mechanisms of Radon Injury* project, this volume] are completed. These experiments clarify the induction-promotion relationships of radon and cigarette-smoke exposures. Exposures

TABLE 1. Exposure-Response Relationship Study for Radon-Progeny Carcinogenesis in Rats (6000 and 7000 Series Experiments)

Number of Animals[a]		Exposure Regimem[b,c]	Total Exposure, WLM[d]
6000 Series	7000 Series		
64	0	1000-WL radon progeny 15 mg/m^3 uranium ore dust	10,240
56	32	1000-WL radon progeny 15 mg/m^3 uranium ore dust	5,120
56	32	1000-WL radon progeny 15 mg/m^3 uranium ore dust	2,560
56	32	1000-WL radon progeny 15 mg/m^3 uranium ore dust	1,280
88	64	1000-WL radon progeny 15 mg/m^3 uranium ore dust	640
152	128	1000-WL radon progeny 15 mg/m^3 uranium ore dust	320
64	96	Controls	

(a) Number of animals is sufficient to detect the predicted incidence of lung tumors at the 0.05 to 0.1 level of significance, assuming linearity of response between 0 and 9200 WLM (see footnote d) and 0.13% spontaneous incidence.
(b) Exposure rate, 90 hr/wk; planned periodic sacrifice.
(c) Study will be repeated at 100-WL rate (without periodic sacrifice) to augment previous limited exposure-rate data (7000 Series experiments).
(d) Working level (WL) is defined as any combination of the short-lived radon progeny in 1 liter of air that will result in the ultimate emission of 1.3×10^5 MeV of potential α energy. Working-level month (WLM) is an exposure equivalent to 170 hours at a 1-WL concentration. Previous exposure at 900 WL for 84 hr/wk to 9200 WLM produced an 80% incidence of carcinoma.

of female rats (12,000 Series experiments; Table 5) are completed. These experiments provide comparative risk data to exposures of male animals. Tables 1 through 5 are shown here with the actual numbers of animals (including serial-sacrifice animals) used at each exposure level. Previous reports showed design protocol numbers of animals needed to detect lung tumors at a particular level of significance; actual numbers employed always equaled or exceeded the design protocols.

Rat Respiratory Tract Pathology

A current summary of primary tumors of the respiratory tract for 8000 Series animals is shown in Table 6. These sampled data continue to show that the incidence of lung tumors decreases in proportion to the decrease in cumulative radon-progeny exposure and, in comparison to the approximate 0.13% spontaneous incidence, remains elevated at exposures comparable to those found in houses (20 to 40 WLM). Histopathological

TABLE 2. Low Exposure-Response Relationship Study for Radon-Progeny Carcinogenesis in Rats (8000 Series Experiments)

Number of Animals[a]	Exposure Regimen [b]	Total Exposure, WLM[c]
96	100-WL radon progeny 15 mg/m^3 uranium ore dust	640[d]
96	100-WL radon progeny 15 mg/m^3 uranium ore dust	320[d]
192	100-WL radon progeny 15 mg/m^3 uranium ore dust	160
384	100-WL radon progeny 15 mg/m^3 uranium ore dust	80
480	100-WL radon progeny 15 mg/m^3 uranium ore dust	40
544	100-WL radon progeny 15 mg/m^3 uranium ore dust	20
192	Controls	

(a) Number of animals is sufficient to detect lung tumors at the 0.05 to 0.1 level of significance, assuming linearity of response between 0 and 640 WLM (see footnote c) and 0.13% spontaneous incidence.
(b) Exposure rate, 90 hr/wk; planned periodic sacrifice.
(c) Previous exposures indicated a tumor incidence of 16% at 640 WLM. Working level (WL) is defined as any combination of the short-lived radon progeny in 1 liter of air that will result in the ultimate emission of 1.3 x 10^5 MeV of potential α energy. Working-level month (WLM) is an exposure equivalent to 170 hours at a 1-WL concentration.
(d) Repeat exposure is for normalization with Table 1 data.

examinations are in progress on the remainder of tissues from 8000, 9000, 10,000, 11,000, and 12,000 Series animals.

Histopathological examination was completed on all IPI Series rats sacrificed at 25, 52, and 78 weeks from beginning of mixed exposures to radon, radon progeny, uranium ore dust, and cigarette smoke (Table 7). Exposure-related lesions were limited to the lungs and tracheobronchial lymph nodes.

TABLE 3. Ultralow Exposure-Rate Study for Radon-Progeny Carcinogenesis in Rats (9000 Series Experiments)

Number of Animals[a]	Exposure Regimen [b]	Total Exposure, WLM[c]
64	10-WL radon progeny 15 mg/m^3 uranium ore dust	320
64	10-WL radon progeny 3 mg/m^3 uranium ore dust	320
384	10-WL radon progeny 15 mg/m^3 uranium ore dust	80
384	10-WL radon progeny 3 mg/m^3 uranium ore dust	80
512	10-WL radon progeny 15 mg/m^3 uranium ore dust	20
512	10-WL radon progeny 3 mg/m^3 uranium ore dust	20
192	Controls	

(a) Number of animals is sufficient to detect lung tumors at the 0.05 to 0.1 level of significance, assuming linearity of response between 0 and 640 WLM (tumor incidence is approximately 16% at 640 WLM) and 0.13% spontaneous incidence.
(b) Exposure rate, 90 hr/wk; planned periodic sacrifice.
(c) Working level (WL) is defined as any combination of the short-lived radon progeny in 1 liter of air that will result in the ultimate emission of 1.3 x 10^5 MeV of potential α energy. Working-level month (WLM) is an exposure equivalent to 170 hours at a 1-WL concentration.

Exposure-Related Lung Lesions in IPI Series Rats

Focal accumulations of alveolar macrophages with dust ("dust macrophages"), focal interstitial reaction, adenomatosis, and primary lung tumors were the principal experimental effects observed in IPI sacrificed animals. The focal accumulations of alveolar macrophages with dust were randomly distributed or occurred near terminal bronchioles. The dust consisted of uranium ore and, in rats exposed to smoke, probably smoke particulates that blended with and were not distinguishable from the uranium ore dust. The foci frequently had

TABLE 4. Control Study for Uranium Ore-Dust Carcinogenesis in Rats (10,000 Series Experiments)

Number of Animals	Exposure Regimen [a]
96	15 mg/m^3 uranium ore dust
64	Sham-exposed controls

(a) Exposures, 12 to 18 months at 72 hr/wk; planned periodic sacrifice.

TABLE 5. Exposure of Female Rats to Radon Progeny and Uranium Ore Dust (12,000 Series Experiments)

Number of Animals	Exposure Regimen [a]
96	100-WL radon progeny; 640 WLM 5 mg/m^3 uranium ore dust
96	Sham-exposed controls

(a) Exposure rate, 72 hr/wk; planned periodic sacrifice. Working level (WL) is defined as any combination of the short-lived radon progeny in 1 liter of air that will result in the ultimate emission of 1.3×10^5 MeV of potential α energy. Working-level month (WLM) is an exposure equivalent to 170 hours at a 1-WL concentration.

TABLE 6. Current Summary of Primary Tumors of the Respiratory Tract in Life-Span Animals (8000 Series Experiments)

		Extrathoracic Tumors				Lung Tumors						
Nominal Exposure, WLM	Nominal Ore Dust Conc., mg/m^3	Nasal	Laryngeal	Tracheal	No. Animals Examined	No. Animals to Be Examined	Adenoma	Adenocarcinoma	Epidermoid Carcinoma	Adenosquamous Carcinoma	Sarcoma[a]	No. Animals with Lung Tumors
20	15	0/122[b]	0/82	0/119	127	399	0	0	1	0	0	1
40[c]	15	0/135	0/91	0/132	142	320	0	1	0	0	1	2
160	15	0/161	0/97	0/158	171	0	4	5	1	0	1	11
640	15	0/72	0/44	0/71	76	0	5	3	2	1	0	10
Controls		0/60	0/46	0/55	64	109	0	0	0	0	0	0

(a) One malignant hemangiopericytoma and one malignant fibrous histiocytoma, considered radon-progeny-exposure-related.
(b) Number tumors/number examined.
(c) One malignant oropharyngeal hemangiosarcoma, considered radon-progeny-exposure-related; found in tissue not routinely sectioned for histopathology.

a minimal amount of thickened alveolar septa and occasionally had interstitially located macrophages. There was a tendency for dust-laden macrophages to be more aggregated by 52 and 78 weeks after initiation of exposures than in rats sacrificed at 25 weeks; fewer alveolar macrophages were observed at 78 weeks than at earlier sacrifice times.

Focal interstitial reactions were the principal inflammatory lesions related to the exposures. The focal interstitial reactions were generally randomly disseminated and consisted of thickened alveolar septa with a mild mononuclear or mixed-cellular inflammatory response. The interstitial reactions frequently had some associated macrophages in the alveoli, but increased numbers of alveolar macrophages were not the most prominent reaction present. Minimal amounts of alveolar epithelial hyperplasia was associated with the thickened alveolar septa.

The proliferative reaction of alveolar epithelium, more than the minimal amounts associated with an interstitial reaction, was tabulated as adenomatosis. Adenomatosis consisted of foci where alveoli

TABLE 7. Primary Lesions of the Lung in 25-, 52-, and 78-Week Sacrificed Rats (11,000 Series IPI Experiments)[a]

Group Number	Exposure Regimen[c]	Sacrifice Time, wk	Number of Rats (and Group Average Severity)[b] of: Interstitial Reaction	Dust Macrophages	Adenomatosis	Tumors
1	320	25	5 (0.5)	10 (1.9)	0	0
		52	7 (1.0)	10 (2.0)	6 (1.0)	4
		78	9 (1.6)	10 (1.3)	8 (2.2)	5
2	Sham-exposed controls	25	0	0	1 (0.1)	0
		52	2 (0.2)	0	2 (0.3)	0
		78	0	0	1 (0.2)	0
3	160/Shelf/160	25	1 (0.1)	10 (1.2)	1 (0.1)	0
		52	5 (0.5)	10 (2.0)	3 (1.4)	1
		78	9 (1.4)	10 (1.6)	8 (1.5)	1
4	Sham-exposed controls	25	0	0	0	0
		52	1 (0.1)	0	1 (0.3)	0
		78	1 (0.1)	0	1 (0.2)	0
5	160/Smoke/160	25	0	10 (1.6)	2 (0.5)	0
		52	8 (1.6)	10 (2.0)	5 (1.2)	0
		78	10 (1.4)	10 (1.7)	8 (2.1)	2
6	Sham-exposed controls	25	0	0	0	0
		52	2 (0.2)	0	0	0
		78	6 (0.7)	0	2 (0.3)	0
7	320/Smoke	25	3 (0.4)	10 (2.0)	1 (0.1)	0
		52	6 (0.7)	10 (1.9)	5 (1.1)	0
		78	9 (1.2)	10 (1.7)	8 (1.3)	2
8	Sham-exposed controls	25	0	0	0	0
		52	2 (0.3)	0	0	0
		78	3 (0.3)	0	0	0
9	Smoke/320	25	1 (0.1)	10 (1.9)	0	0
		52	4 (0.5)	10 (1.9)	1 (0.1)	0
		78	8 (1.2)	10 (1.2)	4 (0.9)	1
10	Sham-exposed controls	25	0	0	0	0
		52	1 (0.2)	0	0	1
		78	0	0	0	0
11	Ore dust/smoke	25	0	10 (2.0)	0	0
		52	2 (0.3)	10 (1.9)	0	0
		78	2 (0.2	10 (1.6)	0	0
12	Sham-exposed controls	25	0	0	0	0
		52	0	0	0	0
		78	2 (0.3)	0	0	0

(a) Moderately low concentrations (5-6 mg/m^3) of uranium ore dust (2% U content) accompanied radon exposures as a carrier aerosol for the daughters; 10 animals were sacrificed in each group at each sacrifice time.

(b) Group average lesion severity is given in parentheses: +1 (very slight); +2 (slight); +3 (moderate); +4 (marked); +5 (extreme).

(c) Radon-progeny exposures shown are nominal;
320 = 320-WLM (100-WL) radon progeny + uranium ore dust delivered in 8-wk exposure period
160/Shelf/160 = 160 WLM (4 wk)/Shelf (17 wk)/160 WLM (4 wk).
All exposures except group 1 were completed in 25 weeks; cigarette-smoke exposures were 1 hr/d, 5 d/wk for 17 weeks at 0.5 mg/L total particulate mass concentration. Working level (WL) is defined as any combination of the short-lived radon progeny in 1 liter of air that will result in the ultimate emission of 1.3×10^5 MeV of potential α energy. Working-level month (WLM) is an exposure equivalent to 170 hours at a 1-WL concentration.

were lined with prominent cuboidal epithelial cells resembling alveolar type 2 pneumocytes. The alveolar septa were thickened, but the increased thickness was principally caused by the alveolar epithelial hyperplasia and not the inflammatory response as was tabulated with the focal interstitial reaction. In the grade of +3 (observed), the adenomatosis is moderately extensive. The grade +4 (observed) would include some atypical hyperplasia of alveolar epithelium. Grade +5, not observed with these rats, would include atypia and replacement of the architecture of the lung parenchyma so as to be difficult to distinguish from neoplasia. One additional proliferative lesion, alveolar squamous metaplasia, was present in one rat from group 5 (r-S-r).

Primary lung tumors (21 total in 17 rats) were papillary adenomas (10), solid adenomas (1), bronchioloalveolar carcinomas (8), and adenosquamous carcinomas (2). The papillary adenomas occurred in alveolar parenchyma and consisted of fairly well circumscribed nodules of proliferating cuboidal epithelial cells having a papillary pattern replacing normal architecture. The one solid adenoma was composed of a well-circumscribed mass of densely packed epithelial cells having fine connective tissue stroma. The bronchioloalveolar carcinomas consisted of cuboidal epithelial cells proliferating in a bronchioloalveolar pattern with a tendency to extend into adjacent tissues. The two adenosquamous carcinomas had major portions of both bronchioloalveolar pattern and stratified squamous epithelium. Assuming spherical volumes, the average volume and standard deviation of benign tumors was 1.3 $\pm$1.4 mm^3, while carcinomas were 7.6 $\pm$ 5.7 mm^3. The average size of all tumors combined (benign and malignant) were the same at 52 and 78 wk.

The data in Table 7 suggest that cigarette smoke ameliorates radon-induced lung tumors; however, adenomatosis (considered to be a preneoplastic lung lesion) was more prevalent in rats exposed to cigarette smoke after radon exposures (Groups 5 and 7) than before radon exposure (Group 9). Adenomatosis was essentially absent in rats exposed to cigarette smoke without accompanying radon exposures (Group 11).

Exposure-Related Tracheobronchial Lymph Node Lesions in IPI Series Rats

Phagocytosed dust was tabulated as dust macrophages. In grades of +3 (observed), or higher, broad sheets of macrophages partially replace the parenchyma of the medulla.

Reactive hyperplasia usually consisted of increased numbers of plasma cells causing increased thickness of the medullary cords. In grades of +3 (observed) or higher, broad sheets of lymphocytes in the cortex start to extend into pericapsular tissues.

Cystic degeneration, common in older rats and beginning to appear in this population, consisted of dilated spaces partially filled with lymph. The spaces were lined with a single layer of flattened cells and could represent dilated lymphatics.

Finally, the validity of the dosimetric approach for estimating risks of plutonium exposures from radon exposures was examined in collaboration with Drs. E. S. Gilbert, C. L. Sanders, and G. E. Dagle, PNL. The dosimetric approach is based on the assumption that a specified dose to the lung produces the same lung tumor risk independent of the radionuclide producing the dose. If lung tumors are assumed to be fatal, radon and plutonium dose-response curves differ, with a linear function providing a good description of the radon data and a pure quadratic function providing a good description of the plutonium data. These results suggest that the use of the dosimetric approach would be likely to overestimate lung tumor risks from plutonium at low doses. However, if lung tumors are found incidentally at death, dose-response curves for the two exposures are very similar and thus support the dosimetric approach for estimating plutonium lung tumor risks from radon exposures.

Mechanisms of Radon Injury

Principal Investigator: *F. T. Cross*

Other Investigators: *R. L. Buschbom, G. E. Dagle, E. W. Fleck,[a] M. E. Foreman, M. E. Frazier, R. A. Gies, A. C. James, R. F. Jostes, F. C. Leung, L. S. McCoy, S. H. Moolgavkar,[b] T. L. Morgan, J. L. Schwartz,[c] L. G. Smith, and G. L. Stiegler*

Technical Assistance: *T. L. Curry and C. R. Petty*

In this project we conduct molecular, cellular, and whole-animal research relevant to understanding the mechanisms of radon and radon-progeny injury to the respiratory tract. The work specifically addresses the exposure-rate effect in radon-progeny carcinogenesis; the induction-promotion relationships associated with exposure to radon and cigarette-smoke mixtures; the role of oncogenes in radon-induced cancers; the effects of radon on DNA as well as on DNA repair processes; and the involvement of growth factors and their receptors in radon-induced carcinogenesis.

In vitro radon and radon-progeny exposures of adult and fetal rat lung cells were initiated to correlate with data on growth factor and growth factor receptor involvement in radon-exposed rats. The analysis of survival response data on Chinese hamster ovary cells (CHO-C18) exposed to radon and radon progeny in intercalibration experiments continued using a model to calculate dose to the cell nucleus for cells exposed in suspension culture. Southern blot analyses of x-ray- and radon-induced mutations at the CHO-HGPRT locus showed a high percentage of deletion-type events in contrast to a low percentage of deletion-type events in spontaneous mutants. No alterations were seen in spontaneous mutants although to date they comprise about 28% of the mutants from x- and radon-irradiated cells. Initiation-promotion-initiation experiments continued in male SPF Wistar rats exposed to radon and cigarette-smoke mixtures. Biological/statistical modeling of PNL experimental data on radon-induced lung tumors in rats also continued.

In an effort to correlate molecular data with pathological data derived from the animal radon studies, Drs. Marla Foreman, Linda McCoy, and Marvin Frazier (PNL) isolated DNA from fixed, archived, radon- induced lung tumors in rats, amplified the oncogene of interest by the polymerase chain reaction method, and analyzed it by sequencing. (This collaborative work appears in *Oncogenes in Radiation-Induced Carcinogenesis*, this volume.)

In Vitro Radon Cell-Exposure System and Molecular/Cellular Studies

The PNL in vitro radon cell-exposure system was extensively employed in PNL experiments as well as in several collaborative and intercalibration experiments with other laboratories. Collaborations included: (1) Dr. Earl Fleck, Whitman College, on isolating radon-induced HGPRT mutations for Southern blot analysis; (2) Dr. Helen Evans, Case-Western Reserve University (CWRU), on mutational response of radiosensitive and radioresistant L5178Y cells as well as the dosimetric evaluation of the CWRU in vitro radon-exposure system; (3) Drs. Sheldon Wolff and John Wiencke, University of California San Francisco (UCSF), on adaptation studies using x-irradiation followed by radon exposure and vice versa; (4) Drs. James Cleaver and Louise Lutze, UCSF, on radon exposure of shuttle vectors for molecular analysis; and (5) Dr. William Au, University of Texas, on scoring aberrations in first-division metaphases from quiescent human lymphocytes.

(a) Whitman College, Walla Walla, Washington.
(b) Fred Hutchinson Cancer Research Center, Seattle, Washington.
(c) Argonne National Laboratory, Argonne, Illinois.

The PNL-designed alpha probe, used to monitor alpha-particle irradiation of cells in suspension culture, was calibrated with the chelated and unchelated ^{212}Bi and ^{212}Pb suspension system at Argonne National Laboratory (ANL) in collaboration with Drs. Jeffrey Schwartz, Rick Jostes, and Edmond Hui. A comparison of the calculated and measured degraded alpha-energy spectrum for chelated ^{212}Bi is shown in Figure 1. Agreement is good over a wide range of energy. The two shoulders of the curve correspond to the two alpha energies (~6.06 MeV of ^{212}Bi and 8.78 MeV of ^{212}Po) in the medium. The extremely high count rate below 1 MeV results principally from beta particles.

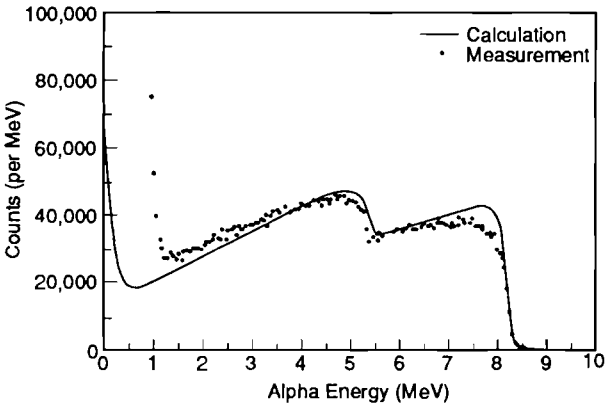

FIGURE 1. Calculated and Measured Energy Spectrum for ^{212}Pb

The effect of plateout on surfaces was measured using unchelated ^{212}Bi and ^{212}Pb. Alphas attached to the Mylar window of the alpha probe act as a thin source in contrast to the thick source of the medium. The additional source produces a peak on each shoulder of the spectrum (Figure 2). Figure 2 also shows the additional beta counts below 1 meV from ^{212}Pb. Additional measurements with the alpha probe, and development of algorithms by Dr. T. E. Hui (PNL) to unfold alpha spectra to obtain concentrations of individual alpha emitters in culture media, are planned.

The analysis of survival response data from intercalibration experiments with CHO-C18 cells continued, using a model to calculate dose to the nucleus of cells exposed in radon suspension systems. The model (manuscript submitted to *Radiation Research*) takes into account the contribution of dose from different radionuclides using scintillation counts of the medium and the incorporated activity in cells. The model produced a D_0 value of about 64-cGy alpha dose to the nucleus in PNL ^{222}Rn suspension system experiments; the previously reported value of about 75 cGy was determined with an interim calculational model. The revised value is similar to that obtained at ANL and CWRU using the updated model.

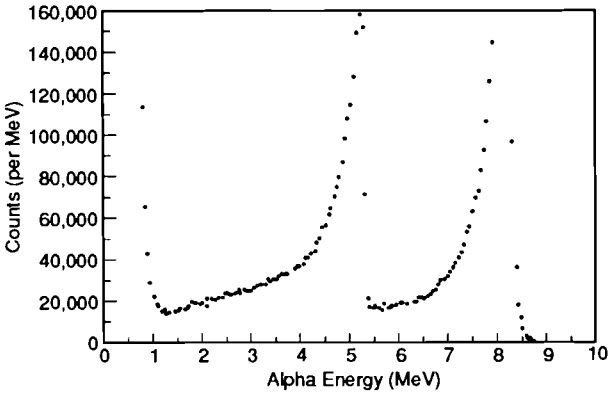

FIGURE 2. Measured Energy Spectrum for Unchelated ^{212}Bi and ^{212}Pb

Work continued on evaluating radon-induced mutations at the CHO-HGPRT locus after 76-cGy alpha doses to the nucleus (previously reported to be 100 cGy). Mutations obtained with radon exposures are predominantly deletion-type events (48%), with 24% showing no change from the parental line and 28% showing a rearrangement of the Southern blot banding patterns. X-ray-induced mutations show a spectrum of damage similar to that obtained from radon exposures. In contrast, spontaneous mutants exhibit a low percentage of deletion-type events (11%) compared with 0% alterations and 89% showing no change. Rigorous selection techniques were employed to ensure that mutants were not sibling isolates. These selection techniques produced banding patterns in spontaneous mutants that were quite different from previously reported values. A current summary of HGPRT mutation types is shown in Table 1. Additional data are needed to determine any differences in radon-exposed and x-irradiated populations.

In vitro radon exposures of fetal and adult rat lung cells were initiated to examine growth factor/growth factor receptor (GF/GFR) gene expressions for correlation with GF/GFR expressions in radon-induced rat lung tumors. This work is being conducted in collaboration with Dr. Frederick Leung (PNL).

Biological/Statistical Modeling and Initiation-Promotion-Initiation Studies

These studies, conducted in collaboration with Dr. Suresh Moolgavkar of the Fred Hutchinson Cancer Research Center, Seattle, are (1) to analyze PNL experimental data on radon-induced lung tumors in rats [the data are to be analyzed using current survival data methods] and also the two-mutation model of carcinogenesis, which is a generalization of the recessive oncogenesis model; (2) to estimate the parameters of the two-mutation carcinogenesis model, to generate testable hypotheses regarding radon-induced lung carcinogenesis, and to study parameters of the model in terms of the effect of radon progeny on mutation rates and cell proliferation kinetics; and (3) to design and analyze data from initiation-promotion-initiation experiments in rats with radon progeny as the initiator and cigarette smoke as the promoter.

An analysis in the context of the two-mutation model of a data set of approximately 1800 rats exposed to between 320 WLM and 10,000 WLM with exposure rates ranging from 5 WLM/week to 500 WLM/week was reported in *Radiation Research* (Moolgavkar et al. 1990). A further analysis of the data set using current survival data methods to determine risk is in progress.

Initiation-promotion-initiation (IPI) experiments continued in male SPF Wistar rats with radon and cigarette-smoke mixtures. The exposure protocols are shown in Table 2.

Initial radon-progeny exposures were at 100-WL concentrations with cumulative levels of 320 WLM; uranium ore-dust concentrations ranged from about 5 to 6 mg/m^3. Cigarette smoke from Kentucky 1R4F cigarettes, in exposures of 1 hr/day, 5 days/week, for 17 weeks, contained total particulate mass concentrations of about 0.5 mg/L and carbon monoxide concentrations between 650 and 700 ppm. Mean plasma concentrations of nicotine and cotinine were about 260 and 125 ng/mL, respectively, in cigarette-smoke-exposed animals; carboxyhemoglobin levels were about 29%. Blood samples were obtained within 15 minutes after exposures ended.

Histopathological examination was completed on all exposed and sham-exposed sacrifice groups at 25, 52, and 78 weeks from start of exposures. These data are reported under the co-project *Inhalation Hazards to Uranium Miners* (this volume).

TABLE 1. Current Summary of HGPRT Mutation Types[a]

Treatment	Full Deletion[b]	Alteration[c]	No Change[d]	Total
None (spontaneous)	2 (11%)	0 (0%)	17 (89%)	19
76 cGy radon	12 (48%)	7 (28%)	6 (24%)	25
300 cGy x rays	5 (33%)	5 (33%)	5 (33%)	15

(a) DNA from each mutant cell line was digested with one or more restriction enzymes.
(b) Full deletion, no residual HGPRT-specific coding sequences detectable.
(c) Alteration, loss of bands and/or appearance of new bands.
(d) No change, banding pattern not different from that of untreated parental controls.

TABLE 2. Initiation-Promotion-Initiation Protocol for Radon (R), Dust (D), and Cigarette-Smoke (S) Inhalation Exposure of Rats[a]

	Duration of Exposure, weeks					
Group	0	4	8	17	21	25
1	R+D---------->					
2	R+D----->					R+D->
3	R+D---->S---------->					R+D->
4	R+D---------->	S---------->				
5	S---------->			R+D---------->		
6	D---------->	S---------->				

(a) Moderately low concentrations of uranium ore dust (D) accompany radon exposures as the carrier aerosol for radon progeny; sham-exposed control animals (not shown) are included in each exposure group. Animals from each group are killed at 25, 52, and 78 weeks to evaluate developing lesions. Protocol may be repeated for different radon-progeny exposure rates and levels.

Reference Cited

Moolgavkar, S. H., F. T. Cross, G. Luebeck, and G. E. Dagle. 1990. A two-mutation model for radon-induced lung tumors in rats. *Radiat. Res.* 121:28-37.

Dosimetry of Radon Progeny

Principal Investigator: *A. C. James*

Other Investigators: *D. R. Fisher, T. E. Hui, F. T. Cross, J. S. Durham, P. Gehr,[a] M. J. Egan,[b] W. Nixon,[b] D. L. Swift,[c] and P. K. Hopke[d]*

The purpose of this project is to provide key dosimetric models that are needed to evaluate human cancer risks from exposures to radon and thoron progeny and to relate risk to the conditions of exposure. The research encompasses modeling and experimental studies that are necessary (1) to interpret human exposures to radon and thoron progeny in terms of effective dose to sensitive cells, and (2) to integrate findings of the DOE/OHER Radon Research Program, including the effects observed in experimental animals and the cellular and molecular responses observed in vitro, into a coherent and comprehensive assessment of human cancer risks. We report here the development and application of a dosimetric model to evaluate radiation doses to sensitive cells throughout the bronchial epithelium of the human adult, child, and infant, and also the corresponding microdosimetric probabilities of radiation events at the subcellular level. The dosimetric model has been used by a Committee of the National Research Council/ National Academy of Sciences to examine the extrapolation of risk estimates developed from studies of underground miners to the general population exposed in the home environment.

Last year we reported work in progress to model lung deposition and bronchial dose for male and female adults and for children exposed to radon (or thoron) progeny (James 1990). We also reported the development of methods for calculating the microdosimetry of cells irradiated in vitro by alpha particles (Fisher 1990). This year we have updated the bronchial dosimetry model to incorporate new research information from the DOE Radon Program; modeled aerosol deposition and bronchial doses in the immature infant lung; applied the updated dosimetry model to compare biologically significant doses from unit exposure in mine and home environments; and linked the microdosimetric calculation to the exposure-dose model and thus evaluated the frequency of radiation events in target cell nuclei as a function of the rate at which a subject is exposed to radon progeny.

Updating the Dosimetry Model

The depth distributions of sensitive tissue beneath the surface of the bronchial and bronchiolar epithelia were determined from the morphometric data reported by Mercer et al. (in press). Figure 1 shows the structure of the bronchial epithelium and the ranges of depth through which the sensitive targets (basal cell and secretory cell nuclei) are taken to occur in healthy subjects independently of age and gender (James et al., in press, a). In the bronchioles, the epithelium and the overlying mucus and ciliary layer are substantially thinner, and the sensitive targets are composed only of secretory cells. In addition to updating the calculation of doses received by these epithelial target tissues from alpha disintegrations in mucus or in the epithelium itself, we have developed methods to calculate the doses received from beta particles that are also emitted by radon and thoron progeny (James et al., in press, a).

Further experimental studies of the penetration of unattached radon progeny through hollow casts of the human nasal passages, pharynx, and larynx, carried out by J. C. Strong and D. L. Swift (at the Biomedical Research Laboratory, AEA Technology, Harwell, England) and also by P. K. Hopke with

---

(a) Institute of Anatomy, University of Berne, Switzerland.
(b) AEA Safety and Reliability, Culcheth, England.
(c) The Johns Hopkins University, Baltimore, Maryland.
(d) Clarkson University, Potsdam, New York.

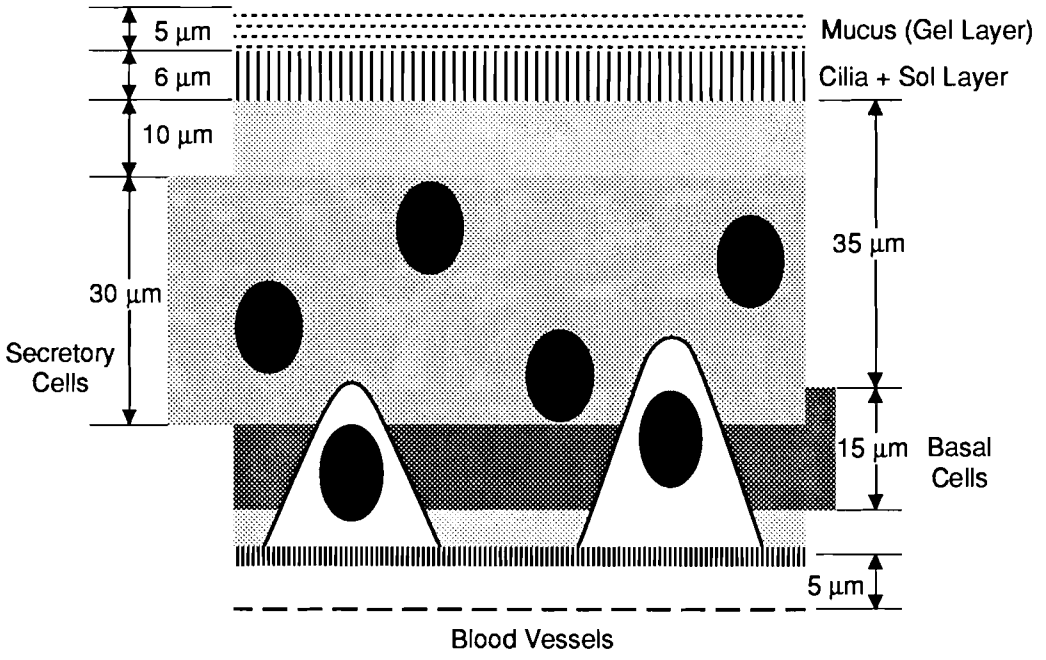

FIGURE 1. Schematic Model of Bronchial Epithelium with Dimensions and Spatial Distributions of Secretory and Basal Cell Nuclei

D. L. Swift (at Clarkson University, Potsdam, New York), now support the unexpectedly high values of nasal filtration efficiency for ultrafine particles and unattached thoron progeny that were found by Cheng et al. (1989). Similar results have been obtained with several accurately made casts, including one from a magnetic resonance image (MRI) scan of a 1.5-year-old infant. The emerging congruence of experimental data indicates that estimates of nasal penetration based on George and Breslin's (1969) study of human subjects, which have been used in previous dosimetric models, may well be twofold high. Thus, previous estimates of exposure-dose conversion coefficients for unattached radon progeny may also have been approximately twofold high. In deriving the dosimetric modeling results outlined here, we assumed for the adult male the nasal penetration efficiency that was expressed in terms of the flow rate (in liters per minute) and particle diffusion coefficient by Cheng et al. (1989):

$$P = \exp(-13.2\, Q^{-1/8}\, D^{1/2}) \qquad (1)$$

We also assumed that penetration of aerosols through the nasal passages in the adult female, in children, and in infants is related to that in the adult male by dimensional scaling factors based on airway size (Swift 1989).

There are no human data on oral deposition of particles as small as unattached radon progeny. Studies with hollow casts of the oral passageway down to the larynx have shown that the deposition efficiency of this pathway may be as high as 75% of that of the nose for the same flow rate and particle size (Cheng et al. 1989). However, in the absence of confirmatory data in vivo, we assumed for the present a more conservative oral deposition efficiency that is 50% of the nasal value (James et al., in press, b). To evaluate doses for so-called mouth breathers and for normal subjects who are exercising heavily, we assumed the typical pattern of change between nasal and oral breathing that was found for adult subjects by Niinimaa et al. (1980, 1981). Thus, the proportion of the total airflow inhaled nasally by mouth breathers is taken to decrease from 70% at rest to 30% under heavy work. Normal nose breathers are assumed to switch from 100% nasal breathing to partial mouth breathing at a total respiratory rate of about 2.1 m^3/h for the adult male.

To calculate the fractional deposition of particles in each branching airway of the lower respiratory tract, we used the theoretical model of aerosol transport and deposition that was developed by Egan et al. (1989). However, for the bronchi (the first through eighth airway generation), we corrected the theoretical deposition estimates to account for the observations of Cohen et al. (1990) of enhanced deposition of submicron-sized particles in the complex flow fields simulated in a hollow bronchial cast. The correction factor shown in Figure 2 is applied to the likelihood of particle deposition that is calculated to arise from the thermodynamic process of diffusion under laminar flow conditions. Although Cohen et al. studied only particles of diameter between 0.04 and 0.2 μm, their data indicated that the deposition enhancement factor approaches unity for very small particles. Shimo and Ohashi (in press) have since observed directly that the deposition efficiency of unattached radon progeny (with a particle diameter of approximately 0.001 μm) in a hollow bronchial model does correspond to the value calculated for diffusion in laminar flow, as we have assumed.

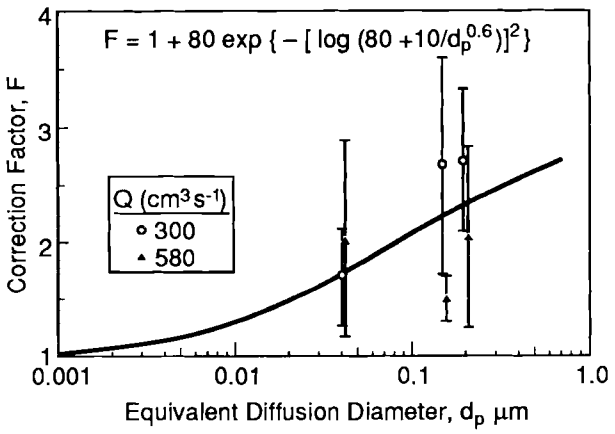

FIGURE 2. Factors by Which Deposition Efficiencies of Submicron-Sized Particles Measured by Cohen et al. (1990) for Cyclic Flow in Hollow Bronchial Casts Exceed Values Calculated for Diffusion in Laminar Flow

Modeling the Infant Lung

Typical dimensions of respiratory airways in the developmental stage from birth to 2 years of age were estimated by scaling a model of the fully developed respiratory acinus according to lung volume, the number of airways, and the degree of alveolization. The number of airways is virtually complete at birth, but alveolization of these immature airways is not (Zeltner et al. 1987). At 1 month, about 20% of the typical number of alveoli in the adult are present. By 1 year, alveolization has increased to about 80%.

Exposure-Dose Conversion Coefficients

Table 1 shows how the doses received by basal cell targets in the bronchi of different subjects are calculated to depend on the activity median thermodynamic diameter (AMTD) attained by the radon-progeny aerosol within the respiratory tract and also on the subject's breathing rate (represented by different levels of physical exertion). It is seen that the assumed value of nasal deposition efficiency has a major impact on doses that are calculated to result from exposure to unattached radon progeny (characterized by an aerosol AMTD of 0.0011 μm). The doses received by secretory cell nuclei are found to be approximately twofold higher than the values shown in Table 1 (for basal cell nuclei only).

Representative Exposure Conditions in Mines and Homes

Table 2 summarizes the unattached fractions of airborne potential alpha energy (f_p) and the characteristic sizes of the attached radon-progeny aerosols, which are taken to represent the different exposure conditions in underground mines and in the home environment (NRC, in press). The condensation nuclei to which radon progeny attach are unstable in saturated air. According to the available information, we assume that condensation nuclei grow on inhalation, such that the AMTD of the radon-progeny aerosol within the respiratory tract is double that in ambient air (Sinclair et al. 1974).

TABLE 1. Summary of Coefficients to Convert Exposure to Radon-Progeny Potential Alpha Energy[a] into Dose Received by Basal Cell Nuclei in Bronchi of Different Subjects (normal nose breathers) as a Function of Radon-Progeny Aerosol Size and Subject's Level of Physical Exertion

Subject	Radon-Progeny AMTD (μm) with Assumed Nasal Deposition	Exposure-Dose Conversion Coefficient (mGy per WLM) for Various Levels of Physical Exertion			
		Sleep	Rest	Light Work	Heavy Work
Adult male	0.0011[b]	48.9	59.6	153.0	321.2
	0.0011[c]	23.4	28.9	80.9	210.7
	0.02	18.3	20.0	31.5	41.6
	0.15	4.66	5.04	7.86	11.8
	0.25	3.35	3.64	6.31	14.9
	0.3	3.03	3.31	6.22	18.4
	0.5	2.63	2.93	7.51	38.6
Adult female	0.0011[b]	39.9	48.8	152.5	340.9
	0.0011[c]	18.6	23.1	80.0	223.2
	0.02	19.1	21.4	36.2	49.2
	0.15	4.66	5.17	8.62	13.4
	0.25	3.29	3.64	6.75	17.1
	0.3	2.95	3.27	6.59	21.1
	0.5	2.48	2.77	7.77	44.4
Child, age 10 yr	0.0011[b]	48.8	60.2	166.5	-
	0.0011[c]	23.0	28.8	87.5	-
	0.02	22.3	24.9	40.1	-
	0.15	5.38	5.98	9.58	-
	0.25	3.81	4.25	7.61	-
	0.3	3.43	3.84	7.47	-
	0.5	2.89	3.30	8.80	-
Child, age 5 yr	0.0011[b]	55.7	74.9	129.4	-
	0.0011[c]	26.1	36.0	65.6	-
	0.02	25.8	29.7	38.2	-
	0.15	6.04	6.98	8.94	-
	0.25	4.34	5.05	6.66	-
	0.3	3.93	4.61	6.26	-
	0.5	3.33	4.08	6.42	-
Infant, age 1 yr	0.0011[b]	63.8	94.3	148.6	-
	0.0011[c]	29.6	45.2	74.3	-
	0.02	33.2	39.6	48.2	-
	0.15	7.77	9.06	10.9	-
	0.25	5.56	6.65	8.19	-
	0.3	5.02	6.11	7.69	-
	0.5	4.17	5.47	7.67	-
Infant, age 1 mo	0.0011[b]	50.1	-	78.8	-
	0.0011[c]	22.4	-	36.7	-
	0.02	36.8	-	45.9	-
	0.15	9.02	-	10.9	-
	0.25	6.25	-	7.35	-
	0.3	5.54	-	6.47	-
	0.5	4.25	-	5.01	-

(a) The airborne concentration of potential alpha energy is commonly quoted in the unit working level (WL) which is defined as any combination of short-lived progeny in 1 liter of air that will result in the ultimate emission of 1.3×10^5 MeV of potential alpha energy. The working-level month (WLM) is an exposure equivalent to 170 hours at a 1-WL concentration. AMTD, activity median thermodynamic diameter.

(b) Nasal deposition of unattached progeny according to George and Breslin (1969).

(c) Nasal deposition of unattached progeny according to Cheng et al. (1989).

TABLE 2. Radon-Progeny Aerosol Characteristics Assumed to Represent Exposure Conditions in Mines and Homes

Exposure Scenario	f_p	AMTD of Ambient Aerosol (μm)	AMTD of Aerosol in Respiratory Tract (μm)
Mine			
Mining	0.005	0.25	0.5
Haulageway	0.03	0.15	0.3
Lunchroom	0.08	0.15	0.3
Living Room			
Normal	0.08	0.15	0.3
Smoker, average	0.03	0.25	0.5
Smoker, during smoking	0.01	0.25	0.5
Cooking/vacuuming	0.05	0.02/0.15[a] (15%/80%)	0.02/0.3 (15%/80%)
Bedroom			
Normal	0.08	0.15	0.3
High	0.16	0.15	0.3

(a) The radon-progeny aerosol produced by cooking/vacuuming has three size modes; 5% of potential alpha energy is unattached, 15% has an AMTD of 0.02 μm, and 80% an AMTD of 0.15 μm. The 0.02-μm AMTD mode is hydrophobic and does not increase in size within the respiratory tract. AMTD, activity median thermodynamic diameter.

To evaluate doses received from given exposures in underground mines, we consider that a miner who is engaged in rock-breaking or other dusty "mining" activities (see Table 2) spends 25% of his time doing heavy work and 75% doing light work. We consider that transport and maintenance work in less dusty "haulageways" corresponds to light work. We also examine the case of exposure in a "lunchroom" or other less active and dusty areas of a mine, where the miner is assumed to spend 50% of his time resting and 50% doing light work.

For the home, we take into account differences in the level of each subject's physical exertion during exposures in living rooms and bedrooms. Thus, for living rooms, adults, children and 1-year-old infants are assumed normally to spend 50% of their time resting and 50% doing light work. The 1-month-old infant is assumed to spend 70% of the time asleep and 30% in light activity. During exposure to the special aerosol conditions that arise during cooking or vacuuming (see Table 2), we assume that adults spend 75% of their time doing light work and 25% resting. We assume that subjects are asleep during most of their exposure in a bedroom.

Extrapolation of Dose per Unit Exposure from Mines to Homes

Using the terminology of the BEIR IV report (NRC 1988), we consider that the risk per unit exposure in the home, $(\text{Risk})_h/(\text{WLM})_h$ (WLM, working-level month), is related to that from exposure in mines, $(\text{Risk})_m/(\text{WLM})_m$, by a dimensionless factor, K.

$$K = \frac{(\text{Risk})_h/(\text{WLM})_h}{(\text{Risk})_m/(\text{WLM})_m} \qquad (2)$$

On the premise that risk is related primarily to the doses received by the appropriate cellular targets, the value of the risk extrapolation factor K is given by the ratio of the doses that result from unit exposure in each environment.

$$K = \frac{(\text{Dose})_h/(\text{WLM})_h}{(\text{Dose})_m/(\text{WLM})_m} \qquad (3)$$

Figure 3 compares doses received by secretory and basal cell nuclei in bronchial epithelium that are calculated for an adult female (a homemaker), for unit exposure to radon progeny under various

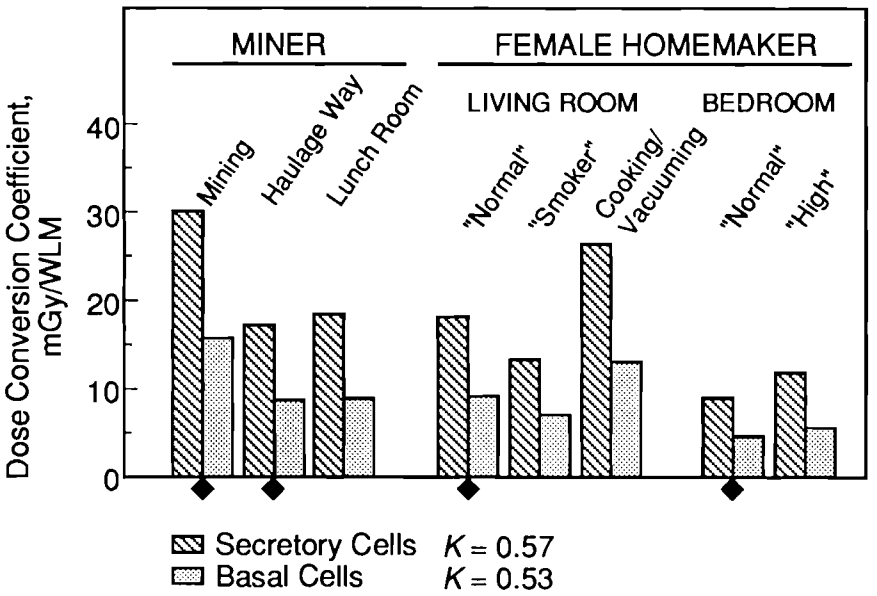

FIGURE 3. Comparison of Doses to Bronchial Target Cell Nuclei Received by Miner and by Female Homemaker for Unit Exposure Under Various Environmental Conditions

conditions in the home, with the values calculated for a male underground miner. It is seen that secretory cell nuclei receive approximately twofold higher doses than basal cell nuclei. When we consider that the exposure of a population of miners is divided equally between "mining" and work in "haulageways," and that the exposure of a homemaker is divided equally between the "normal" living room and bedroom, we find that the K factor based on comparative doses to secretory cell nuclei is 0.57, and also that the K factor based on doses to basal cell nuclei is not significantly different (at $K = 0.53$).

Figure 4 shows the calculated variability in the mean doses received by secretory and basal cell nuclei for different subjects (all nose breathers) exposed under various conditions in the home. It is found that doses per unit exposure tend to be higher for children than for adults, but not by large factors. The corresponding K factors that are assessed by comparison with bronchial doses received by a normal nose-breathing miner are summarized in Table 3. These K factors are found to range from 0.47 for a 1-month-old infant (based on comparative doses received by basal cell nuclei) to 0.81 for a 1-year-old infant (based on comparative doses received by secretory cell nuclei). On the basis of bronchial doses averaged for all nose-breathing subjects exposed in the home relative to the healthy nose-breathing miner, the overall value of this exposure risk extrapolation factor is found to be 0.62.

Table 3 also gives values of the K factor calculated for the adult male by comparing doses received by just the lobar and segmental bronchi or by the bronchioles. The former are similar to K factors calculated for target cells throughout all bronchial airways, but the K factor based on comparative doses received by bronchiolar target cells is marginally higher (at 0.8). Finally, Table 3 shows that values of the K factor calculated by comparing mouth-breathing subjects in the home with nose-breathing miners are generally higher than the corresponding values for nose breathers. The overall average exposure risk extrapolation factor for mouth-breathing subjects is found to be 0.76.

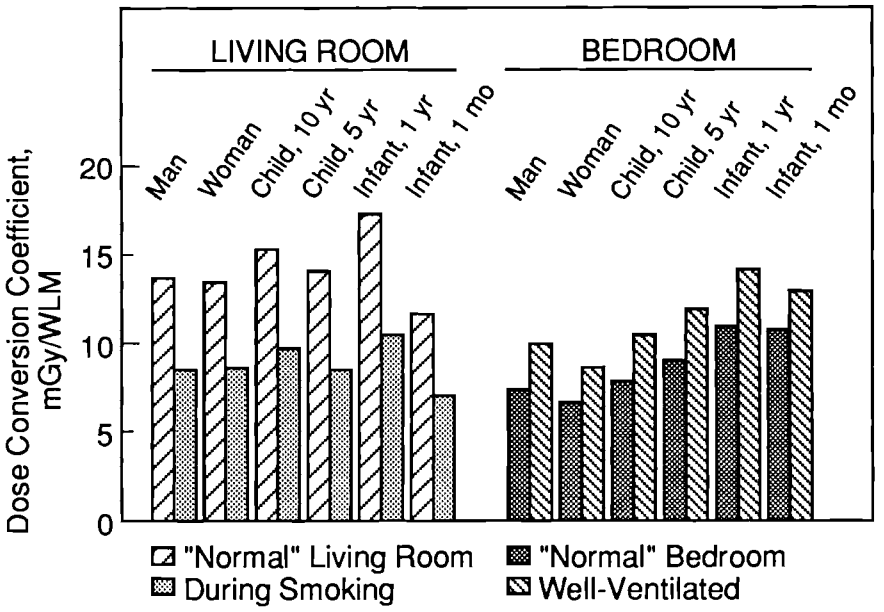

FIGURE 4. Influence of Environmental Conditions on Bronchial Doses Received by Subjects Exposed in the Home

Comparative Microdosimetry

We have calculated the microdosimetric probability densities in specific energy for secretory and basal cell nuclei in bronchial epithelium of the adult male and for the various exposure conditions in mines and homes (Fisher et al., in press). We have also applied microdosimetric calculations to relate the frequency of radiation events during the lifetime of an epithelial cell to the rate at which a subject is exposed to radon progeny. For example, Figure 5 shows the alpha-particle hit probabilities calculated for secretory cell nuclei at levels of cumulative exposure from 0.15 to 100 WLM. The lowest rate of exposure corresponds to that received over a 6-month period in the average U.S. home (with a mean radon concentration of approximately 1.5 pCi/liter). The highest exposure rate (100 WLM over 6 months) corresponds to the highest exposed group of uranium miners from the Colorado Plateau epidemiological study (NRC 1988). The intermediate rate of 10 WLM over 6 months corresponds to the average exposure of uranium miners in the Ontario study.

For all except the highest exposure rate considered for the Colorado Plateau miners, it is found that the probability of a single alpha-particle hit to the secretory cell nucleus during the normal lifetime of a cell (which is approximately 6 months) increases linearly with the exposure rate. The corresponding probabilities of multiple hits are small (less than 0.01 at a cumulative exposure of 10 WLM). However, for the very high cumulative exposure of 100 WLM in 6 months, the probability of a single hit is significantly lower, and the overall probability of multiple hits exceeds 0.1. These findings support the notion that the significantly lower excess risk of lung cancer in relationship to radon-progeny exposure that was found for the most highly exposed group of Colorado Plateau miners is related to the relatively low number of single alpha-particle events in target cell nuclei.

We will proceed to develop a model of target cell transformation and survival in the human respiratory tract (Fisher 1990) based on the cellular responses to radon-progeny exposure observed in vitro and the specific energy distributions computed for basal and secretory cell nuclei in relationship to the environmental conditions of exposure.

TABLE 3. Summary of *K* Factors Calculated for Healthy Subjects in the Home Relative to the Normal Healthy Miner

Subject	Target Region	Target Cell	Radon-Progeny Solubility	*K* Factor
Nose Breathers				
Adult male	Bronchi	Secretory	Insoluble	0.63
			Partially soluble	0.56
		Basal	Insoluble	0.61
			Partially soluble	0.52
Adult male	Lobar/ segmental bronchi	Secretory	Insoluble	0.61
			Partially soluble	0.52
		Basal	Insoluble	0.60
			Partially soluble	0.46
Adult male	Bronchioles	Secretory	Mean	0.80
Adult male	Bronchi	Secretory	Mean	0.60
		Basal	Mean	0.56
Adult female	Bronchi	Secretory	Mean	0.57
		Basal	Mean	0.53
Child, age 10 yr	Bronchi	Secretory	Mean	0.66
		Basal	Mean	0.61
Child, age 5 yr	Bronchi	Secretory	Mean	0.66
		Basal	Mean	0.61
Infant, age 1 yr	Bronchi	Secretory	Mean	0.81
		Basal	Mean	0.74
Infant, age 1 mo	Bronchi	Secretory	Mean	0.64
		Basal	Mean	0.47
Mouth Breathers				
Adult Male	Bronchi	Secretory	Mean	0.75
		Basal	Mean	0.69
Adult Female	Bronchi	Secretory	Mean	0.72
		Basal	Mean	0.66
Child, age 10 yr	Bronchi	Secretory	Mean	0.83
		Basal	Mean	0.77
Child, age 5 yr	Bronchi	Secretory	Mean	0.81
		Basal	Mean	0.74
Infant, age 1 yr	Bronchi	Secretory	Mean	1.00
		Basal	Mean	0.92
Infant, age 1 mo	Bronchi	Secretory	Mean	0.73
		Basal	Mean	0.55

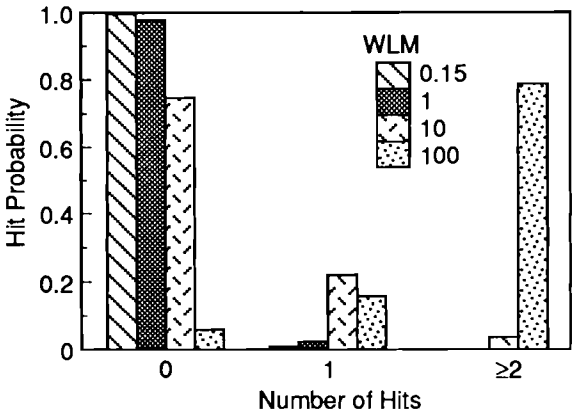

FIGURE 5. Alpha-Particle Hit Probabilities for Secretory Cell Nuclei for Different Cumulative Exposures to Radon Progeny

References Cited

Cheng, Y. S., D. L. Swift, Y. F. Su, and H. C. Yeh. 1989. Deposition of radon progeny in human head airways. In: *Inhalation Toxicology Research Institute Annual Report 1988-89*, pp. 29-30. LMF-126, Lovelace Biomedical and Environmental Research Institute, Albuquerque, New Mexico.

Cohen, B. S., R. G. Sussman, and M. Lippmann. 1990. Ultrafine particle deposition in a human tracheobronchial cast. *Aerosol Sci. Technol.* 12:1082-1091.

Egan, M. J., W. Nixon, N. I. Robinson, A. C. James, and R. F. Phalen. 1989. Inhaled aerosol transport and deposition calculations for the ICRP Task Group. *J. Aerosol Sci.* 20:1301-1304.

Fisher, D. R. 1990. Microdosimetry of radon daughters. In: *Pacific Northwest Laboratory Annual Report for 1989 to the DOE Office of Energy Research*, Pt. 1, pp. 57-60. PNL-7200, Pacific Northwest Laboratory, Richland, Washington.

Fisher, D. R., T. E. Hui, and A. C. James. Model for assessing radiation dose to epithelial cells in the human respiratory tract from radon progeny. *Radiat. Prot. Dosim.* (in press).

George, A. C., and A. J. Breslin. 1969. Deposition of radon daughters in humans exposed to uranium mine atmospheres. *Health Phys.* 17:115-124.

James, A. C. 1990. Behavior and dosimetry of radon. In: *Pacific Northwest Laboratory Annual Report for 1989 to the DOE Office of Energy Research*, Pt. 4, pp. 19-24. PNL-7200, Pacific Northwest Laboratory, Richland, Washington.

James, A. C., P. Gehr, R. Masse, R. G. Cuddihy, F. T. Cross, A. Birchall, J. S. Durham, and J. K. Briant. Dosimetry model for bronchial and extrathoracic tissues of the respiratory tract. *Radiat. Prot. Dosim.* (in press, a).

James, A. C., W. Stahlhofen, G. Rudolf, M. J. Egan, W. Nixon, P. Gehr, and J. K. Briant. The respiratory tract deposition model proposed by the ICRP Task Group. *Radiat. Prot. Dosim.* (in press, b).

Mercer, R. R., M. L. Russell, and J. D. Crapo. Airway cell and nuclear depth distribution in human and rat lungs. *Health Phys.* (in press).

National Research Council (NRC). 1988. *Health Risks of Radon and Other Internally Deposited Alpha-Emitters.* BEIR IV. Committee on the Biological Effects of Ionizing Radiation. National Academy Press, Washington, D.C.

National Research Council (NRC). *Comparative Dosimetry of Radon in Mines and Homes.* Report by a Scientific Panel. National Academy Press, Washington, D.C. (in press).

Niinimaa, W., P. Cole, S. Mintz, and R. J. Shephard. 1980. The switching point from nasal to oronasal breathing. *Respir. Physiol.* 42:61-71.

Niinimaa, W., P. Cole, S. Mintz, and R. J. Shephard. 1981. Oronasal distribution of respiratory airflow. *Respir. Physiol.* 43:69-75.

Shimo, M., and A. Ohashi. Deposition distribution of unattached RaA atoms in the tracheobronchial region. In: *Indoor Radon and Lung Cancer: Reality or Myth?,* 29th Hanford Symposium on Health and the Environment, October 16-19, 1990, Richland, Washington (in press).

Sinclair, D. R., R. J. Countess, and G. S. Hoopes. 1974. The effect of relative humidity on the size of atmospheric aerosol particles. *Atmos. Environ.* 8:1111-1117.

Swift, D. L. 1989. Age-related scaling for aerosol and vapor deposition in the upper airways of humans. In: *Modeling for Scaling to Man: Biology, Dosimetry, and Response*, Proceedings of the 26th Hanford Life Sciences Symposium, October 20-23, 1987, Richland, Washington. *Health Phys.* 57(Suppl. 1):293-298 (Special Issue).

Zeltner, T. B., J. H. Caduff, P. Gehr, J. Pfenninger, and P. H. Burri. 1987. The postnatal development and growth of the human lung: I. Morphometry. *Respir. Physiol.* 67:247-267.

Aerosol Technology Development

Principal Investigator: *A. C. James*

Other Investigators: *J. K. Briant, B. J. Greenspan, and M. A. Parkhurst*

The purpose of this project is to develop and transfer aerosol technology to basic and applied research in biology and chemistry, especially in the areas of health and environmental effects of energy-related materials. The ongoing objective is to improve systems for the control, monitoring, and characterization of exposures of laboratory animals to toxic aerosols, gases, and vapors. The current thrust is to improve the metrology, control, and characterization of exposures to radon progeny in studies of the mechanisms of radon-induced respiratory tract cancer and to provide a new and simpler technique to characterize exposure to unattached radon progeny in domestic or occupational settings. We report here the design and development of an Unattached Radon Progeny Size-Spectrometer to measure the concentration and unattached fraction of potential alpha energy in air and also the activity-size distribution of the unattached progeny.

The Unattached Radon Progeny Size-Spectrometer (URPSS) is based on the principle of diffusion in a parallel-plate channel.[a] Sampled air is drawn at a constant flow rate of 0.5 liter/min through unobstructed channels formed by the outer parallel walls of the spectrometer and a strip of track-etch detector material (poly[ethylene glycol *bis*-(allyl carbonate)], commonly known as CR-39). The sampling channels are designed to effectively allow all the radon-progeny activity associated with ambient condensation nuclei or other forms of vector aerosol (such as the uranium ore dust used in PNL's studies of radon-induced lung cancer) to pass through and be collected on a separate filter. Laminar airflow and unobstructed sampling channels eliminate inertial deposition of these particles. Vertical orientation of the channels prevents significant loss of particles by sedimentation.

Unattached radon progeny, that is, those progeny existing as ions or molecules or those associated with molecular clusters of airborne contaminants, deposit according to their particulate size by diffusion to the walls of the sampling channels. Figure 1 shows the profiles of particle deposition along either 15-cm channel of the URPSS (shown as the logarithm of fraction deposited per centimeter of length) that are calculated for particles of several different diameters using the theoretical treatment reviewed by Soderholm (1979). Particles of 0.5-nm diameter are calculated to deposit entirely within 2 cm of the channel entrance. For larger particles, the deposition profile is calculated to spread progressively along each channel. This pattern of diffusive particle deposition is determined by the width of the sampling channels and the total sampling flow rate, and both parameters can be varied to extend the particle-size range analyzed by the spectrometer.

The profile of radon-progeny alpha (α) activity deposited along each of the sampling channels is recorded as damage tracks in the exposed surfaces of the CR-39 detector strip. Radon progeny α activity attached to particles large enough to pass through the sampling channels is recorded by a separate CR-39 detector chip mounted in front of the 25-mm-diameter filter used to collect these particles. The exposed CR-39 detectors are batch-processed by controlled etching in a sodium hydroxide solution to produce a permanent record of radon-progeny α decays in the form of etched tracks (Figure 2).

The number of α-particle tracks is counted under a microscope in contiguous fields along the whole length (and on both sides) of the 15-cm CR-39

(a) This design is similar in concept to the "radon progeny detector" patented by RAD-X Ltd. of 719 Genesee St., Syracuse, New York 13210.

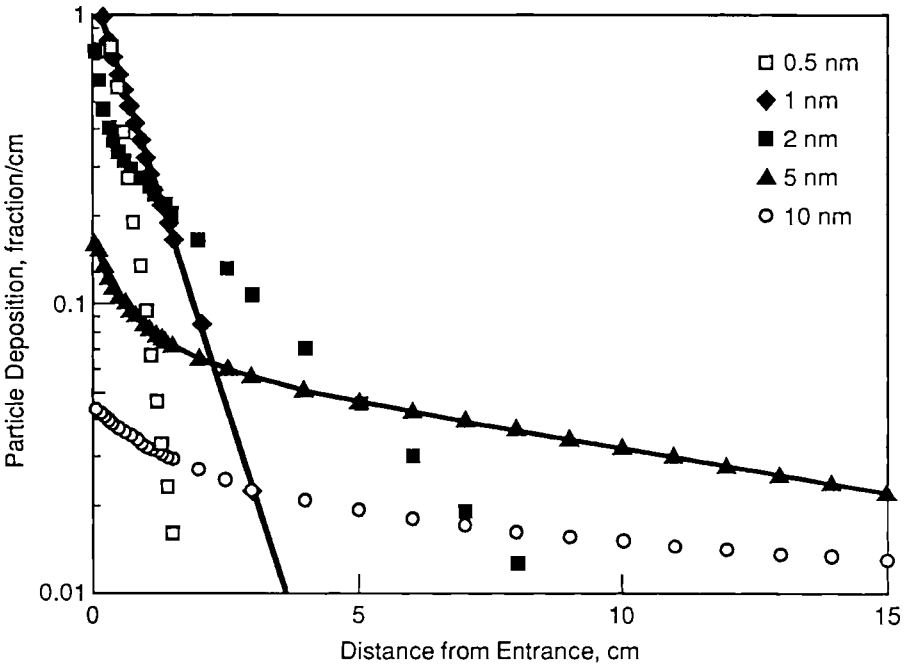

FIGURE 1. Calculated Profiles of Particle Deposition Along the Spectrometer Channel

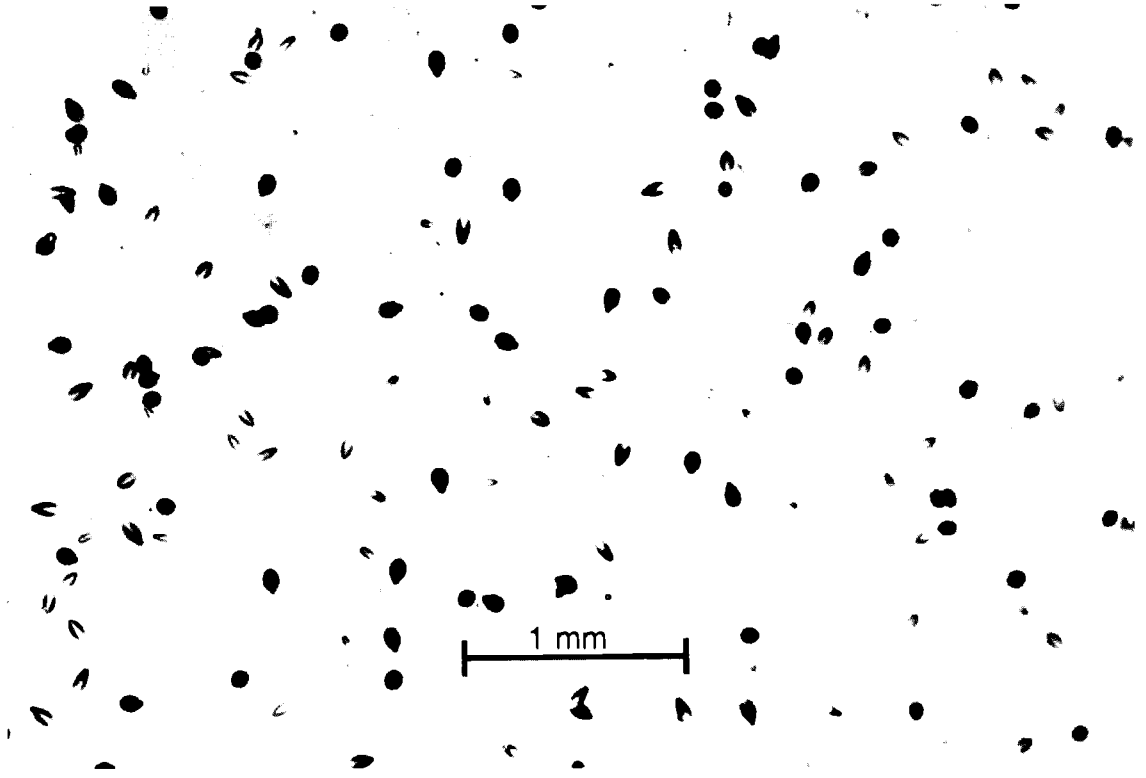

FIGURE 2. Alpha Tracks Developed in Poly[ethylene glycol *bis*-(allyl carbonate)] by Chemical Etching

detector strip. The measured track density is recorded as a function of distance from the front edge of the strip. In the case of the CR-39 chip that measures radon-progeny α activity collected in the filter, the average α-track density is measured by scanning an appropriate number of optical fields. We are calibrating both of these source/detector configurations in terms of the response of the CR-39 detectors to total α energy emitted by the short-lived radon progeny.

Processed CR-39 detectors are scanned by a computer-controlled optical microscope (Southern Micro Instruments, Inc., Atlanta, Georgia). Software to enable the scanning microscope to automatically recognize and focus on α-particle-etched tracks in CR-39 is being developed for us by the manufacturer of the instrument. We will interface this with software developed by Dr. D. L. Henshaw's group at the H. H. Wills Physics Laboratory, University of Bristol, England[(a)] (Fews 1986; Hatzialekau and Henshaw 1988) for fully automated image analysis of the spatial distribution of α tracks in CR-39 autoradiographs.

Figure 3 shows the profile of α activity measured along the CR-39 detector strip when the URPSS was used to sample the unattached ^{218}Po aerosol formed in an exposure chamber supplied with ^{222}Rn in filtered laboratory air (at 40% relative humidity with no animals present). The measured pattern of α tracks is fitted by the profile of deposition calculated for particles with an activity average diffusion coefficient of 0.067 cm^2 s^{-1} (which corresponds to a particle diameter of 0.68 nm). Under the test conditions, the diffusion coefficient of ^{218}Po was expected to be less than the maximum value of 0.078 cm^2 s^{-1} found for neutral ^{218}Po atoms in dry air (Ramamurthi and Hopke 1991). We are testing the theoretically determined profile of deposition in the sampling channel by exposing the URPSS at various flow rates to ^{218}Po of known diffusion coefficient.

The activity-weighted size distribution of unattached radon progeny is known to vary

(a) Used by PNL under license from the University of Bristol.

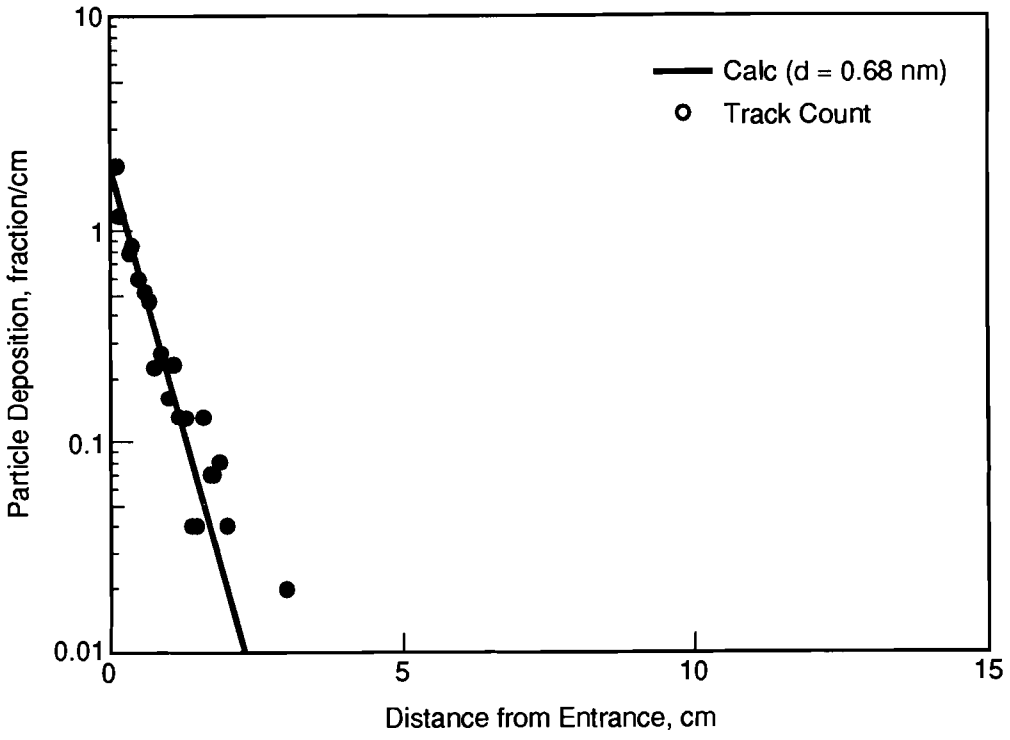

FIGURE 3. Alpha-Track Density Measured Along the Spectrometer Channel Compared with Best-Fit Theoretical Deposition Profile for Particles of 0.68-nm Diameter

substantially with environmental conditions. In indoor air, the activity average diffusion coefficient is thought to be about 0.04 cm^2 s^{-1} (Ramamurthi and Hopke 1991). This value corresponds to an average particle diameter of about 1 nm. However, in the presence of relatively high concentrations of vapors, such as those produced during and after cooking, the median activity-weighted particle size is shifted into the range 1.5 nm to 10 nm. This range of particle size corresponds to a range of activity average diffusion coefficients from 0.02 cm^2 s^{-1} to 0.0005 cm^2 s^{-1}. Using the URPSS, we have found that the size of unattached radon progeny also grows significantly in the contaminated atmosphere of an animal exposure chamber.

Figure 4 shows the profile of α activity measured along the CR-39 detector strip when the URPSS was used to sample the ultrafine radon progeny produced in a reconstruction of PNL's exposures of laboratory rats to uranium mine aerosols. In this preliminary study, 64 rats were exposed to ^{222}Rn at a concentration of 290 nCi/liter with 2.5 mg/m^3 of uranium ore-dust aerosol. The resulting concentration of radon-progeny potential α energy was 160 working level (WL). The ultrafine fraction f_p was approximately 15%, as measured by PNL's conventional wire-screen technique. The measured dependence of radon-progeny penetration through the wire screen as a function of flow rate indicated an effective diffusion diameter of 1.0 nm. However, the URPSS showed that a second component of ultrafine radon progeny, composed of larger particles that are not detected by a wire-screen sampler, was also present (as shown in Figure 4).

From measurements of the α-track profile along the URPSS channel, we were able to resolve the ultrafine fraction of radon-progeny activity into its discrete components; 54% with an equivalent particle diameter of 0.94 nm and 46% with a median equivalent particle diameter of about 4.1 nm.

Data on the filtration efficiency of the nasal passages in the rat (Cheng et al. 1990) show that only 2% of inhaled 0.94-nm-diameter particles are expected to escape deposition in the nose. In contrast, a much higher fraction (33%) of the 4.1-nm-diameter component of the true ultrafine fraction is expected to deposit in the lung and thus contribute to the measured higher incidence of lung tumors in rats exposed to so-called unattached progeny.

To unfold the activity-weighted size distribution for a polydisperse aerosol of ultrafine radon progeny, we use the characteristic penetration curves calculated for the spectrometer channel (Figure 5). The CR-39 strip can be divided into an optimum number of segments that is determined by the

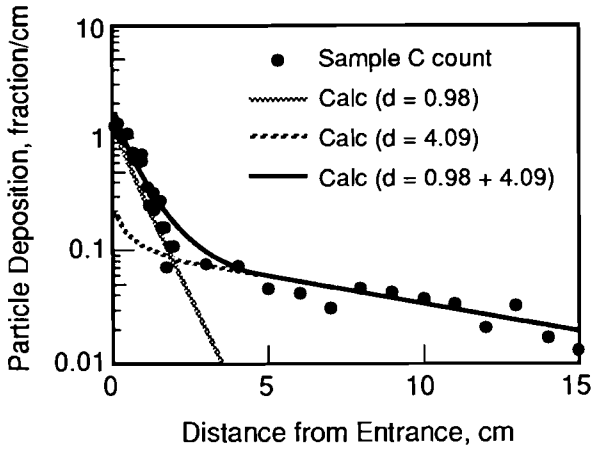

FIGURE 4. Measured Profile of Alpha Tracks from Ultrafine Progeny Obtained in Reconstruction of PNL's Past Exposures of Rats to Uranium Mine Aerosols

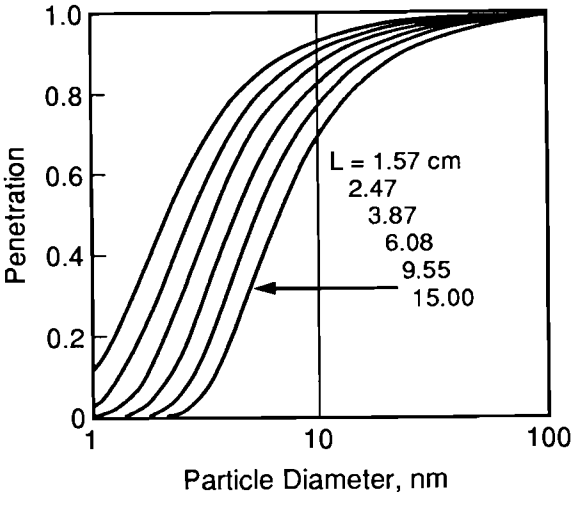

FIGURE 5. Penetration Through Six Different Lengths of Spectrometer Channel Calculated as Function of Particle Diameter

measured distribution of α tracks. Based on the calculated penetration values for each segment, the activity-weighted size distribution of particles that deposited in the spectrometer channel can be unfolded from the measured penetration profile of α activity. We are developing an unfolding procedure based on the method of Wolfenbarger and Seinfeld (1990). We are also developing the software needed to calculate the activity-size distribution of unattached radon progeny, the total airborne concentration of potential α energy, and the "unattached fraction" directly from the α-track densities measured along the spectrometer channel and on the CR-39 chip that records activity on the final filter.

We expect the URPSS to improve significantly the characterization of radon-progeny exposures of laboratory animals and thus the modeling of doses received by target tissues in the respiratory tract. The URPSS will also enable economical characterization and monitoring of human exposures to unattached radon progeny at low concentrations in indoor air for a wide variety of situations, with integrated averages over extended, and thus representative, periods of exposure.

References Cited

Cheng, Y. S., G. K. Hansen, Y. F. Su, H. C. Yeh, and K. T. Morgan. 1990. Deposition of ultrafine aerosols in rat nasal molds. *Toxicol. Appl. Pharmacol.* 106:222-233.

Fews, A. P. 1986. Fully automated image analysis of alpha particle and proton etched tracks in CR-39. *Nucl. Tracks* 12:221-225.

Hatzialekou U., and D. L. Henshaw. 1988. Automated image analysis of alpha-particle autoradiographs of human bone. *Nucl. Instrum. Methods* 263:504-514.

Ramamurthi, M., and P. K. Hopke. 1991. An automated, semicontinuous system for measuring indoor radon progeny activity-weighted size distributions, d_p: 0.5-500 nm. *Aerosol Sci. Technol.* 14:82-92.

Soderholm, S. C. 1979. Analysis of diffusion battery data. *J. Aerosol Sci.* 10:163-175.

Wolfenbarger, J. K., and J. H. Seinfeld. 1990. Inversion of aerosol size distribution data. *J. Aerosol Sci.* 21:227-248.

Growth Factors in Radiation Carcinogenesis

Principal Investigator: *F. C. Leung*

Other Investigators: *D. P. Chandler, J. F. Park, G. E. Dagle, and F. T. Cross*

This research project examines the involvement of growth factors (GF) and their receptors (GFR) in radiation-induced carcinogenesis of the lung in animals. We used immunocytochemical assays for detecting GF/GFR in lung tumors from dogs and rats exposed to inhaled radionuclides including $^{239}PuO_2$, $^{238}PuO_2$, $^{239}Pu(NO_3)_4$, and radon progeny. Immunocytochemical analysis of epidermal growth factor (EGF) receptor (EGFR) expression was performed on paraffin-block sections of 51 primary lung tumors from dogs exposed to inhaled plutonium and 6 primary lung tumors from control dogs. Four of six (67%) primary lung tumors from control dogs and 21 of 51 (41%) primary lung tumors from plutonium-(Pu-) exposed dogs stained positively. In the Pu-exposed dog lung tumors, EGFR-positive staining was observed in 2 of 5 epidermoid carcinomas, 11 of 19 bronchioloalveolar carcinomas, 5 of 15 papillary adenocarcinomas, and 3 of 11 adenosquamous carcinomas. In the control dog lung tumors, EGFR staining was positive in 2 of 2 bronchioloalveolar carcinomas, 2 of 3 papillary adenocarcinomas, and 0 of 1 adenosquamous carcinoma. EGFR-positive staining was observed in 1 of 16 dog lung tumors at the three lowest exposure levels and in 20 of 35 dog lung tumors at the two highest exposure levels. In radon-induced rat lung tumors, EGF, EGFR, transforming growth factor-alpha (TGF-α), and bombesin were found to be abnormally expressed. The abnormal expressions of these GF/GFR were mainly associated with epidermoid carcinoma of the lung and were not found in other histotypes.

Introduction

Radiation exposure causes DNA damage (double- and single-strand DNA breaks, chromosomal translocation, deletion, and mutation, etc.) and tumor development. The mechanisms of radiation-induced carcinogenesis are not known. Activation of oncogenes, deletion of suppressor genes, and abnormal expression of growth factor and growth factor receptor (GF/GFR) have been reported as being involved in the carcinogenesis processes in human lung cancers, but very few data are available for animal lung tumors, especially radiation-induced lung tumors.

Growth factors (GF) are polypeptides that regulate cell growth and differentiation through binding to specific cell membrane receptors; however, their function in cell growth and differentiation is complex. Recent advances in molecular cellular biology have provided links between GF, oncogenes, and cancer, including: (1) activation and overexpression of GF; (2) activation and overexpression of GF receptors (GFR); (3) activation of a postreceptor pathway that bypasses the GF requirement; and (4) suppression of an inhibitory GF such as TGF-β. Human lung tumor tissues synthesize many types of GF that are not usually found in normal lung tissues. Also, GFR binding is reportedly different in human normal and lung tumor tissue demonstrating that GF/GFR play a role in human lung tumorigenesis (Yamaguchi et al. 1989).

Epidermal growth factor (EGF) is a 53-amino-acid, small polypeptide with a molecular weight of 6045 that was first isolated from mouse salivary glands and was subsequently shown to be present in a variety of tissues. Regulation of EGF of cellular growth and proliferation is mediated by the binding of EGF to a specific membrane glycoprotein receptor with a molecular weight of 170,000. This epidermal growth factor receptor (EGFR) consists of an extracellular ligand binding domain, a transmembrane portion, and an intracellular domain with tyrosine kinase activity. The EGFR also phosphorylates a number of protein substrates in addition to mediating autophosphorylation of tyrosine residues located near the carboxyl terminal.

The molecular cellular role of EGF and its receptor in normal and disease states is under active investigation but the mechanism is still poorly understood. EGF has been shown to increase cell growth by increasing DNA synthesis and also to be involved in cell proliferation, differentiation, and wound healing in epithelial tissue. Conversely, EGF has also been shown to be a negative growth factor.

The EGFR gene shares a high significant homology to the *erb-B* family of oncogenes. The *V-erb-B* oncogene, derived from a strain of avian erythroblastosis virus, encodes a transforming protein with homology to a truncated form of EGFR that lacks the extracellular ligand binding domain. EGFR is overexpressed in various malignant tumors and appears to play an important role in the pathogenesis of these carcinomas. In human lung cancer, there are reports of increased EGFR using the radioreceptor binding assay and immunocytochemical assay (Berger et al. 1987; Cerny et al. 1986; Hwang et al. 1986; Sherwin et al. 1981; Sobol et al. 1987). The overexpression of EGFR is mainly associated with non-small-cell carcinomas of the lung, particularly with epidermoid carcinomas (Berger et al. 1987; Cerny et al. 1986; Sobol et al. 1987).

We recently reported increased EGFR expression in radiation-induced dog lung tumors by radioreceptor binding assay (Leung et al. 1991). Dog lung tumors are mainly non-small-cell carcinomas including epidermoid and adenocarcinomas; dogs do not have small-cell carcinomas. This report describes the cell types that overexpress EGFR in plutonium- (Pu-) induced dog lung tumors and radon progeny-induced rat lung tumors, as indicated by immunocytochemical assay. The rat lung tumors were also examined for EGFR, EGF, TGF-α, and bombesin.

Materials and Methods

Formalin-fixed, paraffin-embedded dog and rat lung tumor samples were obtained from our ongoing long-term experiments designed to determine the life-span dose-effect relationships of inhaled plutonium (dogs) and radon (rats). For the immunocytochemical staining procedure, we employed the standard procedure using the avidin-biotin complex (ABC) immunoperoxidase method. Reagents for the staining procedure were obtained from Vector Laboratories (Burlingame, California). A commercial monoclonal antibody (29.1) against EGFR from human-derived A431 cell membranes was purchased from Sigma (St. Louis, Missouri). Polyclonal rabbit antiserum generated against EGF was obtained from Collaborative Research Inc. (Bedford, Massachusetts); polyclonal goat antiserum against TGF-α was obtained from Biotop (Seattle, Washington); and a polyclonal rabbit antiserum against bombesin was obtained from ICN Immunobiologicals (Lisle, Illinois). The slides were counterstained with hematoxylin and examined by light microscopy. Sections were assessed subjectively, and tumor cells were graded as either positive or negative.

Results and Discussion

Plutonium-Induced Dog Lung Tumors

Dogs were exposed to either inhaled $^{239}PuO_2$, $^{238}PuO_2$, or $^{239}Pu(NO_3)_4$; 51 randomly selected primary lung tumors were obtained from Pu-exposed dogs and compared with 6 primary lung tumors from control dogs. Of the Pu-exposed dog lung tumors, 1 was from dose-level Group 1, 5 were from dose-level Group 2, 10 from dose-level Group 3, 27 from dose-level Group 4, and 8 from dose-level Group 5. Histopathological diagnosis followed the W.H.O. classification system.

The results of anti-EGFR monoclonal antibody staining with control and Pu-induced dog lung tumors are shown in Table 1. Four of 6 (67%) control dog lung tumors stained positively for EGFR, whereas 21 of 51 (41%) of the lung tumors from Pu-exposed dogs stained positively. Most dog lung tumor (16/21, 76%) staining was heterogeneous and patchy; in a few tumors (5/21, 24%), however, staining was homogeneous. Most positive-staining tumor cells displayed moderate to strong staining intensity. Examples of anti-EGFR monoclonal antibody staining of control and exposed dog lung tumors are shown in Figure 1. There were no obvious differences in the characteristics of 29.1 staining between EGFR-positive lung tumors on the basis of histopathological classification. In the Pu-exposed dog lung tumors, EGFR staining was positive in 2 of 5 epidermoid carcinomas, 11 of 19 bronchioloalveolar carcinomas, 5 of 15 papillary adenocarcinomas, and 3 of 11 adenosquamous carcinomas. In the control dog lung tumors, EGFR staining was positive in 2

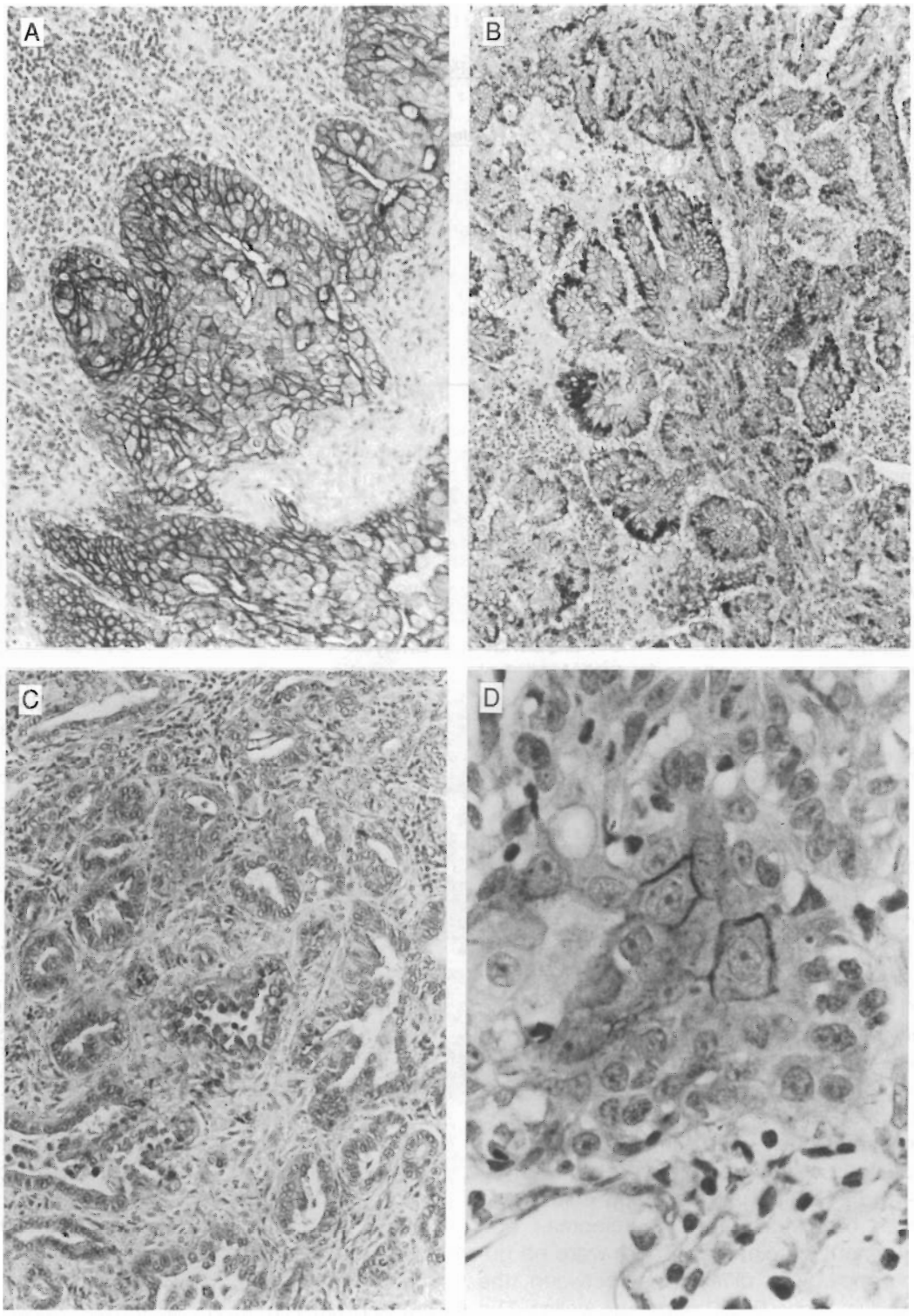

FIGURE 1. (A) Epidermoid Carcinoma Immunostained with Anti-Epidermal Growth Factor Receptor (anti-EGFR) Shows Intense Homogeneous Immunoreactivity. (B) Papillary Adenocarcinoma Immunostained with Anti-EGFR. Most tumor cells stained positively; note few negative-staining cells. (C) Bronchioloalveolar Carcinoma Immunostained with Anti-EGFR. Most cells immunostained distinctly although variably. (D) Epidermoid Carcinoma Immunostained with Anti-EGFR. Note variable staining.

TABLE 1. Anti-EGFR Monoclonal Antibody Staining of Lung Tumors from Control and Plutonium-Exposed Dogs

Dose-Level Group	Mean Initial Lung Deposition (nCi/g lung)	Number Positive/Number Examined					
		Epidermoid Carcinoma	Bronchiolo-alveolar Carcinoma	Papillary Adenocarcinoma	Adenosquamous Carcinoma	Solid Carcinoma	Total Carcinoma
Control	0	0/0	2/2	2/3	0/1	0/0	4/6
1	~0.01	0/1	0/0	0/0	0/0	0/0	0/1
2	0.18	0/2	1/3	0/0	0/0	0/0	1/5
3	0.53	0/0	0/1	0/7	0/2	0/0	0/10
4	2.33	0	8/10	5/8	3/8	0/1	16/27
5	9.53	2/2	2/5	0/0	0/1	0/0	4/8
Total Carcinoma (exposed)		2/5	11/19	5/15	3/11	0/1	21/51

of 2 bronchioloalveolar carcinomas, 2 of 3 papillary adenocarcinomas, and 0 of 1 adenosquamous carcinoma. In relationship to different dose-exposure groups, there seemed to be fewer EGFR-positive reactions among dose-level groups 1 through 3 (0/1, 1/5, and 0/10) compared to dose-level groups 4 and 5 (16/27, 4/8). We have observed that anti-EGFR monoclonal antibody also stained normal bronchial epithelium identified within positive lung tumor sections in 1 of 4 control dog lung tumors and 16 of 21 lung tumors from Pu-exposed dogs. In addition, there were no apparent morphological differences between EGFR-positive and EGFR-negative lung tumor cells.

The immunocytochemical localization of EGFR in lung tumors of dogs confirmed our earlier observations of elevated EGFR determined by the radioreceptor binding assay (Leung et al. 1991). The radioreceptor binding assay demonstrated that EGFR increased as much as 10 fold in Pu-induced dog lung tumors compared to normal lungs. The immunocytochemical procedure, although it did not provide the quantitative data obtained with radioreceptor binding assays, demonstrated specific cell types associated with EGFR expressions that had not previously been demonstrated in lung tumors of dogs. We have observed both EGFR-positive- and EGFR-negative-staining epidermoid carcinomas, bronchioloalveolar carcinomas, and adenosquamous carcinomas. There were no obvious morphological differences between the EGFR-positive and EGFR-negative cells. The existence of EGFR-positive and EGFR-negative cells in epidermoid carcinomas and adenocarcinomas may reflect variations in the differentiation status among these carcinomas.

We used a commercial monoclonal antibody that is generated against a human cervical cancer cell line membrane, A431, because the canine EGF and EGFR have not been purified and characterized. This monoclonal antibody has been demonstrated to have a strong reactivity to dog liver EGF receptor. It is important for future research to purify the dog EGFR for sequence analysis and for use as ligand and reagent for generating antibodies and to clone the EGFR genomic gene and cDNA for sequence analysis and comparison to the human sequence.

Our current data agree well with the EGFR expression found in human lung epidermoid carcinomas and adenocarcinomas (Berger et al. 1987; Cerny et al. 1986; Sobol et al. 1987). The percentage of EGFR-positive epidermoid carcinomas in human lung tumors ranged from 62% to 100% and the percentage of EGFR-positive adenocarcinomas from 34% to 75%. There were no EGFR-positive-staining cells in small-cell carcinoma of the human lung tumors. The similar percentages of EGFR-positive and EGFR-negative tumor cells found in both epidermoid and adenocarcinomas suggest that Pu-induced dog lung tumors and human non-small-cell lung carcinoma share similar molecular and cellular abnormalities in terms of EGFR expression. Our data demonstrated that elevated EGFR expression may be one of the molecular cellular characteristics of radiation-induced lung tumors in the dog, and that EGF and its receptor may play a role in radiation-induced carcinogenesis of the dog lung. The data also suggested that radiation-induced dog lung tumors may be a suitable animal model for studying human non-small-cell lung carcinoma.

Radon-Induced Rat Lung Tumors

We have examined 72 radon-induced rat lung tumors for EGFR expression; 37 radon-induced rat lung tumors for EGF expression; 37 radon-induced rat lung tumors for TGF-α expression; 38 radon-induced rat lung tumors for bombesin expression; and 31 normal control rat lungs. One lung tumor from a control rat was also examined. There were no positive staining reactivities of anti-EGFR, anti-EGF, anti-TGF-α, and anti-bombesin with the 32 lung samples from normal control rats (data not shown). The control rat lung tumor, a histocytoma, did not stain positively with anti-EGFR, anti-EGF, anti-TGF-α, and anti-bombesin.

The results of anti-EGFR reactivity with radon-induced rat lung tumors and the 1 tumor obtained from a control rat are summarized in Table 2. Twenty-six (36%) of 72 radon-induced rat lung tumors showed positive EGFR staining; the 1 lung tumor from a control rat showed no positive staining to EGFR antibody. When lung tumors were separated into different histopathological classifications, 25 of 37 radon-induced epidermoid carcinomas of the lung stained positively. In most cases, tumor expression of EGFR was heterogeneous and patchy. None of the other histopathological types of lung tumors stained positively except the squamous portion of adenosquamous carcinomas.

TABLE 2. Reactivity of EGFR Antibodies with Radon-Induced Rat Lung Tumors

	Number Examined	Number Positive	Percent Positive
Treatment			
Control	1	0	0
Radon-induced	72	26	36
Tumors			
Epidermoid carcinoma	37	25	68
Adenocarcinoma	30	0	0
Sarcoma	4	0	0
Adenosquamous carcinoma	1	1[(a)]	-

(a) Adenosquamous carcinoma; squamous portion positive.

The results of anti-EGF reactivity with radon-induced rat lung tumors and the tumor obtained from a control rat are summarized in Table 3. Sixteen (43%) of 37 radon-induced rat lung tumors showed positive EGF staining, and the 1 lung tumor from a control rat showed no positive staining to EGF antibody. When lung tumors were separated into different histopathological classifications, all 15 radon-induced epidermoid carcinomas of the lung stained positively. In most instances, tumor expression of EGF was heterogeneous and patchy. None of the other histopathological types of lung tumors stained positively except the squamous portion of adenosquamous carcinomas.

TABLE 3. Reactivity of EGF Antibodies with Radon-Induced Rat Lung Tumors

	Number Examined	Number Positive	Percent Positive
Treatment			
Control	1	0	0
Radon-induced	37	16	43
Tumors			
Epidermoid carcinoma	15	15	100
Adenocarcinoma	17	0	0
Sarcoma	4	0	0
Adenosquamous carcinoma	1	1[(a)]	-

(a) Adenosquamous carcinoma; squamous portion positive.

The results of anti-TGF-α reactivity with radon-induced rat lung tumors and the tumor obtained from a control rat are summarized in Table 4. Sixteen (43%) of the 37 radon-induced rat lung tumors showed positive TGF-α staining; the 1 lung tumor from a control rat showed no positive staining to TGF-α antibody. When lung tumors were separated into different histopathological classifications, all 15 radon-induced epidermoid carcinomas of the lung stained positively. In most instances, tumor expression of TGF-α was also heterogeneous and patchy. None of the other histopathological types of lung tumors stained positively except the squamous portion of adenosquamous carcinomas.

TABLE 4. Reactivity of TGF-α Antibodies with Radon-Induced Rat Lung Tumors

	Number Examined	Number Positive	Percent Positive
Treatment			
Control	1	0	0
Radon-induced	37	16	43
Tumors			
Epidermoid carcinoma	15	15	100
Adenocarcinoma	17	0	0
Sarcoma	4	0	0
Adenosquamous carcinoma	1	1[(a)]	-

(a) Adenosquamous carcinoma; squamous portion positive.

The results of anti-bombesin reactivity with radon-induced rat lung tumors and the tumor obtained from a control rat are summarized in Table 5. Sixteen (42%) of the 38 radon-induced rat lung tumors showed positive bombesin staining; the 1 lung tumor from a control rat showed no positive staining to bombesin antibody. When lung tumors were separated into different histopathological classifications, 15 of 16 radon-induced epidermoid carcinomas of the lung stained positively. In most instances, tumor expression of bombesin was also heterogeneous and patchy. None of the other histopathological types of lung tumors stained positively except the squamous portion of adenosquamous carcinomas.

TABLE 5. Reactivity of Bombesin Antibodies with Radon-Induced Rat Lung Tumors

	Number Examined	Number Positive	Percent Positive
Treatment			
Control	1	0	0
Radon-induced	38	16	42
Tumors			
Epidermoid carcinoma	16	15	94
Adenocarcinoma	17	0	0
Sarcoma	4	0	0
Adenosquamous carcinoma	1	1[(a)]	-

(a) Adenosquamous carcinoma; squamous portion positive.

We have demonstrated that the expression of EGFR, EGF, TGF-α, and bombesin in radon-induced rat lung tumors is significantly elevated compared to that in normal rat lung tissue as determined by immunocytochemical assay. The abnormal expression of EGFR, EGF, TGF-α, and bombesin was predominantly associated with epidermoid carcinomas. Current data showing positive expression of GF/GFR in radon-induced rat lung tumors agree well with previous radioreceptor binding assay data showing significantly elevated EGFR in Pu-induced dog lung tumors when compared with normal dog lung tissue (Leung et al. 1991). Elevated EGFR levels were also demonstrated by Immunocytochemical analyses of Pu-induced dog lung tumors. These results suggest that the immunocytochemical assay is useful for identifying and characterizing abnormal expression of GF/GFR in radiation-induced animal lung tumors.

Our results do not definitely rule out GF/GFR expression in radon-induced adenocarcinomas. The low levels of GF/GFR expression in radon-induced adenocarcinomas may not have been detectable in our assays. We have demonstrated that the immunocytochemical assay is less sensitive in measuring abnormal expressions of EGFR than is the radioreceptor binding assay when the same tissue samples are examined. Therefore, it is important that additional assays such as radioimmunoassay and northern blot analysis corroborate the abnormal expression of GF/GFR. However, the immunocytochemical assay does provide relative differences in expression among cell types.

Abnormal expressions of GF/GFR found in radon-induced rat lung tumors do not necessarily imply a causal relationship, because oncogenesis has been demonstrated to be a multistep process. The definitive molecular and cellular mechanism of abnormal expressions of GF/GFR in radon-induced cancer remains to be determined and can be studied in gene transfer experiments. Flavin et al. (1990) reported that bovine lung fibroblasts exposed to a 5-Gy radiation dose showed growth factor release into conditioned medium, and Shoji et al. (1990) demonstrated that human lung fibroblasts produced an apparent 6000-dalton growth factor that possessed growth stimulatory activity for bronchial epithelial cells. These studies

demonstrated that lung cells are capable of producing GF and possibly GFR. It would be useful to examine early GF/GFR gene expression in rat lung cells exposed to radon in vitro and compare it with the expression of GF/GFR found in carcinomas.

It is well established that human lung tumors are hormone-producing tumors, and it has also been shown that many human lung tumors possess abnormal expression of GF/GFR. In many instances, multiple hormones and GF/GFR are produced by human lung carcinomas. Even though the multiple production of hormones and GF/GFR is a rather common feature in human lung carcinomas, the exact biological significance of such phenomena is not known. Because GF/GFR are involved in normal cell growth and differentiation, and because their abnormal expression has been shown to be associated with human carcinomas, it has been suggested that abnormal expressions of GF/GFR may be involved in oncogenesis in the human lung. It is reasonable to hypothesize that different profiles of GF/GFR expression may also reflect variations in the differentiation or histogenesis of lung carcinomas. In addition, there seems to be a significant difference in GF/GFR expression between human small-cell and non-small-cell carcinomas. Such differences in GF/GFR expression in human lung tumors suggest that characterizing the expression of GF/GFR in humans may find application in distinguishing clinically significant subtypes of lung carcinomas. Our current results suggest that radon-induced rat lung and human lung carcinomas may share a similar molecular and cellular pathway as regards the expression of GF/GFR during carcinogenesis.

References Cited

Berger, M. S., W. J. Gullick, C. Greenfield, B. J. Addis, and M. D. Waterfield. 1987. Epidermal growth factor receptors in lung tumours. *J. Pathol.* 152:297-307.

Cerny, T., D. M. Barnes, P. Hasleton, P. V. Barber, K. Healy, W. Gullick, and N. Thatcher. 1986. Expression of epidermal growth factor receptor (EGF-R) in human lung tumours. *Br. J. Cancer* 54:265-269.

Flavin, M. P., L. A. Parton, and C. M. Bowman. 1990. Conditioned medium from irradiated bovine pulmonary artery endothelial cells stimulates increased protein synthesis by irradiated bovine lung fibroblasts in vitro. *Exp. Lung Res.* 16:405-422.

Hwang, D. L., T. Yee-Chaw, S. S. Lin, and A. Lev-Ran. 1986. Expression of epidermal growth factor receptors in human lung tumors. *Cancer* 58:2260-2263.

Leung, F. C., L. R. Bohn, and G. E. Dagle. 1991. Elevated epidermal growth factor reception binding in plutonium-induced lung tumors from dogs. *Proc. Soc. Exp. Biol. Med.* 196:385-389.

Sherwin, S. A., J. D. Minna, A. F. Gazdar, and G. J. Todaro. 1981. Expression of epidermal and nerve growth factor receptors and soft agar growth factor production by human lung cancer cells. *Cancer Res.* 41:3538-3542.

Shoji, S., K. A. Rickard, H. Takizawa, R. F. Ertl, J. Linder, and S. I. Rennard. 1990. Lung fibroblasts produce growth stimulatory activity for bronchial epithelial cells. *Am. Rev. Respir. Dis.* 141:433-439.

Sobol, R. E., R. W. Astarita, C. Hofeditz, H. Masui, R. Fairshter, I. Royston, and J. Mendolsohn. 1987. Epidermal growth factor receptor expression in human lung carcinomas defined by a monoclonal antibody. *J. Natl. Cancer Inst.* 79:403-407.

Yamaguchi, K., K.-I. Imanishi, K. Maruno, Y. Miyake, Y. Shimosata, and K. Abe. 1989. Lung cancer and autocrine growth factors. *Chest* 96:29S-31S.

Oncogenes in Radiation-Induced Carcinogenesis

Principal Investigator: *M. E. Frazier/G. L. Stiegler*

Other Investigators: *E. Sisk, L. C. Stillwell, T. M. Seed,[a] M. E. Foreman, and R. P. Schneider*

We are studying the role of activated oncogenes in radiation-induced carcinogenesis. Lung tumor and leukemic cells have been obtained from studies of life-span dose-effect relationships in experimental animals exposed to either plutonium, inhaled radon progeny, or external whole-body radiation. We have done molecular analysis of the *ras* oncogene family in selected samples using the polymerase chain reaction (PCR) method and direct DNA sequencing of the amplified gene products. We have identified specific activating *ras* mutations in about one-half of the samples and are characterizing their frequency and specficity to the particular source of inducing radiation. Ultimately, we will use the accumulated data to describe a pattern of genetic change that might provide a basis for distinguishing damage caused by different forms of radiation and chemical mutagens.

More than 30 oncogenes have been identified and partially characterized. None has been totally biochemically defined as to its specific cellular function. It is generally agreed that the known oncogenes are directly or indirectly connected to cellular proliferation or to a specific developmental process, that is, their genetic expression is important to the flow of specific information bringing about these biological events. Experimental evidence strongly indicates that the molecular changes which activate proto-oncogenes (the normal cellular oncogene counterpart) result from point mutations, translocations, and deletions, and that the resulting gene protein product is altered so that its normal cellular function is altered. The end result is carcinogenesis.

Our preliminary analysis of radiation-induced canine malignancies indicates that dominant-acting oncogenes are present in DNA prepared from these canine tumors. These data were obtained from NIH 3T3 transformation assays using isolated canine lung tumor DNA. Experimental data from other groups have shown that the activated genes causing the NIH 3T3 transformation often belong to the *ras* gene family. We previously reported experimental evidence of *ras* gene activation in radiation-induced canine tumors showing tumor-specific restriction fragment-length polymorphisms and elevated levels of *ras* gene transcription.

Initial studies have focused on activation of the *ras* oncogene family, which contains the best-characterized group of oncogenes at both the molecular and the biochemical level. Published experimental data about the chemical induction of these genes provide our study of radiation activation with a large database of comparable chemical methods of activation (Table 1). Mammalian *ras* genes are activated and acquire transforming potential by alteration in their coding sequence, most often brought about by single-point mutations.

These point mutations have been localized in codons 12, 13, 59, and 61. The presence of a glycine residue at position 12 appears to be necessary for normal gene function; substitution of any other amino acid except proline results in gene activation. Substitution of glutamic acid at codon 61 by any other amino acid residue except proline or glutamine yields an activated *ras* gene. The exact function of the *ras* proteins is not known, but they closely approximate the biochemical properties of G proteins, which are involved in the modulation of signal transduction through transmembrane signaling systems. Through these systems, *ras* proteins play a role in cell proliferation and possibly terminal differentiation.

(a) Argonne National Laboratory, Argonne, Illinois.

TABLE 1. Activation of *ras* Oncogenes in Carcinogen-Induced Tumors

Species	Carcinogen	Tumor	*ras* gene	Incidence, %
Rat	NMU[a]	Mammary carcinoma	H-*ras*	86
	DMBA[a]	Mammary carcinoma	H-*ras*	23
	DMN[b]	Kidney mesenchymal	K-*ras*	40
Mouse	DBACR[c]	Skin carcinoma	H-*ras*	80
	DMBA[d]	Mammary carcinoma	H-*ras*	100
	MCA[e]	Thymic lymphoma	K-*ras*	80
	HOAFF[f]	Hepatocellular carcinoma	H-*ras*	100
	VC[f]	Hepatocellular carcinoma	H-*ras*	100

(a) Zarbl, H., A. V. Sukumar, M.-Z. Dionisio, and M. Barbacid. 1985. Direct mutagenesis of Ha-*ras*-1 oncogenes by *N*-nitroso-*N*-methylurea during initiation of mammary carcinogenesis. *Nature* 315:382-385.

(b) Sukumar, S., A. Perantoni, C. Reed, J. Rice, and M. L. Wenk. 1986. Activated K-*ras* and N-*ras* oncogenes in primary renal mesenchymal tumors induced in F344 rats by methyl-(methoxymethyl)-nitrosamine. *Mol. Cell. Biol.* 6:2716-2720.

(c) Bizub, D., A. W. Wood, and M. S. Skalka. 1986. Mutagenesis of the Ha-*ras* oncogene in mouse skin tumors induced by polycyclic aromatic hydrocarbons. *Proc. Natl. Acad. Sci. USA* 83:6048-6052.

(d) Dandekar, S., S. Sukumar, H. Zarbl, L. J. Young, and R. D. Cardiff. 1986. Specific activation of the cellular Harvey-*ras* oncogene in dimethylbenzanthracene-induced mouse mammary tumors. *Mol. Cell. Biol.* 6:4104-4107.

(e) Eva, A., and S. A. Aaronson. 1983. Frequent activation of c-*kis* as a transforming gene in fibrosarcomas induced by methylchoanthrene. *Science* 220:955-956.

(f) Wiseman, R. W., S. J. Stowers, E. C. Miller, M. W. Anderson, and J. Miller. 1986. Activating mutations of the c-Ha-*ras* proto-oncogene in chemically induced hepatomas of the male B6C3F mouse. *Proc. Natl. Acad. Sci. USA* 83:5825-5829.

Identification of the receptor and effector systems that interact with the *ras* proteins has so far been elusive, although some experimental evidence connects *ras* and the epidermal growth factor that enhances the *ras* protein guanosine 5'-diphospate (GDP) binding activity.

The tumor material that we are analyzing to provide a large database on radiation-induced *ras* gene activation has been fixed in formalin and embedded in paraffin, or frozen. This material can be used for detailed molecular analysis by the polymerase chain reaction (PCR) method. Only small quantities of valuable assay material are required; less than 1 μg of DNA or total cellular RNA is necessary per assay.

Preliminary DNA sequencing of canine genomic material was necessary to establish the normal molecular structure of the H-, K-, and N-*ras* gene 1st and 2nd exons (Figures 1A and 1B, respectively). The sequences have been obtained either directly from PCR-amplified material or from DNA sequence analysis of molecular clones isolated from a canine-specific genomic or cDNA library (the cDNA library was commercially obtained from Stratagene, Inc.).

Direct DNA sequence analysis of frozen plutonium-induced lung tumor samples has so far not shown *ras* gene mutational activation in the regions of the 12th and 61st codons. This does not preclude the event of mutations in these regions; it only predicts that a more careful analysis of the samples must be made using molecular cloning techniques. We have previously reported (see *Pacific Northwest Laboratory Annual Report for 1989 to the DOE Office of Energy Research, Part 1*) that one tumor we examined had an alteration in amino acid codons 15 and 16 of the N-*ras* 1st exon. These mutations resulted in a change in the amino acid specificity at these two positions. The codon changes have not been reported in the literature for any mammalian species, and it is not known whether these mutations cause *ras* gene transforming activity.

We have examined DNA from frozen spleen samples of dogs with myelomonocytic leukemia induced by whole-body gamma radiation. Direct DNA sequence analysis of the K-*ras* 1st exon PCR products has revealed a transformation-specific mutation in the 12th codon. The autoradiograph of the sequencing gel (Figure 2) shows a mixture of nucleotide bases at the second position of the codon where the sequence GGT (glycine) has been replaced by GTT (valine) in what we assumed to be a background of normal 1st exon sequences. When we further characterized the mutation and determined its frequency in the tumor by cloning and sequencing individual products of the PCR reaction, we found that the amplified material consisted of sequences of H-, K-, and N-*ras* 1st exons rather than a mixture of

(A)

K-ras first exon

5'-ATG ACT GAG TAC AAA CTG GTG GTG GTT GGA GCT GGT GGC
GTA GGC AAG AGT GCC TTG ACG ATA CAG CTA ATT CAG AAC
CAT TTT GTG GAC GAA TAT GAT CCC ACC ATA GAG- 3'

N-ras first exon

5'-ATG ACT GAG TAC AAA CTG GTG GTG GTT GGA GCA GGT GGT
GTT GGG AAA AGC GCA TCG ACA ATG CAG CTA ATC CAG AAC
CAC TTT GTA GAT GAA CAC GAC CCC ACC ATA GAG- 3'

H-ras first exon

5'-ATG ACT GAG TAC AAA CTG GTG GTG GTG GGC GCT GGA GGC
GTG GGA AAG AGT GCC CTG ACC ATC CAG CTG ATC CAG AAC
CAT TTT GTG GAC GAA TAT GAT CCC ACC ATA GAG- 3'

(B)

K-ras second exon

5'-GAT TCC TAC AGG AAG CAA GTA GTA ACC GAT GGA GAA ACC TGT CTC
TTG GAT ATT CTC GAC ACA GCA GGT CAA GAG GAG TAC GGT GCA ATG
AGG GAC CAG TAC GTG AGG ACT GGG GAG GGC TTT CTT TGT GTG TTT
GCC ATA AAT AAT ACT AAA TCA TTT GAA GAT ATT CAC CAT TAT- 3'

N-ras second exon

5'-GAT TCT TAC CGA AAA CAG GTG GTT ATA GAC GGT GAA ACC TGT CTG
TTG GAT ATA CTG GAT ACA GCT GGT CAA GAA GAG TAC AGT GCC ATG
AGA GAC CAA TAC ATG AGG ACA GGC GAA GGC TTC CTC TGT GTA TTT
GCC ATC AAT AAT AGC AAA TCA TTT GCA GAC ATT AAC CTC TAC -3'

H-ras second exon

5'-GAC TCC TAC CGG AAA CAG GTG GTC ATT GAT GGG GAG ACG TGT TTA
CTG GAC ATC TTA GAC ACA GCA GGT CAA GAA GAG TAT AGT GCC ATG
CGG GAC CAG TAC ATG CGC ACA GGG GAG GGC TTC CTC TGT GTA TTT
GCC ATC AAC AAC ACC AAG TCC TTC GAG GAC ATC CAT CAG TAC- 3'

FIGURE 1. (A) Sequences of K-*ras*, N-*ras*, and H-*ras* 1st exons. Sequences used for primers are underlined. Primers were chemically synthesized with restriction sites to facilitate molecular cloning. (B) Sequences of K-*ras*, N-*ras*, and H-*ras* 2nd exons. Primer sequences are underlined.

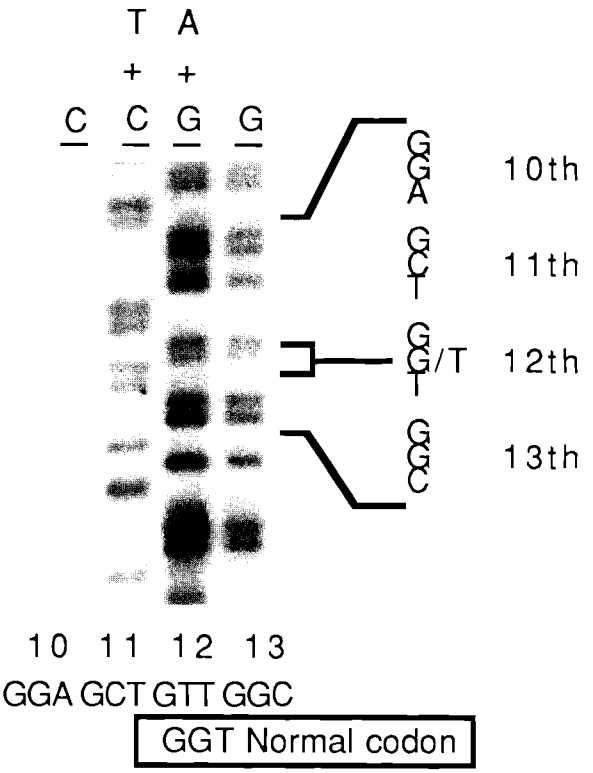

FIGURE 2. Chemical sequence analysis of polymerase chain reaction- (PCR-) amplified canine K-*ras* 1st exon from dog myeloid leukemia cells. Interpretation of banding patterns in autoradiograph are shown above photograph. The 10th, 11th, 12th, and 13th codons are identified on right. Double banding pattern is seen in middle base of 12th codon. Coding sequence and normal 12th codon sequence are shown below photograph.

normal and mutated K-*ras* 1st exons. The sequences were predominantly K-*ras* and N-*ras* with H-*ras* occurring at a frequency of approximately 1 in 10 examined. The amplification mixture resulted from the design of the PCR primers, which match the first 20 bases of coding sequence on the 5' and 3' terminus of the 1st exon, in this case N-*ras*.

The sequences of the K-, N-, and H-*ras* 1st exon are highly homologous with H-*ras* being the most divergent. Obtaining this mixture proved to be fortuitous. When we examined the nucleotide sequence of the H-*ras* gene, another activating lesion was found in its 12th codon in which GGA, normally coding for glycine, was altered to AGA. The codon is now specific for arginine and brings about *ras* transformational activation. The sequence and interpretation are shown in Figure 3. We are currently performing a detailed analysis of the *ras* 1st and 2nd exon sequences in a number of the chronic myeloproliferative (CMP) tumors and have found the K-*ras* 1st exon lesions in four CMP tumors and the H-*ras* mutation in two of the four CMP tumors examined. Analysis of the K-, N-, and H-*ras* 2nd exon sequences has not been completed.

We have preliminary evidence of K-*ras* activation in radon-induced rat lung tumors. One tumor has been characterized and shown to have an altered 12th codon (GGT altered to GTT), changing the amino acid preference from the normal glycine to valine, similar to the CMP observation discussed previously. We are now examining control and tumor samples to determine the frequency and significance of this lesion in radon-induced carcinogenesis.

Translocations are important in defining a chromosomal basis of neoplasia. Many chromosomal translocations have been defined in malignant myeloid diseases, and certain chromosomal defects are consistently associated with some types of human cancer. One of the first translocations identified was the 9;22 translocation in human chronic myeloid leukemia (CML), which became known as the Philadelphia (Ph) chromosome. It is important to identify and, if possible, clone the genes involved at the rearrangement site, which probably have functions that are critical to cellular growth potential. The gene that is associated with the Ph translocation is the Abelson (*abl*) proto-oncogene located on human chromosome 9. This *abl* proto-oncogene has sequence homology with the viral oncogene (*v-abl*) first isolated from a mouse pre-B-cell leukemia.

We are characterizing the molecular arrangement of the *abl* gene in the dog genome. Our interest is in investigating the *abl* gene locus and its possible association with an observed canine cytogenetic alteration in the q arm of the karyotypic first chromosome. This rearrangement has been observed in a number of animals that either have or are developing radiation-induced chronic myeloproliferative disorders. In humans, the locus for the *abl* gene is large, more than 200 kbp; it is a logical assumption that the canine gene size is equivalent. We will analyze the *abl* gene with

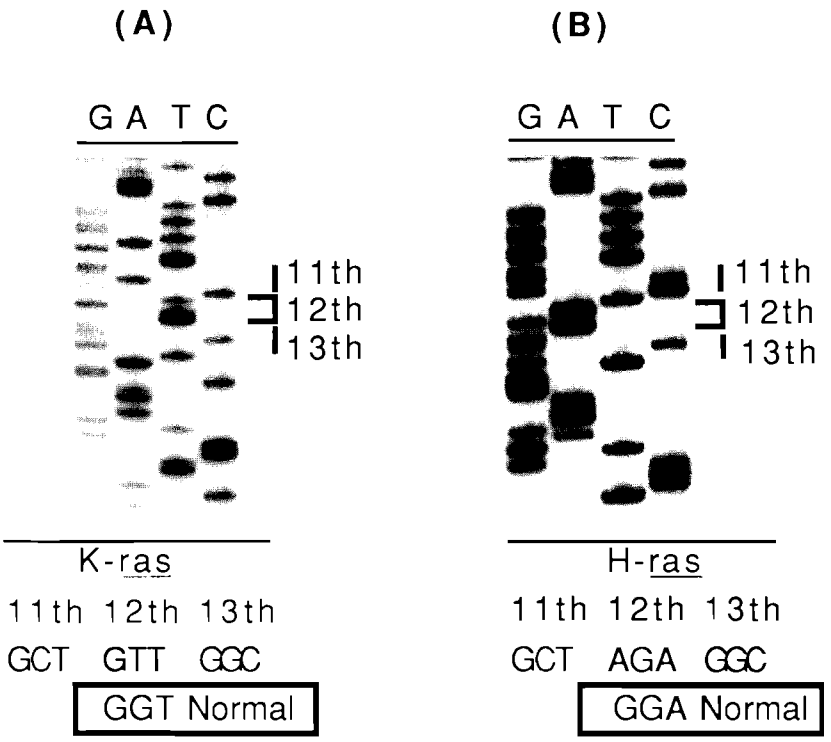

FIGURE 3. Dideoxy sequencing gel autoradiograms of canine K-*ras* (A) and H-*ras* (B) gene 1st exons. Specific lanes are marked at top of photographs as G, A, T, or C; regions of the 11th, 12th, and 13th codons of A and B are indicated on right; specific gene and codon sequences are shown below each photograph. Normal 12th codon sequence is below codon 12.

pulse-field gel electrophoresis (PFGE), a technique capable of separating large DNA restriction fragments (100,000 to 2.5 million bp). The probes used for detection of *abl* gene rearrangement, the *v-abl* cDNA clone, and specific canine PCR-generated *abl* gene fragments, will be labeled and used for PFGE/Southern blot analysis of canine CML DNA samples.

In addition to detailed DNA sequence information, we hope to provide more information on gene expression in tumors identified with an activated *ras* gene. We have available frozen tumor material suitable for analysis of isolated mRNA. We are developing methods, using PCR, to directly amplify and sequence *ras*-specific mRNA transcripts (Figure 4). The method uses the retroviral enzyme reverse transcriptase to make a cDNA copy of the K-, N-, or H-*ras* sequence. Using standard PCR procedures, the cDNA copy is amplified, molecularly cloned, and examined for mutation by DNA sequence analysis. This information provides evidence that the gene is being transcribed and used as a translational template.

The myeloproliferative canine DNA samples provide more than the single experimental observation of a *ras* point mutation. The importance of this study focuses on the availability of tumor samples. Bone marrow as well as spleen samples have been collected from dogs at various stages in the progression of CMP disease. Each sample will provide a unique analytical time point. We intend to use the point mutations identified in K-*ras*, H-*ras,* and possibly *abl* as genetic markers for following the genetic malignant progression of the disease. It is hoped that a stage-specific pattern of mutational oncogene activation will be identified that will define sequential events leading to radiation-induced oncogenesis.

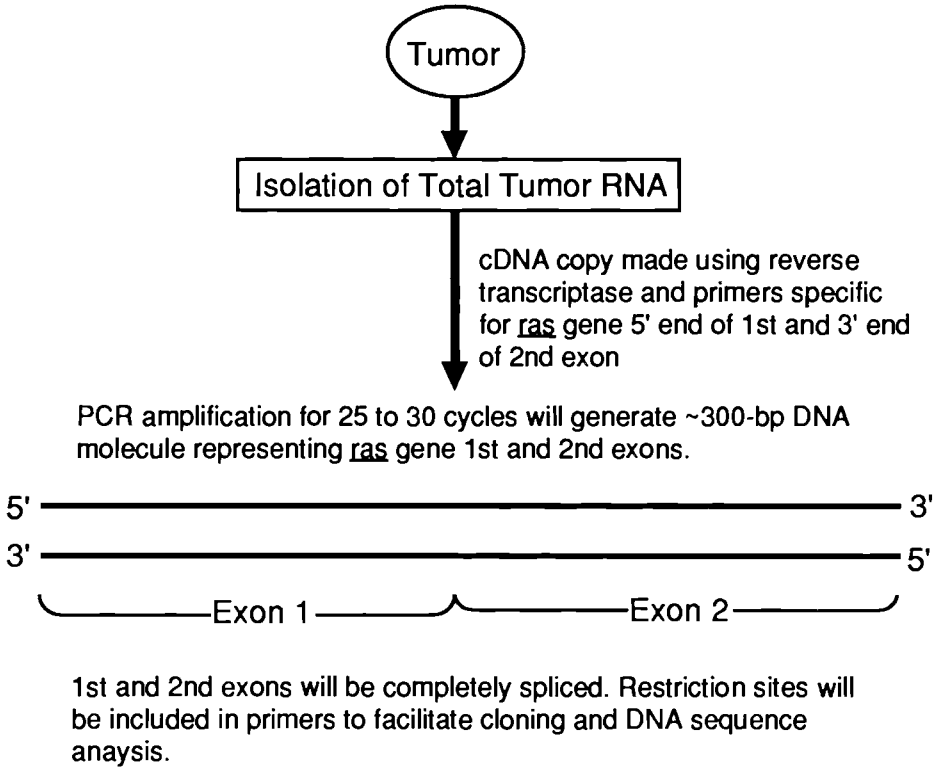

FIGURE 4. Amplification of mRNA by polymerase chain reaction. After reverse transcriptase copying using specific primers, resultant molecule respresents 1st and 2nd *ras* gene exons.

Mutation of DNA Targets

Principal Investigator: *R. P. Schneider*

Other Investigators: *J. E. Hulla, S. J. Rogers, and G. L. Stiegler*

The project is testing the hypothesis that tumor suppressor genes are important targets in radiation carcinogenesis. We have prepared specific DNA probes and primers to dog Rb and rat p53 genes to characterize their integrity in preserved tumor tissue from animals exposed to radiation. We have amplified, cloned, and analyzed the sequence of a 534-bp fragment of dog Rb cDNA. Methods and primers were developed for amplification and analysis of the rat p53 gene. Amplification of the p53 gene from rat genomic DNA results in amplification of fragments of the predicted size of a cDNA copy of the gene, suggesting the presence of a processed pseudogene.

During 1990, a study of mutation of tumor suppressor genes as targets in radiation carcinogenesis was started. The current objective is to characterize the status of these genes in radiation-induced cancer tissue.

The loss of function of the product of tumor suppressor genes apparently contributes to carcinogenesis. In other words, their *normal* function provides essential control of cell division. Defects in the gene, mRNA, or gene products of retinoblastoma susceptibility (Rb) and p53 genes have been observed in many tumor types. For Rb, these include human retinoblastoma, osteosarcoma, and small-cell carcinoma of the lung (SCCL). Defects in the p53 gene, mRNA, or protein have been commonly seen in human lung cancers of all types (except SCCL), in colorectal cancer, and in many other types. Transfection of transformed cells (or cotransfection with *ras* oncogenes) with either Rb or p53 cDNA can suppress the malignant phenotype. We suspect that tumor suppressor gene inactivation by deletions is a mechanism of radiation carcinogenesis, because evidence from PNL and elsewhere indicates that large deletions are a major component of genetic damage by ionizing radiation. It is possible, in radiation carcinogenesis, that tumor suppressor genes are inactivated by larger deletions than those characterized in cancers caused by other means, such as chemicals, thus providing a means to identify radiation-induced cancer.

Our approach is to examine p53 and Rb genes in tumor tissue preserved from life-span animal experiments at PNL and other DOE laboratories. We have a small number of frozen rat and dog lung tumors and dog bone tumors (osteosarcomas) induced by inhaled plutonium and radon. We also have a large number of plutonium-induced rat and dog lung tumors that have been fixed in formalin and embedded in paraffin. Myelogenous leukemia cells from dogs that were chronically exposed to x rays and gamma radiation at Argonne National Laboratory are also available. When tissue of sufficient quality is available, we plan to analyze Rb and p53 gene expression by analysis of their mRNA using the polymerase chain reaction (PCR) and northern blot methods. The fixed and embedded tissues do not have mRNA or large molecular weight DNA for northern or Southern analysis; thus, PCR is being used to amplify specific regions of these genes for analysis by gel electrophoresis. Further analysis by methods that detect base-pairing mismatches caused by mutations and deletions is also planned. The first step required for this approach has been to prepare primers for PCR and Rb gene-specific DNA probes for northern and Southern blot analysis.

Because the Rb gene is commonly defective in human osteosarcomas, and because dogs exposed to $^{239}PuNO_2$ and $^{238}PuO_2$ developed this form of cancer, we prepared reagents for analysis

of the dog Rb gene. The human Rb gene is encoded in 200 kb containing 27 exons with a 4.7-kb mRNA and a coding sequence of 2.7 kb; the human and mouse cDNA sequences are known but that of the dog is not. Our strategy was to amplify specific exons by PCR, assuming a high degree of sequence homology with the human gene, to design primers. We have amplified a segment with synthetic primers to human exon 17 from dog genomic DNA and a canine cDNA library. However, we have not been successful in obtaining amplification of other exons except in a fragment that includes exons 17 through 20 from the canine cDNA library. To verify that it is part of the dog Rb gene and to assess sequence homology with the human gene, we analyzed the sequence of this fragment after subcloning it in a plasmid. The sequence (Figure 1) is highly homologous to the human sequence, differing only by 43 base and 12 amino acid changes. The sequence differs from that of the mouse gene by 63 bases. We are now using this amplified fragment to screen the dog cDNA and cosmid libraries to obtain more information about its sequence and have probes for in situ hybridization. We will also use it as a probe to screen radiation-induced myelogenous leukemia cells of the dog by northern blot techniques for deletions in Rb mRNA. We plan to culture dog bone tumor cells that we have maintained frozen for investigation of Rb expression and size of its mRNA.

Because the rat p53 gene has yet to be cloned and sequenced, we used sequence information from the mouse gene to estimate the location and size of intervening sequences within the rat cDNA. The resulting gene structure is outlined in Figure 2. From reports of mouse investigations, we know that of the 11 exons, only exons 2 through 11 code for the protein product. The 1st exon is separated from the other coding regions by a 6100-bp intron and is spliced from the mRNA before protein synthesis. Additionally, in the human ortholog, mutational hot spots have been localized to the region encompassing exons 4 through 8. These findings allow us to focus our attention to the functionally significant regions of the gene; it is these sequences that have the greatest potential as markers for radiation-induced damage.

We plan to determine if deletions within the p53 gene have an increased occurrence in radiation-induced rat lung tumors compared to the surrounding normal tissue. We synthesized a series of primers and probes sufficient to amplify and detect each of the 10 coding exons of the gene. Using freshly isolated rat live DNA as a template, we effectively amplified 8 of the coding exons individually (Figure 3). Additionally, we amplified larger fragments of the gene to include most of the intervening sequences within the targeted region. These fragments are indicated by the underlined stretches of the gene in Figure 2; the products of the amplifications are shown in Figure 4. The identity of the amplification products was confirmed by blotting the fragments and probing with radiolabeled oligonucleotide (Figure 5). The probes consisted of sequences complementary to the predicted amplification products and were internal to the sequences used for priming the amplification. With these preliminary data for comparison, we began using formalin-fixed tissues as the source of p53 template. When we used DNA isolated from archived tissues, we successfully amplified fragments of the p53 gene containing exons 5 and 6 and exons 8 and 9 as well as the two intervening sequences. These fragments contain the sequences known to be altered most often in human tumors.

An interesting finding resulted from our initial investigations. When fragments containing more than one exon are amplified, two major products are apparent on agarose gels (see Figure 4). In each case, the size of the longer amplification product is consistent with the expected p53 gene fragment. The size of the shorter amplification products suggests that they are amplified from a processed (sans introns) p53 pseudogene in the rat genome. A pseudogene that includes the same priming sites will always be amplified in concert with the functional gene. Because the gene and putative pseudogene are distinguishable on the basis of size when the amplified fragment contains intron sequences, we plan to use the pseudogene as an internal control in our PCR assays. We are now attempting to confirm the identity of the shorter fragments with sequence analysis.

Our future direction is to use the assays we developed to compare the structure of p53 gene fragments amplified from a series of well-characterized, archived, normal and tumor tissues. Through these experiments, we will determine whether aberrations within the p53 gene are

HUMAN RB GENE BASE 1665

ACA GAT TTG TCT TTC CCA TGG GTT CTG AAT GTA CTT AAT
PCR Primer

TTA AAA GCC TTT GAT TTT TAC AAA GTG ATT GAA AGT TTT

ATC AAA GCA GAA GCC AAC TTG ACC AGA GAA ATG ATA AAA

CAT TTA GAA CGA TGT GAA CAT CGA ATC ATG GAA TCA CTT

GCA TGG CTC TCT GAT TCA CCT TTA TTT GAT CTG ATT AAA

CAA GCA AAA GAC CGA GAA GGA CCA GCT GAT CAC CTT GAA

TCT GCT TGT ACT CTG AAC CTT CCT CTC CAG AGT AAT CAC

ACT GCA GCA GAT ATG TAT CTT TCT CCT GTA AGA TCC CCA

AAG AAA AAA GGA TCA ACT ATA CGT GTA AAT TCT ACT GTA

AAC ACA GAG GCA CAA GCA ACC TCA GCC TTC CAG ACT CAG

AAG CCA TTG AAA TCT ACC TCC CTT TCA CTT TTT TAC AAA

AAA GTG TAC CGA CTA GCT TAT CTT CGA CTA AAT ACG CTG

TGT GCA CGC CTC CTA TCT GAC CAC CCA GAA CTA GAA CAC

ATC ATC TGG ACC CTT TTT CAG CAC ACA CTG CAA AAT GAG

TAT GAA CTC ATG AGA GAC AGG CAT TTG GA
PCR Primer

FIGURE 1. Sequence of Fragment of Dog Rb Gene Amplified by Polymerase Chain Reaction (PCR) from Canine cDNA Library was Obtained by Dideoxy Method Using Sequenase from Fragment Cloned into Plasmid pUC18. Underlined regions indicate PCR primer sequences; vertical lines indicate location of introns in human gene. Bases differing from human cDNA sequence have corresponding base in human gene printed above them; amino acid changes are shown below appropriate codon with human amino acid in parentheses.

significant to the tumorigenic process induced by radiation. This will lead to increased understanding of the mechanisms of radiation carcinogenesis. Further, we will characterize the nature of the genetic damage that inactivated the mechanisms.

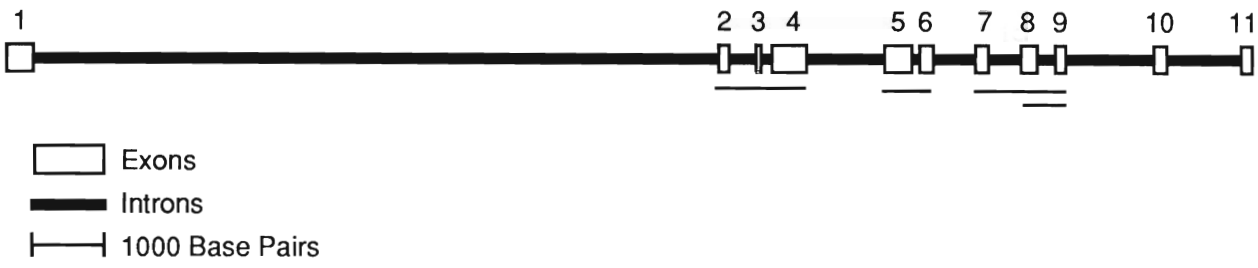

FIGURE 2. Schematic Pepresentation of Rat p53 Gene. Location and size of exons and introns have been estimated from sequence information from mouse and rat. Only exons 2 through 11 are coding sequences. Each of the exons 4 through 11, in addition to the underlined regions, have been successfully amplified (see Figures 3 and 4).

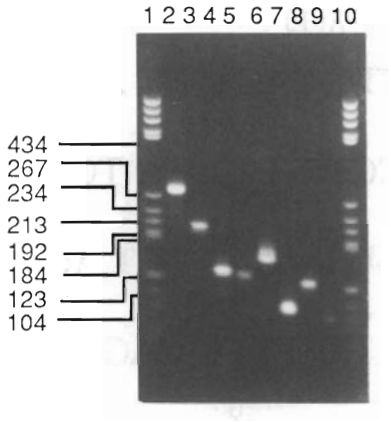

FIGURE 3. Amplification Products Were Electrophoretically Separated Using 2% Agarose Gel and Stained with Ethidium Bromide. Table below outlines contents of each lane with expected sizes of amplified fragments; apparent sizes are consistent with predicted sizes. Lanes 1 and 10 contain molecular size markers.

Lane	Exon	Predicted Size (bp)
2	4	278
3	5	204
4	6	133
5	7	131
68155		
7995		
810128		
911101		

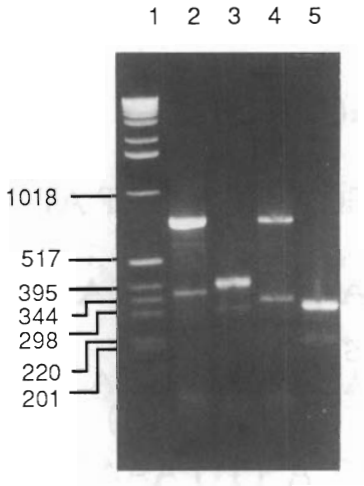

FIGURE 4. Amplification Products Were Electrophoretically Separated on 1.5% Agarose Gel and Stained with Ethidium Bromide. Table below outlines contents of each lane with expected sizes of amplified fragments. Apparent fragment sizes are consistent with predicted sizes. Lane 1 contains molecular size markers.

Lane	Primers Flank Exons	Predicted Size Gene/Pseudogene (bp)
2	2 and 4	740/380
3	5 and 6	397/317
4	7 and 9	741/341
5	8 and 9	310/230

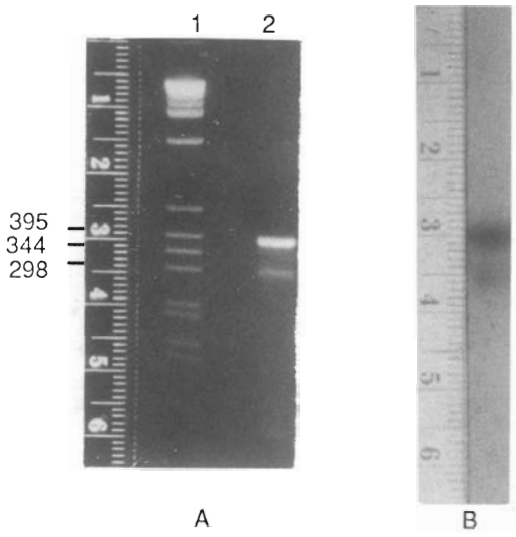

FIGURE 5. Primers flanking exons 5 and 6 Were Used to Amplify p53 Gene and Putative Pseudogene Fragments. (A) Amplification products were separated by electrophoresis on 1.5% agarose gel. Lane 1 contains molecular weight markers; lane 2 contains amplified gene and pseudogene fragments (molecular size given in numbers of base pairs). Gel was blotted to nylon membrane and probed with radiolabeled oligonucleotide having sequence complementary to internal stretch of exon 5. (B) Autoradiograph shows both fragments contain complementary exon 5 sequence.

Molecular Events During Tumor Initiation

Principal Investigator: *D. L. Springer*

Other Investigators: *D. B. Mann, G. L. Stiegler, and B. D. Thrall*

Many in vitro studies have been conducted with benzo[a]pyrene diol-epoxide (BPDE) binding to DNA; in vivo, however, this binding may be altered by association of numerous proteins with the DNA. The fundamental unit of DNA in chromatin is the nucleosome, where the DNA wraps around a core of histone proteins. At this level, the DNA lies on the surface of the protein core particles, and this association protects the DNA from nucleases. An unanswered question is: Does this close association between DNA and proteins protect the DNA from damage by chemical carcinogens or radiation? Studies with very small molecules such as dimethyl sulfate have indicated unrestricted access to the nucleosomal DNA, whereas larger molecules may bind preferentially to naked DNA over nucleosomal DNA. Because BPDE is a large bulky carcinogen, it may bind differently to chromatin compared to naked DNA. Further, BPDE intercalates into the DNA prior to covalently binding to the exocyclic amino groups of deoxyguanosine or deoxyadenine. This suggests that the influence of BPDE binding on chromatin structure may be critical to tumor initiation and progression. Thus, the purpose of our work includes determining: (1) the location and frequency of BPDE adducts to naked versus nucleosomal DNA; (2) the influence of BPDE adducts on nucleosome positioning; and (3) whether these adducts alter the expression of genes.

Many lines of evidence support the hypothesis that tumor initiation and development may involve adduct-induced changes in chromatin structure. It has been well established that many carcinogens either bind directly to DNA or are converted by mixed-function oxidases to reactive intermediates that covalently attach to the DNA. Although the relationship between covalent binding and tumor yield is only loosely correlated, this mechanism for tumor initiation has been widely accepted. Studies designed to obtain fundamental information about the way the three-dimensional structure of chromatin is involved in gene regulation have indicated that actively transcribed chromatin is more loosely coiled than other forms of chromatin and thus is more susceptible to nuclease digestion. Thus, it is not surprising that certain oncogenes have sensitivity to nuclease digestion that increases throughout tumor progression.

It is known that benzo[a]pyrene-diol-epoxide (BPDE) binds to DNA and inhibits its replication (Mizusawa and Kakefuda 1979). However, little is known about the effects of BPDE adducts on transcriptional processes. Bulky DNA adducts may alter transcriptional regulatory processes in genes, and this may ultimately contribute to the progression of malignancy. For example, recessive-acting anti-oncogenes or other tumor-suppressing genes may be key targets for adduction, and altered transcription of these may contribute to the carcinogenic process. An early study by Leffler et al. (1977) demonstrated that adduction of calf thymus DNA with BPDE resulted in decreased average RNA chain length. Studies by Koostra et al. (1989) also demonstrated that transcription was inhibited when as little as 0.01% of pGAL plasmid DNA was modified by BPDE. In fact, Koostra et al. (1989) showed that transcription of BPDE-modified plasmid DNA was terminated in a region that contains GC-box sequences (GGGCGG), which are important eukaryotic promoter elements found in the 5′ region of some oncogenes. Koostra speculated that these regions are preferential targets for BPDE adduction. Because the chromatin structure in the 5′ region of many active genes is in open (non-nucleosomal) form (Benezra et al. 1986), it may be that these regions are susceptible to adduction with BPDE. Thus, preferential adduction of 5′ (promoter) regions of genes could conceivably lead to decreased transcription or loss of regulation of transcription.

Using a well-characterized 5S rRNA gene system, we are evaluating transcriptional processes in BPDE-modified DNA in an effort to extend our understanding of the influence of DNA adducts on

gene regulation. The plasmid pXP-14, provided by Dr. D. Brown (Carnegie Institute, Baltimore, Maryland), was used in preliminary transcription studies. This plasmid contains the 5S rRNA gene from *Xenopus borealis* and the bacteriophage SP6 promoter region. Primers containing 30 nucleotides with a unique restriction site sequence were synthesized for polymerase chain reaction (PCR) amplification of a 310-bp fragment containing the SP6 promoter region and the 5S rRNA gene from the pXP-14 plasmid. This fragment was then adducted by incubation with radiolabeled (±)-r-7,t-8-dihydroxy-t(-)9,10-epoxy-7,8,9,10-tetrahydrobenzo[a]pyrene (BPDE), and unbound BPDE decomposition products were removed by consecutive extractions with diethylether. As is shown in Table 1, incubation of the 310-bp fragment with 250 μM BPDE resulted in 0.55% modification of the bases. This corresponds to approximately 1.0 adduct per 180 bases, or 3.4 adducts per 310-bp fragment. In addition, incubation of pXP-14 plasmid DNA with 250 μM BPDE resulted in a similar level of adduction (0.64%), suggesting that adduction was consistent between the plasmid and PCR fragment.

TABLE 1. Adduction of 310-bp PCR Fragment and pXP-14 Plasmid DNA

Template	BPDE (μm)	Modification (%)	Bases/Adduct
310 bp	250	0.55	180.2
pXP-14	250	0.64	157.3

We have developed several methods for determining the effects of adduction on transcription. Adducted and nonadducted 310-bp fragments were used as a template for transcription by bacteriophage SP6 RNA polymerase. In these studies (Figure 1A), 100 ng DNA was incubated for 30 minutes in the presence of 1.25 mM nucleotide triphosphates, 25 units SP6 polymerase, and 20 μCi [α-^{32}P]UTP (uridine 5′-triphosphate). The RNA transcripts were then precipitated with ethanol and electrophoresed on a 6% polyacrylamide 7 M urea gel. Transcription of nonadducted 310-bp template resulted in primarily full-length transcripts of approximately 250 bp, with lesser amounts of shorter transcripts. We speculated that the short transcripts produced with the nonadducted template are due to secondary DNA structures that impede transcription by SP6 polymerase. When transcription was carried out using three different adducted 310-bp templates, distinct transcriptional breakpoints were noted as compared to the control template. DNA adducted at the level of 0.1 to 0.3 adducts per 310 bp showed a series of short RNA transcripts not seen in the control template. At a higher level of adduction (3.4 adducts per 310 bp or 0.55% modification), similar breaks in transcription were observed, but the overall amount of RNA produced was

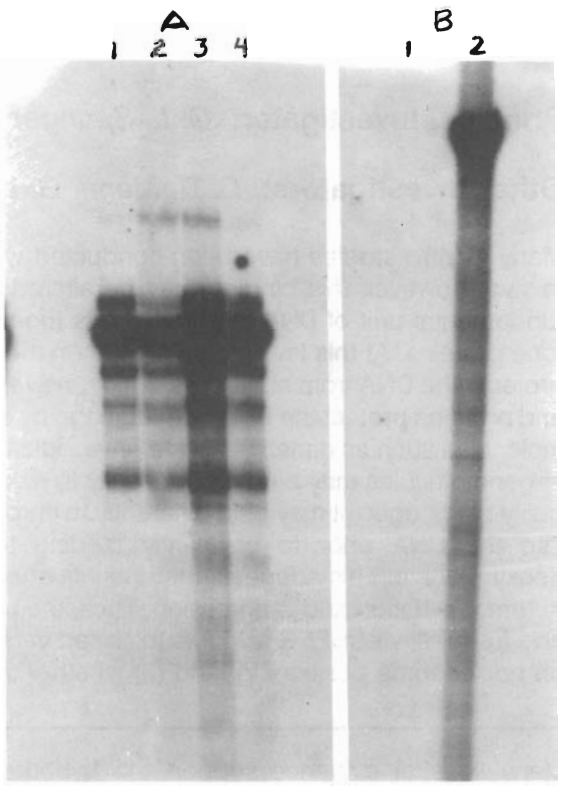

FIGURE 1. SP6 Transcripts and T4 Polymerase Digestions of Unadducted and Adducted 310-bp DNA. (A) Transcription runoff was done using 100 ng of unadducted or adducted 310-bp DNA fragments using SP6 RNA polymerase. RNA transcripts were then separated on a 6.0% polyacrylamide sequencing gel and autoradiographed. Lane 1, unadducted 310-bp template; lanes 2 through 4, 310-bp templates adducted with BPDE at the level of 1.7, 0.1, and 0.3 adducts per strand, respectively. (B) DNA (310 bp) was 5′-end labeled with [^{32}P]ATP using T4 kinase and digested with *Eco*RI, leaving only the coding strand labeled with radioactivity. The DNA was then digested with T4 DNA polymerase in absence of deoxynucleotide triphosphates, separated on a 6% sequencing gel, and autoradiographed overnight. Lane 1, unadducted 310-bp template; Lane 2, 310-bp template adducted at level of 1.7 adducts per strand.

decreased. In a separate experiment, the primary transcript was excised from the gel and counted by liquid scintillation counting. The 310-bp template adducted at the 0.03% modification level showed a 23% inhibition in the amount of primary transcript produced, while template adducted at the 0.55% modification level showed more than 80% decrease in the amount of primary transcript. This may be because adducts in the SP6 promoter region of the template prevent the initiation of transcription.

To determine the precise position of BPDE adducts on the 5S gene fragment, we are currently employing methods using the 3'→5' exonuclease activity of T4 DNA polymerase. This enzyme, in the absence of nucleotide triphosphates, digests DNA to short fragments. When the enzyme encounters blocks in exonuclease activity, such as bulky adducts, a family of fragments of defined lengths can be separated and visualized by gel electrophoresis and autoradiography. Preliminary results using this methodology are shown in Figure 1B. A 2-hour incubation with T4 polymerase completely digested the nonadducted 310-bp fragment, yet a series of fragments were seen in the adducted fragment. In addition, dark bands in the T4-digested fragment corresponded closely in size to the transcriptional breaks seen in the adducted 310-bp template, indicating there are "hot spots" for BPDE adduction in the template that stop transcription. Currently, studies using dideoxy-sequencing methods to determine the precise position of these putative adducts are being performed.

In addition to ongoing studies with pXP-14 plasmid DNA, a new plasmid ("pGEM-5S") (Figures 2 and 3) has been successfully constructed by subcloning the 5S rRNA gene from pXP-14 into the pGEM-9Z-f(-) expression vector. The resulting plasmid contains the 5S gene and opposing SP6

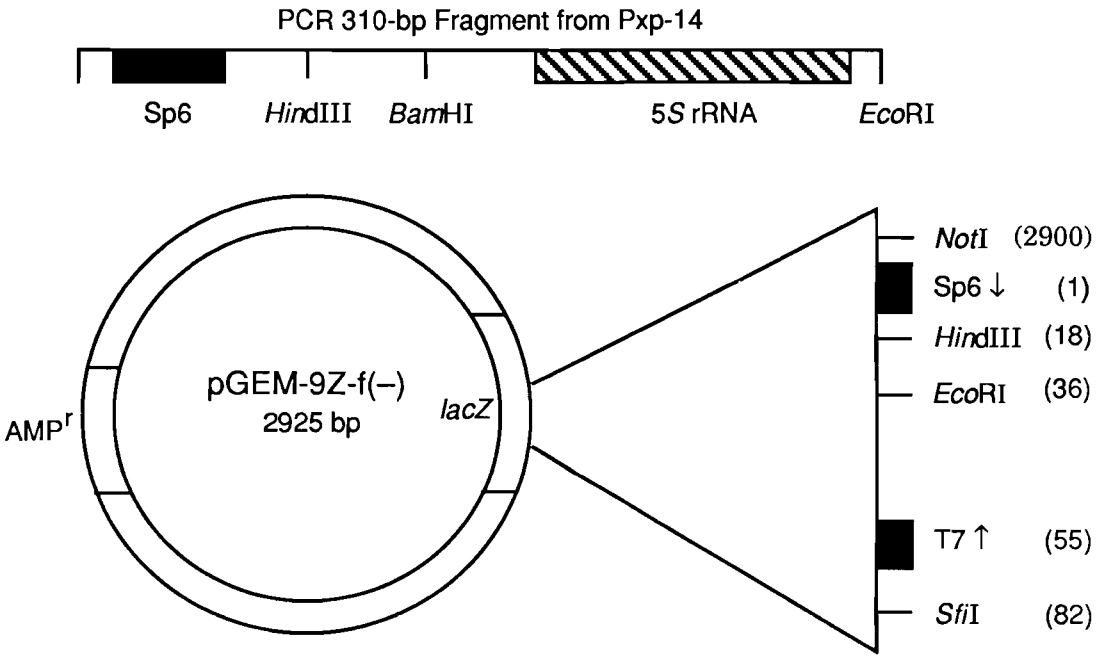

FIGURE 2. Construction of "pGEMS-5S" plasmid. The 310-bp PCR fragment from plasmid pXP-14 and plasmid pGEM-9Z-f(-) were digested with *Hin*dIII and *Eco*RI restriction enzymes. The 219-bp fragment containing the 5S rRNA gene was then ligated into the *lacZ* region of pGEM-9Z-f(-) at the *Hin*dIII/*Eco*RI site using T4 DNA ligase. Resulting plasmid "pGEM-5S" contains 5*S* gene with opposing SP6 and T7 promoter regions, as confirmed by restriction mapping (see Figure 3). Transcription of coding strand is done with SP6 RNA polymerase.

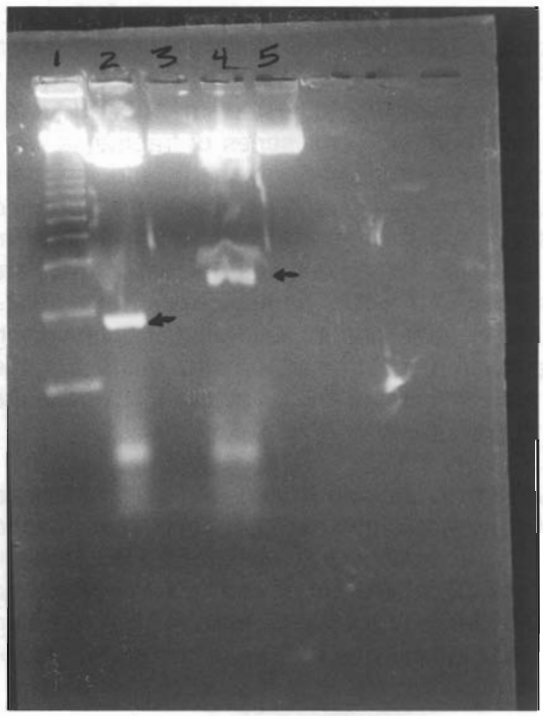

FIGURE 3. Restriction mapping of "pGEMS-5S" plasmid. Plasmid pGEMS-5S and parent pGEM-9Z-f(-) were digested with *Eco*RI and *Hin*dIII (lanes 2 and 3), or *Not*I and *Sfi*I (lanes 4 and 5) and electrophoresed on a 2.0% agarose gel. *Eco*RI/*Hin*dIII (219 bp) and *Not*I/*Sfi*I fragments (308 bp) are indicated by arrows. Lane 1, 123-bp DNA ladder; lanes 2 and 4, pGEM-5S; lanes 3 and 5, pGEM-9Z-f(-).

and T7 promoters. This will allow us to selectively determine the transcriptional effects of BPDE adducts on the coding or noncoding strand of the template. In addition, the pGEM-5S plasmid contains *Sfi*1 and *Not*1 restriction sites, which allow a 308-bp fragment containing the gene and promoter regions to be excised from the plasmid without extraneous DNA. Thus, unlike PCR techniques, milligram quantities of DNA can be prepared for adduction and transcription studied with relatively little expense.

Other studies now in progress are directed at determining the specific effects of adduction in the promoter region of the 5S gene fragment. For instance, the 5S fragment (308 bp) from pGEM-5S will be digested with *Bam*HI, which cleaves between the SP6 promoter and the 5S gene. The SP6 promoter will then be adducted with BPDE and ligated to nonadducted 5S gene. Incubation of the 308-bp fragment with SP6 polymerase in the absence of nucleotide triphosphates should result in a stable transcription complex. This complex can then be "footprinted" by digestion with DNAse I and polyacrylamide gel electrophoresis. By these methods, we will determine whether adduction of the SP6 promoter region with BPDE interferes with binding of SP6 RNA polymerase.

Nucleosome positioning was recently demonstrated to be sequence dependent, and the placement of nucleosomes along the chromatin fiber may be involved in regulation of gene activation or inactivation. Further, it has been shown that Z-DNA is a more rigid structure and that regions containing this DNA conformation do not form nucleosomes. It has also been reported that BPDE adducts stabilize DNA structure in the B conformation in the area proximal to the adduct and destabilize distal base pairing so that the transition of the B to Z conformation is favored (Chen 1985). Thus, it follows that chromatin structure and possible gene expression may be altered in regions where bulky adducts are present.

In an attempt to elucidate some of the regulatory processes involved in tumor development, we are conducting studies to determine the influence of BPDE adducts with respect to nucleosome positioning and other structural changes in chromatin. For this we are also using the 5S rRNA gene as a model system. It has been shown that the gene will form a single nucleosome either by incubation with core histone particles or by exchange with chick erythrocyte chromatin. The position of the nucleosome is known with respect to the DNA sequence, and the positioning is fixed with respect to location along the 5S rRNA gene. The model therefore allows manipulation of bulky adducts and lends itself to experimental designs that address questions on the influence of bulky adducts on nucleosome positioning.

Recently we prepared and stored a large quantity of chicken erythrocyte nuclei, which will be used as a source of core histone particles for nucleosome studies. The 5S rRNA gene will be incubated with the erythrocyte chromatin under the appropriate concentrations of salts so that the 5S rRNA gene becomes associated with core histone particles. After these samples are adducted with BPDE, we will map the location of the adducts, determine the influence of the adducts on nucleosome positioning and determine whether the adducts alter transcription.

References Cited

Benezra, R., C. R. Cantor, and R. Axel. 1986. Nucleosomes are phased along the mouse β-major globin gene in erythroid and nonerythroid cells. *Cell* 44:697-704.

Chen, F.-M. 1985. Covalent binding of (+)- and (-)-trans-7,8-dihydroxy-anti-9,10-epoxy-7,8,9,10-tetrahydrobenzo[a]pyrene to B and Z DNAs. *Biochemistry* 24:6219-6227.

Koostra, A., L. K. Lew, R. S. Nairn, and M. C. MacLeod. 1989. Preferential modification of GC boxes by benzo[a]pyrene-7,8-diol-9,10-epoxide. *Mol. Carcinogen.* 1:239-244.

Leffler, S., P. Pulkrabek, D. Grunberger, and B. I. Weinstein. 1977. Template activity of calf thymus DNA modified by a dihydrodiol epoxide derivative of benzo[a]pyrene. *Biochemistry* 16:3133-3136.

Mizusawa, H., and T. Kakefuda. 1979. Inhibition of DNA sythesis *in vitro* by binding of benzo[a]pyrene metabolite diol-epoxide I to DNA. *Nature* 279:75-78.

Genotoxicity of Inhaled Energy Effluents

Principal Investigator: *A. L. Brooks*

Other Investigators: *K. E. McDonald, C. Mitchell, and R. M. Kitchin*

The interaction between cellular and genetic damage induced by low- and high-LET radiation and damage produced by chemicals is being studied. We have concentrated our research on metals, organic solvents, and fibers used in the nuclear industry and present at nuclear waste sites. Research on metals has demonstrated a multiplicative interaction between beryllium and x rays for induction of chromosome aberrations. Silicon carbide (SiC) fibers used in space nuclear systems were evaluated in lung epithelial cells (LEC) and Chinese hamster ovary cells (CHO). SiC produced a concentration-related increase in cell killing in both cell types but induced no increase in the frequency of micronuclei in either cell type. The fibers interfered with cytokinesis, causing a significant increase in the frequency of multinucleated giant cells in CHO cells but having little effect on LEC cells. No interaction between damage from gamma rays and that from SiC fibers was demonstrated using micronuclei as an endpoint.

Research has begun on the genotoxic responses of cells in culture to organic solvents such as methyl isobutyl ketone (hexone), which was used to reprocess nuclear fuels and is now present in large amounts in nuclear waste sites. Hexone caused a concentration-related increase in cell killing and a small increase in the frequency of micronuclei induced in LEC cells. No interaction between damage from gamma rays and hexone was detected by induction of micronuclei. Expansion of this research in vitro and in vivo will provide a mechanistic foundation on which to define the interaction of radiation and chemicals in production of chromosome and cellular damage. Awareness of these mechanisms flags potential problem areas and allows adequate worker protection both in the nuclear industry and during nuclear waste-site cleanup.

Introduction

Many workers are involved in nuclear energy and weapons production, and in the future additional workers may be exposed to internally deposited radioactive materials, external radiation, and promoting and carcinogenic chemicals during cleanup of nuclear waste sites. Because the normal incidence of cancer in the human population is high, more than 20%, many workers in the nuclear industry or involved in waste-site cleanup operations will develop cancer independent of their work or exposure history. Current standards are designed to protect worker populations from excessive radiation and chemical exposure. However, standards are set for one compound at a time; little consideration is given to potential interaction between physical and chemical factors or the interaction of biological damage produced by combined exposure to multiple environmental insults. It has been demonstrated that combined exposure to environmental agents can produce risks that are either greater or less than would be predicted by an additive model.

Studies are being conducted to define the relationships between combined exposures and cellular responses, measured as changes in cell killing, micronuclei induction, chromosome number, aberration type and frequency, and oncogene or anti-oncogene location in the karyotype. The data derived from these studies will aid in evaluation of health risks in nuclear industry and during nuclear waste-site cleanup.

Results and Discussion

Exposure to Radiation and Metals

Beryllium is widely used in space nuclear systems, creating a potential for combined exposures. Research has determined that x rays and beryllium

interact to increase the frequency of chromatid-type aberrations above that predicted by an additive model. It was noted that the interaction was limited to cells in the S stage of the cell cycle. To further understand the mechanisms of this interaction, the influence of cell cycle on the interaction was evaluated. Changes induced in the cell cycle by combined exposure to x rays and beryllium were measured using a flow cytometer. It was determined that exposure of cells to beryllium alone delayed the progression of cells through the cycle; cells accumulated in the S stage of the cell cycle. A 7-hour recovery period allowed the cells to move through the cycle, resulting in an increased number in the G_2/M stage. When cells were exposed to x rays only or x rays plus beryllium, there was a similar change in the distribution of cells through the cell cycle. These data supported the idea of a partial synchronization or blockage of the cells in the S phase of the cycle by beryllium. The difference in the response of the cells to the combined exposure could not be totally explained by the observed shifts in the cycle. Other factors, such as changes in repair of chromosome damage, seem to be important in the production of the increased level of damage by the interactions between radiation and beryllium.

Exposure to Radiation and Fibers

Many new fiber materials are being developed for use in space nuclear systems and reinforcement of advanced ceramics. Studies were conducted on the toxicity of one of these, silicon carbide (SiC) (Table 1). Detailed studies were conducted to determine if and how SiC fibers altered the genetic make-up of cells. The effect of SiC fibers on the induction of cell killing, micronuclei, and multinucleated cells was evaluated in both fibroblasts, Chinese hamster ovary cells (CHO), and lung epithelial cells (LEC).

The fibers were cytotoxic to both cell types (Figure 1). Fibers were more effective per unit of concentration in killing LEC cells than CHO cells. No change in the frequency of micronuclei was observed in either cell type (Figure 2), however, suggesting that chromosome aberrations are not a major contributor to the failure of cells to divide and form colonies.

TABLE 1. Physical Characteristics of Silicon Carbide Fibers (SiC) Used in These Studies and in Advanced Ceramics

Surface area, 3.6 m^2/g
Average diameter, 0.32 μm
Density, 3.2 g/cm^3
Average length, 6.5 μm
Fiber number/mass, 1.05 x 10^7 fibers/mg

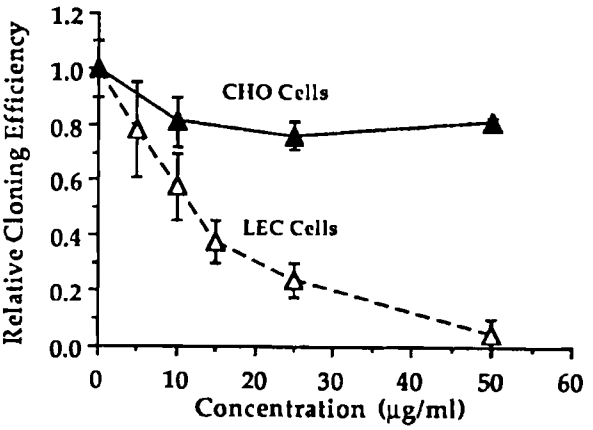

FIGURE 1. Induction of Cell Killing by SiC Fibers in Lung Epithelial Cells (LEC) and in Fibroblasts (Chinese hamster ovary cells, CHO)

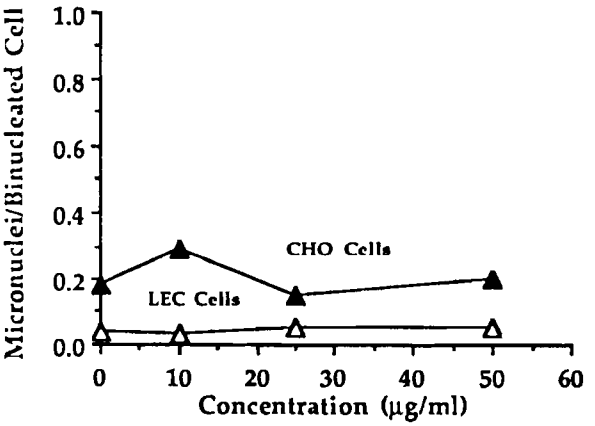

FIGURE 2. Induction of Micronuclei in Chinese Hamster Ovary Cells (CHO) and Lung Epithelial Cells (LEC) by SiC fibers. No micronuclei were induced in either cell line.

If fibers cause problems with chromosome segregation or segregation of chromosome fragments, one could postulate that fibers should increase the frequency of micronuclei present in cells that had been exposed to ionizing radiation. Figure 3

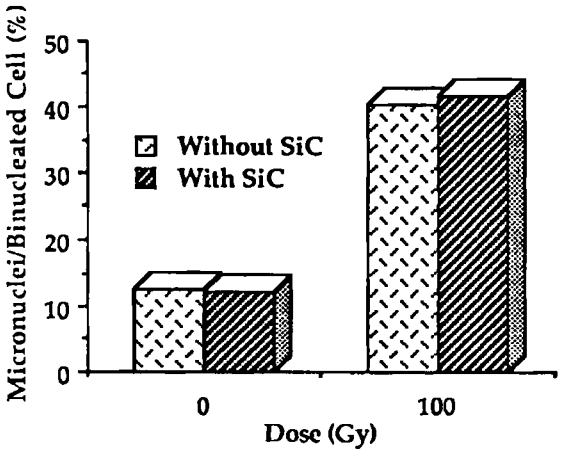

FIGURE 3. Induction of Micronuclei in Lung Epithelial Cells (LEC) by Radiation with and Without SiC Fibers. No interaction was apparent.

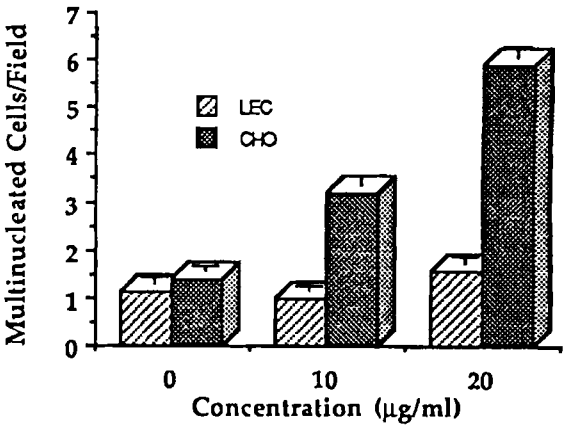

FIGURE 4. Induction of Multinucleated Giant Cells by SiC Fibers in Lung Epithelial Cells (LEC) and Chinese Hamster Ovary (CHO) Cells

illustrates that our studies found no interaction between damage produced by fibers and that from radiation as indicated by induction of micronuclei.

A special protocol was developed to determine if the fibers interfered with cytokinesis during normal cell division. Cells were treated with fibers for an extended period of time. The cells were exposed to fibers during the log growth phase; after reaching confluency they were subcultured and again allowed to grow to confluency. Cells were then fixed and stained and the frequency of multinucleated giant cells scored per microscopic field, providing a measure of improper cell division. For CHO cells there was a linear increase in the induction of multinucleated cells as a function of fiber concentration (Figure 4). Over the range of fibers tested, the frequency of giant cells increased more than threefold. The frequency of multinucleated giant cells induced by the SiC fibers in LEC cells was very low. The fact that epithelial cells were not altered by the SiC exposure to the same degree as CHO cells suggests that LEC cells may have a lower intake of fibers or a lower cell turnover rate than the fibroblasts. Fibers were observed in most of the giant cells illustrated for CHO cells (Figure 5). Additional research is being conducted to determine if radiation can interact with damage produced by fibers to alter the induction of the multinucleated giant cells.

Exposure to Radiation and Organic Solvents

Extensive effort will be involved in removing, containing, and decontaminating nuclear waste sites. Many organic solvents are present in these sites, creating a potential for worker exposure. Solvents such as trichloroethylene were used to remove lubricants from the copper jackets that covered the fuel elements; other solvents such as methyl isobutyl ketone (hexone), tributyl phosphate, and isobutyl butyl phosphonate were used during separation of uranium and plutonium from fission products. These materials, disposed of in large quantities at the waste disposal sites, are mixed with radioactive fission products and alpha-emitting radioisotopes.

Research is being conducted to determine the toxicity of these materials in vitro and to evaluate the interaction of solvent-induced with radiation-induced cellular damage. To date, the toxicity of hexone and hexone-induced micronuclei in LEC cells have been evaluated. Hexone is toxic at rather low concentrations (Figure 6). Preliminary research to evaluate the potential for interaction between radiation and hexone (1 mM) demonstrated that hexone alone produces an increase in micronuclei but that the combined exposure to radiation and hexone had an additive effect on the frequency of micronuclei (Figure 7). Other endpoints and solvents will be evaluated in vitro to determine if there are interactive effects. Such interactive effects would be cause for concern and should be addressed with animal studies.

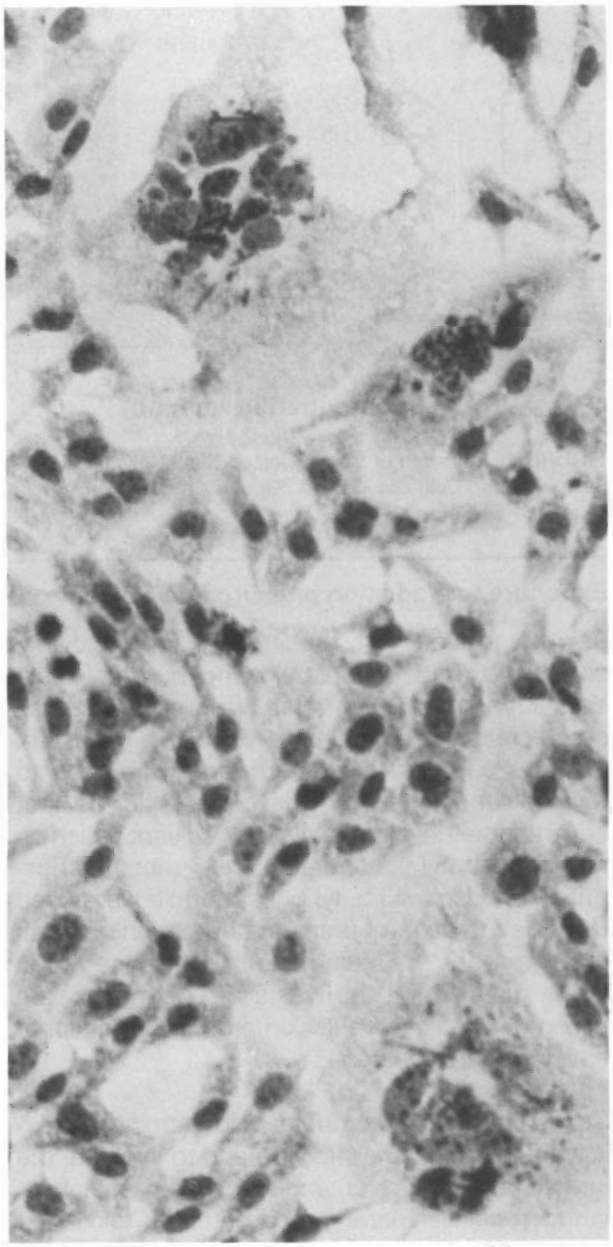

FIGURE 5. Presence of SiC Fibers in Multinucleated Giant Chinese Hamster Ovary (CHO) Cells

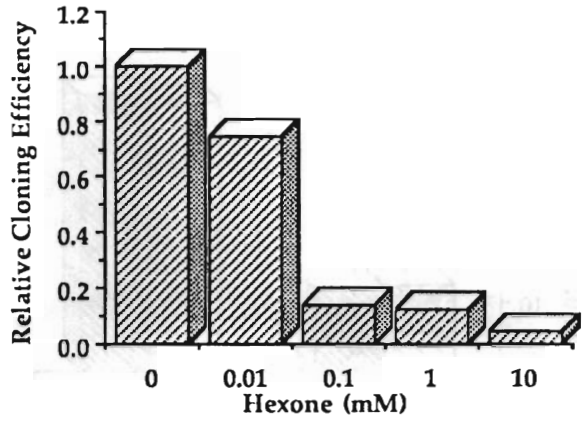

FIGURE 6. Relative Cloning Efficiency of Lung Epithelial Cells (LEC) as a Function of Hexone Concentration

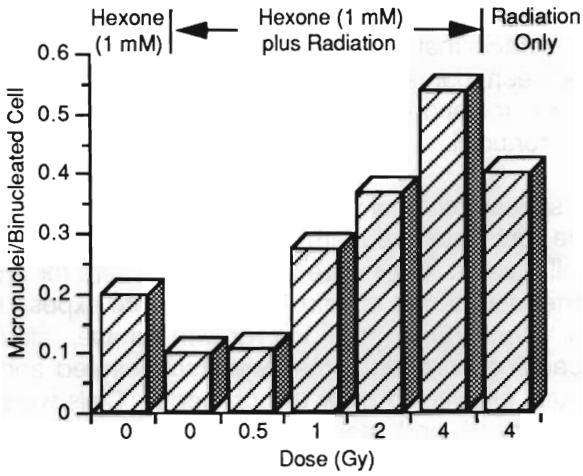

FIGURE 7. Frequency of Micronuclei/Binucleated Cells in Lung Epithelial Cells (LEC) Induced by Radiation and Hexone Given Alone or in Combination

Exposure to Acute and Protracted Radiation

Studies are being conducted to determine the influence of internally deposited ^{239}Pu or ^{144}Ce on the induction and repair of x-ray-induced chromosome aberrations in the bone marrow of Chinese hamsters. Hamsters with a body burden of plutonium or cerium were exposed to x rays. The responsiveness of the cells to the induction of chromosome damage by the challenge dose of x rays is being followed as a function of time and radiation dose. This will make it possible to determine if a plutonium or cerium body burden alters the ability of the cells to repair radiation-induced damage. This project will provide a broad database on the interaction of environmental pollutants with radiation exposure. It has demonstrated that beryllium and x rays interact to increase the amount of chromosome damage. However, no interaction was detected between

radiation and SiC fibers or radiation and hexone exposure for the induction of micronuclei. Information derived from this project is very important in evaluation of occupational radiation exposure, radiation accidents, and nuclear waste-site cleanup.

Fetal and Juvenile Radiotoxicity

Principal Investigator: *M. R. Sikov*

Other Investigators: *R. L. Buschbom, F. T. Cross, G. E. Dagle, A. C. James, T. J. Mast, and H. K. Meznarich*

This project is involved with the deposition, dosimetry, and toxicity of radionuclides relative to prenatal or postnatal age. Recent emphasis is directed at performing comparative and predictive analyses, modeling patterns and phenomenological interactions to facilitate extrapolations to man, and investigating teratogenic mechanisms. This information is being used in setting radiological protection standards for pregnant women and for rapidly growing infants and children. We have completed evaluations of specimens and data from previous experiments, including dosimetric assessments that demonstrated that radon progeny were restricted in their transfer to the fetus during inhalation exposures of pregnant rats. The dosimetry confirmed predictions that the major dose to the conceptus would come from radon that crossed the placenta and its decay products and that 18-hour exposures to 124 WLM (working-level months) per day for 13 days would not be teratogenic. We further examined relationships between radionuclide transfer to the embryo/fetus and fractional absorption from gut; metabolites showed greater similarities and toxic materials greater differences. Immunocytochemical studies of alterations of extracellular matrix and cell surfaces by radiation effects on limb development in vitro have demonstrated fibronectin changes that correlate with histological and histochemical changes in cartilage differentiation. Related experiments have provided parallel information about radiation effects on the processes and roles of intercellular communication during early interactions among blastomeres.

We analyzed specimens and data that provided information and concepts about placental transfer, fetoplacental radiation doses, and perinatal or long-term toxicity to address continuing questions concerning the identity of target cells and tissues associated with teratogenesis or oncogenesis during prenatal life and the magnitude of the radiation doses to these targets from radionuclides. This effort included examining archived tissues, slides, and related experimental materials, and evaluating data to complete and extend previous results.

A paucity of data on the prenatal dosimetry and effects of inhaled radon and progeny led us to perform computational and empirical dosimetric and toxicological evaluations following daily 18-hour inhalation exposures of pregnant rats to 124 working-level months (WLM) through 6 to 19 days of gestation for a total exposure of 1612 WLM. On the basis of our previous results with krypton, kinetic models for radon in adults, and information on heavy nuclide placental transfer, we predicted and empirically confirmed that radon would freely cross the placenta in both directions, that in situ decay of radon and its progeny, rather than transferred progeny, would provide the primary contribution to the radiation dose to the embryo/fetus, and that significant levels of reproductive or developmental toxicity would not be detected even at these high concentration levels.

Two rats were removed from the radon chambers on the last day of exposure to provide radioanalytic samples to estimate distribution and dosimetry. Specific activities of ^{214}Pb in tissues of the pregnant rats were calculated from the measurements made on the last day of exposure, and the corresponding dose-equivalent rates were determined using a value of 20 for the quality factor.

Predicted and measured values of specific activities in these tissues and organs are presented in Figure 1. The ^{222}Rn human model had not predicted that the lung would have the greatest deposition, and the measured specific activity was almost 1000 times greater than predicted

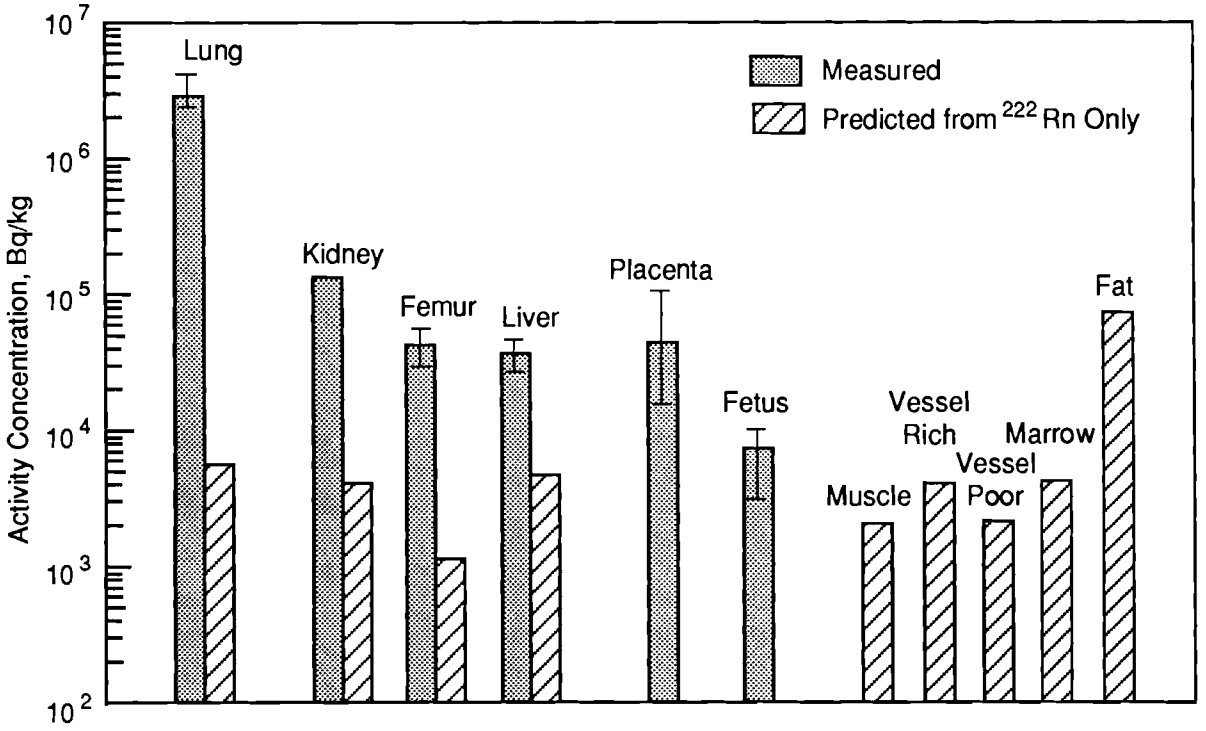

FIGURE 1. Comparison of Specific Activity of ^{214}Pb in Tissues of Pregnant Rats and Fetoplacental Unit as Predicted from ^{222}Rn Exposure Only and as Measured After Multiple Daily Exposures

because of the retention of radon progeny in lung. Many nuclides in the radon decay chain are excreted through the kidney, but this organ had the highest specific activity of the other tissues and organs evaluated, although it was an order of magnitude less than lung. The measured activity again was markedly higher than predicted on the basis of the radon, but the differential was substantially less than with lung, presumably because of a lesser role of retention. The radionuclide concentration in the placenta was similar to that in the femurs and livers of the pregnant rats.

The specific activity in the fetus was substantially lower than that in the placenta, by about a factor of 3, which contrasted with krypton results in which fetoplacental concentrations were more uniform and the doses were similar to those received by tissues of the dams. This difference is interpreted as indicating that the placenta restricts the transfer of radon progeny to the conceptus during inhalation exposures to radon. There is probably some sequestration of these nuclides in the placental tissues, but measurable quantities of these nuclides cross the placenta and enter the fetus. The dose-equivalent rates at the end of the exposure period essentially mirror the measured specific activities and thus reflect the reduced levels of translocated radon progeny in the fetus. The dose-equivalent rate was calculated to be 1.4 mSv hr^{-1}, or 34 mSv to the fetus on the last day of exposure. This corresponds to an absorbed dose of 1.7 mGy (0.17 rad) on this day or to 23.5 mGy (2.4 rad) during the 14-day postimplantation period of the rat, if this rate was maintained throughout gestation. An absorbed dose of this magnitude would not be expected to produce detectable developmental toxicity, nor would the corresponding dose-equivalent of 48 cSv (48 rem) when protracted over this period. This conclusion is consistent with the findings of the biological evaluations in the study, which provided no indication of reproductive toxicity (*Pacific Northwest Laboratory Annual Report for 1988 to the Office of Energy Research, Part 1*).

The findings of the radon studies relate to epidemiological findings with radon progeny and related nuclides and to ongoing questions that we

have raised concerning the identity of target tissues and radiation doses that are involved in perinatal oncogenesis. Associated implications illustrate the need for mechanistic studies of dosimetry, pathogenesis, and altered homeostasis of control factors. Our ongoing efforts to quantify placental transfer and perinatal doses and to develop operational models relate to the foregoing questions and are of importance in establishing dose-response relationships. Such relationships for prenatal effects are often developed on the basis of the amount administered to the pregnant woman or animal, rather than quantities reaching the fetal tissues that are exposed, that is, the fetoplacental dose. Predictive dose-response relationships for the human embryo/fetus are limited by these dosimetric uncertainties, as well as by extrapolation problems relative to effect.

We have described our initial efforts to establish correlations between placental transfer of radionuclides, their chemical and physical characteristics, and results obtained with compartmental and physiologically based pharmacokinetic models. It was desired to have numerical factors for comparisons, for developing and testing hypotheses and predictions about placental transfer, and for subsequent modeling. We have integrated all available data, including clearance measurements from placental perfusion experiments and serial sacrifice studies, and have developed composite values that are predictive of fractional placental transfer. We found that these composite values, denoted Θ, displayed good general correlation with gastrointestinal or pulmonary fractional absorption, expressed as values of f_1, but there was marked deviation in many instances.

One approach to determining reasons for this pattern involved examining characteristics of those values that fit and did not fit the generalization (Table 1). We now find that agreement is good for materials that are commonly involved in normal metabolism and bodily processes. In contrast, there tends to be disagreement for several materials that are accepted as being toxic, especially under experimental conditions, and the lack of agreement may relate to biological actions including phenomena such as effects on blood flow, altered physical form of materials that enter blood, potentially bidirectional transfer processes, and transport proteins.

TABLE 1. Correspondence Between Degree to Which Selected Metabolic and Toxic Materials Are Absorbed from the Gastrointestinal (GI) Tract (f_1) and Fraction Crossing the Placenta from Transfer Compartment into Embryo/Fetus (Θ)

Materials	f_1 (GI)	Θ	
Metabolic Materials			
H_2O	1	1	
CO_2	1	0.6	
Na^+	1	0.8	
PO_4^{2-}	0.8	0.9	
K^+	1	1	
Ca^{2+}	0.3	0.5	
Sr^{2+}	0.3	0.5	
I^-	1	1	
Cs^+	1	1	
Toxic Materials			
Cd^{2+}	0.05	0.6	(guinea pig)
Cd^{2+}	0.05	0.06	(human)
Hg^{2+}	0.02	0.02	
Hg (Me)	1	0.8	
Pb	0.3	0.2	
U	0.05	0.03	
Pu	1E-3	4E-3	
Am	1E-3	6E-4	

As was noted in 1989 (*Pacific Northwest Laboratory Annual Report for 1989 to the DOE Office of Energy Research, Part 1*), prenatal irradiation was among the first agents for which cause-and-effect and dose-response relationships for teratogenesis were demonstrated, but that analysis of mechanisms was limited. We began efforts in this direction, concentrating on cell-cell interactions that involve their surfaces and the extracellular matrix. It was postulated that radiogenic interference with communication between mesenchymal cells might interfere with chondrogenesis. Thus, we initiated studies on dose and stage relationships for teratogenesis, using mouse forelimb buds in organ culture as a model. One bud was irradiated to obtain a graded degree of developmental abnormalities, and the contralateral bud served as control. Limb buds were fixed at the time of explantation, after 1, 2, or 3 days in culture, and from embryos removed from untreated dams at the same stages of development.

Our studies showed that exposure to 1 Gy did not produce gross morphological effect but affected differentiation. We concluded that this dose was the upper limit for mechanistic studies because the limb buds were visually smaller than controls after exposure and development was unduly retarded at higher doses. Procedures have been developed to use the indirect peroxidase staining method to detect polyclonal antibodies to fibronectin, which is the primary extracellular matrix component in embryonic tissues. Unstained slides from the prior study were retained for immunocytochemical investigation, and these slides have now been stained and evaluated. Staining of limbs from unirradiated 15-dg (days of gestation) mice that had developed in vivo showed that fibronectin was present in cell populations of the early developmental stages and the matured chondrocytes, in the premyoblasts, and adjacent to the aggregated prechondrocytes. The limb bud fibronectin was located in the extracellular matrix as well as in the cytoplasm of more mature chondrocytes.

A dose of 1 Gy reduced aggregation of prechondrocytic mesenchyme, and led to less cell-to-cell contact and a less well ordered arrangement of cells than in the controls. The mesenchymal cells of nonchondrogenic areas of irradiated limbs showed reduced differentiation at 3 days. In our current evaluations of specimens taken at the time of explantation, fibronectin in limb buds of 12-dg mice could be detected among nonchondrocytes located in the area between the apical ectodermal ridge and the predigital chondrocytes but was not present in the aggregated prechondrocytes. Almost immediately after irradiation, the level of fibronectin was reduced relative to controls. Fibronectin was detectable in the region between the apical ectodermal ridge and the predigital chondrocytes after 3 days in culture of limb buds explanted from unirradiated 12-dg embryos and had appeared in the chondrocytes. In irradiated buds at this time, fibronectin levels either were reduced or fibronectin was not present in nonchondrocytes, although it could be detected in chondrocytes.

Research on this project continued to be coordinated with that of project staff who are developing a study in which single blastomeres of two- to four-cell embryos will be irradiated with microbeams of charged particles. Preimplantation mouse embryos were selected for that project because their cells (blastomeres) and subsequent presumptive tissues must undergo precisely sequenced interactions to attain recognizable developmental endpoints. Previously, standard procedures for harvesting and culturing two-cell embryos to the blastocyst stage had been modified to conditions appropriate to the irradiation facility. Studies of intercellular interactions during early development were performed to obtain data complementary to those obtained after irradiation of limb during organogenesis. Two-cell embryos were irradiated with 1 Gy of x rays or were sham irradiated. Pooled results across experiments showed that 92% of 66 control embryos developed to the blastocyst stage within 3 days, but only 55% of a similar number of irradiated embryos had reached this stage and these required a longer incubation time to become blastocysts (Figure 2). At the end of incubation, embryos were fixed in 3% glutaraldehyde for immunochemical staining. Readily detectable levels of fibronectin were found in control blastocysts, although positive levels could not be established at the earliest developmental stages. Even after adjustment for the reduced extent of development, fibronectin levels were decreased in the irradiated embryos, which is consistent with the possible involvement of fibronectin in the teratogenic effects of radiation (Figure 3).

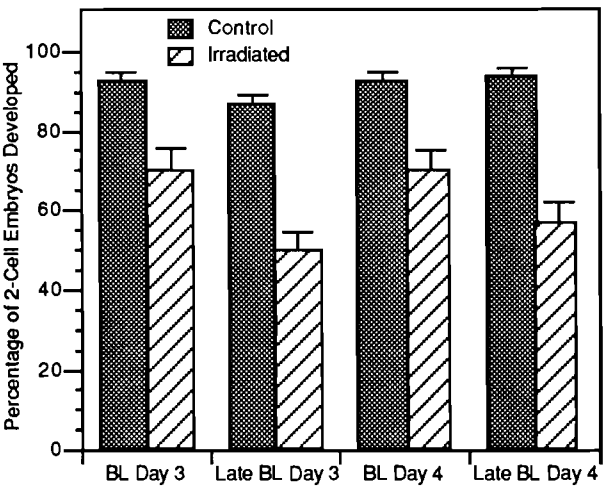

FIGURE 2. Effect of Exposure of Two-Cell Mouse Embryos in Culture to 1 Gy of X Rays on Development to Blastocyst (BL) or Late Blastocyst Stage After 3 or 4 Days in Culture. All differences between irradiated and control groups are statistically significant ($p \leq 0.02$).

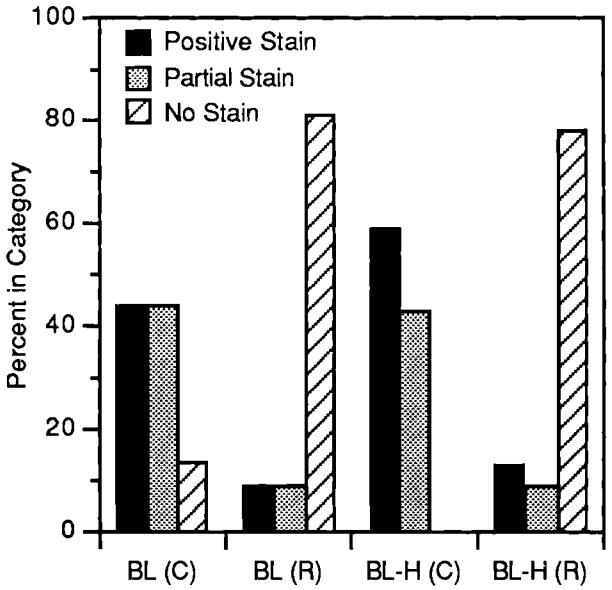

FIGURE 3. Effect of Irradiation of Two-Cell Mouse Embryos with 1 Gy on Amount of Immunohistochemically Detectable Fibronectin in Control (C) and Irradiated (R) Blastocysts (BL) and in Hatched Blastocysts (BL-H)

General
Life Sciences
Research

GnomeView II: A Graphical Interface to the Human Genome

Principal Investigator: *R. J. Douthart*

Other Investigator: *D. A. Thurman*

GnomeView is a graphical computer interface to the human genome. The central units of information organization are genome maps and DNA sequence. Although GnomeView contains its own Data Base Management System (DBMS), it is not a data repository such as GenBank and Genetics Data Base (GDB). GnomeView is guided by user queries, and abstracts information from these databases to draw genomic maps. Currently information is abstracted automatically from GenBank but must be abstracted manually from GDB (Genome Data Base) and other sources of mapping information.

An examination of any compendium of genetic maps, textbooks, and journals about modern genetics and molecular biology attests to the fact that the preferred method of presenting genomic information is pictorial: for example, chromosomes, physical maps, and regions related to DNA sequence are drawn as boxes, shaded regions, etc., on a linear map, and objects are identified with labels on drawings. If there are too many objects, their location is defined by some metric, such as chromosome band or base number, and they are listed in a table.

The GnomeView graphical user interface provides scientists with graphical representations of genomic maps. It provides access to many types of maps, from chromosomes and genetic maps to physical maps and DNA sequence. Ancillary information such as description of loci and genetic objects and bibliographic information is also available to the user.

System Design

GnomeView uses db_VISTA, a network-model database management system, to store and manipulate genomic mapping data. This type of database is excellent for storing and accessing the object relationships inherent in genomic data. Various genetics objects can be stored as the same record type, and maps are stored as collections of these objects linked together through ownership definitions and map metrics. Objects common to more than one mapping need to be stored only once in the database. Various querying mechanisms are being developed to locate objects, maps, and descriptive information. The system allows simultaneous display of maps at different levels in the hierarchy and of conflicting and contradictory maps. Hybrid or new maps can be created by the user and saved as user-specific objects in the database.

We are developing the user interface on a SUN workstation in portable-C using the UNIX operating system. The graphics display is written using the network-transparent, device-independent X-window system.

Progress

The GenBank sequence database has recently changed the format of the sequence headers. Overall this change is for the better, but routines that reference sequence features information had to be changed in GnomeView. The Genbank changes provide a direct reference between objects mapped to human chromosomes and GenBank sequences. This addition allows GnomeView to connect these extremes in mapping in a very straightforward way.

GnomeView's central organizing information unit is the map-object, which can be described in a number of ways (Figure 1). For example, a given object can have a database-specific name (locus name) and accession number, a map-specific description, and a more global description that is common among various mappings or databases. In addition to the description field, a keyword field or dictionary of attributes can be extremely useful for conducting queries.

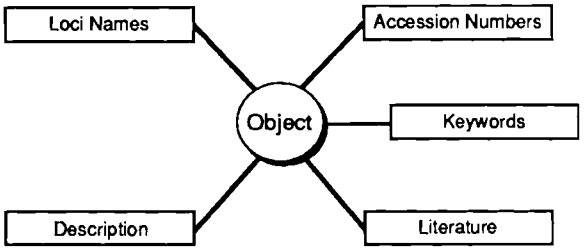

FIGURE 1. Query-Fields Associated with a Map-Object

GnomeView is a user interface to information, not a database or information repository; however, it does have an internal database management system. The network model management system db_VISTA was chosen for its efficiency in modeling complex data representations, anticipating large increases in the number of objects that will eventually be mapped.

A conservative estimate is that about 100,000 genes make up the human genome. Considering only the sequence level in the mapping hierarchy, an average of about 20 features may describe each gene. This implies an estimated 2 million database objects for sequence mapping alone. The smallest set of information necessary to identify objects and draw maps is selected from comprehensive database such as GBD (Genome Data Base), OMIM (Online Mendelian Inheritance in Man), and GenBank. Except for GenBank, information about map-objects is currently entered manually into GnomeView. Fortunately, these databases have been recently restructured using relational database management systems. The system of choice seems to be Sybase. A translator that captures information from comprehensive databases in the GnomeView form is needed. As the form of the comprehensive databases becomes better defined, so does the form of the translator.

Figure 1 depicts the information associated with a map-object that constitutes the basis of a GnomeView query. The closer a comprehensive database is to ordering information in this fashion, the easier it is to abstract into GnomeView. All the fields in Figure 1 exist in the new GenBank headers. This allows direct assess to a resident copy of the database without use of a translator.

At the chromosome level, loci have been manually abstracted from HGML (Human Genome Mapping Library) Chromosome Plots. This publication has appropriate loci names and descriptions but lacks an appropriate set of keywords or attributes that can be used to query map-objects. A study was made of the attribute quality of loci that have been mapped to the chromosomes of the human genome. A dictionary of 22 keywords was developed and integrated into the X-window choice panel (Figure 2). All the loci of the last HGML mapping have been assigned keywords and respond to attribute queries. The chromosome query panel shown in Figure 2 allows location of objects on the basis of names (locus names and numbers), a

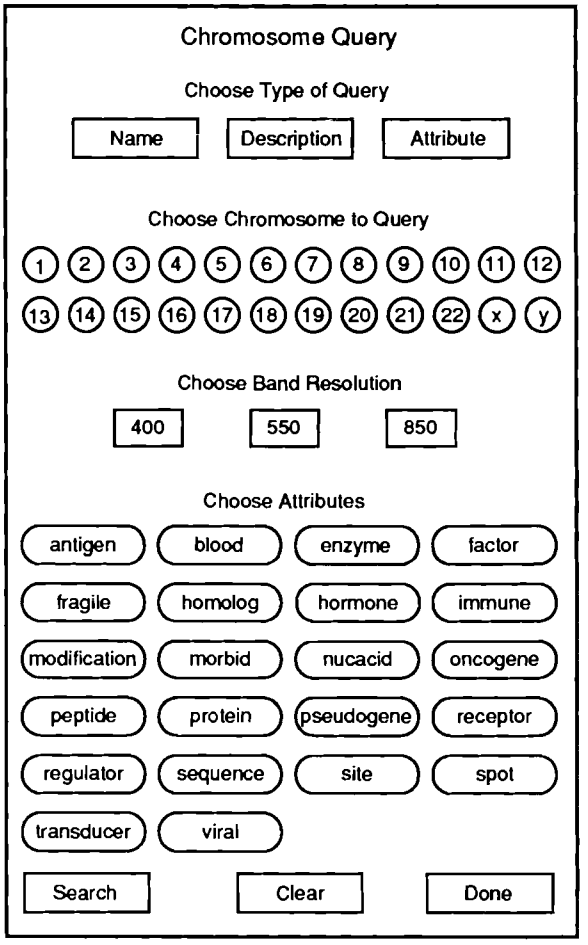

FIGURE 2. Chromosome Query Menu Box

description that scans short loci descriptors and attributes (selected set of keywords). Mapping is available at three different band resolutions. The use of GDB (Genetic Data Base) and an appropriate translator should allow automatic information abstraction rather than manual entry.

Map Representations

Figure 3 shows a simplified representation of two maps, A and B, as they are stored in GnomeView's Network-Model Database. Maps A and B have common objects 1, 3, and 4. Object 2

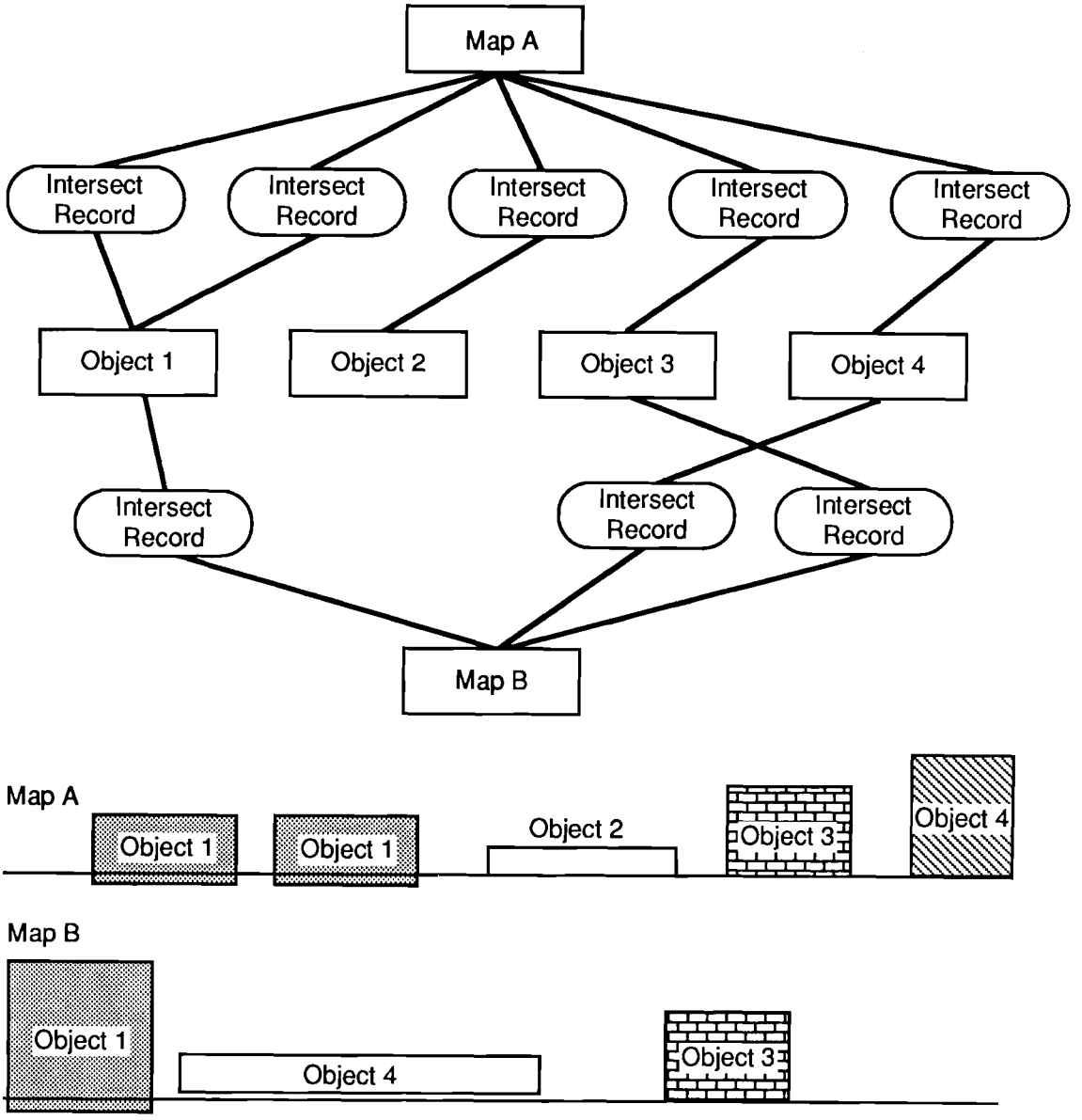

FIGURE 3. Map Storage Within GnomeView's Network-Model Database

has only been mapped to Map A. The intersect records that link map to object contain information on the type of map, its metric, and specific instructions for drawing graphic representations.

Map A generated by this network contains two copies of object 1. Map A and Map B have objects 1, 3, and 4 in common. Each map can have its own local metric that may be only tangentially related to other maps. Common objects can be of entirely different sizes on different maps. For example, the superoxide dismutase loci SOD1 is located on band q22.1 of chromosome 21. This band consists of millions of base pairs. Band location is the accepted chromosome metric. At the sequence level, the superoxide dismutase gene is represented by locus HUMSOD in GenBank, which is a 874-base mRNA sequence, in addition to HUMSOD1 and HUMSOD2, which are also mRNA sequences containing superoxide dismutase isolated from different tissue sources. Loci HUMSODG1. . . HUMSODG5 contain sequenced exons and flanks. The total superoxide dismutase at the sequence level is about 11 kb (kilobases). In this example, the object SOD1 at the chromosome level maps into a number of objects at the sequence level, a subset of which represents the genomic sequence of which less than 20% has actually been sequenced. The superoxide dismutase gene was the first test of map location and representation at different levels in the hierarchy. A 1000-kb restriction enzyme map and a combined map of sequence and features were constructed manually to test the GnomeView architecture.

Future

Progress in development of both GenBank and GDB databases is facilitating the evolution of GnomeView into a useful interface. Objects such as DNA probes, restriction fragment-length polymorphisms (RFLPs), and specific tagged sequence (STSs) are being listed in these databases and can be mapped to the chromosome level and in some cases related to sequence. Our focus is to directly access these databases for information so as to develop a usable B-test version of GnomeView in 1991-1992.

Synthesis of Human Genome Information

Principal Investigator: *J. E. Schmaltz*

Computer science expertise was provided to the Human Genome Task Group by an OHER detailee. The Human Genome community uses the term "informatics" to refer to computation, analysis, and database components of this multidisciplinary effort. Expertise in the area of informatics was provided, including reviewing research proposals, facilitating interagency and interlaboratory cooperation, liaising with the Human Genome newsletter group at Oak Ridge National Laboratory, and representing the U.S. Department of Energy at technical meetings.

Research Proposal Review

Two regular meetings of the OHER Research Committee were attended. Arrangments were made for the panels that reviewed the Human Genome proposals. A copy of the Federal Register announcement on the Human Genome e-mail bulletin board resulted in a number of additional proposals. Support was provided for the review of Small Business Innovative Research (SBIR) grants that pertained to the Human Genome program.

Site reviews of the three Human Genome Centers took place this summer; support was provided for selecting informatics reviewers, attending the reviews (2 days at each laboratory), and summarizing the reviewers' comments on the informatics portion of each center's efforts. This was the second such review for the centers, and the first time that reviewers for the informatics portion were specifically included.

Interagency Cooperation

Cooperation and coordination among the various agencies involved is a cornerstone of the national Human Genome program. In addition to the DOE and National Institutes of Health (NIH), other agencies prominent in the genome effort are the Howard Hughes Medical Institute (HHMI) (a private agency), the National Library of Medicine (NLM), and the National Science Foundation (NSF). As part of DOE's interagency coordination, the NIH review panel on Physical Mapping Databases (February 20, 1990) was attended as an observer.

The DOE and the NIH formalized their coordination and cooperation with a Memorandum of Understanding (MOU) in October 1988. Both the DOE Human Genome Coordinating Committee and the NIH Human Genome Program Advisory Committee had appointed informatics subcommittees. These subcommittees met informally twice (Crystal City, Virginia, July 19, 1989; Herndon, Virginia, November 8, 1989). These meetings resulted in a document on genome informatics needs and goals and a recommendation on the makeup of the formal Joint Informatics Task Force (JITF). This Task Force was formally constituted following action by the two parent agency committees. Support was provided for these meetings and for formulation of the document. The first formal meeting of the JITF was held in Rockville, Maryland, on March 8-9, 1990.

The DOE and the NIH jointly published a document entitled "Understanding Our Genetic Inheritance - The US Human Genome Project: The First Five Years FY 1991-1995" encompassing the joint plan developed by their advisory committees.

Interlaboratory Cooperation

Representation was provided for the DOE informatics community at the Human Genome Coordinating Committee (HGCC) meetings; attendance was provided to the NIH Program Advisory Committee (PAC) meetings and the joint HGCC-PAC meetings.

The DOE Human Genome Contractor/Grantee Workshop, held in Sante Fe, New Mexico, November 3-4, 1989, convened the people working on the DOE genome program and provided an overview of the program. With the help of Slyvia Splengler of Lawrence Berkeley Laboratory (LBL),

an informal reception for computer professionals before the meeting resulted in many interesting discussions.

Another outcome was a meeting of human genome computer scientists from Los Alamos National Laboratory (LANL), LBL, Lawrence Livermore National Laboratory (LLNL), and PNL that was held at LBL on December 1, 1989. Each laboratory presented the software they were currently working on and the additional software they needed. Numerous arrangements for sharing software and collaborations were made; some were already under way.

Oak Ridge Liaison

In February 1988, the Human Genome Task Group initiated a project at Oak Ridge National Laboratory (ORNL) called Human Genome Management Information System (HGMIS). The project began with four components: (1) a quarterly newsletter, (2) an annual DOE program report, (3) technical reports, and (4) an electronic bulletin board. Liaison was provided as the primary DOE contact with Betty Mansfield, the Task Leader for ORNL. The highlights for this year were producing the DOE program report and seeing the newsletter become a joint DOE/NIH effort.

The *Human Genome 1989-90 Program Report* was a 156-page, full-color report on the current status of the DOE program containing sections on history, background, management, and abstracts. It has become the cornerstone of the DOE's public relations on the genome program.

The NIH was also sufficiently impressed with the quarterly newsletter last year to join with the DOE this year to produce a bimonthly newsletter featuring news from both agencies. The joint newsletter, renamed "Human Genome News" instead of "Quarterly," was first published in April 1990 and will continue to be produced by the ORNL group. Liaison was provided with the public relations people at NIH who were responsible for their input into the newsletter. DOE continues to receive many favorable comments about the usefulness of this publication. The mailing list, which grew this year from 2100 to more than 4500 names, includes scientists, administrators, staff of other agencies, members of the press, upper DOE and National Laboratory management, and Congressional staff.

Meeting Attendance

Interest in the national Human Genome Project engendered many meetings on this topic (and sessions on human genome at tangentially related meetings). The DOE sent representatives to many of these meetings, often in response to invitations, to make presentations and bring reports back to the Task Group. Representation was provided to a number of informatics-related meetings:

- NSF Workshop on Computational Biology, Washington, D.C., December 13-15, 1989
- 1st International Conference on Electrophoresis, Supercomputing, and the Human Genome, Tallahassee, Florida, April 10-13, 1990
- Workshop on Computing and Molecular Biology, Washington, D.C., April 30-May 1, 1990
- Cold Spring Harbor Laboratory meeting on Genome Mapping and Sequencing, Cold Spring Harbor, New York, May 3-6, 1990
- Panel session on Database Issues of the Human Genome Project at SIGMOD '90, Atlantic City, New Jersey, May 25, 1990
- Federal Technology Transfer -- Biotechnology Conference, Washington, D.C., July 10, 1990
- Human Genome hearing before the Senate Subcommittee on Energy Research and Development, Washington, D.C., July 11, 1990
- Software and Database Developers Conference, Bethesda, Maryland, July 16, 1990. This meeting was sponsored by the National Center for Biotechnology Information (NCBI) of the National Library of Medicine.

Regular meetings of two groups were attended as an observer for OHER and the Human Genome Task Group. The first is the ESnet (Energy Sciences network) Steering Committee (ESSC), which is an effort to consolidate several existing special purpose networks within Energy Research programs and at the same time significantly upgrade the capacity of the network. The OHER research community is not now a significant user of this network but will be in the future. Meetings of the ESSC were attended as an observer for the OHER staff. With George Duda of the Health Effects Research Division, a survey was conducted of OHER-funded researchers to determine their current network uses and future network needs. The results of this survey were used in OHER's input to ESnet planning.

The second regular meeting was that of the semi-annual GenBank Advisors meeting, of interest to DOE because of its relevance to the genome program and because part of the contract is carried out at LANL. The GenBank Sponsor's Forum was also attended, at which the NIH GenBank staff reviewed the Advisors' meeting with other agency staff.

Other Human Genome Efforts

One major focus was to find a replacement detailee. OHER received approval to hire a permanent Computational Biologist rather than a temporary assignee, and the national labs and universities were polled for candidates and also an announcement was sent out on electronic mail. Support was provided in the interviewing of candidates for this position and for a new Molecular Biologist position.

The Human Genome Program is highly visible and is often a major topic in briefings to the Director of Energy Research, the Secretary of Energy, the Office of Management and Budget, and Congress. Support was provided preparing materials for these briefings.

Appendix

Appendix

Dose-Effect Studies with Inhaled Plutonium in Beagles

On the following pages (pp. 119-131), data are presented for all dogs assigned to current life-span dose-effect studies with inhaled $^{239}PuO_2$, $^{238}PuO_2$, and ^{239}Pu nitrate. Information is presented on the estimated initial lung deposition, based on external thorax counts and on estimated lung weights (0.011 x body weight) at time of exposure. Information is also provided (see column headed "Comments on Dead Dogs") on the current interpretation of the most prominent clinicopathological features associated with the death of animals. These data represent information presently available, and are presented as reference material for scientists who desire to follow in detail the progress of these experiments.

DOSE-EFFECT STUDIES WITH INHALED PU-239 OXIDE IN BEAGLES

DOSE GROUP	DOG IDENT	INITIAL ALVEOLAR DEPOSITION NCI	NCI/G LUNG	NCI/ KG	INHALATION EXPOSURE WEIGHT (KG)	AGE* (MO)	DATE	DATE OF DEATH	MONTHS SINCE INHALATION 9/30/90	DEATH	COMMENTS ON DEAD DOGS
CONTROL	738 F	0	0.00	0.00				08/11/83		171.5*	Hemangiosarcoma, Heart
CONTROL	740 F	0	0.00	0.00				06/18/83		169.8*	Malignant Lymphoma
CONTROL	749 F	0	0.00	0.00				09/14/84		183.4*	Adrenalitis
CONTROL	755 M	0	0.00	0.00				12/10/82		162.2*	Status Epilepti, Nephrosclero
CONTROL	766 M	0	0.00	0.00				06/26/84		180.3*	Lung Tumor
CONTROL	775 F	0	0.00	0.00				10/05/81		147.3*	Pulmonary Thromboembolism
CONTROL	785 M	0	0.00	0.00				09/02/87		217.5*	Luxated Vertebral Disc
CONTROL	789 M	0	0.00	0.00				07/25/83		167.9*	Malignant Lymphoma
CONTROL	792 M	0	0.00	0.00				04/28/76		79.5*	Oral Tumor
CONTROL	800 F	0	0.00	0.00				11/17/86		204.9*	Malignant Pheochromocytoma
CONTROL	801 M	0	0.00	0.00				02/23/82		148.1*	Lung Tumor
CONTROL	811 F	0	0.00	0.00				02/24/85		183.1*	Oral cav.: Malignant Melanoma
CONTROL	846 M	0	0.00	0.00				04/08/83		159.6*	Nephrosclerosis
CONTROL	861 M	0	0.00	0.00				11/18/86		202.6*	Cushing's,Intestinal Carcinom
CONTROL	868 F	0	0.00	0.00				03/24/87		205.4*	Chronic Nephropathy
CONTROL	872 F	0	0.00	0.00				11/05/82		152.8*	Lung Tumor
CONTROL	878 M	0	0.00	0.00				01/22/85		177.4*	Chronic Nephropathy
CONTROL	882 M	0	0.00	0.00				11/06/81		138.7*	Hemangiosarcoma, Liver
CONTROL	885 F	0	0.00	0.00				02/18/83		153.5*	Lung Tumor
CONTROL	903 F	0	0.00	0.00				01/30/85		174.6*	Malignant Lymphoma
CONTROL SACRIFICE	701 F	0	0.00	0.00				04/18/79		121.0*	Sacrificed
CONTROL SACRIFICE	703 M	0	0.00	0.00				03/24/77		96.2*	Sacrificed
CONTROL SACRIFICE	724 M	0	0.00	0.00				03/30/78		107.9*	Sacrificed
D-1 LOWEST	756 M	0	0.00	0.00	13.0	19.5	01/19/71	04/21/83	147.0		Epilepsy
D-1 LOWEST	762 M	0	0.00	0.00	11.5	19.3	01/19/71	01/24/77	72.2		Sacrificed
D-1 LOWEST	847 M	0	0.00	0.00	13.0	18.5	07/06/71	01/23/85	162.6		Kidney Failure
D-1 LOWEST	858 M	0	0.00	0.00	13.5	18.2	07/06/71	10/01/86	182.9		Lymphocytic Leukemia
D-1 LOWEST	865 F	0	0.00	0.00	9.0	17.4	07/06/71	09/16/86	182.4		Acute Pneumonia, Lung Tumor
D-1 LOWEST	879 M	0	0.00	0.00	14.5	17.9	10/07/71	07/27/84	153.7		Hemangiosarcoma, Liver,Spleen
D-1 LOWEST	886 F	0	0.00	0.00	10.5	18.2	11/10/71	04/04/84	148.8		Meningioma, Malignant
D-1 LOWEST	907 F	0	0.00	0.00	11.5	15.9	11/10/71	05/10/86	174.0		Pneumonia
D-1 LOWEST	825 F	1	0.01	0.12	11.5	18.1	06/08/71	11/17/82	137.3		Hemangiosarcoma, Spleen
D-1 LOWEST	849 F	1	0.01	0.10	10.0	21.3	10/07/71	10/26/72	12.6		Sacrificed
D-1 LOWEST	904 F	1	0.01	0.07	9.5	15.9	11/10/71	12/19/83	145.3		Chondrosarcoma, Nasal
D-1 LOWEST	832 F	2	0.02	0.22	9.0	16.5	04/26/71	03/03/86	178.2		Malignant Lymphoma
D-1 LOWEST	900 M	3	0.02	0.22	13.0	16.0	11/10/71	05/21/82	126.3		Round Cell Sarcoma
D-1 LOWEST	870 F	4	0.03	0.32	12.0	16.9	07/06/71	05/04/84	154.0		Pneumonia
D-1 LOWEST	899 F	4	0.03	0.31	11.5	16.0	11/10/71	03/29/81	112.6		Hemangiosarcoma, Heart
D-1 LOWEST	867 M	5	0.04	0.41	11.5	17.4	07/06/71	02/07/86	175.1		Malignant Lymphoma
D-1 LOWEST	891 M	6	0.04	0.41	14.0	16.0	11/10/71	06/26/81	115.5		Septicemia
D-1 LOWEST	853 M	8	0.05	0.51	15.0	21.3	10/07/71	12/12/84	158.2		Bronchopneumonia
D-1 LOWEST	875 M	8	0.05	0.54	14.0	16.8	07/06/71	05/21/78	82.5		Kidney: Malignant Lymphoma
D-1 LOWEST	770 F	6	0.06	0.63	9.5	19.1	01/19/71	11/29/84	166.3		Glomerulosclerosis

* Indicates age in months since birth, all other ages are in months since exposure.

DOSE-EFFECT STUDIES WITH INHALED PU-239 OXIDE IN BEAGLES

DOSE GROUP	DOG IDENT	INITIAL ALVEOLAR DEPOSITION NCI	NCI/G LUNG	NCI/ KG	INHALATION EXPOSURE WEIGHT (KG)	AGE* (MO)	DATE	DATE OF DEATH	MONTHS SINCE INHALATION 9/30/90	DEATH	COMMENTS ON DEAD DOGS
D-1 LOWEST	788 M	8	0.06	0.62	13.0	18.8	02/10/71	04/13/84		158.1	Chronic Nephropathy
D-1 LOWEST	850 F	5	0.06	0.63	8.0	21.3	10/07/71	06/06/83		140.0	Bone Tmr, Chronic Nephropathy
D-1 LOWEST	893 M	9	0.06	0.61	14.0	14.9	10/07/71	07/01/86		176.8	Pneumonia
D-1 LOWEST	807 F	8	0.07	0.73	11.0	14.6	02/10/71	07/24/81		125.4	Pituitary Tumor, Cushing's
D-1 LOWEST	841 F	6	0.07	0.75	8.0	17.7	06/08/71	04/01/86		177.8	Malignant Lymphoma
D-1 LOWEST	908 M	9	0.07	0.77	11.0	15.9	11/10/71	04/01/80		100.7	Unknown, Pulmon. Hyalinosis
D-2 LOW	776 M	10	0.07	0.74	13.5	20.2	03/04/71	09/19/84		162.6	Bronchopneumonia
D-2 LOW	842 M	10	0.07	0.77	13.5	18.6	07/06/71	05/01/85		165.8	Lung Tmr, Chronic Nephropathy
D-2 LOW	767 M	10	0.08	0.83	12.0	18.2	12/21/70	12/09/85		179.6	Valvular Endocardiopathy
D-2 LOW	920 M	11	0.08	0.92	12.0	16.0	06/08/72	07/07/72		1.0	Sacrificed
D-2 LOW	862 M	13	0.09	1.00	13.0	17.3	06/08/71	06/25/83		144.6	Peritonitis
D-2 LOW	871 M	13	0.09	0.96	13.5	16.9	07/06/71	07/24/86		180.6	Malignant Melanoma, Oral
D-2 LOW	874 M	16	0.11	1.24	13.0	16.8	07/06/71	04/09/85		165.1	Chronic Nephropathy
D-2 LOW	754 M	22	0.15	1.69	13.0	19.5	01/19/71	01/10/78		83.7	Epilepsy
D-2 LOW	845 F	19	0.15	1.63	11.5	17.6	06/08/71	08/09/84		158.1	Urinary Bladder Tumor
D-2 LOW	748 F	14	0.16	1.75	8.0	19.5	01/19/71	08/19/81		127.0	Unknown Cause
D-2 LOW	798 F	16	0.16	1.78	9.0	15.7	02/10/71	08/29/74		42.6	Sacrificed
D-2 LOW	826 F	19	0.17	1.90	10.0	19.1	07/06/71	04/17/84		153.4	Hemangioma, Spleen
D-2 LOW	831 F	21	0.18	2.00	10.5	17.9	06/08/71	05/14/84		155.2	Pneumonia
D-2 LOW	881 F	19	0.19	2.09	9.0	17.7	10/07/71	12/20/86		182.4	Acute Pneumonia
D-2 LOW	780 F	24	0.22	2.40	10.0	18.2	01/19/71	04/08/82		134.6	Pheochromocytoma
D-2 LOW	859 M	35	0.22	2.41	14.5	18.2	07/06/71	04/22/84		153.6	Urinary Bladder Tumor
D-2 LOW	757 M	36	0.23	2.57	14.0	18.5	12/21/70	11/26/86		191.2	Leiomyosarcoma,Kidney,Lung Tm
D-2 LOW	876 F	19	0.24	2.69	7.0	17.9	10/07/71	05/05/86		174.9	Nephropathy,Lung Tumor
D-2 LOW	806 F	26	0.25	2.74	9.5	15.3	03/04/71	10/29/82		139.9	Palate: Malignant Melanoma
D-2 LOW	813 F	32	0.29	3.20	10.0	15.1	03/04/71	12/15/83		153.4	Multilobular Sarcoma, Skull
D-2 LOW	877 F	34	0.29	3.24	10.5	17.9	10/07/71	05/06/86		174.9	Lung Tumor
D-2 LOW	769 F	28	0.32	3.50	8.0	18.2	12/21/70	06/23/78		90.1	Ovarian Tumor
D-2 LOW	802 M	40	0.33	3.64	11.0	18.1	04/26/71	12/28/84		164.1	Pneumonia
D-3 MED-LOW	781 F	48	0.38	4.17	11.5	17.3	12/21/70	02/20/81		122.0	Kidney Tumor, Lung Tumor
D-3 MED-LOW	771 F	44	0.40	4.40	10.0	19.2	01/20/71	11/02/83		153.4	Lung Tumor
D-3 MED-LOW	782 M	62	0.42	4.59	13.5	19.0	02/10/71	05/27/83		147.5	Neurofibrosarcoma,Brach.Pl.
D-3 MED-LOW	786 M	62	0.42	4.59	13.5	19.5	03/04/71	05/29/86		182.8	Adrenocortical Carc, Lung Tmr
D-3 MED-LOW	752 M	62	0.43	4.77	13.0	18.6	12/21/70	02/22/79		98.1	Lung Tumor, Adrenal Tumor
D-3 MED-LOW	823 M	65	0.44	4.81	13.5	16.8	04/26/71	05/24/84		156.9	Urinary Bladder Tumor
D-3 MED-LOW	883 M	63	0.44	4.85	13.0	17.7	10/07/71	01/25/88		195.6	Chronic Nephropathy
D-3 MED-LOW	778 M	74	0.46	5.10	14.5	20.2	03/04/71	08/26/79		101.7	Pulmonary Thromboembolism
D-3 MED-LOW	838 M	56	0.46	5.09	11.0	17.8	06/08/71	07/20/84		157.4	Malignant Lymphoma, Lung Tmr
D-3 MED-LOW	795 F	54	0.49	5.40	10.0	15.0	01/20/71	09/06/83		151.5	Lung Tumor
D-3 MED-LOW	815 M	68	0.52	5.67	12.0	16.8	04/26/71	05/22/73		24.9	Sacrificed
D-3 MED-LOW	851 F	53	0.54	5.89	9.0	21.3	10/07/71	12/07/86		182.0	Thyroid Carc, Hypothyroidism
D-3 MED-LOW	918 M	74	0.58	6.43	11.5	16.0	06/08/72	07/06/72		0.9	Sacrificed
D-3 MED-LOW	834 F	67	0.68	7.44	9.0	17.8	06/08/71	07/05/79		96.9	Pyometra

* Indicates age in months since birth, all other ages are in months since exposure.

DOSE-EFFECT STUDIES WITH INHALED PU-239 OXIDE IN BEAGLES

DOSE GROUP	DOG IDENT	INITIAL ALVEOLAR DEPOSITION NCI	NCI/G LUNG	NCI/ KG	INHALATION EXPOSURE WEIGHT (KG)	AGE* (MO)	DATE	DATE OF DEATH	MONTHS SINCE INHALATION 9/30/90	DEATH	COMMENTS ON DEAD DOGS
D-3 MED-LOW	797 F	85	0.70	7.73	11.0	16.4	03/04/71	05/16/86		182.4	Lung Tumor
D-3 MED-LOW	848 F	75	0.72	7.94	9.5	21.3	10/07/71	10/02/86		179.8	Acute Pneumonia
D-3 MED-LOW	827 F	89	0.74	8.09	11.0	16.7	04/26/71	01/06/85		164.4	Acute Pneumonitis
D-3 MED-LOW	697 M	140	0.85	9.33	15.0	19.5	10/30/70	05/08/80		114.3	Cardiac Valve Insufficiency
D-3 MED-LOW	750 M	118	0.93	10.26	11.5	19.6	01/20/71	06/28/84		161.2	Lung Tmr, Malignant Lymphoma
D-3 MED-LOW	884 M	123	1.12	12.30	10.0	17.8	10/08/71	09/12/84		155.2	Lung Tumor
D-3 MED-LOW	844 F	135	1.17	12.86	10.5	17.6	06/08/71	08/08/85		170.0	Nephropathy,Lung Tumor
D-3 MED-LOW	905 F	127	1.36	14.94	8.5	15.9	11/10/71	02/07/83		134.9	Malignant Lymphoma
D-4 MEDIUM	866 M	200	1.35	14.81	13.5	17.4	07/06/71	06/27/84		155.7	Lung Tumor
D-4 MEDIUM	809 F	157	1.36	14.95	10.5	15.3	03/04/71	05/28/81		122.8	Liver Cirr,Thy Tm,Addison's
D-4 MEDIUM	764 F	158	1.37	15.05	10.5	18.2	12/21/70	07/07/82		138.5	Lung Tumor
D-4 MEDIUM	835 F	163	1.48	16.30	10.0	16.4	04/26/71	06/25/78		86.0	Reticulum Cell Sarcoma
D-4 MEDIUM	839 F	189	1.49	16.43	11.5	16.3	04/26/71	02/03/86		177.3	Lung Tumor,Bile Duct Carcinom
D-4 MEDIUM	814 F	140	1.50	16.47	8.5	15.1	03/04/71	10/17/79		103.5	Lung Tumor, Thyroid Adenoma
D-4 MEDIUM	836 M	256	1.66	18.29	14.0	17.8	06/08/71	03/16/81		117.3	Lung Tumor
D-4 MEDIUM	819 F	163	1.74	19.18	8.5	18.2	06/08/71	08/20/85		170.4	Nephropathy,Lung Tumor
D-4 MEDIUM	888 M	274	1.78	19.57	14.0	17.1	10/08/71	07/02/79		92.8	Lung Tumor
D-4 MEDIUM	824 F	227	1.79	19.74	11.5	18.1	06/08/71	01/26/81		115.6	Bronchopneumonia
D-4 MEDIUM	860 M	254	1.85	20.32	12.5	17.3	06/08/71	06/24/82		132.5	Lung Tumor
D-4 MEDIUM	833 F	248	2.37	26.11	9.5	16.5	04/26/71	04/04/83		143.3	Metritis,Adrenal & Thyr Tumr
D-4 MEDIUM	810 F	302	2.39	26.26	11.5	15.3	03/04/71	09/09/81		126.2	Lung Tumor
D-4 MEDIUM	794 M	444	2.60	28.65	15.5	17.7	03/04/71	02/17/81		119.5	Pituitary Tumor, Cushing's
D-4 MEDIUM	854 M	465	2.64	29.06	16.0	21.3	10/08/71	01/25/82		123.6	Lung Tumor
D-4 MEDIUM	478 M	298	2.71	29.80	10.0	64.0	10/09/70	10/16/70		0.2	Sacrificed
D-4 MEDIUM	808 F	270	2.89	31.76	8.5	14.6	02/10/71	09/09/82		138.9	Lung Tumor
D-4 MEDIUM	805 F	257	3.12	34.27	7.5	18.5	06/08/71	07/22/82		133.5	Esophageal & Lung Tumor
D-4 MEDIUM	812 M	438	3.19	35.04	12.5	17.1	04/26/71	11/12/79		102.6	Lung Tumor
D-4 MEDIUM	857 M	486	3.40	37.38	13.0	17.3	06/08/71	07/01/80		108.8	Lung Tumor
D-4 MEDIUM	892 M	494	3.59	39.52	12.5	16.0	11/10/71	10/26/81		119.5	Lung Tumor
D-4 MEDIUM	816 M	398	3.62	39.80	10.0	16.8	04/25/71	05/11/71		0.5	Sacrificed
D-4 MEDIUM	777 M	546	3.97	43.68	12.5	20.2	03/04/71	03/26/80		108.7	Lung Tumor
D-4 MEDIUM	803 M	547	4.32	47.57	11.5	18.1	04/26/71	11/10/77		78.5	Interstitial Pneumonitis
D-5 MED-HIGH	787 M	651	4.73	52.08	12.5	19.5	03/04/71	02/08/79		95.2	Lung Tumor, Intestinal Tumor
D-5 MED-HIGH	840 F	703	4.92	54.08	13.0	17.7	06/08/71	04/29/80		106.7	Lung Tumor
D-5 MED-HIGH	727 M	733	5.33	58.64	12.5	18.8	10/26/70	11/10/76		72.5	Lung Tumor
D-5 MED-HIGH	898 F	711	5.39	59.25	12.0	16.0	11/10/71	02/03/81		110.8	Uri Bladr & Lung & Adr Tumor
D-5 MED-HIGH	856 F	818	5.72	62.92	13.0	18.2	07/07/71	05/02/79		93.8	Lung Tumor
D-5 MED-HIGH	759 M	809	6.13	67.42	12.0	18.3	12/21/70	06/02/75		53.4	Lung Tumor
D-5 MED-HIGH	864 F	801	6.62	72.82	11.0	17.4	07/07/71	11/02/79		99.9	Lung Tumor
D-5 MED-HIGH	909 M	737	6.70	73.70	10.0	15.9	11/10/71	06/04/81		114.8	Lung Tumor
D-5 MED-HIGH	734 M	914	6.92	76.17	12.0	19.2	11/10/70	04/01/71		4.7	Sacrificed
D-5 MED-HIGH	837 M	1283	8.04	88.48	14.5	18.8	07/07/71	07/21/77		72.5	Lung Tumor
D-5 MED-HIGH	863 F	980	8.48	93.33	10.5	17.4	07/07/71	10/21/77		75.5	Lung Tumor

* Indicates age in months since birth, all other ages are in months since exposure.

DOSE-EFFECT STUDIES WITH INHALED PU-239 OXIDE IN BEAGLES

DOSE GROUP	DOG IDENT	INITIAL ALVEOLAR DEPOSITION NCI	NCI/G LUNG	NCI/ KG	INHALATION EXPOSURE WEIGHT (KG)	AGE* (MO)	DATE	DATE OF DEATH	MONTHS SINCE INHALATION 9/30/90	DEATH	COMMENTS ON DEAD DOGS
D-5 MED-HIGH	820 F	847	8.56	94.11	9.0	18.2	06/08/71	06/01/79		95.8	Lung Tumor
D-5 MED-HIGH	852 F	1187	9.38	103.22	11.5	21.3	10/08/71	02/22/78		76.5	Lung Tumor
D-5 MED-HIGH	880 F	840	9.55	105.00	8.0	17.8	10/08/71	12/04/78		85.9	Lung Tumor
D-5 MED-HIGH	889 F	1089	9.90	108.90	10.0	16.0	11/10/71	09/20/79		94.3	Lung Tumor, Osteoarthropathy
D-5 MED-HIGH	783 M	1394	10.14	111.52	12.5	19.0	02/10/71	12/03/75		57.7	Lung Tumor
D-5 MED-HIGH	804 M	1344	10.18	112.00	12.0	20.5	07/07/71	08/18/74		37.4	Lung Tumor, Rad. Pneumonitis
D-5 MED-HIGH	873 M	1767	10.71	117.80	15.0	16.8	07/07/71	09/03/76		61.9	Lung Tumor
D-5 MED-HIGH	760 M	1378	10.89	119.83	11.5	19.3	01/20/71	08/15/73		30.8	Radiation Pneumonitis
D-5 MED-HIGH	796 F	1318	11.41	125.52	10.5	15.7	02/10/71	09/17/75		55.2	Lung Tumor, Osteoarthropathy
D-5 MED-HIGH	761 M	1460	12.07	132.73	11.0	19.3	01/20/71	11/02/76		69.4	Lung Tumor
D-5 MED-HIGH	709 M	1726	12.55	138.08	12.5	19.6	11/10/70	03/31/71		4.6	Sacrificed
D-5 MED-HIGH	772 M	1896	14.99	164.87	11.5	19.8	02/10/71	06/26/75		52.5	Lung Tumor, Osteoarthropathy
D-5 MED-HIGH	702 F	1682	15.29	168.20	10.0	19.8	11/10/70	03/31/71		4.6	Sacrificed
D-5 MED-HIGH	739 F	1511	17.17	188.88	8.0	18.5	11/10/70	04/01/71		4.7	Sacrificed
D-6 HIGH	753 F	2448	23.43	257.68	9.5	18.5	12/21/70	10/02/76		69.4	Lung Tumor
D-6 HIGH	817 M	3164	23.97	263.67	12.0	19.2	07/07/71	03/26/73		20.6	Radiation Pneumonitis
D-6 HIGH	829 M	3515	24.58	270.38	13.0	19.1	07/07/71	09/13/73		26.3	Radiation Pneumonitis
D-6 HIGH	890 F	3101	31.32	344.56	9.0	16.0	11/10/71	06/13/74		31.1	Radiation Pneumonitis
D-6 HIGH	435 F	3840	33.25	365.71	10.5	75.5	11/05/70	11/12/70		0.2	Sacrificed
D-6 HIGH	913 M	4900	35.64	392.00	12.5	17.4	07/19/72	08/18/72		1.0	Sacrificed
D-6 HIGH	906 F	6632	63.46	698.11	9.5	15.9	11/09/71	11/22/72		12.5	Radiation Pneumonitis
D-6 HIGH	896 F	5515	66.85	735.33	7.5	16.0	11/10/71	02/12/73		15.1	Radiation Pneumonitis
D-6 HIGH	747 F	7476	97.09	1068.00	7.0	19.6	01/20/71	01/13/72		11.8	Radiation Pneumonitis
D-6 HIGH	910 M	14267	103.76	1141.36	12.5	15.9	11/10/71	10/12/72		11.1	Radiation Pneumonitis

* Indicates age in months since birth, all other ages are in months since exposure.

DOSE-EFFECT STUDIES WITH INHALED PU-238 OXIDE IN BEAGLES

DOSE GROUP	DOG IDENT	INITIAL ALVEOLAR DEPOSITION NCI	NCI/G LUNG	NCI/ KG	INHALATION EXPOSURE WEIGHT (KG)	AGE* (MO)	DATE	DATE OF DEATH	MONTHS SINCE INHALATION 9/30/90 DEATH	COMMENTS ON DEAD DOGS
CONTROL	939 M	0	0.00	0.00				10/01/82	136.9*	Urinary Bladder Tumor
CONTROL	949 F	0	0.00	0.00				10/30/84	161.7*	Malignant Lymphoma
CONTROL	978 M	0	0.00	0.00				04/07/88	202.8*	Cervical Disc Disease
CONTROL	990 F	0	0.00	0.00				07/08/79	97.4*	Pyometra
CONTROL	996 F	0	0.00	0.00				07/06/84	157.2*	Malignant Lymphoma
CONTROL	1005 M	0	0.00	0.00				02/24/87	188.8*	Lung Tumor
CONTROL	1007 F	0	0.00	0.00				03/29/88	201.9*	Chronic Nephropathy
CONTROL	1024 M	0	0.00	0.00				07/13/87	192.9*	Trans. Cell Carc. Urethra
CONTROL	1038 M	0	0.00	0.00				12/16/86	183.9*	Hemangiosarcoma, Spleen
CONTROL	1045 M	0	0.00	0.00				06/08/86	177.6*	Renal Amyloidosis,Spl Hemangi
CONTROL	1054 F	0	0.00	0.00				12/05/88	207.3*	Chronic Nephropathy
CONTROL	1061 F	0	0.00	0.00				07/07/81	118.2*	Malignant Lymphoma
CONTROL	1093 M	0	0.00	0.00				11/04/83	142.4*	Pituitary Tumor, Cushing's
CONTROL	1097 F	0	0.00	0.00				09/15/88	200.1*	Nasal Transitional Carcinoma
CONTROL	1112 M	0	0.00	0.00				12/02/86	178.4*	Malignant Lymphoma
CONTROL	1116 F	0	0.00	0.00				04/07/89	206.3*	Hemangiosarcoma, Omentum
CONTROL	1186 F	0	0.00	0.00				07/26/85	155.3*	Urinary Bladder Tumor
CONTROL	1197 M	0	0.00	0.00				04/25/89	199.8*	Pneumonia
CONTROL	1209 M	0	0.00	0.00				12/27/88	195.6*	Pulmonary Interstial Fibrosis
CONTROL	1225 F	0	0.00	0.00				10/10/87	180.2*	Pituitary Adenoma
CONTROL SACRIFICE	966 M	0	0.00	0.00				04/30/77	71.6*	Sacrificed
CONTROL SACRIFICE	1011 F	0	0.00	0.00				06/01/78	83.9*	Sacrificed
CONTROL SACRIFICE	1013 F	0	0.00	0.00				05/29/79	95.8*	Sacrificed
CONTROL SACRIFICE	1087 M	0	0.00	0.00				12/14/76	60.0*	Sacrificed
CONTROL SACRIFICE	1118 M	0	0.00	0.00				01/13/76	47.5*	Sacrificed
CONTROL SACRIFICE	1223 M	0	0.00	0.00				05/15/75	31.9*	Sacrificed
CONTROL SACRIFICE	1227 M	0	0.00	0.00				12/01/76	49.9*	Sacrificed
CONTROL SACRIFICE	1228 M	0	0.00	0.00				10/31/78	72.9*	Sacrificed
D-1 LOWEST	998 M	0	0.00	0.00	10.5	19.6	01/18/73	04/11/86	158.7	Lung Tumor
D-1 LOWEST	1003 M	0	0.00	0.00	14.0	19.6	01/18/73	04/01/87	170.4	Transitional Carc, Uri Bladr
D-1 LOWEST	1023 F	0	0.00	0.00	12.5	19.2	01/18/73	03/27/88	182.2	Pneumonia
D-1 LOWEST	1039 M	0	0.00	0.00	11.0	17.0	01/18/73	07/04/86	161.5	Heart Failure
D-1 LOWEST	1044 F	0	0.00	0.00	11.5	17.0	01/18/73	08/31/88	187.4	Epilepsy
D-1 LOWEST	1055 M	0	0.00	0.00	13.0	16.8	01/18/73	06/04/87	172.5	Malignant Melanoma, Oral
D-1 LOWEST	1063 M	0	0.00	0.00	14.5	16.7	01/18/73	11/11/80	93.8	Brain Tumor, Heart Tumor
D-1 LOWEST	1105 F	0	0.00	0.00	10.0	16.4	05/31/73	02/08/85	140.3	Malignant Lymphoma
D-1 LOWEST	1194 F	0	0.00	0.00	10.5	19.8	04/18/74	12/03/85	139.5	Malignant Lymphoma
D-1 LOWEST	1215 M	0	0.00	0.00	15.5	19.3	04/18/74	04/26/77	36.3	Sacrificed
D-1 LOWEST	1230 M	0	0.00	0.00	12.5	18.4	04/18/74	09/30/86	149.4	Hemangiosarcoma, Liver
D-1 LOWEST	951 M	2	0.01	0.14	14.0	19.3	12/19/72	02/14/83	121.9	Anesthetic Death
D-1 LOWEST	1008 M	2	0.01	0.15	13.5	19.6	01/18/73	10/24/85	153.2	Fibrosarcoma, Spleen
D-1 LOWEST	1193 F	2	0.01	0.16	12.5	19.8	04/18/74	01/22/86	141.2	Immune Hemolytic Anemia
D-1 LOWEST	959 M	3	0.02	0.22	13.5	19.2	12/19/72	06/22/84	138.1	Liver Abcess

* Indicates age in months since birth, all other ages are in months since exposure.

DOSE-EFFECT STUDIES WITH INHALED PU-238 OXIDE IN BEAGLES

DOSE GROUP	DOG IDENT	INITIAL ALVEOLAR DEPOSITION NCI	NCI/G LUNG	NCI/ KG	INHALATION EXPOSURE WEIGHT (KG)	AGE* (MO)	DATE	DATE OF DEATH	MONTHS SINCE INHALATION 9/30/90	DEATH	COMMENTS ON DEAD DOGS
D-1 LOWEST	1069 F	2	0.02	0.24	8.5	18.1	05/31/73	06/24/83		120.8	Malignant Lymphoma
D-1 LOWEST	1095 F	2	0.02	0.19	10.5	16.6	05/31/73	08/12/87		170.4	Chronic Nephropathy
D-1 LOWEST	921 F	3	0.03	0.31	10.0	19.5	11/30/72	12/27/72		0.9	Sacrificed
D-1 LOWEST	923 F	3	0.03	0.35	8.5	19.5	11/30/72	01/26/73		1.9	Sacrificed
D-1 LOWEST	989 F	3	0.03	0.32	9.5	18.8	12/19/72	03/05/81		98.5	Bone Tumor, Fibrosarcoma
D-1 LOWEST	925 M	5	0.04	0.40	12.5	19.5	11/30/72	02/27/73		2.9	Sacrificed
D-1 LOWEST	1204 M	6	0.04	0.43	14.0	17.7	02/26/74	02/23/89		179.9	Trans. Cell Carc, Urethra
D-1 LOWEST	970 F	6	0.05	0.55	11.0	19.2	12/19/72	01/04/77		48.5	Sacrificed
D-1 LOWEST	993 F	6	0.05	0.50	12.0	18.8	12/19/72	07/01/86		162.4	Malignant Lymphoma
D-1 LOWEST	1106 F	5	0.05	0.50	10.0	16.4	05/31/73	03/14/83		117.4	Adrenal Tmr,Osteoarthropathy
D-2 LOW	1065 F	6	0.05	0.60	10.0	18.3	05/31/73	04/10/86		154.3	Malignant Lymphoma, Lung Tmr
D-2 LOW	1082 M	11	0.06	0.69	16.0	18.0	05/31/73	12/04/79		78.1	Paralysis, Spinal Cord Degen.
D-2 LOW	1188 M	11	0.06	0.71	15.5	18.4	02/26/74	01/15/84		118.6	Metastatic Lng Tmr, Prim. Unk
D-2 LOW	1084 M	13	0.07	0.76	17.0	17.5	05/31/73	08/19/89		194.6	Malignant Lymphoma, Heart
D-2 LOW	1090 F	10	0.08	0.83	12.0	17.3	05/31/73	05/10/87		167.3	Heart Failure
D-2 LOW	1222 M	15	0.10	1.07	14.0	19.0	04/18/74	03/19/86		143.0	Malign (mediast) Mesothelioma
D-2 LOW	971 F	13	0.11	1.24	10.5	19.2	12/19/72	05/04/83		124.5	Hemangiosarcoma, Spleen
D-2 LOW	999 F	11	0.11	1.16	9.5	18.7	12/19/72	01/31/86		157.4	Nasal Sarcoma, Lung Tumor
D-2 LOW	1229 M	16	0.11	1.19	13.5	16.8	02/26/74	05/25/84		122.9	Pneumonia, Thyroid Tumor
D-2 LOW	1070 M	22	0.12	1.33	16.5	18.1	05/31/73	12/13/83		126.4	Round Cell Sarcoma: Kidney
D-2 LOW	1214 M	17	0.12	1.36	12.5	19.3	04/18/74	05/12/75		12.8	Sacrificed
D-2 LOW	955 M	17	0.14	1.55	11.0	19.2	12/19/72	01/27/87		169.3	Lng Tumor, Bile Duct Adenoma
D-2 LOW	1033 M	17	0.14	1.55	11.0	19.1	02/22/73	12/17/85		153.8	Lung Tumor
D-2 LOW	1036 F	16	0.14	1.52	10.5	18.2	02/22/73	05/06/87		170.4	Malignant Melanoma, Oral
D-2 LOW	1216 M	23	0.16	1.77	13.0	19.3	04/18/74	04/22/87		156.1	Malignant Lymphoma
D-2 LOW	1060 F	22	0.18	2.00	11.0	17.8	02/22/73	12/21/84		141.9	Pneumonia
D-2 LOW	981 M	30	0.21	2.31	13.0	19.0	12/19/72	01/12/89		192.8	Chronic Nephropathy
D-2 LOW	1046 M	27	0.22	2.45	11.0	18.1	02/22/73	12/15/87		177.7	Lung Tumor
D-2 LOW	1050 F	22	0.22	2.44	9.0	18.1	02/22/73	05/14/86		158.7	Lung Tumor
D-2 LOW	1078 F	29	0.22	2.42	12.0	18.0	05/31/73	11/09/83		125.3	Meningioma, Malignant
D-2 LOW	1207 F	22	0.24	2.59	8.5	17.6	02/26/74	08/11/88		173.5	Herniated Vert Disc
D-2 LOW	1196 F	28	0.25	2.80	10.0	17.9	02/26/74	12/26/88		178.0	Salivary Squam. Carc, Lng Tmr
D-2 LOW	1189 M	38	0.26	2.81	13.5	20.0	04/18/74	04/25/79		60.2	Sacrificed
D-2 LOW	930 M	38	0.27	2.92	13.0	19.2	11/30/72	12/28/72		0.9	Sacrificed
D-3 MED-LOW	1066 M	54	0.31	3.38	16.0	18.3	05/31/73	06/21/83		120.7	Malignant Lymphoma
D-3 MED-LOW	972 F	40	0.33	3.64	11.0	19.2	12/19/72	03/04/86		158.5	Allergic Bronchitis
D-3 MED-LOW	1089 F	41	0.34	3.73	11.0	17.3	05/31/73	08/21/88		182.7	Chronic Nephropathy
D-3 MED-LOW	1310 M	54	0.34	3.72	14.5	18.5	03/04/75	04/01/77		24.9	Sacrificed
D-3 MED-LOW	1312 M	58	0.34	3.74	15.5	18.5	03/04/75	03/26/79		48.7	Sacrificed
D-3 MED-LOW	1311 M	54	0.36	4.00	13.5	18.5	03/04/75	04/03/78		37.0	Sacrificed
D-3 MED-LOW	1219 F	46	0.40	4.38	10.5	19.0	04/18/74	12/05/86		151.6	Chronic Nephropathy
D-3 MED-LOW	1317 M	72	0.41	4.50	16.0	18.1	03/04/75	04/01/77		24.9	Sacrificed
D-3 MED-LOW	1158 M	73	0.43	4.71	15.5	17.7	11/06/73	06/16/88		175.3	Nasal Carcinoma

* Indicates age in months since birth, all other ages are in months since exposure.

DOSE-EFFECT STUDIES WITH INHALED PU-238 OXIDE IN BEAGLES

DOSE GROUP	DOG IDENT	INITIAL ALVEOLAR DEPOSITION NCI	NCI/G LUNG	NCI/ KG	INHALATION EXPOSURE WEIGHT (KG)	AGE* (MO)	DATE	DATE OF DEATH	MONTHS SINCE INHALATION 9/30/90	DEATH	COMMENTS ON DEAD DOGS
D-3 MED-LOW	1165 M	76	0.43	4.75	16.0	17.3	11/06/73	07/21/86		152.4	Acute Pneumonia
D-3 MED-LOW	1309 M	60	0.44	4.80	12.5	18.5	03/04/75	04/22/87		145.6	Hemangiosarcoma, Liver
D-3 MED-LOW	1318 M	67	0.45	4.96	13.5	18.1	03/04/75	03/08/76		12.2	Sacrificed
D-3 MED-LOW	929 F	41	0.50	5.47	7.5	19.2	11/30/72	01/25/73		1.8	Sacrificed
D-3 MED-LOW	1316 M	84	0.53	5.79	14.5	18.1	03/04/75	12/13/88		165.4	Posterior Paralysis
D-3 MED-LOW	960 M	68	0.54	5.91	11.5	19.2	12/19/72	11/07/80		94.6	Malignant Lymphoma
D-3 MED-LOW	1072 M	98	0.54	5.94	16.5	18.1	05/31/73	09/22/83		123.7	Delayed Radiation Pneumonitis
D-3 MED-LOW	1190 F	71	0.54	5.92	12.0	18.1	02/26/74	05/09/85		134.4	Lung Tumor
D-3 MED-LOW	926 M	75	0.55	6.00	12.5	19.5	11/30/72	02/28/73		3.0	Sacrificed
D-3 MED-LOW	1315 M	90	0.55	6.00	15.0	18.1	03/04/75	03/31/77		24.9	Sacrificed
D-3 MED-LOW	982 M	76	0.58	6.33	12.0	19.0	12/19/72	01/29/86		157.3	Pneumonia, Thyroid Carcinoma
D-3 MED-LOW	1040 M	84	0.61	6.72	12.5	18.2	02/22/73	03/04/81		96.3	Parathyroid Adenoma
D-3 MED-LOW	1059 F	71	0.65	7.10	10.0	17.8	02/22/73	08/08/83		125.5	Malignant Lymphoma
D-3 MED-LOW	1319 M	99	0.67	7.33	13.5	18.1	03/04/75	03/09/76		12.2	Sacrificed
D-3 MED-LOW	1108 F	84	0.69	7.64	11.0	16.4	05/31/73	01/14/87		163.5	Posterior Paralysis
D-3 MED-LOW	1000 F	70	0.71	7.78	9.0	18.7	12/19/72	12/02/87		179.4	Transitional Carc, Uri Bladr
D-3 MED-LOW	1056 M	97	0.71	7.76	12.5	17.9	02/22/73	06/17/86		159.8	Pneumonia, Thyroid Carcinoma
D-3 MED-LOW	1004 M	116	0.73	8.00	14.5	19.6	01/18/73	04/30/87		171.3	Malig Lympho, Lng Tmr, Cholan
D-3 MED-LOW	1026 M	116	0.78	8.59	13.5	19.2	01/18/73	11/13/85		153.8	Hepatic Displasia
D-3 MED-LOW	1043 F	98	0.89	9.80	10.0	18.1	02/22/73	09/21/81		102.9	Empyema, Pituit.T., Cushing's
D-3 MED-LOW	1031 F	76	0.92	10.13	7.5	19.1	02/22/73	05/04/84		134.3	Pneumonia
D-3 MED-LOW	1212 F	111	1.12	12.33	9.0	17.6	02/26/74	06/24/88		171.9	Hepatocellular Carcinoma
D-4 MEDIUM	1176 M	129	0.87	9.56	13.5	16.6	11/06/73	12/12/85		145.2	Hemangioma, Spleen
D-4 MEDIUM	1221 F	124	1.13	12.40	10.0	19.0	04/18/74	09/30/88		173.4	Malig Lympho, Cholangiosarcom
D-4 MEDIUM	1195 M	228	1.38	15.20	15.0	18.1	02/26/74	07/29/87		161.0	Chron Nephr,Bile Duct Adenoma
D-4 MEDIUM	1032 M	162	1.40	15.43	10.5	16.3	11/30/72	12/08/72		0.3	Sacrificed
D-4 MEDIUM	1053 F	148	1.42	15.58	9.5	17.9	02/22/73	02/02/85		143.3	Cushing's Disease
D-4 MEDIUM	997 M	203	1.60	17.65	11.5	19.6	01/18/73	05/08/86		159.6	Lung Tumor
D-4 MEDIUM	991 F	194	1.76	19.40	10.0	18.8	12/19/72	06/20/83		126.0	Urinary Bladder & Ovarian Tmr
D-4 MEDIUM	1177 M	262	1.76	19.41	13.5	16.6	11/06/73	03/12/85		136.1	Bone Tumor
D-4 MEDIUM	932 F	216	1.79	19.64	11.0	19.1	11/30/72	01/25/73		1.8	Sacrificed
D-4 MEDIUM	1103 F	260	1.89	20.80	12.5	16.5	05/31/73	04/08/83		118.2	Bone Tumor, Lung Tumor
D-4 MEDIUM	973 F	271	2.24	24.64	11.0	19.2	12/19/72	10/08/84		141.6	Bone Tumor
D-4 MEDIUM	931 F	289	2.39	26.27	11.0	19.1	11/30/72	12/28/72		0.9	Sacrificed
D-4 MEDIUM	1091 F	243	2.60	28.59	8.5	17.3	05/31/73	11/10/86		161.3	Thyroid Carcinoma
D-4 MEDIUM	1114 M	430	2.70	29.66	14.5	16.4	05/31/73	04/23/85		142.8	Bone Tumor,Bile Duct Carcinom
D-4 MEDIUM	1062 M	435	2.93	32.22	13.5	17.8	02/22/73	05/30/84		135.2	Bone Tumor, Lung Tumor
D-4 MEDIUM	934 M	454	3.06	33.63	13.5	19.1	11/30/72	03/01/73		3.0	Sacrificed
D-4 MEDIUM	1081 M	541	3.07	33.81	16.0	18.0	05/31/73	01/18/80		79.6	Hemangiosarcoma, Heart
D-4 MEDIUM	1030 F	340	3.25	35.79	9.5	19.1	02/22/73	04/14/83		121.7	Pneumonia, Rad. Pneumonitis
D-4 MEDIUM	1198 M	539	3.50	38.50	14.0	17.9	02/26/74	09/14/86		150.6	Acute Pneumonia, Lung Tumor
D-4 MEDIUM	952 F	365	3.69	40.56	9.0	19.2	12/19/72	06/03/83		125.4	Bone Tumor
D-4 MEDIUM	1166 M	673	4.08	44.87	15.0	17.3	11/06/73	06/23/84		127.5	Malignant Lymphoma

* Indicates age in months since birth, all other ages are in months since exposure.

DOSE-EFFECT STUDIES WITH INHALED PU-238 OXIDE IN BEAGLES

DOSE GROUP	DOG IDENT	INITIAL ALVEOLAR DEPOSITION NCI	NCI/G LUNG	NCI/ KG	INHALATION EXPOSURE WEIGHT (KG)	AGE* (MO)	DATE	DATE OF DEATH	MONTHS SINCE INHALATION 9/30/90	DEATH	COMMENTS ON DEAD DOGS
D-4 MEDIUM	1220 F	518	4.28	47.09	11.0	19.0	04/18/74	12/09/86		151.7	Malignant Lymphoma, Addison's
D-4 MEDIUM	992 F	555	4.39	48.26	11.5	18.8	12/19/72	07/26/84		139.2	Bone Tumor
D-4 MEDIUM	983 M	617	4.67	51.42	12.0	19.0	12/19/72	12/29/83		132.3	Adrenal & Pituitary Tumor
D-5 MED-HIGH	1191 F	591	4.48	49.25	12.0	19.8	04/18/74	03/21/77		35.1	Interstitial Pneumonitis
D-5 MED-HIGH	1157 M	700	4.71	51.85	13.5	17.7	11/06/73	03/02/84		123.8	Bone Tumor
D-5 MED-HIGH	1035 F	571	5.46	60.11	9.5	18.2	02/22/73	03/04/84		132.3	Bone Tumor, Cushing's Disease
D-5 MED-HIGH	1192 F	754	6.53	71.81	10.5	18.1	02/26/74	03/29/83		109.0	Bone Tumor
D-5 MED-HIGH	1140 M	1014	6.58	72.43	14.0	18.2	11/06/73	12/14/81		97.2	Bone Tumor
D-5 MED-HIGH	1071 M	1269	6.79	74.65	17.0	18.1	05/31/73	01/09/81		91.3	Bone Tumor, Lung Tumor
D-5 MED-HIGH	1173 M	1023	7.75	85.25	12.0	17.3	11/06/73	02/09/82		99.1	Bone Tumor
D-5 MED-HIGH	1178 M	1125	8.52	93.75	12.0	16.6	11/06/73	01/06/83		110.0	Bone Tumor, Lung Tumor
D-5 MED-HIGH	1047 M	900	8.61	94.74	9.5	18.1	02/22/73	10/05/82		115.4	Vertebral Disk Herniation
D-5 MED-HIGH	1109 F	1119	8.85	97.30	11.5	16.4	05/31/73	08/06/80		86.2	Bone & Lung Tumor, Addison's
D-5 MED-HIGH	1160 F	1344	10.18	112.00	12.0	17.3	11/06/73	09/22/81		94.5	Bone Tumor, Lung Tumor
D-5 MED-HIGH	1211 M	1764	11.06	121.66	14.5	17.6	02/26/74	05/17/82		98.6	Bone Tumor
D-5 MED-HIGH	1096 F	1476	12.20	134.18	11.0	16.6	05/31/73	05/08/78		59.2	Addison's Disease
D-5 MED-HIGH	1218 F	1710	12.95	142.50	12.0	17.3	02/26/74	04/24/81		85.9	Bone Tumor
D-5 MED-HIGH	1092 M	1848	13.44	147.84	12.5	17.3	05/31/73	10/23/78		64.8	Bone Tumor
D-5 MED-HIGH	1027 M	2148	13.95	153.43	14.0	19.2	01/18/73	12/01/78		70.4	Bone Tumor, Lung Tumor
D-5 MED-HIGH	1115 F	1885	14.90	163.91	11.5	16.1	05/31/73	07/11/78		61.3	Bone Tumor
D-5 MED-HIGH	974 F	1718	15.62	171.80	10.0	20.2	01/18/73	05/24/78		64.1	Bone Tumor
D-5 MED-HIGH	1079 M	2620	15.88	174.67	15.0	18.0	05/31/73	02/12/78		56.4	Addison's Disease, G.I. Tumor
D-5 MED-HIGH	1058 F	1907	16.51	181.62	10.5	17.8	02/22/73	11/01/79		80.3	Bone Tumor, Adrenal Tumor
D-6 HIGH	1002 M	2907	18.88	207.64	14.0	19.6	01/18/73	01/21/80		84.1	Bone Tumor, Lung Tumor
D-6 HIGH	1057 M	3116	20.98	230.81	13.5	17.9	02/22/73	03/07/79		72.4	Bone Tumor
D-6 HIGH	1009 M	3630	26.40	290.40	12.5	19.6	01/18/73	04/01/78		62.4	Lung Tumor, Osteoarthropathy
D-6 HIGH	1042 F	2959	28.32	311.47	9.5	18.1	02/22/73	11/10/78		68.6	Bone Tumor, Lung Tumor
D-6 HIGH	994 F	3453	31.39	345.30	10.0	19.6	01/18/73	07/04/76		41.5	Addison's Disease
D-6 HIGH	1006 F	3810	31.49	346.36	11.0	19.6	01/18/73	01/18/79		72.0	Bone Tumor, Lung Tumor
D-6 HIGH	975 F	3968	36.07	396.80	10.0	20.2	01/18/73	07/25/78		66.2	Bone Tumor, Lung Tumor
D-6 HIGH	1037 M	4854	44.13	485.40	10.0	18.2	02/22/73	11/21/78		68.9	Bone Tumor
D-6 HIGH	1143 M	7691	53.78	591.62	13.0	18.2	11/06/73	12/05/77		49.0	Bone Tumor, Lung Tumor
D-6 HIGH	1025 M	8479	57.10	628.07	13.5	19.2	01/18/73	03/17/77		49.9	Lung Tumor
D-6 HIGH	1064 M	9453	63.66	700.22	13.5	16.7	01/18/73	04/14/77		50.8	Bone Tumor, Lung Tumor
D-6 HIGH	1162 F	6959	70.29	773.22	9.0	17.3	11/06/73	12/19/78		61.4	Bone Tumor, Addison's Disease
D-6 HIGH	1175 F	6201	75.16	826.80	7.5	16.6	11/06/73	02/24/78		51.6	Lung Tumor

* Indicates age in months since birth, all other ages are in months since exposure.

INHALED PLUTONIUM NITRATE IN DOGS

DOSE GROUP	DOG IDENT	INITIAL ALVEOLAR DEPOSITION NCI	NCI/G LUNG	NCI/ KG	INHALATION EXPOSURE WEIGHT (KG)	AGE* (MO)	DATE	DATE OF DEATH	MONTHS SINCE INHALATION 9/30/90	DEATH	COMMENTS ON DEAD DOGS
CONTROL	1356 M	0	0.00	0.00				04/07/87		154.9*	Adrenal Tumor
CONTROL	1365 M	0	0.00	0.00				07/16/88		170.1*	Pneumonia
CONTROL	1376 F	0	0.00	0.00				05/11/80		70.8*	Pneumonia
CONTROL	1388 M	0	0.00	0.00				09/11/81		86.7*	Sacrificed
CONTROL	1393 M	0	0.00	0.00				06/19/87		155.9*	Pneumonia
CONTROL	1405 M	0	0.00	0.00				08/13/84		121.3*	Sacrificed, Heart Base Tumor
CONTROL	1409 M	0	0.00	0.00				07/17/89		180.3*	Processing
CONTROL	1418 M	0	0.00	0.00				08/26/89		181.4*	Processing
CONTROL	1425 M	0	0.00	0.00				08/02/82		96.5*	Status Epilepticus
CONTROL	1450 F	0	0.00	0.00				11/04/81		87.4*	Sacrificed
CONTROL	1455 F	0	0.00	0.00				08/20/87		156.5*	Pyometra
CONTROL	1483 F	0	0.00	0.00					192.9*		
CONTROL	1509 M	0	0.00	0.00				10/30/86		145.1*	Sacrificed
CONTROL	1516 F	0	0.00	0.00					191.8*		
CONTROL	1525 M	0	0.00	0.00				11/14/87		157.1*	Prostate Tumor
CONTROL	1526 M	0	0.00	0.00				08/28/90		190.5*	Processing
CONTROL	1528 F	0	0.00	0.00				04/06/87		149.2*	Cerebral hemorrhage
CONTROL	1543 M	0	0.00	0.00				08/12/86		141.3*	Vertebral Disc
CONTROL	1563 F	0	0.00	0.00					180.8*		
CONTROL	1572 F	0	0.00	0.00				02/01/90		172.8*	Endocarditis
CONTROL	1577 M	0	0.00	0.00				04/04/90		174.9*	Splenic Tumor
CONTROL	1584 F	0	0.00	0.00				11/29/88		158.6*	Thyroid Tumor
CONTROL	1594 F	0	0.00	0.00					180.6*		
CONTROL	1608 M	0	0.00	0.00					180.3*		
CONTROL	1633 F	0	0.00	0.00				11/10/86		126.9*	Thyroid Tumor
CONTROL	1638 F	0	0.00	0.00				09/08/87		136.5*	Sacrificed
VEHICLE	1361 M	0	0.00	0.00	8.5	21.0	02/13/76	04/04/89		157.7	Processing
VEHICLE	1381 F	0	0.00	0.00	8.5	19.8	02/13/76	12/05/89		165.7	Processing
VEHICLE	1392 M	0	0.00	0.00	13.0	22.0	04/22/76	01/16/90		164.8	Processing
VEHICLE	1406 M	0	0.00	0.00	13.5	21.6	04/22/76	01/21/88		141.0	Malignant Melanoma
VEHICLE	1412 F	0	0.00	0.00	9.0	19.0	02/13/76	07/06/89		160.7	Processing
VEHICLE	1421 M	0	0.00	0.00	13.0	23.3	06/23/76	02/26/88		140.1	Mastocytoma
VEHICLE	1457 F	0	0.00	0.00	12.0	20.6	04/22/76	11/07/89		162.5	Processing
VEHICLE	1491 F	0	0.00	0.00	8.0	21.6	06/23/76	05/10/89		154.5	Mammary Tumor
VEHICLE	1504 F	0	0.00	0.00	10.0	20.9	06/23/76	02/22/89		152.0	Malignant Lymphoma
VEHICLE	1514 M	0	0.00	0.00	14.0	20.9	06/23/76	08/06/82		73.4	Malignant Lymphoma
VEHICLE	1524 M	0	0.00	0.00	12.0	21.5	07/27/76	03/27/88		140.0	Vertebral Disc
VEHICLE	1531 F	0	0.00	0.00	9.0	20.9	07/27/76		170.1		
VEHICLE	1542 M	0	0.00	0.00	12.0	20.8	07/27/76	05/01/89		153.1	Malignant Lymphoma
VEHICLE	1566 M	0	0.00	0.00	14.0	18.3	03/15/77	01/18/90		154.2	Malignant Lymphoma
VEHICLE	1578 M	0	0.00	0.00	10.5	18.2	03/15/77	02/13/90		155.0	Nephropathy
VEHICLE	1593 F	0	0.00	0.00	11.0	18.0	03/15/77		162.5		
VEHICLE	1601 F	0	0.00	0.00	8.5	18.0	03/15/77	04/08/90		156.8	Nephropathy

* Indicates age in months since birth, all other ages are in months since exposure.

INHALED PLUTONIUM NITRATE IN DOGS

DOSE GROUP	DOG IDENT	INITIAL ALVEOLAR DEPOSITION NCI	NCI/G LUNG	NCI/ KG	INHALATION EXPOSURE WEIGHT (KG)	AGE* (MO)	DATE	DATE OF DEATH	MONTHS SINCE INHALATION 9/30/90	DEATH	COMMENTS ON DEAD DOGS
VEHICLE	1620 M	0	0.00	0.00	11.0	21.1	12/01/77	01/06/87		109.2	Vertebral Disc
VEHICLE	1634 F	0	0.00	0.00	10.5	19.6	12/01/77		154.0		
VEHICLE	1651 F	0	0.00	0.00	11.0	19.2	12/01/77		154.0		
D-1 LOWEST	1416 M	0	0.00	0.00	12.0	22.1	05/20/76	02/15/90		164.9	Processing
D-1 LOWEST	1458 F	0	0.00	0.00	10.5	21.5	05/20/76	09/21/89		160.1	Processing
D-1 LOWEST	1489 F	0	0.00	0.00	8.0	20.5	05/20/76	08/04/84		98.5	Esophageal Tumor
D-1 LOWEST	1501 M	0	0.00	0.00	14.0	20.4	05/20/76	01/03/84		91.5	Thyroid Tumor
D-1 LOWEST	1515 M	0	0.00	0.00	13.5	19.8	05/20/76		172.4		
D-1 LOWEST	1573 M	0	0.00	0.00	11.5	19.4	04/19/77	09/06/90		160.6	Processing
D-1 LOWEST	1581 M	0	0.00	0.00	16.5	19.3	04/19/77	07/31/86		111.4	Hemangiosarcoma
D-1 LOWEST	1596 M	0	0.00	0.00	14.0	19.2	04/19/77		161.4		
D-1 LOWEST	1600 F	1	0.01	0.11	11.0	19.2	04/19/77	06/27/90		158.3	Processing
D-1 LOWEST	1603 M	2	0.01	0.12	14.0	19.2	04/19/77		161.4		
D-1 LOWEST	1339 F	2	0.02	0.22	9.0	17.5	10/16/75	11/13/75		0.9	Sacrificed
D-1 LOWEST	1519 M	2	0.02	0.18	12.5	19.5	05/20/76	07/13/90		169.8	Processing
D-1 LOWEST	1570 F	2	0.02	0.18	10.0	19.4	04/19/77	06/19/87		122.0	Stomach tumor
D-1 LOWEST	1465 F	4	0.03	0.35	12.0	21.0	05/20/76	05/16/89		155.9	Nephropathy
D-1 LOWEST	1470 F	3	0.03	0.29	10.5	21.0	05/20/76	04/09/84		94.7	Meningioma
D-1 LOWEST	1507 M	4	0.03	0.32	14.0	19.8	05/20/76	06/07/88		144.6	Malignant Melanoma
D-1 LOWEST	1592 F	4	0.03	0.29	13.5	19.2	04/19/77	10/17/89		149.9	Pneumonia
D-1 LOWEST	1607 M	5	0.03	0.35	13.0	19.0	04/19/77	07/26/88		135.2	Liver Tumor
D-1 LOWEST	1335 M	5	0.04	0.42	11.5	18.0	10/16/75	11/13/75		0.9	Sacrificed
D-1 LOWEST	1487 F	6	0.04	0.46	13.0	20.5	05/20/76	07/05/90		169.5	Processing
D-1 LOWEST	1583 F	4	0.04	0.40	9.5	19.2	04/19/77	10/13/89		149.8	Thyroid Tumor
D-1 LOWEST	1351 M	7	0.06	0.61	11.0	17.2	10/16/75	11/13/75		0.9	Sacrificed
D-1 LOWEST	1565 F	8	0.06	0.67	11.5	19.4	04/19/77	09/28/85		101.3	Hemangiosarcoma
D-2 LOW	1513 M	0	0.00	0.00	11.5	19.8	05/20/76		172.4		
D-2 LOW	1520 M	1	0.01	0.12	10.5	19.5	05/20/76	05/21/90		168.0	Processing
D-2 LOW	1415 M	2	0.02	0.20	11.5	22.2	05/20/76	12/27/89		163.3	Processing
D-2 LOW	1575 M	3	0.02	0.19	14.0	19.4	04/19/77	12/28/87		128.3	Prostate Tumor
D-2 LOW	1466 F	5	0.03	0.37	14.0	21.0	05/20/76	01/04/90		163.5	Processing
D-2 LOW	1606 F	5	0.04	0.42	12.5	19.0	04/19/77	06/22/90		158.1	Processing
D-2 LOW	1579 M	8	0.05	0.59	14.0	19.3	04/19/77	06/05/90		157.5	Processing
D-2 LOW	1590 F	6	0.05	0.51	12.0	19.2	04/19/77	03/18/87		118.9	Mammary Tumor
D-2 LOW	1585 F	8	0.06	0.68	12.0	19.2	04/19/77	08/31/89		148.4	Thyroid Tumor
D-2 LOW	1580 F	9	0.07	0.82	11.0	19.3	04/19/77		161.4		
D-2 LOW	1591 M	11	0.07	0.76	15.0	19.2	04/19/77	08/15/89		147.9	Malignant Lymphoma
D-2 LOW	1417 M	11	0.08	0.89	12.0	22.1	05/20/76	10/05/89		160.5	Processing
D-2 LOW	1423 M	10	0.08	0.87	11.0	22.1	05/20/76	06/27/89		157.2	Processing
D-2 LOW	1567 M	10	0.08	0.83	12.0	19.4	04/19/77	06/15/90		157.9	Processing
D-2 LOW	1472 F	10	0.09	1.01	10.0	21.0	05/20/76	11/22/89		162.1	Processing
D-2 LOW	1503 F	9	0.09	1.03	8.5	19.8	05/20/76	12/13/84		102.8	Thyroid Tumor
D-2 LOW	1602 M	15	0.09	1.03	14.5	19.2	04/19/77	08/10/86		111.7	Epilepsy

* Indicates age in months since birth, all other ages are in months since exposure.

INHALED PLUTONIUM NITRATE IN DOGS

DOSE GROUP	DOG IDENT	INITIAL ALVEOLAR DEPOSITION NCI	NCI/G LUNG	NCI/ KG	INHALATION EXPOSURE WEIGHT (KG)	AGE* (MO)	DATE	DATE OF DEATH	MONTHS SINCE INHALATION 9/30/90	DEATH	COMMENTS ON DEAD DOGS
D-2 LOW	1484 F	11	0.10	1.08	10.0	20.5	05/20/76		172.4		
D-2 LOW	1599 F	10	0.10	1.14	9.0	19.2	04/19/77	03/12/86		106.7	Adrenal Tumor
D-2 LOW	1490 F	16	0.15	1.65	9.5	20.5	05/20/76	10/19/88		149.0	Mammary Tumor
D-3 MED-LOW	1336 M	21	0.14	1.52	13.5	18.0	10/16/75	11/13/75		0.9	Sacrificed
D-3 MED-LOW	1341 F	19	0.16	1.78	10.5	17.2	10/16/75	11/13/75		0.9	Sacrificed
D-3 MED-LOW	1605 F	25	0.20	2.19	11.5	17.8	03/15/77	03/24/82		60.3	Sacrificed
D-3 MED-LOW	1386 M	34	0.21	2.36	14.5	22.0	04/20/76	01/04/86		116.5	Hemangiosarcoma
D-3 MED-LOW	1389 M	27	0.23	2.54	10.5	21.9	04/20/76	05/04/76		0.5	Sacrificed
D-3 MED-LOW	1413 F	29	0.24	2.68	11.0	18.2	01/20/76	03/01/85		109.3	Malignant Lymphoma
D-3 MED-LOW	1445 F	34	0.24	2.60	13.0	21.0	04/20/76	05/05/76		0.5	Sacrificed
D-3 MED-LOW	1568 M	46	0.29	3.17	14.5	18.3	03/15/77	12/02/86		116.6	Pneumonia
D-3 MED-LOW	1595 M	50	0.29	3.23	15.5	18.0	03/15/77	01/09/90		153.9	Nephropathy
D-3 MED-LOW	1390 M	43	0.30	3.29	13.0	21.9	04/20/76	05/04/76		0.5	Sacrificed
D-3 MED-LOW	1391 M	54	0.30	3.26	16.5	21.9	04/20/76	07/22/85		111.0	Thyroid Tumor, Lung Tumor
D-3 MED-LOW	1587 M	53	0.31	3.40	15.5	18.1	03/15/77	01/14/86		106.0	Hemangiosarcoma, Lung Tumor
D-3 MED-LOW	1359 M	50	0.32	3.57	14.0	20.2	01/20/76	01/23/76		0.1	Sacrificed
D-3 MED-LOW	1540 M	54	0.32	3.51	15.5	20.7	07/22/76	11/25/86		124.1	Lung tumor
D-3 MED-LOW	1344 F	41	0.33	3.60	11.5	17.2	10/16/75	11/14/75		1.0	Sacrificed
D-3 MED-LOW	1589 F	41	0.34	3.75	11.0	18.0	03/15/77	06/08/82		62.8	Sacrificed, Lung Tumor
D-3 MED-LOW	1588 M	50	0.36	3.98	12.5	18.1	03/15/77	03/22/78		12.2	Sacrificed
D-3 MED-LOW	1529 F	43	0.37	4.08	10.5	20.8	07/22/76	10/19/76		2.9	Sacrificed
D-3 MED-LOW	1574 M	46	0.38	4.21	11.0	18.2	03/15/77	07/14/90		160.0	Processing
D-3 MED-LOW	1375 F	50	0.40	4.35	11.5	19.1	01/20/76	01/23/76		0.1	Sacrificed
D-3 MED-LOW	1564 F	40	0.40	4.44	9.0	18.3	03/15/77	03/20/78		12.2	Sacrificed
D-3 MED-LOW	1444 F	49	0.41	4.50	11.0	21.0	04/20/76	05/17/90		168.9	Processing
D-3 MED-LOW	1439 F	53	0.42	4.61	11.5	21.0	04/20/76	03/30/88		143.3	Malignant Lymphoma
D-3 MED-LOW	1523 F	55	0.42	4.60	12.0	21.3	07/22/76		170.3		
D-3 MED-LOW	1539 M	65	0.45	4.99	13.0	20.7	07/22/76	10/20/76		3.0	Sacrificed
D-3 MED-LOW	1380 M	63	0.46	5.06	12.5	19.1	01/20/76	05/24/87		136.1	Pneumonia
D-3 MED-LOW	1407 F	50	0.51	5.56	9.0	18.5	01/20/76	01/23/76		0.1	Sacrificed
D-3 MED-LOW	1569 F	58	0.53	5.82	10.0	18.2	03/15/77	09/27/87		126.4	Lung tumor
D-3 MED-LOW	1576 M	70	0.53	5.86	12.0	18.2	03/15/77	03/17/82		60.1	Sacrificed
D-3 MED-LOW	1582 F	57	0.54	5.96	9.5	18.1	03/15/77	08/12/88		136.9	Mammary Tumor,Liver Tumor
D-3 MED-LOW	1571 F	68	0.57	6.22	11.0	18.2	03/15/77	03/21/78		12.2	Sacrificed
D-3 MED-LOW	1427 F	68	0.62	6.81	10.0	21.1	04/20/76	08/23/89		160.1	Processing
D-3 MED-LOW	1522 F	78	0.71	7.78	10.0	21.3	07/22/76	10/18/76		2.9	Sacrificed
D-3 MED-LOW	1363 M	85	0.74	8.09	10.5	20.2	01/20/76	05/12/87		135.7	Pneumonia, Adrenal/Liver Tmrs
D-3 MED-LOW	1604 M	85	0.74	8.10	10.5	18.0	03/15/77	04/03/90		156.6	Processing
D-3 MED-LOW	1530 F	72	0.76	8.41	8.5	20.8	07/22/76	09/17/86		121.9	Bone Tumor, Lung Tumor
D-3 MED-LOW	1456 F	61	0.79	8.68	7.0	20.5	04/20/76	04/21/87		132.0	Pneumonia
D-3 MED-LOW	1598 F	93	1.06	11.65	8.0	18.0	03/15/77	03/10/82		59.8	Sacrificed
D-3 MED-LOW	1422 F	99	1.12	12.35	8.0	18.1	01/20/76	07/11/90		173.7	Processing
D-4 MEDIUM	1637 M	192	1.45	15.99	12.0	18.9	11/07/77	11/28/88		132.7	Lung Tumor

* Indicates age in months since birth, all other ages are in months since exposure.

INHALED PLUTONIUM NITRATE IN DOGS

DOSE GROUP	DOG IDENT	INITIAL ALVEOLAR DEPOSITION NCI	NCI/G LUNG	NCI/ KG	INHALATION EXPOSURE WEIGHT (KG)	AGE* (MO)	DATE	DATE OF DEATH	MONTHS SINCE INHALATION 9/30/90	DEATH	COMMENTS ON DEAD DOGS
D-4 MEDIUM	1404 M	260	1.48	16.25	16.0	21.5	04/20/76	02/03/84		93.5	Pleuritis
D-4 MEDIUM	1521 F	205	1.49	16.37	12.5	21.3	07/22/76	06/07/85		106.5	Bone Tumor, Lung Tumor
D-4 MEDIUM	1656 M	211	1.54	16.90	12.5	18.4	11/07/77		154.7		
D-4 MEDIUM	1379 M	278	1.74	19.16	14.5	19.1	01/20/76	01/20/88		144.0	Liver, Lung, & Bone Tumors
D-4 MEDIUM	1362 M	267	1.87	20.54	13.0	20.2	01/20/76	12/20/88		155.0	Bone, Liver, & Lung Tumors
D-4 MEDIUM	1639 F	248	2.05	22.57	11.0	18.5	11/07/77	12/24/89		145.5	Rad. Pneumonitis, Lung Tumor
D-4 MEDIUM	1647 M	294	2.05	22.58	13.0	18.5	11/07/77	01/13/90		146.2	Lung Tumor, Liver Tumor
D-4 MEDIUM	1640 M	307	2.06	22.71	13.5	18.5	11/07/77	03/20/84		76.4	Lung Tumor
D-4 MEDIUM	1645 F	257	2.13	23.39	11.0	18.5	11/07/77	08/07/86		105.0	Lung Tumor
D-4 MEDIUM	1534 M	295	2.14	23.57	12.5	20.8	07/22/76	05/26/85		106.1	Congestive Heart Failure
D-4 MEDIUM	1414 F	233	2.35	25.86	9.0	18.2	01/20/76	08/14/86		126.8	Bone, Lung, and Liver tumors
D-4 MEDIUM	1618 F	277	2.40	26.36	10.5	20.3	11/07/77	07/12/89		140.1	Bone Tumor
D-4 MEDIUM	1385 M	373	2.42	26.63	14.0	19.0	01/20/76	07/12/84		101.7	Bone Tumor, Lung Tumor
D-4 MEDIUM	1408 F	331	2.62	28.77	11.5	18.5	01/20/76	10/12/83		92.7	Bone Tumor
D-4 MEDIUM	1428 F	378	3.12	34.36	11.0	21.1	04/20/76	10/28/85		114.3	Bone Tumor, Lung Tumor
D-4 MEDIUM	1535 F	345	3.13	34.48	10.0	20.7	07/22/76	10/06/86		122.5	Bone and lung tumors
D-4 MEDIUM	1446 F	354	3.22	35.40	10.0	21.0	04/20/76	08/10/86		123.7	Pyometra, Liver tumor
D-4 MEDIUM	1364 M	463	3.24	35.65	13.0	20.2	01/20/76	08/02/84		102.4	Lung Tumor
D-4 MEDIUM	1387 F	345	4.48	49.30	7.0	19.0	01/20/76	08/13/80		54.8	Bone Tumor
D-5 MED-HIGH	1329 F	363	3.30	36.27	10.0	18.0	10/16/75	11/14/75		1.0	Sacrificed
D-5 MED-HIGH	1346 M	656	4.42	48.59	13.5	17.2	10/16/75	11/14/75		1.0	Sacrificed
D-5 MED-HIGH	1648 M	811	5.90	64.90	12.5	18.5	11/07/77	07/11/85		92.1	Bone Tumor, Lung Tumor
D-5 MED-HIGH	1347 F	688	6.95	76.47	9.0	17.2	10/16/75	11/14/75		1.0	Sacrificed
D-5 MED-HIGH	1659 F	990	7.32	80.51	12.3	18.3	11/07/77	08/19/83		69.4	Bone Tumor
D-5 MED-HIGH	1636 M	1212	8.48	93.25	13.0	18.9	11/07/77	05/03/83		65.8	Bone Tumor
D-5 MED-HIGH	1621 M	1334	8.66	95.26	14.0	20.3	11/07/77	11/19/84		84.4	Bone Tumor, Lung Tumor
D-5 MED-HIGH	1646 F	1061	8.77	96.45	11.0	18.5	11/07/77	11/11/82		60.1	Bone Tumor
D-5 MED-HIGH	1429 M	1376	9.62	105.85	13.0	23.2	06/23/76	05/29/81		59.2	Bone Tumor, Lung Tumor
D-5 MED-HIGH	1641 M	1275	9.66	106.24	12.0	18.5	11/07/77	06/28/85		91.7	Lung Tumor
D-5 MED-HIGH	1660 M	1518	10.22	112.41	13.5	18.3	11/07/77	09/05/84		81.9	Bone Tumor, Lung Tumor
D-5 MED-HIGH	1508 M	1716	10.76	118.37	14.5	20.9	06/23/76	01/24/80		43.0	Bone Tumor
D-5 MED-HIGH	1655 M	1094	11.05	121.56	9.0	18.4	11/07/77	03/18/85		88.3	Bone Tumor, Lung Tumor
D-5 MED-HIGH	1652 F	1320	12.00	131.95	10.0	18.4	11/07/77	07/20/83		68.4	Bone Tumor, Lung Tumor
D-5 MED-HIGH	1619 F	1490	12.32	135.50	11.0	20.3	11/07/77	01/21/83		62.5	Bone Tumor
D-5 MED-HIGH	1512 M	2411	14.61	160.71	15.0	20.9	06/23/76	12/23/79		42.0	Bone Tumor
D-5 MED-HIGH	1419 M	1559	14.92	164.11	9.5	23.3	06/23/76	10/22/82		76.0	Bone Tumor, Lung Tumor
D-5 MED-HIGH	1498 F	2018	16.68	183.45	11.0	21.5	06/23/76	04/09/82		69.5	Bone Tumor, Lung Tumor
D-5 MED-HIGH	1502 F	3008	20.25	222.80	13.5	20.9	06/23/76	01/21/81		55.0	Bone Tumor, Lung Tumor
D-5 MED-HIGH	1485 F	2330	21.18	233.00	10.0	21.7	06/23/76	12/30/80		54.2	Bone Tumor
D-5 MED-HIGH	1471 F	2508	21.71	238.82	10.5	22.1	06/23/76	05/01/79		34.2	Radiation Pneumonitis
D-5 MED-HIGH	1492 F	2473	24.98	274.82	9.0	21.6	06/23/76	10/16/80		51.8	Bone Tumor
D-5 MED-HIGH	1459 F	2645	26.72	293.89	9.0	22.6	06/23/76	09/25/80		51.1	Rad. Pneumonitis, Lung Tumor
D-6 HIGH	1518 M	3565	29.46	324.09	11.0	20.6	06/23/76	12/18/79		41.8	Rad. Pneumonitis, Lung Tumor

* Indicates age in months since birth, all other ages are in months since exposure.

INHALED PLUTONIUM NITRATE IN DOGS

DOSE GROUP	DOG IDENT	INITIAL ALVEOLAR DEPOSITION NCI	NCI/G LUNG	NCI/ KG	INHALATION EXPOSURE WEIGHT (KG)	AGE* (MO)	DATE	DATE OF DEATH	MONTHS SINCE INHALATION 9/30/90	DEATH	COMMENTS ON DEAD DOGS
D-6 HIGH	1420 M	3840	30.36	333.91	11.5	23.3	06/23/76	07/12/78		24.6	Radiation Pneumonitis
D-6 HIGH	1517 F	5185	49.62	545.79	9.5	20.6	06/23/76	11/02/77		16.3	Radiation Pneumonitis
D-6 HIGH	1510 F	6969	55.09	606.02	11.5	20.9	06/23/76	11/09/77		16.6	Radiation Pneumonitis
D-6 HIGH	1424 M	7681	69.83	768.12	10.0	23.2	06/23/76	08/31/77		14.3	Radiation Pneumonitis

* Indicates age in months since birth, all other ages are in months since exposure.

Publications and Presentations

Publications

1989

Bair, W. J. 1989. Human respiratory tract model for radiological protection--A revision of the ICRP dosimetric model for the respiratory system. In: *Proceedings, Seventh International Congress of the International Radiation Protection Association*, April 10-17, 1988, pp. 158-161, Sydney, Australia. Pergamon Press, Sydney, Australia.

Bair, W. J., J. F. Park, G. E. Dagle, and A. C. James. 1989. Overview of biological consequences of exposure to plutonium and higher actinides. *Radiat. Prot. Dosim.* 26(1/4)125-139.

Bean, R. M., B. L. Thomas, D. A. Dankovic, D. B. Mann, G. A. Ross, and D. L. Springer. 1989. Analysis of classical and nonclassical adducts. In: *Multilevel Health Effects Research: From Molecules to Man,* J. F. Park and R. A. Pelroy, eds., pp. 429-434, Proceedings of the 27th Hanford Symposium on Health and the Environment, October 18-21, 1988, Richland, Washington. Battelle Press, Columbus, Ohio.

Birchall, A., and A. C. James. 1989. A microcomputer algorithm for solving first-order compartment models involving recycling. *Health Phys.* 56:857-868.

Briant, J. K., and B. S. Cohen. 1989. Flow distribution through human and canine airways during inhalation and exhalation. *J. Appl. Physiol.* 67:1649-1654.

Brooks, A. L., and W. C. Griffith. 1989. Chromosomal binding and clearance of benzo[a]pyrene-diol-epoxide. In: *Multilevel Health Effects Research: From Molecules to Man,* J. F. Park and R. A. Pelroy, eds., pp. 307-312, Proceedings of the 27th Hanford Symposium on Health and the Environment, October 18-21, 1988, Richland, Washington. Battelle Press, Columbus, Ohio.

Brooks, A. L., W. C. Griffith, N. F. Johnson, G. L. Finch, and R. G. Cuddihy. 1989. The induction of chromosome damage in CHO cells by beryllium and radiation given alone and in combination. *Radiat. Res.* 120:494-507.

Cohen, B. S., and J. K. Briant. 1989. Flow distribution in human and canine tracheobronchial airway casts. In: *Modeling for Scaling to Man: Biology, Dosimetry, and Response,* Proceedings of the 26th Hanford Life Sciences Symposium, October 20-23, 1987, Richland, Washington. *Health Phys.* 57(Suppl. 1):21-27.

Cross, F. T. 1989. Evidence of lung cancer risk from animal studies. In: *Radon*, N. H. Hartley, ed., pp. 129-140, Proceedings of the Twenty-Fourth Annual NCRP Meeting, March 30-31, 1988. National Council on Radiation Protection and Measurements, Bethesda, Maryland.

Cross, F. T., G. E. Dagle, and R. A. Gies. 1989. Reply to Dr. Archer's comment on "A Histologic Study of the Influence of Cigarette Smoking in Suppressing Rn Daughter Carcinogenesis in Dogs." *Health Phys.* 56:256 (Correspondence).

Dagle, G. E., J. F. Park, E. S. Gilbert, and R. E. Weller. 1989. Risk estimates for lung tumors from inhaled $^{239}PuO_2$, $^{238}PuO_2$, and $^{239}Pu(NO_3)_4$ in beagle dogs. *Radiat. Prot. Dosim.* 26(1/4):173-176.

Dankovic, D. A., C. W. Wright, R. C. Zangar, and D. L. Springer. 1989. Complex mixture effects on the dermal absorption of benzo[a]pyrene and other polycyclic aromatic hydrocarbons from mouse skin. *J. Appl. Toxicol.* 9(4):239-244.

Dankovic, D. A., B. L. Thomas, R. C. Zangar, D. W. Later, and D. L. Springer. 1989. Inhibition of benzo[a]pyrene-7,8-diol formation in vitro by complex organic mixtures. *Toxicology* 55:93-103.

Dankovic, D. A., D. L. Springer, D. B. Mann, L. G. Smith, B. L. Thomas, and R. M. Bean. 1989. Preparation of microgram quantities of Bap-DNA adducts using isolated rat hepatocytes *in vitro*. *Carcinogenesis* 10(4):789-791 (Short Communication).

Egan, M. J., W. Nixon, N. I. Robinson, A. C. James, and F. F. Phalen. 1989. Inhaled aerosol transport and deposition calculations for the ICRP Task Group. *J. Aerosol. Sci.* 20:1305-1308.

Filipy, R. E., K. E. Lauhala, D. R. McGee, W. C. Cannon, R. L. Buschbom, J. R. Decker, E. G. Juffel, J. F. Park, H. A. Ragan, S. S. Yaniv, and B. R. Scott. 1989. *Inhaled ^{147}Pm and/or Total-Body Gamma Radiation: Early Mortality and Morbidity in Rats.* NUREG/CR-5353/PNL-6891, Pacific Northwest Laboratory, Richland, Washington. U.S. Nuclear Regulatory Commission, Washington, D.C.

Finch, G. L., A. L. Brooks, M. D. Hoover, and R. G. Cuddihy. 1989. Influence of physicochemical properties of beryllium particles on toxicity to cultured cells. *In Vitro Toxicol.* 2(4):287-297.

Finch, G. L., A. L. Brooks, J. M. Benson, M. D. Hoover, J. A. Mewhinney, A. F. Eidson, R. G. Cuddihy, R. F. Henderson, and C. H. Hobbs. 1989. Influence of physicochemical properties of beryllium and nickel compounds on cultured cell toxicity. In: *Effects of Mineral Dusts on Cells*, Fourth International Workshop, NATO ASI Series, Vol. H30, B. T. Mossman and R. O. Begin, eds., pp. 85-92. Springer-Verlag, Berlin and Heidelberg.

Frazier, M. E. 1989. State of the Art Address: Oncogenes and Tumor-Suppressing Genes. In: *Proceedings of the American College of Veterinary Internal Medicine,* G. Pidgeon, ed., pp. 896-904, Seventh Annual Veterinary Medical Forum, May 1989, San Diego, California. Omnipress, Madison, Wisconsin.

Frazier, M. E., T. M. Seed, L. L. (Scott) Whiting, and G. L. Stiegler. 1989. Evidence for oncogene activation in radiation-induced carcinogenesis. In: *Multilevel Health Effects Research: From Molecules to Man,* J. F. Park and R. A. Pelroy, eds., pp. 197-205, Proceedings of the 27th Hanford Symposium on Health and the Environment, October 18-21, 1988, Richland, Washington. Battelle Press, Columbus, Ohio.

Gilbert, E. S. 1989. Issues in analysing the effects of occupational exposure to low levels of radiation. *Stat. Med.* 8:173-187.

Gilbert, E. S., and F. T. Cross. 1989. Radon risks in animals with reference to man. In: *Multilevel Health Effects Research: From Molecules to Man,* J. F. Park and R. A. Pelroy, eds., pp. 359-371, Proceedings of the 27th Hanford Symposium on Health and the Environment, October 18-21, 1988, Richland, Washington. Battelle Press, Columbus, Ohio.

Gilbert, E. S., J. F. Park, and R. L. Buschbom. 1989. Time-related factors in the study of risks in animals and humans. *Health Phys.* 57(Suppl. 1):379-385.

Gilbert, E. S., G. R. Petersen, and J. A. Buchanan. 1989. Mortality of workers at the Hanford Site: 1945-1981. *Health Phys.* 56(1):11-25.

Gilbert, E. S., G. R. Petersen, and J. Buchanan. 1989. Mortality of Hanford workers: A reply. *Health Phys.* 57:841.

Gilbert, E. S., S. A. Fry, L. D. Wiggs, G. L. Voelz, D. L. Cragle, and G. R. Petersen. 1989. Analyses of combined mortality data on workers at the Hanford Site, Oak Ridge National Laboratory, and Rocky Flats Nuclear Weapons Plant. *Radiat. Res.* 120:19-35.

Guilmette, R. A., N. A. Gillett, A. F. Eidson, W. C. Griffith, and A. L. Brooks. 1989. The influence of non-uniform alpha-irradiation of Chinese hamster liver on chromosome damage and the induction of cancer. In: *Risks from Radium and Thorotrast*, D. M. Taylor, C. W. Mays, G. B. Gerber, and R. G. Thomas, eds., pp. 142-149. BIR Report 21, British Institute of Radiology, London, U.K.

James, A. C. 1989. *Evaluation of the Efficacy of the Amway Pureflow™ Air Treatment System (APATS) in Mitigating Dose from Radon Daughters.* PNWD-1440. Prepared for Amway Corporation, Ada, Michigan, by Battelle, Pacific Northwest Laboratories, Richland, Washington.

James, A. C., and A. Birchall. 1989. Progress in lung modelling by the ICRP Task Group. *Radiat. Prot. Dosim.* 26(1/):227-235.

James, A. C., A. Birchall, F. T. Cross, R. G. Cuddihy, and J. R. Johnson. 1989. The current approach of the ICRP Task Group for modeling doses to respiratory tract tissues. In: *Modeling for Scaling to Man: Biology, Dosimetry, and Response,* Proceedings of the 26th Hanford Life Sciences Symposium, October 20-23, 1987, Richland, Washington. *Health Phys.* 57(Suppl. 1):271-282.

Kelly, G., P. R. Kerkof, A. L. Brooks, and P. J. Haley. 1989. Oncogene activation in radiation-induced lung tumors. In: *Low Dose Radiation: Biological Bases of Risk Assessment*, K. F. Beverstock and J. W. Stather, eds., pp. 286-295. Taylor and Francis, London.

Leung, F. C., and G. Saccomanno. 1989. Expression of epidermal growth-factor receptor and bombesin in archived paraffin-block uranium-miner lung tumors. In: *Multilevel Health Effects Research: From Molecules to Man,* J. F. Park and R. A. Pelroy, eds., pp. 373-382, Proceedings of the 27th Hanford Symposium on Health and the Environment, October 18-21, 1988, Richland, Washington. Battelle Press, Columbus, Ohio.

Leung, F. C., J. R. Coleman, G. E. Dagle, and F. T. Cross. 1989. Involvement of growth factors and their receptors in radiation-induced carcinogenesis. In: *Multilevel Health Effects Research: From Molecules to Man,* J. F. Park and R. A. Pelroy, eds., pp. 207-218, Proceedings of the 27th Hanford Symposium on Health and the Environment, October 18-21, 1988, Richland, Washington. Battelle Press, Columbus, Ohio.

Lynch, T. P., R. L. Kathren, G. E. Dagle, and J. F. McInroy. 1989. Comparative skeletal distribution of Am and Pu in man, monkey, and baboon. *Health Phys.* 57(Suppl. 1):81-88.

Mahaffey, J. A., ed. 1989. *Modeling for Scaling to Man: Biology, Dosimetry, and Response*, Proceedings of the 26th Hanford Life Sciences Symposium, October 20-23, 1987, Richland, Washington. *Health Phys.* 57(Suppl. 1):1-461.

Mahlum, D. D., D. B. Mann, D. A. Dankovic, and D. L. Springer. 1989. Can carcinogenicity be predicted from chemical analysis and DNA adduction? In: *Multilevel Health Effects Research: From Molecules to Man,* J. F. Park and R. A. Pelroy, eds., pp. 453-462, Proceedings of the 27th Hanford Symposium on Health and the Environment, October 18-21, 1988, Richland, Washington. Battelle Press, Columbus, Ohio.

Mann, D. B., G. L. Stiegler, and D. L. Springer. 1989. Mapping of BaP adducts to the 5*S* rRNA gene carried on a plasmid target. In: *Multilevel Health Effects Research: From Molecules to Man,* J. F. Park and R. A. Pelroy, eds., pp. 435-440, Proceedings of the 27th Hanford Symposium on Health and the Environment, October 18-21, 1988, Richland, Washington. Battelle Press, Columbus, Ohio.

Masse, R., and F. T. Cross. 1989. Risk considerations related to lung modeling. In: *Modeling for Scaling to Man: Biology, Dosimetry, and Response*, Proceedings of the 26th Hanford Life Sciences Symposium, October 20-23, 1987, Richland, Washington. *Health Phys.* 57(Suppl. 1):283-289.

Mast, T. L., R. L. Rommereim, J. R. Coleman, and F. C. Leung. 1989. Fetal pulmonary development in the rat: Effect of chemical mixtures on cellular morphology and growth factors. In: *Multilevel Health Effects Research: From Molecules to Man,* J. F. Park and R. A. Pelroy, eds., pp. 257-266, Proceedings of the 27th Hanford Symposium on Health and the Environment, October 18-21, 1988, Richland, Washington. Battelle Press, Columbus, Ohio.

Nelson, M. A., A. J. Lansing, I. M. Sanchez, R. J. Bull, and D. L. Springer. 1989. Dichloroacetic acid and trichloroacetic acid-induced DNA strand breaks are independent of peroxisome proliferation. *Toxicology* 58:239-248.

Park, J. F., C. L. Sanders, R. E. Weller, E. S. Gilbert, R. L. Buschbom, K. E. Lauhala, and K. E. McDonald. 1989. Comparative toxicology of inhaled $^{239}PuO_2$ in dogs and rats. In: *Modeling for Scaling to Man: Biology, Dosimetry, and Response*, J. A. Mahaffey, ed., Proceedings of the 26th Hanford Life Sciences Symposium, Richland, Washington. *Health Phys.* 57(Suppl. 1):331 (abstract).

Perry, R. E., R. E. Weller, and G. E. Dagle. 1989. Transitional cell carcinoma of the bladder with skeletal metastases in a dog. *J. Am. Anim. Hosp. Assoc.* 25:547-551.

Perry, R. E., R. E. Weller, R. L. Buschsbom, G. E. Dagle, and J. F. Park. 1989. Radiographically determined growth kinetics of primary lung tumors in the dog. In: *Proceedings of the Veterinary Cancer Society Ninth Annual Conference*, pp. 41-42, October 16, 1989, Raleigh, North Carolina. North Carolina University Press, Raleigh, North Carolina.

Rithidech, K., B. T. Chen, J. L. Mauderly, E. B. Whorton, Jr., and A. L. Brooks. 1989. Cytogenetic effects of cigarette smoke on pulmonary alveolar macrophages of the rat. *Environ. Mol. Mutagen.* 14:27-33.

Sanders, C. L., K. E. Lauhala, and K. E. McDonald. 1989. Quantitative scanning electron microscopic autoradiography of inhaled $^{239}PuO_2$. *Health Phys.* 56(3):321-325.

Sanders, C. L., K. E. Lauhala, and K. E. McDonald. 1989. Scanning electron microscopy of lung following alpha irradiation. *Scanning Microsc.* 3(3):907-918.

Sanders, C. L., K. E. Lauhala, and K. E. McDonald. 1989. Tritiated thymidine-labeled bronchioloalveolar cells and radiation dose following inhalation of plutonium in rats. *Exp. Lung Res.* 15:755-769.

Sanders, C. L., K. E. McDonald, and K. E. Lauhala. 1989. Threshold model of lung tumor induction in rats following inhalation of plutonium. *Health Phys.* 56 (Suppl. 1):46 (abstract).

Sanders, C. L., K. E. McDonald, R. R. Adee, and K. E. Lauhala. 1989. Phagocytosis of pulmonary deposited particles by type 1 alveolar epithelium. In: *Proceedings of the 47th Annual Meeting of the Electron Microscopy Society of America*, G. W. Bailey, ed., pp. 922-923. San Francisco Press, San Francisco, California.

Sanders, C. L., K. E. McDonald, K. E. Lauhala, and M. E. Frazier. 1989. Use of archived tissues for studies of plutonium-induced lung tumors. In: *Multilevel Health Effects Research: From Molecules to Man*, J. F. Park and R. A. Pelroy, eds., pp. 189-196, Proceedings of the 27th Hanford Symposium on Health and the Environment, October 18-21, 1988, Richland, Washington. Battelle Press, Richland, Washington.

Sasser, L. B., D. L. Lundstrom, R. C. Zangar, D. L. Springer, and D. D. Mahlum. 1989. Elevated blood pressure and heart rate in rats exposed to a coal-derived complex organic mixture. *J. Appl. Toxicol.* 9(1):47-52.

Scott, B. R., R. E. Filipy, and E. F. Hahn. 1989. *Models for Pulmonary Lethality and Morbidity after Irradiation from Internal and External Sources.* NUREG/CR-5351//TI89 013606. Prepared for the U.S. Nuclear Regulatory Commission, Washington, D. C., by Inhalation Toxicology Research Institute, Albuquerque, New Mexico, and Pacific Northwest Laboratory, Richland, Washington.

Seed, T. M., L. V., Kaspar, D. V. Tolle, T. E. Fritz, and M. E. Frazier. 1989. Analyses of critical target cell responses during preclinical phases of evolving chronic radiation-induced myeloproliferative disease. In: *Multilevel Health Effects Research: From Molecules to Man*, J. F. Park and R. A. Pelroy, eds., pp. 245-255, Proceedings of the 27th Hanford Symposium on Health and the Environment, October 18-21, 1988, Richland, Washington. Battelle Press, Columbus, Ohio.

Sikov, M. R. 1989. Tumour development following internal exposures to radionuclides during the prenatal period. In: *Perinatal and Multigeneration Carcinogenesis*, N. P. Napalkov, J. M. Rice, L. Tomatis, and H. Yamasaki, eds., pp. 403-419. IARC Scientific Publications No. 96, International Agency for Research on Cancer, Lyon, France.

Sikov, M. R., and B. J. Kelman. 1989. Factors affecting the placental transfer of actinides. In: *Modeling for Scaling to Man: Biology, Dosimetry, and Response*, J. A. Mahaffey, ed., Proceedings of the 26th Hanford Life Sciences Symposium, Richland, Washington. *Health Phys.* 57(Suppl. 1):109-114.

Sikov, M. R., D. D. Mahlum, G. E. Dagle, J. L. Daniel, and M. Goldman. 1989. Mechanistic explanations for the elevated susceptibility of the perinatal thyroid gland to radiogenic cancer. In: *Multilevel Health Effects Research: From Molecules to Man*, J. F. Park and R. A. Pelroy, eds., pp. 283-293, Proceedings of the 27th Hanford Symposium on Health and the Environment, October 18-21, 1988, Richland, Washington. Battelle Press, Richland, Washington.

Springer, D. L., and R. C. Zangar. 1989. Influence of imprinting agents on cytochrome P-450 expression. In: *Multilevel Health Effects Research: From Molecules to Man*, J. F. Park and R. A. Pelroy, eds., pp. 239-244, Proceedings of the 27th Hanford Symposium on Health and the Environment, October 18-21, 1988, Richland, Washington. Battelle Press, Richland, Washington.

Springer, D. L., D. B. Mann, D. A. Dankovic, B. L. Thomas, C. W. Wright, and D. D. Mahlum. 1989. Influences of complex organic mixtures on tumor-initiating activity, DNA-binding and adducts of benzo[a]pyrene. *Carcinogenesis* 10(1):131-137.

Stahlhofen, W., G. Rudolf, and A. C. James. 1989. Intercomparison of experimental regional aerosol deposition data. *J. Aerosol Med.* 2(3):285-308.

Stevens, R. G., D. Y. Jones, M. S. Micozzi, and P. R. Taylor. 1989. Response to correspondence: Body iron store and the risk of cancer. *N. Engl. J. Med.* 320:1012-1014.

Stiegler, G. L., and M. E. Frazier. 1989. Molecular analysis of specific DNA sequences using the polymerase chain-reaction method. In: *Multilevel Health Effects Research: From Molecules to Man*, J. F. Park and R. A. Pelroy, eds., pp. 119-125, Proceedings of the 27th Hanford Symposium on Health and the Environment, October 18-21, 1988, Richland, Washington. Battelle Press, Richland, Washington.

Thompson, R. C. 1989. *Life-Span Effects of Ionizing Radiation in the Beagle Dog.* Pacific Northwest Laboratory, Richland, Washington.

Weller, R. E. 1989. Diagnosis and management of endocrine gland neoplasms. In: *Proceedings of the American College of Veterinary Internal Medicine,* G. Pidgeon, ed., pp. 873-880, Seventh Annual Veterinary Medical Forum, May 1989, San Diego, California. Omnipress, Madison, Wisconsin.

Zangar, R. C., D. L. Springer, R. L. Buschbom, and D. D. Mahlum. 1989. Comparison of fetotoxic effects of a dermally applied complex organic mixture in rats and mice. *Fundam. Appl. Toxicol.* 13:662-669.

1990

Arnold, G. E., A. K. Dunker, S. J. Johns, and R. J. Douthart. 1990. The sequence attributes method for determining correlations between amino acid sequence and protein secondary structure. In: *Current Research in Protein Chemistry: Techniques, Structure, and Function*, J. J. Villefranche, ed., pp. 405-415. Academic Press, New York.

Briant, J. K. 1990. Calculation of equivalent aerosol particle mobility in different mixtures of gases used to study convective transport in airways. *J. Aerosol Med.* 3(4):221-232.

Briant, J. K., and A. C. James. 1990. *Dissolution and Particle Size Characterization of Radioactive Contaminants in Hanford Facilities: Criteria for Methods of Measurement.* PNL-7438, Pacific Northwest Laboratory, Richland, Washington.

Brooks, A. L., G. J. Newton, L. J. Skyr, F. A. Seiler, and B. R. Scott. 1990. The combined effects of alpha particles and x rays on cell killing and micronucleii induction in lung epithelial cells. *Int. J. Radiat. Biol.* 58:799-811.

Cross, F. T. 1990. Health effects and risks of radon exposure. In: *Environmental Radon: Occurrence, Control and Health Hazards*, S. K. Majumdar, R. F. Schmalz, and E. W. Miller, eds., pp. 223-237. Pennsylvania Academy of Science, Easton, Pennsylvania.

Dagle, G. E., L. G. Smith, K. E. McDonald, J. F. McShane, and D. L. Stevens, Jr. 1990. Pulmonary carcinogenesis in rats given implants of shale oil in beeswax pellets. *J. Toxicol. Environ. Health* 29:399-407.

Fisher, D. R. 1990. Alpha-particle emitters in medicine. In: *Dosimetry of Administered Radionuclides*, S. J. Adelstein, A. E. Kassis, and R. W. Burt, eds., pp. 194-204. American College of Nuclear Physicians, Washington, D.C.

Gilbert, E. S. 1990. *A. Study of Detailed Dosimetry Methods for a Selected Group of Workers Included in the Hanford Mortality Study.* PNL-7439, Pacific Northwest Laboratory, Richland, Washington.

Gilbert, E. S. 1990. Statistical methods for analyzing and combining data on low level exposures to ionizing radiation. *Radiat. Res.* 124(3):348-349 (abstract).

Gilbert, E. S., G. R. Petersen, and J. A. Buchanan. 1990. Failing to prove danger is no proof of safety: A reply. *Health Phys.* 59(4):483-484.

Gilbert, E. S., J. F. Park, F. T. Cross, and G. E. Dagle. 1990. Recent Pacific Northwest Laboratory animal studies: Methods and results. *Radiat. Res.* 124(3):368-369 (abstract).

Gilbert, E. S., S. A. Fry, L. D. Wiggs, G. L. Voelz, D. L. Cragle, and G. R. Petersen. 1990. Methods for analyzing combined data from studies of workers exposed to low doses of radiation. *Am. J. Epidemiol.* 131(5):917-927.

Hobbs, C. H., and F. T. Cross. 1990. Health effects of radon exposure in laboratory animals. *Fundam. Appl. Toxicol.* 13:630-632.

Hui, T. E., J. W. Poston, and D. R. Fisher. 1990. The microdosimetry of radon decay products in the respiratory tract. *Radiat. Prot. Dosim.* 31(1/4):405-411.

James, A. C. 1990. Reassessment of factors influencing lung dose from radon daughters. In: *Proceedings of the Technical Exchange Meeting on Assessing Radon Health Risks*, September 18-19, 1989, Grand Junction, Colorado, J. R. Duray, G. H. Langner, et al., eds. NTIS, Springfield, Virginia.

Moolgavkar, S. H., F. T. Cross, G. Luebeck, and G. E. Dagle. 1990. A two-mutation model for radon-induced lung tumors in rats. *Radiat. Res.*121:28-37.

Morgan, T. L., E. W. Fleck, K. A. Poston, B. A. Denovan, C. N. Newman, B. J. F. Rossiter, and J. H. Miller. 1990. Molecular characterization of x-ray-induced mutations at the HPRT locus in plateau-phase Chinese hamster ovary cells. *Mutat. Res.* 232:171-182.

Petersen, G. R., E. S. Gilbert, J. A. Buchanan, and R. G. Stevens. 1990. A case-cohort study of lung cancer, ionizing radiation, and tobacco smoking among males at the Hanford Site. *Health Phys.* 58(1):3-11.

Rithidech, K., J. A. Hotchkiss, W. C. Griffith, R. F. Henderson, and A. L. Brooks. 1990. Chromosome damage in rat pulmonary alveolar macrophages following ozone inhalation. *Mutat. Res.* 24:67-73.

Sanders, C. L., and J. A. Mahaffey. 1990. Inhalation carcinogenesis of repeated exposures to high-fired $^{244}CmO_2$ in rats. *Health Phys.* 58(5):631-638.

Sikov, M. R., R. J. Traub, and H. K. Meznarich. 1990. *Contribution of Maternal Radionuclide Burdens to Prenatal Radiation Doses.* NUREG/CR-5631//PNL-7445. Prepared for the U.S. Nuclear Regulatory Commission by Pacific Northwest Laboratory, Richland, Washington.

Stevens, R. G. 1990. Iron and the risk of cancer. *Med. Oncol. Tumor Pharmacother.* 7:177-182.

Stevens, R. G., and B. S. Blumberg. 1990. Serum albumin and mortality. *Lancet* 335:351.

Stevens, R. G., and D. R. Kalkwarf. 1990. Iron, radiation, and cancer. *Environ. Health Perspect.* 87:291-300.

Stram, D. O., S. Akiba, K. Neriishi, R. G. Stevens, and Y. Hosoda. 1990. Smoking and serum proteins in atomic-bomb survivors in Japan. *Am. J. Epidemiol.* 131:1038-1045.

Wilson, B. W., R. G. Stevens, and L. E. Anderson, eds. 1990. *Extremely Low Frequency Electromagnetic Fields: The Question of Cancer.* Battelle Press, Columbus, Ohio.

Wilson, R. H., J. J. Fix, W. V. Baumgartner, and L. L. Nichols. 1990. *Description and Evaluation of the Hanford Personnel Dosimeter Program from 1944 Through 1989.* PNL-7447, Pacific Northwest Laboratory, Richland, Washington.

1991

Leung, F. C., L. R. Bohn, and G. E. Dagle. 1991. Elevated epidermal growth factor reception binding in plutonium-induced lung tumors from dogs. *Proc. Soc. Exp. Biol. Med.* 196:385-389.

Meznarich, H. K., L. A. Braby, and M. R. Sikov. 1991. Expression of fibronectin in mouse blastocysts following irradiation. *Proc. Soc. Exp. Biol. Med.* 196(1):115 (*Abstracts*, Northwest Section).

Sever, L. E. 1991. Low-level ionizing radiation: Paternal exposure and children's health. *Health Environ. Digest* 5(1):1-3.

Sikov, M. R., F. T. Cross, T. J. Mast, E. Palmer, and A. C. James. 1991. Developmental toxicology and dosimetry studies of prenatal exposures in rats. *Proc. Soc. Exp. Biol. Med.* 196(1) (*Abstracts*, Northwest Section).

In Press

Akiba, S., K. Nerishi, W. J. Blot, M. Kabuto, M., R. G. Stevens, H. Kato, and C. E. Land. Serum ferritin and stomach cancer risk among Japanese. *Cancer* (in press).

Alavanja, M. C. R., R. Brownson, M. Wood, Z. Hrubec, J. A. Mahaffey, and J. D. Boice, Jr. Radon dosimetry for a lung cancer study in Missouri. In: *Indoor Radon and Lung Cancer: Reality or Myth?*, F. T. Cross, ed., Proceedings of the 29th Hanford Symposium on Health and the Environment, October 15-19, 1990, Richland, Washington. Battelle Press, Columbus, Ohio (in press).

Bailey, M. R., A. Birchall, R. G. Cuddihy, A. C. James, and M. Roy. Respiratory tract clearance model for dosimetry and bioassay of inhaled radionuclides. *Radiat. Prot. Dosim.* (in press).

Benson, J. M., A. L. Brooks, and R. F. Henderson. Comparative *in vitro* cytotoxicity of nickel compounds to pulmonary alveolar macrophages and to rat lung epithelial cells. *Adv. Environ. Sci. Technol.* (in press).

Birchall, A., M. R. Bailey, and A. C. James. LUDEP: A lung dose evaluation program. *Radiat. Protect. Dosim.* (in press).

Brooks, A. L., K. Rithidech, N. F. Johnson, D. G. Thomassen, and G. J. Newton. Evaluating chromosome damage to estimate dose to tracheal epithelial cells. In: *Indoor Radon and Lung Cancer: Reality or Myth?*, F. T. Cross, ed., Proceedings of the 29th Hanford Symposium on Health and the Environment, October 15-19, 1990, Richland, Washington. Battelle Press, Columbus, Ohio (in press).

Cross, F. T., G. E. Dagle, R. A. Gies, L. G. Smith, and R. L. Buschbom. Experimental animal studies of radon and cigarette smoke. In: *Indoor Radon and Lung Cancer: Reality or Myth?*, F. T. Cross, ed., Proceedings of the 29th Hanford Symposium on Health and the Environment, October 15-19, 1990, Richland, Washington. Battelle Press, Columbus, Ohio (in press).

Dagle, G. E., F. T. Cross, and R. A. Gies. Morphology of respiratory tract lesions in rats exposed to radon/radon progeny. In: *Indoor Radon and Lung Cancer: Reality or Myth?*, F. T. Cross, ed., Proceedings of the 29th Hanford Symposium on Health and the Environment, October 15-19, 1990, Richland, Washington. Battelle Press, Columbus, Ohio (in press).

Dagle, G. E., E. P. Moen, R. A. Adee, T. E. Hui, A. C. James, R. E. Filipy, and R. L. Kathren. Microdistribution of thorium deposited in liver. *Health Phys.* (in press).

Egert, G. H., R. L. Kathren, F. T. Cross, and M. A. Robkin. The effect of home weatherization on indoor radon concentrations. In: *Indoor Radon and Lung Cancer: Reality or Myth?*, F. T. Cross, ed., Proceedings of the 29th Hanford Symposium on Health and the Environment, October 15-19, 1990, Richland, Washington. Battelle Press, Columbus, Ohio (in press).

Fisher, D. R., A. C. James, and T. E. Hui. Model for assessing radiation dose to epithelial cells of the human respiratory tract from radon daughters. *Radiat. Prot. Dosim.* (in press).

Fisher, D. R., T. E. Hui, V. P. Bond, and A. C. James. Microdosimetry of radon progeny: Application to risk assessment. In: *Indoor Radon and Lung Cancer: Reality or Myth?*, F. T. Cross, ed., Proceedings of the 29th Hanford Symposium on Health and the Environment, October 15-19, 1990, Richland, Washington. Battelle Press, Columbus, Ohio (in press).

Foreman, M. E., L. S. McCoy, and M. E. Frazier. Involvement of oncogenes in radon-induced lung tumors in the rat. In: *Indoor Radon and Lung Cancer: Reality or Myth?*, F. T. Cross, ed., Proceedings of the 29th Hanford Symposium on Health and the Environment, October 15-19, 1990, Richland, Washington. Battelle Press, Columbus, Ohio (in press).

Gilbert, E. S., F. T. Cross, C. L. Sanders, and G. E. Dagle. Models for comparing lung-cancer risks in radon- and plutonium-exposed experimental animals. In: *Indoor Radon and Lung Cancer: Reality or Myth?*, F. T. Cross, ed., Proceedings of the 29th Hanford Symposium on Health and the Environment, October 15-19, 1990, Richland, Washington. Battelle Press, Columbus, Ohio (in press).

James, A. C., and A. Birchall. Implications of the ICRP Task Group's proposed lung model for internal dose assessments in the mineral sands industry. In: *Minesafe International, 1990,* Proceedings of an International Conference on Occupational Health and Safety in the Minerals Industry, September 10-14, 1990, Perth, Australia (in press).

James, A. C., W. Stahlhofen, G. Rudolf, M. J. Eagan, W. Nixon, P. Gehr, and J. K. Briant. The respiratory tract deposition model proposed by the ICRP Task Group. *Radiat. Protect. Dosim.* (in press).

James, A. C., P. Gehr, R. Masse, R. G. Cuddihy, F. T. Cross, A. Birchall, J. S. Durham, and J. K. Briant. Dosimetry model for bronchial and extrathoracic tissues of the respiratory tract. *Radiat. Protect. Dosim.* (in press).

Jostes, R. F., E. W. Fleck, R. A. Gies, T. E. Hui, T. L. Morgan, J. L. Schwartz, J. K. Wiencke, and F. T. Cross. Cytotoxic, clastogenic and mutagenic response of mammalian cells exposed *in vitro* to radon and its progeny. In: *Indoor Radon and Lung Cancer: Reality or Myth?*, F. T. Cross, ed., Proceedings of the 29th Hanford Symposium on Health and the Environment, October 15-19, 1990, Richland, Washington. Battelle Press, Columbus, Ohio (in press).

Jostes, R., T. E. Hui, A. C. James, F. T. Cross, J. L. Schwartz, J. Rotmensch, R. W. Atcher, H. H. Evans, J. Mencl, G. Bakale, and P. S. Rao. *In vitro* radon exposure of mammalian cells: Dosimetric considerations. *Radiat. Res.* (in press).

Leung, F. C. Growth factor and growth factor receptor in radiation carcinogenesis. *Radiat. Environ. Biophys.* (in press).

Leung, F. C., G. E. Dagle, and F. T. Cross. Involvement of growth factors and their receptors in radon-induced rat lung tumors. In: *Indoor Radon and Lung Cancer: Reality or Myth?*, F. T. Cross, ed., Proceedings of the 29th Hanford Symposium on Health and the Environment, October 15-19, 1990, Richland, Washington. Battelle Press, Columbus, Ohio (in press).

Mahaffey, J. A., J. R. Johnson, and C. L. Sanders. Robust estimation of nonlinear lung kinetics in animals exposed to alpha-emitting radionuclides. *J. Risk Anal.* (in press).

Mahaffey, J. A., F. T. Cross, J. R. Johnson, and M. C. Baechler. Cost of prevention of lung cancer from residential exposure to radon daughters. *Radiat. Prot. Dosim.* (in press).

Mauderly, J. L., W. E. Bechtold, J. A. Bond, A. L. Brooks, B. J. Chen, R. G. Cuddihy, J. R. Harkema, R. F. Henderson, N. F. Johnson, K. Rithidech, and D. J. Thomassen. Comparison of three methods of exposing rats to cigarette smoke. In: *Proceedings of a Symposium on Assessment of Inhalation Hazards: Integration and Extrapolation Using Diverse Data*, February 19-24, 1989, Hannover, FRG (in press).

Sanders, C. L., R. A. Guilmette, and R. L. Kathren. Autoradiographic examination of soft tissues in a human case of acute ^{241}Am exposure. *Health Phys.* (in press).

Sikov, M. R., H. K. Meznarich, and R. J. Traub. Comparison of placental transfer and localization of cesium, strontium, and iodine in experimental animals and women. In: Meeting Report, CEIR/MRC Forum -- Radionuclides and External Irradiation: Implications for the Embryo and Fetus. *Int. J. Radiat. Biol.* (in press).

Sikov, M. R., F. T. Cross, T. J. Mast, H. E. Palmer, and A. C. James. Developmental toxicity of radon exposures. In: *Indoor Radon and Lung Cancer: Reality or Myth?*, F. T. Cross, ed., Proceedings of the 29th Hanford Symposium on Health and the Environment, October 15-19, 1990, Richland, Washington. Battelle Press, Columbus, Ohio (in press).

Stevens, R. G., and B. S. Blumberg. Serum albumin and risk of cancer. In: *Nutrition and Cancer Prevention*, M. S. Micozzi and T. Moon, eds. Marcel Dekker, New York (in press).

Stevens, R. G., and K. Neriishi. Iron and oxidative damage in human cancer. In: *Mechanisms and Consequences of Oxidative Damage*, A. Bloom and L. Spatz, eds. Environmental Health Institute (in press).

Presentations

1989

Bair, W. J. 1989. Lifespan Studies on the Biological Effects of Inhaled Plutonium and Human Risk Estimation. Presented at the 21st Annual Symposium of the National Institute of Radiological Sciences, Inhalation of Airborne Particles and Induction Mechanisms of Its Biological Effects, December 7-8, 1989, Chiba-shi, Japan, and on December 15, 1989, in Hiroshima, Japan.

Bair, W. J. 1989. Revision of the ICRP Dosimetric Model for the Human Respiratory Tract. Life-Span Studies of Inhaled Plutonium in Beagle Dogs. Invited lectures at the National Institute of Radiological Sciences, December 8, 1989, Chiba, Japan; at Japanese Nuclear Power, December 11, 1989, Toyko, Japan; and at the Radiation Effects Research Foundation, December 15, 1989, Hiroshima, Japan.

Bean, R. M. 1989. Characterization of Biologically Prepared PAH-DNA Adducts as Standards for Analytical Methods Development. Presented at the 12th International Symposium on Polynuclear Hydrocarbons, September 19-21, 1989, Gaithersburg, Maryland.

Bihl, D., R. L. Buschbom, and M. J. Sula. 1989. Results of a Pilot Fecal Sampling Program for Plutonium Workers. Presented at the Conference on Bioassay, Environmental, and Analytical Radiochemistry, October 30-November 2, 1989, Charleston, South Carolina.

Briant, J. K. 1989. Particle Transport by Oscillatory Air Motion in a Tracheobronchial Cast. Presented at the 1989 Annual Meeting of the American Association for Aerosol Research (AAAR), October 9-13, 1989, Reno, Nevada.

Brooks, A. L., F. A. Seiler, and B. R. Scott. 1989. The Combined Effect of Alpha Particles and X-Rays on the Induction of Micronuclei in Rat Lung Epithelial Cells. Presented at the 37th Annual Meeting of the Radiation Research Society, March 18-23, 1989, Seattle, Washington.

Brooks, A. L., B. S. Scott, and L. J. Shyr. 1989. Repair of Alpha-Induced Chromosome Damage. Presented at the 5th International Conference on Environmental Mutagens, July 10-15, 1989, Case Western Reserve University, Cleveland, Ohio.

Brooks, A. L., N. F. Johnson, and G. F. Finch. 1989. The Influence of Cell Cycle Changes on Radiation- and Beryllium-Induced Chromosome Aberrations. Presented at the 6th Annual Meeting of the Pacific Northwest Association of Toxicologists, September 15-16, 1989, Vancouver, B.C., Canada.

Brooks, A. L., N. F. Johnson, G. J. Newton, and D. G. Thomassen. 1989. Radon-Induced Chromosome Damage in Rat Tracheal Epithelial Cells. Presented at the 5th International Conference on Environmental Mutagens, July 10-15, 1989, Case Western Reserve University, Cleveland, Ohio.

Brooks, A. L., K. Rithidech, B. A. Muggenburg, D. Lozano, and D. L. Lundgren. 1989. In Vivo and In Vitro Interaction Between X Rays and Alpha Particles in the Production of Micronuclei. Presented at the 34th Annual Meeting of the Health Physics Society, June 25-29, 1989, Albuquerque, New Mexico.

Carr, F., and J. A. Mahaffey. 1989. DOE/OHER Chernobyl Database. Presented at the Annual Meeting of the Society for Risk Analysis, October 29-November 1, 1989, San Francisco, California.

Cross, F. T., G. E. Dagle, R. A. Gies, and R. L. Buschbom. 1989. Non-Pulmonary Neoplasms Following Radon Inhalation Exposure. Presented at the 34th Annual Meeting of the Health Physics Society, June 2529, 1989, Albuquerque, New Mexico.

Dagle, G. E. 1989. Development of Beagle Pathology Atlas. Presented at the European Late Effects Project (EULEP) Pathology Working Group Meeting, October 27, 1989, Munich, FRG.

Dagle, G. E., and J. F. Park. 1989. Tracheobronchial Lymphadenopathy in Dogs Inhaling Plutonium. Presented at the 37th Annual Meeting of the Radiation Research Society, March 22, 1989, Seattle, Washington.

Dagle, G. E., J. F. Park, and R. E. Weller. 1989. Pathology in Dogs Inhaling Plutonium. Presented at Harwell Laboratories, Environmental and Medical Sciences Division, October 23, 1989, Oxfordshire, United Kingdom.

Dagle, G. E., J. F. Park, R. E. Weller, R. L. Buschbom, and E. S. Gilbert. 1989. Health Effects of Inhaled Soluble Plutonium: Predicting from 11 Years After Exposure. Presented at the 34th Annual Meeting of the Health Physics Society, June 25-29, 1989, Albuquerque, New Mexico.

Douthart, R. 1989. Biotechnology, the Human Genome, and Computers. Presented at the Workshop on Career Opportunities in Biomedical Sciences for Minority Students, March 21, 1989, Long Beach, California (invited presentation).

Douthart, R. J. 1989. Graphics Representation of Large Genomic Structures. Presented to the Society for Industrial Microbiology, August 18, 1989, Seattle, Washington (invited presentation).

Douthart, R. J. 1989. Computers and Genome Mapping. Presented at the INEL Computer Symposium, October 10-12, 1989, Idaho Falls, Idaho (invited lecture).

Douthart, R. J. 1989. Graphics Representation of Genomic Maps. Presented at the INEL Computing Symposium, October 10-12, 1989, Idaho Falls, Idaho (invited presentation).

Douthart, R. J., and D. L. Thurman. 1989. Demonstration of "Gnomeview Interface." Presented at the DOE Contractors Workshop on the Human Genome, November 2-5, 1989, Santa Fe, New Mexico (invited demonstration).

Douthart, R. J., D. L. Thurman, and V. Lortz. 1989. GnomeView: A Graphics Computer Interface to the Human Genome. Presented at the Macromolecules, Genes, and Computers Symposium, August 13, 1989, Waterville Valley, New Hampshire (invited presentation).

Dunker, K., G. Arnold, and R. J. Douthart. 1989. The Sequence Attributes Method of Evaluation of Protein Secondary Structure Predictions. Presented at the Macromolecules, Genes, and Computers Symposium, August 13, 1989, Waterville Valley, New Hampshire (invited presentation).

Fisher, D. R. 1989. Alpha-Particle Emitters in Medicine. Presented at the Joint Symposium on Dosimetry of Administered Radionuclides, September 21-22, 1989, Washington, D.C.

Fisher, D. R. 1989. Antibodies, Radionuclides, and Dosimetry for Cancer Treatment. Presented at the PNL Health Physics Department Seminar, January 4, 1989, Richland, Washington.

Fisher, D. R., T. E. Hui, and J. W. Poston. 1989. The Microdosimetry of Radon Decay Products in the Respiratory Tract. Presented at the 10th Symposium on Microdosimetry, May 22-25, 1989, Rome, Italy.

Frazier, M. E. 1989. Oncogenes and Tumor-Suppressing Genes in Radiation Carcinogenesis. Presented at a seminar at Washington State University, May 1, 1989, Pullman, Washington (invited presentation).

Frazier, M. E. 1989. Oncogenes and Tumor-Suppressing Genes: State of the Art Address. Presented at the 7th Annual Veterinary Medical Forum of the American College of Veterinary Internal Medicine, May 26, 1989, San Diego, California.

Frazier, M. E., G. L. Stiegler, F. T. Cross, and C. L. Sanders. 1989. Use of Archived Paraffin-Embedded Tissues for Studying Oncogene Activation in Radiation-Induced Lung Tumors. Presented at the 37th Annual Meeting of the Radiation Research Society, March 18-23, 1989, Seattle, Washington.

Frazier, M. E., B. J. Kelman, T. M. Seed, L. L. Whiting, and G. L. Stiegler. 1989. Oncogene Activation in Experimentally Induced Lung Tumors. Presented at the 5th International Congress of Toxicology, July 16-21, 1989, Brighton, England.

Fritz, L. K., P. H. Bhatavta, and R. A. Pelroy. 1989. A Study of Mutagenesis Using Synthetic DNA Targets. Presented at the 89th Annual Meeting of the American Society for Microbiology, May 15-19, 1989, New Orleans, Louisiana.

Gilbert, E. S. 1989. The Hanford Mortality Study and Collaborative Combined Populations Studies. Presented at the NAS-NRC Advisory Committee on DOE's Comprehensive Epidemiologic Data Resource, November 20, 1989, Oak Ridge, Tennessee.

Gilbert, E. S. 1989. The Hanford Mortality Study and Collaborative Combined Populations Studies. Presented at the SPEERA Committee Meeting, December 21, 1989, Richland, Washington.

Gillett, N. A., R. A. Guilmette, A. F. Eidson, W. C. Griffith, and A. L. Brooks. 1989. Comparison of Heterogeneous and Homogeneous Patterns of Alpha Irradiation in the Induction of Liver Cancer in the Chinese Hamster. Presented at the 37th Annual Meeting of the Radiation Research Society, March 18-23, 1989, Seattle, Washington.

James, A. C. 1989. The Importance of Particle Size in Respiratory Deposition and Dose. Presented at the DOE Workshop on Unattached Fraction and Radon Decay Product Activity Size Measurements, April 24-25, 1989, University of Illinois, Champaign-Urbana, Illinois.

James, A. C., R. C. Roth, R. W. Kuennen, and F. T. Cross. 1989. The Efficacy of a High-Efficiency Room Air Treatment System in Mitigating Dose from Radon Decay Products. Presented at the Annual Meeting of the American Association for Aerosol Research, October 9-13, 1989, Reno, Nevada.

Jostes, R. F., R. A. Gies, W. F. Morgan, and F. T. Cross. 1989. Radon-Induced Mutagenesis. Presented at the American Society for Cell Biology and the American Society for Biochemistry and Molecular Biology Meeting, January 29-February 2, 1989, San Francisco, California.

Jostes, R. F., R. A. Gies, W. F. Morgan, E. W. Fleck, and F. T. Cross. 1989. Radon-Induced DNA Damage in Mammalian Cell Systems. Presented at the 37th Annual Meeting of the Radiation Research Society, March 19-23, 1989, Seattle, Washington.

Kerkof, P. R., G. Kelly, and A. L. Brooks. 1989. Oncogene Expression in Radiation-Induced Lung Tumors: A Rapid Screening Procedure. Presented at the 4th International Congress of Cell Biology, August 15-19, 1989, Ottawa, Ontario, Canada.

Mahaffey, J. A. 1989. The PNL Epidemiology and Biometry Program. Presented at the Life Sciences Center Advisory Committee Meeting on the Basic and Applied Biomarkers Program, November 30-December 1, 1989, Richland, Washington.

Mahaffey, J. A., and S. E. Dietert. 1989. The Epidemiology Program at Hanford. Presented at the SPEERA Committee Meeting, December 21, 1989, Richland, Washington.

Mahaffey, J. A., A. C. James, J. R. Johnson, and C. L. Sanders. 1989. Robust Estimation of Lung Kinetics in Laboratory Animals Exposed to Alpha-Emitting Radionuclides. Presented at the Annual Meeting of the Society for Risk Analysis, October 29-November 1, 1989, San Francisco, California.

Mahlum, D. D., and M. R. Sikov. 1989. Prenatal Irradiation and Adult Tumor Response. Presented at the 37th Annual Meeting of the Radiation Research Society and 9th Annual Meeting of the North American Hyperthermia Group, March 19-23, 1989, Seattle, Washington.

Meznarich, H. K., and M. R. Sikov. 1989. Development of Mouse Limb Bud in Culture Following Radiation. Presented at the Annual Meeting of the Society for Experimental Biology and Medicine, Northwest Section, October 28, 1989, Richland, Washington.

Meznarich, H. K., M. R. Sikov, and J. E. Ballou. 1989. Kinetics of Inhaled Krypton in the Blood of Pregnant Ewes and Their Fetuses. Presented at the Annual Meeting of the Federation of American Societies for Experimental Biology, March 19-23, 1989, New Orleans, Louisiana.

Park, J. F., G. E. Dagle, R. E. Weller, R. L. Buschbom, and E. S. Gilbert. 1989. Health Effects of Inhaled $^{239}PuO_2$ in Beagle Dogs. Presented at the 34th Annual Meeting of the Health Physics Society, June 29, 1989, Albuquerque, New Mexico.

Rithidech, K., D. G. Thomassen, and A. L. Brooks. 1989. Chromosome Changes During Neoplastic Progression in Rat Tracheal Epithelial (RTE) Cells. Presented at the 5th International Conference on Environmental Mutagens, July 10-15, 1989, Case Western Reserve University, Cleveland, Ohio.

Rithidech, K., D. L. Lundgren, B. A. Muggenberg, D. Lozano, and A. L. Brooks. 1989. The Influence of Plutonium Exposure and Lung Cancer on the Frequency of X-Ray-Induced Micronuclei in Dog Blood Lymphocytes. Presented at the 37th Annual Meeting of the Radiation Research Society, March 18-23, 1989, Seattle, Washington.

Sanders, C. L. 1989. Use of the Scanning Electron Microscope in Radiobiology Studies with Inhaled Transuranics. Presented at the Fall Meeting of the Pacific Northwest Electron Microscopy Society, November 10, 1989, Portland, Oregon.

Sanders, C. L., K. E. McDonald, and K. E. Lauhala. 1989. Relationship Between Bronchiolar Dose and Lung Tumor Induction Following Inhalation of Plutonium. Presented at the 37th Annual Meeting of the Radiation Research Society, March 18-23, 1989, Seattle, Washington.

Sanders, C. L., K. E. McDonald, and K. E. Lauhala. 1989. Scanning Electron Microscopy of Lung Following Alpha Irradiation. Presented at the Annual Meeting of Scanning Microscopy International, May 1-5, 1989, Salt Lake City, Utah.

Sanders, C. L., K. E. McDonald, and K. E. Lauhala. 1989. Threshold Model of Lung Tumor Induction in Rats Following Inhalation of Plutonium. Presented at the 34th Annual Meeting of the Health Physics Society, June 25-29, 1989, Albuquerque, New Mexico.

Sanders, C. L., K. E. McDonald, and K. E. Lauhala. 1989. Phagocytosis of Pulmonary Deposited Particles Following Alpha Irradiation. Presented at the Annual Meeting of the Electron Microscopy Society of America, August 6-11, 1989, San Antonio, Texas.

Scott, B. R., A. L. Brooks, and K. Rithidech. 1989. Distribution of Micronuclei Among Cells Exposed to Ionizing Radiation. Presented at the 34th Annual Meeting of the Health Physics Society, June 25-29, 1989, Albuquerque, New Mexico.

Seiler, F. A., B. R. Scott, and A. L. Brooks. 1989. Dose-Response Model for Combined Effects of Alpha Particles and X-Rays on Lung Epithelial Cells. Presented at the 37th Annual Meeting of the Radiation Research Society, March 18-23, 1989, Seattle, Washington.

Sikov, M. R., R. J. Traub, and H. K. Meznarich. 1989. Expression of Radiation Doses to the Embryo or Fetus from Incorporated Radionuclides. Presented at the 34th Annual Meeting of the Health Physics Society, June 25-29, 1989, Albuquerque, New Mexico.

Sikov, M. R., D. D. Mahlum, G. E. Dagle, and J. L. Daniel. 1989. Possible Mechanisms for Increased Perinatal Sensitivity to Thyroid Carcinogenesis by I-131. Presented at the 37th Annual Meeting of the Radiation Research Society and 9th Annual Meeting of the North American Hyperthermia Group, March 19-23, 1989, Seattle, Washington.

Sikov, M. R., H. K. Meznarich, R. J. Traub, and B. J. Kelman. 1989. Determining Embryo-Fetal Doses from Maternal Exposure. Presented at the Annual Meeting of the Society for Experimental Biology and Medicine, Northwest Section, October 28, 1989, Richland, Washington.

Stevens, R. G. 1989. Iron and the Risk of Cancer. Presented at the American Cancer Society: 31st Annual Science Writers Conference, April 2-5, 1989, Irvine, California (invited participant).

Stevens, R. G. 1989. Iron and the Risk of Cancer. Presented at the 4th International Symposium on Hematology and Oncology: Nutrition and Cancer, Karolinska Hospital, September 20-21, 1989, Stockholm, Sweden (invited Symposium speaker).

Watson, C. R. 1989. Overview of the National Radiobiology Archives Project--Definitions, Personnel, and Progress to Date. Presented at the National Radiobiology Archives Site Review Meeting, March 28-29, 1989, Richland, Washington.

Watson, C. R. 1989. Review of Project Plan--Summary of Technical Aspects. Presented at the National Radiobiology Archives Site Review Meeting, March 28-29, 1989, Richland, Washington.

Watson, C. R. 1989. Selection of Materials--The Evaluation Process at LEHR. Presented at the National Radiobiology Archives Site Review Meeting, March 28-29, 1989, Richland, Washington.

Weller, R. E. 1989. Diagnosis and Management of Endocrine Gland Neoplasms. Presented at the 7th Annual Veterinary Medical Forum of the American College of Veterinary Internal Medicine, May 26, 1989, San Diego, California.

Weller, R. E. 1989. Radiographically Determined Growth Kinetics of Primary Lung Tumors in the Dog. Presented at the Veterinary Cancer Society Annual Conference, October 16, 1989, Raleigh, North Carolina.

Weller, R. E., J. F. Park, G. E. Dagle, H. A. Ragan, and R. Buschbom. 1989. Hepatic Effects of Inhaled Plutonium in Beagle Dogs. Presented at the 34th Annual Meeting of the Health Physics Society, June 25-29, 1989, Albuquerque, New Mexico.

1990

Alavanja, M. C. R., R. Brownson, J. A. Mahaffey, and J. D. Boice, Jr. 1990. Radon Exposure in an Ongoing Lung-Cancer Case-Control Study in Missouri. Presented at the 29th Hanford Symposium on Health and the Environment, October 15-19, 1990, Richland, Washington.

Bair, B. 1990. Health Effects of Radionuclides. Presented at the World Conference on Lung Health, May 20-24, 1990, Boston, Massachusetts.

Briant, J. K. 1990. Calculation of Mean Free Path in Different Gas Mixtures. Presented at the Annual Meeting of the American Association for Aerosol Research (AAAR), June 18-22, 1990, Philadelphia, Pennsylvania.

Brooks, A. L. 1990. The In Vitro Induction of Cell Killing and Chromosome Alterations by SiC Fibers. Presented at the Annual Meeting of the Environmental Mutagen Society, March 25-29, 1990, Albuquerque, New Mexico.

Brooks, A. L. 1990. Induction and Loss of Chromosome Aberrations in Rat Tracheal Epithelial Cells by Inhaled Radon and Its Progeny. Presented at the 38th Annual Meeting of the Radiation Research Society, April 7-12, 1990, New Orleans, Louisiana.

Brooks, A. L., K. Rithidech, N. F. Johnson, D. G. Thomassen, and G. J. Newton. 1990. Evaluating Chromosome Damage to Estimate Dose to Tracheal Epithelial Cells. Presented at the 29th Hanford Symposium on Health and the Environment, October 15-19, 1990, Richland, Washington.

Cross, F. T. 1990. Inhalation Hazards to Uranium Miners. Presented at the OPA Review of the DOE/OHER Radon Research Program, January 27, 1990, Burlington, California.

Cross, F. T. 1990. The Radon Program. Presented at the LSC/DOE/OMB Meeting with Nancy Milton, Executive Office of the President, June 18-20, 1990, Richland, Washington.

Cross, F. T. 1990. Overview of 29th Hanford Symposium on Health and the Environment, "Indoor Radon and Lung Cancer: Reality or Myth?" Presented at a meeting of the Washington State Radon Health Effects Committee, December 18, 1990, Seattle, Washington.

Cross, F. T., and R. F. Jostes. 1990. Mechanisms of Radon Injury. Presented at the OPA Review of the DOE/OHER Radon Research Program, January 27, 1990, Burlington, California.

Cross, F. T., G. E. Dagle, R. A. Gies, L. G. Smith, and R. L. Buschbom. 1990. Experimental Animal Studies of Radon and Cigarette Smoke. Presented at the 29th Hanford Symposium on Health and the Environment, October 15-19, 1990, Richland, Washington.

Dagle, G. E., F. T. Cross, and R. A. Gies. 1990. Morphology of Respiratory Tract Lesions in Rats Exposed to Radon/Radon Progeny. Presented at the 29th Hanford Symposium on Health and the Environment, October 15-19, 1990, Richland, Washington.

Dagle, G. E., E. P. Moen, R. A. Adee, T. E. Hui, A. C. James, R. E. Filipy, and R. L. Kathren. 1990. Microdistribution of Thorium Deposited in the Liver. Presented at the Thorotrast Collaborator's Workshop, July 17, 1990, Rockville, Maryland.

Douthart, R. J. 1990. Computers and the Human Genome. Presented at "New Directions in Science and Technology," May 2, 1990, Western Oregon State College, Monmouth, Oregon (invited seminar).

Douthart, R. J. 1990. A Graphics Computer Interface to the Human Genome. Presented at the Association of Minority Health Professional Schools; and Research Centers in Minority Institutions: Program Planning Meeting for Participation in the Human Genome Initiative, July 21, 1990, Nashville, Tennessee (invited presentation).

Egert, G. H., R. L. Kathren, and F. T. Cross. 1990. The Effect of Home Weatherization on Indoor Radon Concentrations. Presented at the 29th Hanford Symposium on Health and the Environment, October 15-19, 1990, Richland, Washington.

Fisher, D. R. 1990. Microdosimetry of Cells Irradiated by Alpha Particles. Presented at the 38th Annual Meeting of the Radiation Research Society, April 8-12, 1990, New Orleans, Louisiana.

Fisher, D. R. 1990. Alpha-Emitting Monoclonal Antibodies Against Cancer. Presented at the Summer Nuclear Medicine Seminar Series, Westinghouse Hanford Company, July 25, 1990, Richland, Washington.

Fisher, D. R., and T. E. Hui. 1990. Microdosimetry of Cells Irradiated by Alpha Particles. Presented at the 38th Annual Meeting of the Radiation Research Society, April 8-12, 1990, New Orleans, Louisiana (invited paper).

Fisher, D. R., T. E. Hui, and A. C. James. 1990. Model for Assessing Radiation Dose to Epithelial Cells of the Human Respiratory Tract from Radon Progeny. Presented at the 3rd International Workshop on Respiratory Tract Dosimetry, July 1-3, 1990, Albuquerque, New Mexico.

Fisher, D. R., T. E. Hui, V. P. Bond, and A. C. James. 1990. Microdosimetry of Radon Progeny: Application to Risk Assessment. Presented at the 29th Hanford Symposium on Health and the Environment, October 15-19, 1990, Richland, Washington.

Fisher, D. R., C. C. Badger, H. Breitz, J. F. Eary, J. S. Durham, T. E. Hui, R. L. Hill, and W. B. Nelp. 1990. Internal Radiation Dosimetry for Clinical Testing of Radiolabeled Monoclonal Antibodies. Presented at the 3rd Conference on Radioimmunodetection and Radioimmunotherapy of Cancer, November 15-17, 1990, Princeton University, Princeton, New Jersey.

Foreman, M. E., L. S. McCoy, and M. E. Frazier. 1990. Involvement of Oncogenes in Radon-Induced Lung Tumors in the Rat. Presented at the 29th Hanford Symposium on Health and the Environment, October 15-19, 1990, Richland, Washington.

Frazier, M. E. 1990. Cellular and Molecular Markers of Radiation Damage. Presented at the 38th Annual Meeting of the Radiation Research Society, April 7-12, 1990, New Orleans, Louisiana.

Frazier, M. E. 1990. Oncogenes in Radiation Carcinogenesis. Presented at the DOE/OHER Radiation Biology Program Review, June 5-7, 1990, Chicago, Illinois.

Gilbert, E. S. 1990. Statistical Methods for Analyzing and Combining Data on Low Level Exposures to Ionizing Radiation. Presented at the American Statistical Association Conference on Radiation and Health, July 8-13, 1990, Copper Mountain, Colorado.

Gilbert, E. S. 1990. Methods for Analyzing Combined Data from Studies of Workers Exposed to Low-Level Radiation. Presented at the 1990 Joint Statistical Meetings, August 6-10, 1990, Anaheim, California.

Gilbert, E. S. 1990. Modeling Lung Cancer Risks in Laboratory Dogs Exposed to Inhaled Plutonium. Presented at the 1990 Joint Statistical Meetings, August 6-10, 1990, Anaheim, California.

Gilbert, E. S., F. T. Cross, C. L. Sanders, and G. E. Dagle. 1990. Models for Comparing Lung-Cancer Risks in Radon- and Plutonium-Exposed Experimental Animals. Presented at the 29th Hanford Symposium on Health and the Environment, October 15-19, 1990, Richland, Washington.

Gilbert, E. S., J. F. Park, F. T. Cross, and G. E. Dagle. 1990. Recent Pacific Northwest Laboratory Beagle and Rodent Studies: Methods and Results. Presented at the American Statistical Association Conference on Radiation and Health, July 8-12, 1990, Copper Mountain, Colorado.

Hui, T. E., D. R. Fisher, and A. C. James. 1990. Model for Assessing Radiation Dose to Epithelial Cells of the Human Respiratory Tract from Radon Daughters. Presented at the 3rd International Workshop on Respiratory Tract Dosimetry, July 1-3, 1990, Albuquerque, New Mexico.

Hui, T. E., A. L. Brooks, D. R. Fisher, A. C. James, and R. F. Jostes. 1990. Calculation of Dose and Hit Probability to Cells Irradiated in Vitro by Alpha Particles. Presented at the 35th Annual Meeting of the Health Physics Society, June 24-28, 1990, Anaheim, California.

Hulla, J. E., D. B. Mann, and D. L. Springer. 1990. Characterization of Benzo[a]pyrene (BaP) Adducts to the Plasmid, pXP-14. Presented at the Annual Meeting of the Society of Toxicology, February 11-16, 1990, Miami Beach, Florida.

James, A. C. 1990. Dosimetry Modeling: Overview of Radon Dosimetry and the ICRP Task Group's Proposals for a New Lung Model. Presented at the American Statistical Association Conference on Radiation and Health, July 8-12, 1990, Copper Mountain, Colorado (invited lecture).

James, A. C. 1990. Lung Dosimetry Models and the Impact of Proposed Changes. Presented at the Workshop on Radiation Safety in the Mineral Sands Industry, September 12, 1990, Perth, Western Australia (invited lecture).

James, A. C. 1990. Recent Developments in Internal Dosimetry of Plutonium, Thorium, Uranium, and Radon Progeny. Presented at the Australian Radiation Laboratory, September 18, 1990, Melbourne, Victoria, Australia (invited lecture).

James, A. C. 1990. Dosimetry of Radon Exposures: What Does It Imply for Risk and Measurement of Indoor Exposure? Presented at the 29th Hanford Symposium on Health and the Environment, October 15-19, 1990, Richland, Washington (invited overview).

James, A. C. 1990. Respiratory Tract Dosimetry: What Does It Imply for Risk and Measurement of Indoor Exposure? Presented at the 29th Hanford Symposium on Health and the Environment, October 15-19, 1990, Richland, Washington.

James, A. C., and A. Birchall. 1990. Implications of the ICRP Task Group's Proposed Lung Model for Internal Dose Assessments in the Mineral Sands Industry. Presented at Minesafe International 1990, an International Conference on Occupational Health and Safety in the Minerals Industry, September 10-14, 1990, Perth, Western Australia (invited paper).

James, A. C., W. Stahlhofen, G. Rudolf, M. J. Egan, W. Nixon, and J. K. Briant. 1990. The Respiratory Tract Deposition Model Proposed by the ICRP Task Group. Presented at the 3rd International Workshop on Respiratory Tract Dosimetry, July 1-3, 1990, Albuquerque, New Mexico.

James, A. C., P. Gehr, R. Masse, R. G. Cuddihy, F. T. Cross, A. Birchall, J. S. Durham, and J. Briant. 1990. Dosimetry Model for Bronchial and Extrathoracic Tissues of the Respiratory Tract. Presented at the 3rd International Workshop on Respiratory Tract Dosimetry, July 1-3, 1990, Albuquerque, New Mexico.

Jostes, R. 1990. In Vitro Radon-Induced Chromosomal Damage in Human Peripheral Blood Lymphocytes. Presented at the 38th Annual Meeting of the Radiation Research Society, April 7-12, 1990, New Orleans, Louisiana.

Jostes, R. F., J. K. Wiencke, V. Afzal, S. Wolff, and F. T. Cross. 1990. In Vitro Radon-Induced Chromosomal Damage in Human Peripheral Blood Lymphocytes. Presented at the 38th Annual Meeting of the Radiation Research Society, April 7-12, 1990, New Orleans, Louisiana.

Jostes, R. F., T. L. Morgan, R. A. Gies, E. W. Fleck, K. P. Gaspar, and F. T. Cross. 1990. Molecular Analysis of Radon-Induced Mutants. Presented at the UCLA Colloquium on Ionizing Radiation Damage to DNA, January 16-20, 1990, Lake Tahoe, California.

Jostes, R. F., E. W. Fleck, R. A. Gies, T. E. Hui, T. L. Morgan, J. L. Schwartz, J. K. Wiencke, and F. T. Cross. 1990. Cytotoxic, Clastogenic and Mutagenic Response of Mammalian Cells Exposed *in Vitro* to Radon and Its Progeny. Presented at the 29th Hanford Symposium on Health and the Environment, October 15-19, 1990, Richland, Washington.

Kelman, B. J., and M. R. Sikov. 1990. Estimating Fetal Exposure to Toxic Materials. Presented at the Annual Meeting of the Society of Toxicology, February 12-16, 1990, Miami Beach, Florida.

Leung, F. C. 1990. Growth Factors/Receptors as Potential Molecular Markers for Radiation-Induced Lung Cancer. Presented at the 38th Annual Meeting of the Radiation Research Society, April 7-12, 1990, New Orleans, Louisiana.

Leung, F. C. 1990. Growth Factor/Growth Factor Receptor in Radiation Carcinogenesis. Presented at the Symposium on the "Relevance of Animal Models of Radiation Carcinogenesis in the Light of Developments in Molecular Biology," Institute of Applied Radiobiology and Immunology, October 22-23, 1990, TNO, Rijswijk, The Netherlands.

Leung, F. C., G. E. Dagle, and F. T. Cross. 1990. Involvement of Growth Factors and Their Receptors in Radon-Induced Rat Lung Tumors. Presented at the 29th Hanford Symposium on Health and the Environment, October 15-19, 1990, Richland, Washington.

Leung, F. C., G. E. Dagle, J. F. Park, and F. T. Cross. 1990. Growth Factors/Receptors as Potential Molecular Markers for Radiation-Induced Lung Cancer. Presented at the 38th Annual Meeting of the Radiation Research Society, April 7-12, 1990, New Orleans, Louisiana.

Mahaffey, J. A. 1990. Lung Cancer Risk from Residential Exposure to Radon Daughters. Presented at the Workshop on Statistics of Human Exposure to Ionizing Radiation, April 1-3, 1990, Oxford, United Kingdom.

Mahaffey, J. A., F. T. Cross, J. R. Johnson, and M. C. Baechler. 1990. Cost of Prevention of Lung Cancer from Residential Exposure to Radon Daughters. Presented at the Workshop on Statistics of Human Exposure to Ionizing Radiation, April 2-4, 1990, Oxford, United Kingdom.

Mahaffey, J. A., M. C. R. Alavanja, R. Brownson, M. Wood, Z. Hrubec, and J. D. Boice, Jr. 1990. Radon Dosimetry for a Lung Cancer Study in Missouri. Presented at the 29th Hanford Symposium on Health and the Environment, October 15-19, 1990, Richland, Washington.

Mahlum, D. D. 1990. Health Considerations of Complex Chemical Mixtures. Presented at Whitworth College, December 4, 1990, Spokane, Washington.

Minnick, M. F., R. A. Heinzen, M. E. Frazier, and L. P. Mallavia. 1990. Expression and Sequencing of a Unique Gene Cloned from a Plasmid Harbored by Chronic Strains of *Coxiella burnetii*. Presented at the Annual Meeting of the Northwest Branch of the American Society of Microbiology, June 21-23, 1990, Moscow, Idaho.

Meznarich, H. K., and M. R. Sikov. 1990. Effect of Radiation on Mouse Embryonic Limb Development. Presented at the Annual Meeting of the Federation of American Societies for Experimental Biology, April 1-5, 1990, Washington, D.C.

Meznarich, H. K., L. A. Braby, and M. R. Sikov. 1990. Development of Mouse Limb Bud in Culture Following Irradiation. Presented to the Northwest Section of the Society for Experimental Biology and Medicine, October 6, 1990, Newport, Oregon.

Park, J. F., G. E. Dagle, R. E. Weller, R. L. Buschbom, and G. J. Powers. 1990. Comparative Distribution of Inhaled $^{238}PuO_2$ and $^{239}PuO_2$ in Beagles. Presented at the 35th Annual Meeting of the Health Physics Society, June 24-28, 1990, Anaheim, California.

Sanders, C. L. 1990. Low-Level $^{239}PuO_2$ Lifespan Studies. Presented at the DOE Review of Radiobiology Studies, June 6, 1990, Chicago, Illinois.

Sever, L. E. 1990. Reproductive Health Hazards of the Workplace: A Synthesis of Issues. Presented at the Southeastern Safety and Health Conference and Exhibition, May 8, 1990, Atlanta, Georgia.

Sever, L. E. 1990. Reproductive Health Hazards of the Workplace: A Synthesis of Issues. Presented at the 9th Annual Perinatal Workshop sponsored by the Eastern Washington Chapter, March of Dimes Birth Defect Foundation, November 16, 1990, Pasco, Washington.

Sikov, M. R. 1990. Radiation and Chemical Dosimetry of the Embryo and Fetus. Presented at the Teratology Society Meeting, June 6-12, 1990, Victoria, British Columbia.

Sikov, M. R. 1990. Radionuclide Dosimetry of the Embryo and Fetus. Presented at the Lovelace Inhalation Toxicology Research Institute, September 12, 1990, Albuquerque, New Mexico.

Sikov, M. R., H. K. Meznarich, and R. J. Traub. 1990. Comparison of Placental Transfer and Localization of Cesium, Strontium, and Iodine in Experimental Animals and Women. Presented at the CEIR/MRC Forum on Radionuclides and External Irradiation: Implications for the Embryo and Fetus, November 9, 1990, London, England.

Sikov, M. R., F. T. Cross, T. J. Mast, H. E. Palmer, and A. C. James. 1990. Developmental Toxicology and Dosimetry Studies of Prenatal Exposure in Rats. Presented at the Annual Meeting of the Northwest Section of the Society for Experimental Biology and Medicine, October 5-6, 1990, Newport, Oregon.

Sikov, M. R., F. T. Cross, T. J. Mast, H. E. Palmer, and A. C. James. 1990. Developmental Toxicology of Radon Exposures. Presented at the 29th Hanford Symposium on Health and the Environment, October 15-19, 1990, Richland, Washington.

Springer, D. L., J. E. Hulla, M. G. Horstman, B. L. Thomas, and S. C. Goheen. 1990. Preparation and Partial Characterization of Hemoglobin Adducts from Trichloroethylene (TCE). Presented at the Annual Meeting of the Society of Toxicology, February 11-16, 1990, Miami Beach, Florida.

Zangar, R. C., D. W. Later, and D. L. Springer. 1990. Analysis of Carbaryl Metabolites Using HPLC and Supercritical Fluid Chromatograph (SFC). Presented at the Annual Meeting of the Society of Toxicology, February 11-16, 1990, Miami Beach, Florida.

1991

Carr, F., and J. A. Mahaffey. 1991. Chernobyl Database. Presented at the Winter Technical Conference of the American Statistical Association, January 3, 1991, New Orleans, Louisiana.

Douthart, R. D. 1991. Computer Graphics As a Tool in Understanding Genomic Structures. Presented at the workshop "Computer-Based Analysis of Nucleic Acids and Protein Sequences," January 19, 1991, University of Washington Medical Center, Seattle, Washington (invited presentation).

Douthart, R. D. 1991. Computer Visualization of Large Genomic Structures. Presented at BBN, Inc., March 4, 1991, Cambridge, Massachusetts (invited presentation).

Hulla, J. E. 1991. Evidence of the Occurrence of a Processed p53 Pseudogene Within the Rat Genome. Presented at the Radiation Research Society Special Workshop, "Oncogenic Mechanisms in Radiation-Induced Cancer," January 16-19, 1991, Fort Collins, Colorado.

Stiegler, G. E. 1991. Evidence for *ras*-Oncogene Activation in Radiation-Induced Carcinogenesis. Presented at the Radiation Research Society Special Workshop, "Oncogenic Mechanisms in Radiation-Induced Cancer," January 16-19, 1991, Fort Collins, Colorado.

Author Index

Author Index

Adee, R. R., 25
Blot, W. (National Cancer Institute), 9
Briant, J. K., 65
Brooks, A. L., 97
Buchanan, J. A., 1
Buschbom, R. L., 13, 25, 45, 51, 103
Chandler, D. P., 71
Cross, F. T., 45, 51, 55, 71, 103
Dagle, G. E., 13, 25, 45, 51, 71, 103
Douthart, R. J., 109
Durham, J. S., 55
Egan, M. J. (AEA Safety and Reliability, England), 55
Fisher, D. R., 55
Fix, J. J., 1
Fleck, E. W. (Whitman College), 51
Foreman, M. E., 51, 79
Frazier, M. E., 51, 79
Gehr, P. (Institute of Anatomy, Switzerland), 55
Gideon, K. M., 13, 25, 45
Gies, R. A., 45, 51
Gilbert, E. S., 1, 13, 25, 45
Graubard, B. (National Cancer Institute), 9
Greenspan, B. J., 65
Holter, N. A., 1
Hopke, P. K. (Clarkson University), 55
Hui, T. E., 55
Hulla, J. E., 85
James, A. C., 51, 55, 65, 103
Jostes, R. F., 51
Karagianes, M. T., 33
Kitchin, R. M., 97
Land, C. (National Cancer Institute), 9
Lauhala, K. E., 39
Leung, F. C., 51, 71
Lindgren, L. M., 33
Mahaffey, J. A., 39
Mann, D. B., 91
Mast, T. J., 103
McCoy, L. S., 51
McDonald, K. E., 97
Meznarich, H. K., 103
Mitchell, C., 97
Moolgavkar, S. H. (Fred Hutchinson Cancer Research Center), 51
Morgan, T. L., 51
Nelson, J. M., 9
Neriishi, K. (Radiation Effects Research Foundation, Japan), 9
Nixon, W. (AEA Safety and Reliability, England), 55
Park, J. F., 13, 71
Parkhurst, M. A., 65
Powers, G. J., 13, 25
Prather, J. C., 33
Ragan, H. A., 13, 25
Rogers, S. J., 85
Rommereim, D. N., 33
Romsos, C. O., 13, 25
Sanders, C. L., 39
Schmaltz, J. E., 113
Schneider, R. P., 79, 85
Schwartz, J. L. (Argonne National Laboratory), 51
Seed, T. M. (Argonne National Laboratory), 79
Sever, L. E., 7
Sikov, M. R., 103
Sisk, E., 79
Smith, L. G., 33, 51
Smith, S. K., 33
Springer, D. L., 91
Stevens, R. G., 9
Stiegler, G. L., 51, 79, 85, 91
Stillwell, L. C., 79
Swift, D. L. (The Johns Hopkins University), 55
Thompson, R. C., 33
Thrall, B. D., 91
Thurman, D. A., 109
Watson, C. R., 13, 25, 33
Weller, R. E., 13, 25
Wierman, E. L., 13, 25

Distribution

Distribution

OFFSITE

W. R. Albers
EH-12, GTN
Department of Energy
Washington, DC 20545

R. E. Albert, Professor
& Chairman
Department of Environmental
Health
University of Cincinnati
Medical Center
3223 Eden Avenue
Cincinnati, OH 45267-0056

E. L. Alpen
University of California
230 Donner Laboratory
Berkeley, CA 94720

A. Andersen
Center for Devices &
Radiological Health
Food & Drug Administration
5600 Fishers Lane, HFZ-100
Rockville, MD 20857

D. Anderson
ENVIROTEST
1108 NE 200th Street
Seattle, WA 98155-1136

G. Anderson
Department of Oceanography
University of Washington
Seattle, WA 98115

V. E. Archer
Rocky Mountain Center for
Occupational & Environmental
Health
Building 512
University of Utah
50 North Medical Drive
Salt Lake City, UT 84112

Assistant Secretary
Environment, Safety & Health
EH-1, FORS
Department of Energy
Washington, DC 20585

O. Auerbach
VA Hospital
East Orange, NJ 97919

J. A. Auxier
IT Corporation
312 Directors Drive
Knoxville, TN 37701

F. I. Badgley
13749 NE 41st Street
Seattle, WA 98125

R. E. Baker
8904 Roundleaf Way
Gaithersburg, MD 20879-1630

R. M. Baltzo
Radiological Safety Division
University of Washington
Seattle, WA 98105

R. W. Barber
EH-131, GTN
Department of Energy
Washington, DC 20545

M. M. Bashor, Ph.D.
ATSDR, Mail Stop E-28
1600 Clifton Road NE
Atlanta, GA 30333

J. R. Barker
Office of Environmental Audit
and Compliance
Department of Energy
Washington, DC 20545

W. W. Barker, Chairman
Department of Biology
Central Washington University
Ellensburg, WA 98926

B. J. Barnhart
Office of Energy Research
Department of Energy
ER-72, GTN
Washington, DC 20545

N. F. Barr
ER-72, GTN
Department of Energy
Washington, DC 20545

J. W. Baum
Brookhaven National
Laboratory
Bldg. 703-M
Upton,
Long Island, NY 11973

J. R. Beall
ER-72, GTN
Department of Energy
Washington, DC 20545

S. Benjamin
Director, CRHL
Foothills Campus
Colorado State University
Fort collings, CO 80523

G. L. Bennett
Code RP
National Aeronautics & Space
Administration
Washington, DC 20545

R. P. Berube
EH-151, GTN
Department of Energy
Germantown, MD 20545

PNL-7600, Pt. 1
UC-408

M. H. Bhattacharyya
BIM Div., Bldg. 202
Argonne National Laboratory
9700 South Cass Avenue
Argonne, IL 60439

R. W. Bistline
Rockwell International
Rocky Flats Plant
P. O. Box 464
Golden, CO 80401

B. B. Boecker
Inhalation Toxicology Research Institute
The Lovelace Foundation for Medical Education & Research
P. O. Box 5890
Albuquerque, NM 87185

V. P. Bond
Life Sciences, Chemistry and Safety
Brookhaven National Laboratory
Bldg. 460
Upton, Long Island, NY 11973

C. M. Borgstrom
Acting Director, NEPA
EH-25, Room 3E080
Department of Energy
1000 Independence Ave. SW
Washington, DC 20585

J. D. Brain
Professor of Physiology
Director, Harvard Pulmonary Specialized Center of Research
Harvard University School of Public Health
665 Huntington Avenue
Boston, MA 02115

L. C. Brazley, Jr.
NE-22, GTN
Department of Energy
Washington, DC 20545

B. D. Breitenstein
Brookhaven National Laboratory
P.O. Box 83
Upton, NY 11973

A. Brodsky
16412 Kipling Road
Derwood, MD 20855

F. W. Bruenger
Division of Radiobiology
Bldg. 586
University of Utah
Salt Lake City, UT 84112

D. R. Buhler, Chairman
Toxicology Program
Oregon State University
Corvallis, OR 97331

R. J. Bull
Associate Professor of Pharmacology/Toxicology
College of Pharmacy
Pullman, WA 99164-6510

G. Burley
Office of Radiation Programs, ANR-458
Environmental Protection Agency
Washington, DC 20460

W. W. Burr, Chairman
Medical & Health Sciences Division
Oak Ridge Associated Universities
P. O. Box 117
Oak Ridge, TN 37830

L. K. Bustad
College of Veterinary Medicine
Washington State University
Pullman, WA 99163

C. E. Carter
National Institute of Environmental Health Sciences
P. O. Box 12233
Research Triangle Park, NC 27709

G. W. Casarett
Biophysics Department
University of Rochester Medical Center
Rochester, NY 14642

H. W. Casey, Chairman
Department of Veterinary Pathology
School of Veterinary Medicine
Louisiana State University
Baton Rouge, LA 70803

R. J. Catlin, President
Robert J. Catlin Corporation
701 Welch Road, Suite 1119
Palo Alto, CA 94304

N. Cohen
New York University Medical Center
P. O. Box 817
Tuxedo, NY 10987

W. Cool
Nuclear Regulatory Commission
Washington, DC 20545

D. K. Craig
Savannah River Laboratories
P.O. Box 616
Aiken, SC 29802

E. P. Cronkite
Medical Department
Brookhaven National Laboratory
Upton, Long Island, NY 11973

J. Crowell
The Maxima Corporation
107 Union Valley Road
Oak Ridge, TN 37830

Department of Energy
Health Protection Division
P. O. Box 5400
Albuquerque, NM 87115

G. DePlanque, Director
Department of Energy-EMEL
375 Hudson Street
New York, NY 10014

G. P. Dix
26619 Haney Avenue
Damascus, MD 20750

T. J. Dobry, Jr.
DP-221, GTN
Department of Energy
Washington, DC 20545

DOE/Office of Scientific &
Technical Information (12)

DOE - Savannah River
Operations Office
Environmental Division
P. O. Box A
Aiken, SC 29801

D. Doyle
Argonne National Laboratory
9700 South Cass Avenue
Argonne, IL 60439

H. Drucker
Argonne National Laboratory
9700 South Cass Avenue
Argonne, IL 60439

J. A. Louis Dubeau
Urological Cancer Research
Laboratory
USC Comprehensive Cancer
Center
University of Southern California
Los Angeles, CA 90033-0800

G. D. Duda
ER-72, GTN
Department of Energy
Washington, DC 20545

A. P. Duhamel
ER-74, GTN
Department of Energy
Washington, DC 20545

D. Dungworth
Associate Dean of Research
and Professor & Chairman
Department of Veterinary
Pathology
School of Veterinary Medicine
University of California
Davis, CA 95616

Dr. Patricia W. Durbin
Division of Biology and Medicine
Lawrence Berkeley Laboratory
University of California
Berkeley, CA 94704

K. F. Eckerman
Health Studies Section
Health and Safety Research
Division
Oak Ridge National Laboratory
P. O. Box 2008
Oak Ridge, TN 37831-6383

C. W. Edington, Director
National Academy of Sciences
JH 554
2101 Constitution Avenue, NW
Washington, DC 20418

G. R. Eisele
Medical Division
Oak Ridge Associated
Universities
P. O. Box 117
Oak Ridge, TN 37830

M. Eisenbud
711 Bayberry Drive
Chapel Hill, NC 27514

R. J. Engelmann
11701 Karen
Potomac, MD 20854

N. B. Everett
Department of Biological
Structure
University of Washington
School of Medicine
Seattle, WA 98105

H. Falk, M.D.
CDC
CEHIC/EHHE/
1600 Clifton Road NE
Atlanta, GA 30333

K. P. Ferlic
Office of Scientific &
Engineering Recruitment,
Training & Development
TR-1
U.S. Department of Energy
Washington, DC 20545

B. H. Fimiani
Battelle, Pacific Northwest
Laboratories
Washington Operations
370 L'Enfant Promenade,
Suite 900
901 D Street, SW
Washington, DC 20024

PNL-7600, Pt. 1
UC-408

M. E. Frazier
Office of Health and Environment
Office of Energy Research
Department of Energy
ER-72, GTN
Germantown, MD 20545

H. L. Friedell
Biochemical Oncology
Case-Western Reserve University
2058 Abington Road
Wearn B21
Cleveland, OH 44106

T. Fritz
Argonne National Laboratory
9700 South Cass Avenue
Argonne, IL 60439

D. J. Galas
Office of Energy Research
ER-63
Department of Energy
Washington, DC 20545

D. E. Gardner
Northrop Services, Inc.
P. O. Box 12313
Research Triangle Park,
NC 27709

T. F. Gesell
Idaho Operations Office
Department of Energy
785 DOE Place
Idaho Falls, ID 83402-4149

R. D. Gilmore, President
Environmental Health Sciences, Inc.
Nine Lake Bellevue Building
Suite 104
Bellevue, WA 98005

M. Goldman
Department of Radiological Sciences (VM)
University of California
Davis, CA 95616

R. Goldsmith, Director
Office of Epidemiology & Health Surveillance, EH-42
Department of Energy
Washington, DC 20545

G. Goldstein
ES&H
Acting Director
Office of Epidemiology & Health Surveillance
EH-42
Department of Energy
Washington, DC 20545

J. A. Graham
ECAO, Mail Drop 52
Environmental Protection Agency
Research Triangle Park,
NC 27711

R. A. Griesemer, Director
National Toxicology Program
National Institutes of Health
P. O. Box 12233
Research Triangle Park,
NC 27709

G. H. Groenewold
Energy and Mineral Research Center
University of North Dakota
Box 8123, University Station
Grand Forks, ND 58202

F. F. Hahn
Lovelace Inhalation Toxicology Research Institute
P. O. Box 5890
Albuquerque, NM 87115

E. J. Hall
Radiological Research Laboratory
Columbia University
630 West 168th Street
New York, NY 10032

R. Hamlin
Dept. of Veterinary Physiology
The Ohio State University
1900 Coffey Road
Columbus, OH 43201

J. W. Healy
51 Grand Canyon Drive
White Rock, NM 87544

C. H. Hobbs
Inhalation Toxicology Research Institute
The Lovelace Foundation for Medical Education & Research
P. O. Box 5890
Albuquerque, NM 87185

L. M. Holland
Los Alamos National Laboratory
P. O. Box 1663
Los Alamos, NM 87545

R. Hornung
DSHEFS, NIOSH
Robert A. Taft Laboratories
4676 Columbia Parkway
Cincinnati, OH 45220

R. O. Hunter, Jr.
ER-1, FORS
Department of Energy
1000 Independence Ave. SW
Washington, DC 20585

F. Hutchinson
Department of Therapeutic Radiology, HRT 315
Yale University School of Medicine
333 cedar Street
New Haven, CT 06510-8040

H. Ishikawa, General Manager
Nuclear Safety Research Association
P. O. Box 1307
Falls Church, VA 22041

K. L. Jackson, Chairman
Radiological Sciences Group SB-75
University of washington
Seattle, WA 98195

E. D. Jacobson
Center for Devices & Radiological Health
Food & Drug Administration
5600 Fishers Lane, HFZ-100
Rockville, MD 20857

A. W. Johnson
Vice President for Academic Affairs
San Diego State University
San Diego, CA 92182

R. K. Jones
The Lovelace Foundation for Medical Education & Research
Building 9200, Area Y
Sandia Base
Albuquerque, NM 87108

G. Y. Jordy, Director
ER-30, GTN
Department of Energy
Washington, DC 20545

C. M. Kelly
Air Products and Chemicals, Inc.
Corporate Research and Development
P. O. Box 538
Allentown, PA 18105

A. R. Kennedy
Department of Physiology
Harvard School of Public Health
665 Huntington Avenue
Boston, MA 02115

R. T. Kratzke
NP-40
Department of Energy
Germantown, MD 20585

W. Lauder
Office of Health and Environmental Research
Office of Energy Research
Department of Energy
Germantown, MD 20545

W. M. Leach
Food & Drug Administration
5600 Fishers Lane, HFZ-100
Rockville, MD 20857

Librarian
Brookhaven National Laboratory
Research Library, Reference
Upton, Long Island, NY 11973

Librarian
Colorado State University
Documents Department--The Libraries
Ft. Collins, CO 80523

Librarian
Electric Power Research Institute
3412 Hillview Avenue
P. O. Box 10412
Palo Alto, CA 94303

Librarian
Health Sciences Library, SB-55
University of Washington
Seattle, WA 98195

Librarian
Los Alamos National Laboratory
Report Library, MS P364
P. O. Box 1663
Los Alamos, NM 87545

Librarian
Oregon Regional Primate Research Center
505 NW 185th Avenue
Beaverton, OR 97006

Librarian
Washington State University
Pullman, WA 99164-6510

Library
Serials Department (#80-170187)
University of Chicago
1100 East 57th Street
Chicago, IL 60637

J. B. Little
Department of Physiology
Harvard School of Public Health
665 Huntington Avenue
Boston, MA 02115

A. B. Lovins
Rocky Mountain Institute
1739 Snowmass Creek Road
Snowmass, CO 81654-9199

PNL-7600, Pt. 1
UC-408

O. R. Lunt
Laboratory of Biomedical & Environmental Sciences
University of California
900 Veteran Avenue
Los Angeles, CA 90024-1786

J. R. Maher
ER-65, GTN
Department of Energy
Washington, DC 20545

D. D. Mahlum
Board of Radiation Research
Room 342
2101 Constitution NW
Washington, D.C. 20318

T. D. Mahony
750 Swift Boulevard
Richland, WA 99352

S. Marks
8024 47th Place West
Mukilteo, WA 98275

D. R. Mason
Nuclear Safety Branch
Department of Energy
P. O. Box A
Aiken, SC 29801

W. H. Matchett
Graduate School
New Mexico State University
Box 3G
Las Cruces, NM 88003-0001

H. M. McCammon
ER-75, GTN
Department of Energy
Washington, DC 20545

R. O. McClellan, President
Chemical Industry Institute of Toxicology
P. O. Box 12137
Research Triangle Park,
NC 27709

J. F. McInroy
Los Alamos National Laboratory
Mail Stop K484
P. O. Box 1663
Los Alamos, NM 87545

Medical Officer
Monsanto Research Corp.
Mound Laboratory
P. O. Box 32
Miamisburg, OH 45342

C. B. Meinhold
Head, Safety and Environmental Protection Division
Brookhaven National Laboratory
Upton, Long Island, NY 11973

T. Meinhardt
DSHEFS, NIOSH
Robert A. Taft Laboratories
4676 Columbia Parkway
Cincinnati, OH 45220

M. L. Mendelsohn
Biomedical and Environmental Research Program
Lawrence Livermore National Laboratory, L-452
University of California
P. O. Box 5507
Livermore, CA 94550

H. Menkes
Assistant Professor of Medicine & Environmental Medicine
The John Hopkins University
Baltimore, MD 21205

D. B. Menzel
Southern Occupational Health Center
University of California, Irvine
Irvine, CA 92717

S. Michaelson
University of Rochester Medical Center
Rochester, NY 14642

C. Miller
P.O. Box 180
Watermill, NY 11976

S. Miller
Department of Radiobiology
University of Utah
Salt Lake City, UT 84112

W. A. Mills
Committee on Interagency Radiation Research & Policy Coordination (CIRRPC)
1346 Connecticut Avenue N.W.
Suite 530
Washington, DC 20036

K. Z. Morgan
1984 Castleway Drive
Atlanta, GA 30345

P. E. Morrow
Department of Biophysics
Medical Center
University of Rochester
Rochester, NY 14642

O. R. Moss
Chemical Industry Institute of Toxicology
P. O. Box 12137
Research Triangle Park,
NC 27709

W. F. Mueller
New Mexico State University
Box 4500
Las Cruces, NM 88003-4500

D. S. Nachtwey
NASA-Johnson Space Center
Mail Code SD-5
Houston, TX 77058

D. B. Nash, Editorial Assistant
Department of Radiation Biology and Biophysics
University of Rochester
School of Medicine and Dentistry
260 Crittenden Boulevard
Rochester, NY 14620

R. Nathan
Battelle Project Management Division
505 King Avenue
Columbus, Ohio 43201

National Library of Medicine
TSD-Serials
8600 Rockville Pike
Bethesda, MD 20014

N. S. Nelson
Office of Radiation Programs (ANR-461)
Environmental Protection Agency
401 M Street, SW
Washington, DC 20460

P. Nettesheim
National Institutes of Environmental Health Sciences
Research Triangle Park,
NC 27711

W. R. Ney, Executive Director
National Council on Radiation Protection and Measurements
7910 Woodmont Avenue
Suite 1016
Bethesda, DC 20814

S. W. Nielsen
Department of Pathology
New York State Veterinary College
Cornell University
Ithaca, NY 14850

R. A. Nilan
Division of Sciences
Washington State University
Pullman, WA 99164

M. Nolan
10958 Rum Cay Court
Columbia, MD 21044

Nuclear Regulatory Commission
Advisory Committee on Reactor Safeguards
Washington, DC 20555

A. F. Perge
RW-43, FORS
Department of Energy
Washington, DC 20545

D. F. Petersen
Los Alamos National Laboratory
P. O. Box 1663
Los Alamos, NM 87545

G. R. Petersen, Director
Epidemiologic Studies Division
Office of Epidemiology and Health Surveillance, EH-42
U.S. Department of Energy
Washington, DC 20545

L. E. Peterson
NASA/JSC SD23
Houston, TX 77058

H. Pettingill
Deputy Assistant Secretary of Health
EH-40, GTN
U.S. Department of Energy
Washington, DC 20545

H. Pfuderer
Oak Ridge National Laboratory
P. O. Box X
Oak Ridge, TN 37830

O. G. Raabe
Laboratory for Energy-Related Health Research
University of California
Davis, CA 95616

R. Rabson
Division of Biological Energy Research
ER-17, GTN
Department of Energy
Washington, DC 20545

D. P. Rall, Director
National Institutes of Environmental Health Sciences
P. O. Box 12233
Research Triangle Park,
NC 27709

R. D. Reed, Chief
Rocky Flats Area Office
Albuquerque Operations Office
Department of Energy
P. O. Box 928
Golden, CO 80402-0928

C. R. Richmond
Oak Ridge National Laboratory
4500N, MS-62523
P. O. Box 2008
Oak Ridge, TN 37831-6253

B. Robinson
Monsanto Research Corp.
Mound Laboratory
P. O. Box 32
Miamisburg, OH 45342

S. L. Rose
ER-73, GTN
Department of Energy
Washington, DC 20545

G. Runkle, Chief
Department of Energy, AL
HPB/EHD
P. O. Box 5400
Albuquerque, NM 87115

G. Saccomanno
Pathologist and Director of Laboratories
St. Marys and V. A. Hospitals
Grand Junction, CO 81501

U. Saffiotti
Laboratory of Experimental Pathology, DCCP
National Cancer Institute
Bldg. 560, Rm. 32-60
Bethesda, MD 21701

L. Sagan
Electric Power Research Institute
3412 Hillview Avenue
P. O. Box 10412
Palo Alto, CA 94304

J. M. Samet
New Mexico Tumor Registry
University of New Mexico
Cancer Research and Treatment Center
Albuquerque, NM 87131

M. Sage
CDC (F-28)
CEHIC
1600 Clifton Road NE
Atlanta, GA 30333

R. A. Scarano
Mill Licensing Section
Nuclear Regulatory Commission
Washington, DC 20545

R. A. Schlenker
Center for Human Radiobiology
Argonne National Laboratory
9700 South Cass Avenue
Argonne, IL 60439

C. R. Schuller
Battelle - Seattle
4000 NE 41st Street
Seattle, WA 98105

M. Schulman
ER-70, GTN
Department of Energy
Washington, DC 20545

T. M. Seed
BIM 202
Argonne National Laboratory
9700 South Cass Avenue
Argonne, IL 60439

R. B. Setlow
Brookhaven National Laboratory
Upton, Long Island, NY 11973

R. Shikiar
Battelle - Seattle
4000 NE 41st Street
Seattle, WA 98105

T. Sibley
Department of Fisheries, WH-10
University of Washington
Seattle, WA 98195

P. H. Silverman
Lawrence Berkeley Laboratory
Bldg. 50A/5104
Berkeley, CA 94720

W. K. Sinclair, President
National Council on Radiation Protection
7910 Woodmont Avenue
Suite 1016
Bethesda, MD 20814

D. H. Slade
ER-74, GTN
Department of Energy
Washington, DC 20545

D. A. Smith
ER-72, GTN
Department of Energy
Washington, DC 20545

G. S. Smith
New Mexico State University
Box 3-I
Las Cruces, NM 88003-0001

J. M. Smith
CDC
CEHIC
1600 Clifton Road NE
Atlanta, GA 30333

J. N. Stannard
17441 Plaza Animado #132
San Diego, CA 92128

R. W. Starostecki
Department of Energy
1000 Independence Ave. SW
Washington, DC 20585

R. J. Stern
EH-10, FORS
Department of Energy
Washington, DC 20585

K. G. Steyer
Nuclear Regulatory Commission
Washington, DC 20555

E. T. Still
Kerr-McGee Corporation
P. O. Box 25861
Oklahoma City, OK 73125

Dr. B. J. Stover
243 Carolina Meadows
Chapel Hill, NC 27514

B. Stuart
Brookhaven National Laboratory
Upton, Long Island, NY 11973

D. Swanger
Biology Department
Eastern Oregon State College
La Grande, OR 97850

J. Swinebroad
PE-24, GTN
Department of Energy
Washington, DC 20545

G. N. Taylor
Division of Radiobiology
Bldg. 351
University of Utah
Salt Lake City, UT 84112

Technical Information Service
Savannah River Laboratory
Room 773A
E. I. duPont de Nemours & Company
Aiken, SC 29801

H. E. Thomas
FE-13, GTN
U.S. Department of Energy
Washington, DC 20545

R. G. Thomas
20706 Highland Hall Drive
Gaithersburg, MD 20979

T. Thomas
Health Physics and Industrial Hygiene
EH-41
U.S. Department of Energy
Washington, DC 20545

P. W. Todd
Center for Chemical Engineering
National Bureau of Standards (773.10)
325 Broadway
Boulder, CO 80303

P. T'so
Division of Biophysics, Room 3120
School of Hygiene & Public Health
The Johns Hopkins University
615 North Wolfe Street
Baltimore, MD 21205

A. C. Upton
New York University Medical Center
Institute of Environmental Medicine
A. J. Lanza Laboratory
Long Meadow Road
Tuxedo, NY 10987

B. Valett
NORCUS
390 Hanford Street
Richland, WA 99352

E. J. Vallario
15228 Red Clover Drive
Rockville, MD 20853

R. L. Van Citters, Dean
Research and Graduate Programs
University of Washington
Seattle, WA 98105

C. R. Vest
Marymount University
2807 North Glebe Road
Arlington, VA 22207

G. J. Vodapivc
DOE - Schenectady Naval Reactors Office
P. O. Box 1069
Schenectady, NY 12301

G. L. Voelz
Los Alamos National Laboratory
MS-K404
P. O. Box 1663
Los Alamos, NM 87545

B. W. Wachholz
Radiation Effects Branch
National Cancer Institute
EPN,
6130 Executive Blvd.
Rockville, MD 20842

N. Wald
School of Public Health
University of Pittsburgh
Pittsburgh, PA 15213

A. Waldo
Department of Energy (EH-231)
1000 Independence Ave. SW
Washington, DC 20585

R. A. Walters
Assistant to the Associate Director
Los Alamos National Laboratory
MS-A114
P. O. Box 1663
Los Alamos, NM 87545

P. Watson
Associate Professor
Department of Chemistry
Oregon State University
Corvallis, OR 97331

M. E. Weaver
Professor of Anatomy
University of Oregon Health Science Center
School of Dentistry
Portland, OR 97201

M. H. Weeks
U.S. AEHA, Bldg. 2100
Edgewood Arsenal
Aberdeen Proving Ground, MD 21014

I. Wender
Department of Chemical Engineering
1249 Benedum Hall
University of Pittsburgh
Pittsburgh, PA 15261

W. W. Weyzen
Electric Power Research Institute
3412 Hillview Avenue
P. O. Box 10412
Palo Alto, CA 94303

K. Wilzbach
Argonne National Laboratory
9700 South Cass Avenue
Argonne, IL 60439

F. J. Wobber
Department of Energy
ER-75, GTN
Germantown, MD 20545

R. W. Wood
PTRD, OHER
ER-74, GTN
Department of Energy
Washington, DC 20545

M. E. Wrenn
Environmental Radiation & Toxicology Laboratory
University of Utah
1771 South 900 W. #10
Salt Lake City, UT 84104

S. Yaniv
Health Effects Branch
Office of Nuclear Regulatory Research
Nuclear Regulatory Commission
Washington, DC 20555

R. E. Yoder
Rockwell International
P. O. Box 464
Golden, CO 80401

P. L. Ziemer, Ph. D.
Assistant Secretary
Environment, Safety and Health
EH-42, GTN
U.S. Department of Energy
Washington, DC 20545

FOREIGN

G. E. Adams, Director
Medical Research Council
Radiobiology Unit
Harwell, Didcot
Oxon OX11 ORD
ENGLAND

A. L. Alejandrino, Head
Biomedical Research, ARD
Republic of the Philippines
Philippine Nuclear Research Institute
P.O. Box 932
Manila
THE PHILIPPINES

M. Anderson
Library
Department of National Health & Welfare
Ottawa, Ontario
CANADA

R. K. Appleyard
Director, Biology
European Atomic Energy Community, EURATOM
Brussels
BELGIUM

Atomic Energy of Canada, Ltd.
Scientific Document Distribution Office
Station 14
Chalk River Nuclear Laboratories
Chalk River, Ontario KOJ 1JO
CANADA

D. C. Aumann
Institut für Physikalische Chemie
Universität Bonn
Abt. Nuklearchemie
Wegelerstraße 12
5300 Bonn 1
GERMANY

M. R. Balakrishnan, Head
Library & Information Services
Bhabha Atomic Research Centre
Bombay-400 085
INDIA

G. W. Barendsen
Laboratory for Radiobiology
AMC, FO 212
Meibergdreef 9
1105 AZ Amsterdam
THE NETHERLANDS

J. K. Basson, Vice-President
Raad Op Atomic
Atoomkrag Energy Board
Privaatsk X 256
Pretoria 0001
REPUBLIC OF SOUTH AFRICA

A. M. Beau, Librarian
Département de Protection Sanitaire
Commissariat à l'Énergie Atomique
BP 6
F-92265 Fontenay-aux-Roses
FRANCE

G. Bengtsson
Director-General
Statens Stralskyddsinstitut
Box 60204
S-104 01 Stockholm
SWEDEN

D. J. Beninson
Director, Licenciamento de Instalaciones Nulceares
Comisión Nacional de Energía Atómica
Avenida del Libertador 8250
2° Piso Of. 2330
1429 Buenos Aires
ARGENTINA

A. Bianco
ENEA, Dipart. Protezione
Via le Regina Margherita 125
I-00198 Roma
ITALY

J. Booz
KFA Jülich Institut für Medezin
Kernsforschungsanlage Jülich
Postfach 1913
D-5170 Jülich
GERMANY

M. J. Bulman, Librarian
Medical Research Council
Radiobiology Unit
Harwell, Didcot
Oxon OX11 ORD
ENGLAND

M. Calamosia
ENEA-LAB Fisica E Tossicologia Aerosol
Via Mazzini 2
I-40138 Bologna
ITALY

Cao Shu-Yuan, Deputy Head
Laboratory of Radiation Medicine
North China Institute of Radiation Protection
P. O. Box 120
Tai-yuan, Shan-Xi
THE PEOPLE'S REPUBLIC OF CHINA

M. Carpentier
Commission of the European Communities
200 rue de la Loi
J-70 6/16
B-1049 Brussels
BELGIUM

M. W. Charles
Nuclear Electric
Radiological Protection Branch
Berkeley Nuclear Laboratories
Berkeley
Gloucestershire GL 13 9PB
ENGLAND

Chen Xing-An
Laboratory of Industrial Hygiene
Ministry of Public Health
2 Xinkang Street
Deshengmenwai, Beijing
THE PEOPLE'S REPUBLIC OF CHINA

R. Clarke
National Radiological Protection Board
Harwell, Didcot
Oxon OX11 ORQ
ENGLAND

G. F. Clemente, Director
Radiation Toxicology Laboratory
National Committee of Nuclear Energy (CNEN)
Casaccia Centre for Nuclear Studies (CSN)
Casella Postale 2400
I-00100 Roma
ITALY

H. Coffigny
Institut de Protection et de Sûreté Nucléaire
Département de Protection Sanitaire
Service de Pathologie Expérimentale
BP 6
F-92265 Fontenay-aux-Roses
FRANCE

Commission of the European Communities
DG XII - Library SDM8 R1
200 rue de la Loi
B-1049 Brussels
BELGIUM

M. S. Davies
Medical Research Council
20 Park Crescent
London W1N 4AL
ENGLAND

Deng Zhicheng
North China Institute of Radiation Protection
Tai-yuan, Shan-Xi
THE PEOPLE'S REPUBLIC OF CHINA

M. Di Paola
ENEA, PAS/VALEPID
C.R.E. Casaccia
Casella Postale 2400
I-00100 Roma
ITALY

PNL-7600, Pt. 1
UC-408

Director
Commissariat à l'Énergie Atomique
Centre d'Etudes Nucléaires
Fontenay-aux-Roses (Seine)
FRANCE

Director
Laboratorio di Radiobiologia Animale
Centro di Studi Nucleari Della Casaccia
Comitate Nazionale per l'Energia Nucleare
Casella Postale 2400
I-00100 Roma
ITALY

D. Djuric
Institute of Occupational and Radiological Health
11000 Beograd
Deligradoka 29
YUGOSLAVIA

M. Dousset
Health Ministry
Frue de la Gruerie
F-91190 Gifsur Yvette
FRANCE

J. Eapen
Biochemistry Division
Bhabha Atomic Research Centre
Bombay-400 085
INDIA

Estação Agronómica Nacional
Biblioteca
2780 Oeiras
PORTUGAL

L. Feinendegen, Director
Institut für Medezin
Kernsforschungsanlage Jülich
Postfach 1913
D-5170 Jülich
GERMANY

T. M. Fliedner
Institut für Arbeits- u. Sozialmedizin
Universität Ulm
Oberer Eselsberg M 24, 309
D-7900 Ulm
GERMANY

L. Friberg
The Karolinska Institute
Stockholm
SWEDEN

R. M. Fry, Head
Office of the Supervising Scientist for the Alligator Rivers Region
P. O. Box 387
Bondi Junction NSW 2022
AUSTRALIA

A. Geertsema
Sasol Technology (Pty), Ltd.
P. O. Box 1
Sasolburg 9570
REPUBLIC OF SOUTH AFRICA

G. B. Gerber
Biology, Radiation Protection Medical Research
Commission of the European Communities
Rue de la Loi 200
B-1049 Brussels
BELGIUM

T. Giuseppe
ENEA-PAS-FIBI-AEROSOL
Via Mazzini 2
I-40138 Bologna
ITALY

H. L. Gjørup, Head
Health Physics Department
Atomic Energy Commission Research Establishment
Risø, Roskilde
DENMARK

A. R. Gopal-Ayengar
73-Mysore Colony
Mahul Road, Chembur
Bombay-400 074
INDIA

C. L. Greenstock
Radiation Biology
Atomic Energy of Canada Limited
Chalk River Nuclear Laboratories
Chalk River, Ontario
KOJ 1JO
CANADA

R. V. Griffith
International Atomic Energy Agency
Wagramerstraße 5
P. O. Box 200
A-1400 Vienna
AUSTRIA

Y. Hamnerius
Applied Electron Physics
Chalmers University of Technology
S-412 96 Göteborg
SWEDEN

G. P. Hanson, Chief
Radiation Medicine Unit
World Health Organization
CH-1211 Geneva 27
SWITZERLAND

J. L. Head
Department of Nuclear Science & Technology
Royal Naval College, Greenwich
London SE10 9NN
ENGLAND

W. W. Hofmann
Division of Biophysics
University of Salzburg Austria
Hellbrunner Str 34
A-5020 Salzburg
AUSTRIA

J. Inaba, Director
Division of comparative Radiotoxicology
National Institute of Radiological Sciences
9-1, Anagawa-4-chome
Chiba-shi 260
JAPAN

International Atomic Energy Agency
Documents Library
Attn: Mrs. Javor
Kaerntnerring 11
A-1010 Vienna 1
AUSTRIA

E. Iranzo
Jefe, División Protección Radiológica
Junta de Energia Nuclear
Cuidad Universitari
Madrid 3
SPAIN

W. Jacobi
Institut für Strahlenschutz
Post Schleissheim
Ingolstadter Landstrasse 1
D-8042 Neuherberg
GERMANY

K. E. Lennart Johansson
Radiofysiska Inst.
Regionsjukhuset
S-901-82 Umeå
SWEDEN

A. M. Kellerer
Institut für Medezin Strahlenkunde
Universität Würzburg
Versbacher Straße 5
D-8700 Würzburg
GERMANY

T. Kivikas
Studsvik Nuclear
S-611 82 Nyköping
SWEDEN

H.-J. Klimisch
BASF Aktiengesellschaft
Abteilung Toxikologie, Z470
D-6700 Ludwigshafen
GERMANY

H. E. Knoell
Battelle-Institut e.V.
Am Römerhof 35
Postfach 900160
D-6000 Frankfurt am Main 90
GERMANY

T. Kumatori
National Institute of Radiological Sciences
9-1, Anagawa-4-chome
Chiba-shi 260
JAPAN

J. Lafuma, Head
Département de Protection Sanitaire
Commissariat à l'Énergie Atomique/IPSN
BP 6
F-92260 Fontenay-aux-Roses
FRANCE

J. R. A. Lakey
Department of Nuclear Science & Technology
Royal Naval College
Greenwich Naval college
SW10 9NN
ENGLAND

Li De-Ping
Professor and Director of North China
Institute of Radiation Protection, NMI
P.O. Box 120
Tai-yuan, Shan-Xi
THE PEOPLE'S REPUBLIC OF CHINA

Librarian
Alberta Environmental Centre
Bag 4000
Vegreville, Alberta TOB 4LO
CANADA

Librarian
Centre d'Etudes Nucléaires de Saclay
P. O. Box 2, Saclay
Fig-sur-Yvette (S&O)
FRANCE

Librarian
CSIRO
314 Albert Street
P. O. Box 89
East Melbourne, Victoria
AUSTRALIA

Librarian
CSIRO
Division of Wildlife and Ecology
P. O. Box 84
Lyneham, ACT 2602
AUSTRALIA

Librarian
HCS/EHE
World Health Organization
CH-1211 Geneva 27
SWITZERLAND

PNL-7600, Pt. 1
UC-408

Librarian
Kernforschungzentrum
Karlsruhe
Institut für Strahlenbiologie
Postfach 3640
D-75 Karlsruhe 1
GERMANY

Librarian
Max-Planck-Institut für
Biophysics
Forstkasstraße
D-6000 Frankfurt/Main
GERMANY

Librarian
Medical Research Council
Radiobiology Unit
Chilton
Oxon OX11 ORD
ENGLAND

Librarian
Ministry of Agriculture,
Fisheries & Food
Fisheries Laboratory
Lowestoft, Suffolk NR33 OHT
ENGLAND

Librarian
National Institute of
Radiological Sciences
9-1, Anagawa-4-chome
Chiba-shi 260
JAPAN

Librarian
Supervising Scientist for the
Alligator Rivers Region
Level 23, Bondi Junction Plaza
P. O. Box 387
Bondi Junction NSW 2022
AUSTRALIA

Library
Atomic Energy Commission of
Canada, Ltd.
Whiteshell Nuclear Research
Establishment
Pinawa, Manitoba ROE 1L0
CANADA

Library
Department of Meteorology
University of Stockholm
Arrhenius Laboratory
S-106 91 Stockholm
SWEDEN

Library
Risø National Laboratory
DK-4000 Roskilde
DENMARK

B. Lindell
National Institute of Radiation
Protection
Fack S-104 01
Stockholm 60
SWEDEN

J. R. Maisin
Radiobiology Department
C.E.N. - S.C.K.
Mol
BELGIUM

A. M. Marko
9 Huron Street
Deep River, Ontario KOJ 1PO
CANADA

R. Masse
Institut de Protection et de
Sûreté Nucléaire
Département de Protection
Sanitaire
Service d'Etudes Appliquées de
Protection Sanitaire
BP 6
F-92260 Fontenay-aux-Roses
FRANCE

H. Matsudaira,
Director General
National Institute of
Radiological Sciences
9-1, Anagawa-4-chome
Chiba-shi 260
JAPAN

O. Matsuoka
Research Consultant
Abiko Laboratory
Central Research Institute of
Electric Power Industry
1646, Abiko, Abikosi
Chiba-ken 270-11
JAPAN

N. Matsusaka
Department of Veterinary
Medicine
Faculty of Agriculture
Iwate University
Ueda, Morioka
Iwate 020
JAPAN

S. Mattsson
Department of Radiation Physics
Malmö General Hopsital
S-214 01 Malmö
SWEDEN

R. G. C. McElroy
Atomic Energy Commission of
Canada, Ltd.
Dosimetric Research Branch
Chalk River, Ontario KOJ 1JO
CANADA

F.-I. S. Medina
Cytogenetics Laboratory
Biomedical Research Division
A.R.C.
Philippine Atomic Energy
Commission
P. O. Box 932
Manila
THE PHILIPPINES

P. Metalli
ENEA-PAS
CRE Casaccia
Casella Postale 2400
I-00100 Roma
ITALY

H. J. Metivier
Institut de Protection et de Sûreté Nucléaire
Centre d'Études de Service de Fontenay-aux-Roses
BP 6
F-92265 Fontenay-aux-Roses
FRANCE

A. Morgan
Biomedical Research Dept.
AEA Environmental and Energy
Harwell Laboratory
Oxfordshire OX11 ORA
ENGLAND

Y. I. Moskalev
Institute of Biophysics
Ministry of Public Health
Givopisnaya 46
Moscow
USSR

J. Muller
7 Millgate Crescent
Willowdale, Ontario M2K 1L5
CANADA

D. K. Myers, Head
Radiation Biology Branch
Atomic Energy Commission of Canada, Ltd.
Chalk River, Ontario
CANADA

J. C. Nénot, Deputy Director
Département de Protection
Centre d' Etudes Nucléaires
BP 6
F-92260 Fontenay-aux-Roses
FRANCE

R. Osborne
Atomic Energy Commission of Canada, Ltd.
Biology and Health Physics Division
Chalk River Nuclear Laboratories
P. O. Box 62
Chalk River, Ontario KOJ 1JO
CANADA

J. Pacha
Silesian University
Department of Microbiology
Ul. Jagiellonska 28
40-032 Katowice
POLAND

H. G. Paretzke
GSF Institut für Strahlenschutz
Ingolstadter Landstraße 1
D-8042 Neuherberg
GERMANY

N. Parmentier
Département de Protection Sanitaire
Centre d'Etudes Nucléaires
BP 6
F-92260 Fontenay-aux-Roses
FRANCE

G. Patrick
Medical Research Council
Radiobiology Unit
Harwell, Didcot
Oxon OX11 ORD
ENGLAND

O. Pavlovski
Institute of Biophysics
Ministry of Public Health
Givopisnaya 46
Moscow D-182
USSR

R. Perraud
Commissariat à l'Énergie Atomique
BP 1
87640 Razes
FRANCE

G. Premazzi
Commission of the European Communities
Joint Research Centre
Ispra Establishment
I-21020 Ispra
ITALY

V. Prodi
Department of Physics
University of Bologna
Via Irnerio 46
I-40126 Bologna
ITALY

O. Ravera
Commission of the European Communities, C.C.R.
I-21020 Ispra (Varese)
ITALY

D. V. Rebollo
Junta de Energia Nuclear
Sección de Isotopos
Calle de Serrano, 121
6 Madrid
SPAIN

REP Institutes TNO
TNO Division of Health Research Library
P. O. Box 5815
151 Lange Kleiweg
2280 HV Rijswijk
THE NETHERLANDS

Reports Librarian
Harwell Laboratory, Bldg. 465
UKAEA
Harwell, Didcot
Oxon OX11 ORB
ENGLAND

PNL-7600, Pt. 1
UC-408

P. J. A. Rombout
Inhalation Toxicology Department
National Institute of Public Health and Environmental Protection
P. O. Box 1
NL-3720 BA Bilthoven
THE NETHERLANDS

M. Roy
Institut de Protection et de Sûreté Nucléaire
Département de Protection Sanitaire
Service d'Etudes Appliquées de Protection Sanitaire
BP 6
F-92260 Fontenay-aux-Roses
FRANCE

M. Rzekiecki
Commissariat à l'Énergie Atomique
Centre d'Etudes Nucleaires de Cadarache
BP 13-St. Paul
Les Durance
FRANCE

F. A. Sacherer
Battelle-Institut e.V.
Am Römerhof 35
Postfach 900160
D-6000 Frankfurt am Main 90
GERMANY

W. Seelentag, Chief Medical Officer
Radiation Health Unit
World Health Organization
CH-1211 Geneva 27
SWITZERLAND

H. Smith
International Commission on Radiological Protection
P. O. Box 35
Didcot
Oxon OX11 ORJ
ENGLAND

J. W. Stather
National Radiological Protection Board
Building 383
Chilton, Didcot
Oxon OX11 ORQ
ENGLAND

M. J. Suess
Regional Officer for Environmental Hazards
World Health Organization
8, Scherfigsvej
DK-2100 Copenhagen
DENMARK

Sun Shi-quan, Head
Radiation-Medicine Department
North China Institute of Radiation Protection, MNI
P. O. Box 120
Tai-yuan, Shan-Xi
THE PEOPLE'S REPUBLIC OF CHINA

G. Tarroni
ENEA-PAS-FIBI-AEROSOL
Laboratorio Fisica Sanitaria
Via Ercolani 8
I-40138 Bologna
ITALY

D. M. Taylor
G.M.B.H.
Genetik und fur Toxikologie von Spaltstoffen
Postfach 3640
D-7500 Karlsruhe 1
GERMANY

K. H. Tempel
Institut für Pharmakologie, Toxikologie und Pharmazie
Fachbereich Tiermedizin der Universität München
Veterinärstraße 13
D-8000 München 22
GERMANY

J. W. Thiessen
Radiation Effects Research Foundation
9-9 Hamaguchi-machi 5F
Nagasaki 852
JAPAN

United Nations Scientific Committee on the Effects of Atomic Radiation
Vienna International Center
P. O. Box 500
A-1400 Vienna
AUSTRIA

D. Van As
Atomic Energy Corporation
P. O. Box 582
Pretoria 0001
REPUBLIC OF SOUTH AFRICA

Dame Janet Vaughan
1 Fairlawn End
First Turn
Wolvercote
Oxon OX2 8AP
ENGLAND

J. Vennart
Bardon, Ickleton Road, Wantage
Oxon OX12 9OA
ENGLAND

Vienna International Centre Library
Gifts and Exchange
P. O. Box 100
A-1400 Vienna
AUSTRIA

V. Volf
Kernforschungzentrum Karlsruhe
Institut für Genetik und Toxikologie von Spaltstoffen
Postfach 3640
D-7500 Karlsruhe 1
GERMANY

G. Walinder
Unit of Radiological Oncology
University of Agricultural Sciences
P. O. Box 7031
S-750 07 Uppsala
SWEDEN

Wang Hengde
North China Institute of Radiation Protection
P. O. Box 120
Tai-yuan, Shan-Xi
THE PEOPLE'S REPUBLIC OF CHINA

Wang Renzhi
Institute of Radiation Medicine
27# Tai Ping Road
Beijing 100850
THE PEOPLE'S REPUBLIC OF CHINA

Wang Ruifa, Associate Director
Laboratory of Industrial Hygiene
Ministry of Public Health
2 Xinkang Street
P. O. Box 8018
Deshengmenwai, Beijing 100088
THE PEOPLE'S REPUBLIC OF CHINA

Wang Yibing
North China Institute of Radiation Protection
P. O. Box 120
Tai-yuan, Shan-Xi
THE PEOPLE'S REPUBLIC OF CHINA

Wei Lü-Xin
Laboratory of Industrial Hygiene
Ministry of Public Health
2 Xinkang Street
Deshengmenwai, Beijing 100088
THE PEOPLE'S REPUBLIC OF CHINA

J. Wells
Radiobiology Laboratory
Radiation Biophysics
Nuclear Electric
Berkeley Nuclear Laboratories
Berkeley, Gloucestershire
GL 13 9PB
ENGLAND

B. C. Winkler, Director
Licensing
Raad Op Atomic
Atoomkrag Energy Board
Privaatsk X 256
Pretoria 0001
REPUBLIC OF SOUTH AFRICA

Wu De-Chang
Institute of Radiation Medicine
27# Tai Ping Road
Beijing
THE PEOPLE'S REPUBLIC OF CHINA

Yao Jiaxiang
Laboratory of Industrial Hygiene
2 Xinkang Street
Deshengmenwai, Beijing 100088
THE PEOPLE'S REPUBLIC OF CHINA

Kenjiro Yokoro, Director
Research Institute for Nuclear Medicine & Biology
Hiroshima University
Kasumi 1-2-3, Minami-ku
Hiroshima 734
JAPAN

V. Zeleny
Institute of Experimental Biology and Genetics
Czechoslovak Academy of Sciences
Bidekpvocla 1-83
Pragie 4
CSSR

Zhu Zhixian
China Research Institute of Radiation Protection
Ministry of Nuclear Industry
P.O. Box 120
Tai-yuan, Shan-Xi
THE PEOPLES REPUBLIC OF CHINA

ONSITE

DOE Richland Operations Office (3)

P. W. Kruger A5-90
E. C. Norman A5-51
Public Reading Room A1-65

Tri-Cities University Center

J. Cooper, Librarian H2-52

Hanford Environmental Health Foundation (4)

S. E. Dietert H1-03
R. L. Kathren H1-01
W. C. Milroy H1-02
M. J. Swint H1-02

U. S. Testing

V. H. Pettey H2-51

Westinghouse Hanford Co.

D. E. Simpson B3-51

PNL-7600, Pt. 1
UC-408

Pacific Northwest Laboratory
(231)

R. R. Adee P8-13
R. C. Adams K6-52
L. E. Anderson K4-28
R. W. Baalman (5) K1-50
J. F. Bagley K1-45
W. J. Bair (15) K1-50
C. A. Baldwin P7-58
L. A. Braby P8-47
J. K. Briant P7-53
A. L. Brooks P7-53
J. A. Buchanan P7-82
R. L. Buschbom P7-82
D. P. Chandler K4-13
T. D. Chikalla P7-75
B. J. Chou K4-10
M. L. Clark K4-16
T. T. Claudson K1-66
J. A. Creim K4-28
F. T. Cross K4-13
G. E. Dagle K4-10
J. R. Decker K4-16
H. S. DeFord K4-16
J. A. Dill K4-16
R. J. Douthart K4-13
R. D. DuBois P8-47
F. N. Eichner P7-03
C. E. Elderkin K6-08
J. J. Evanoff K4-10
J. W. Falco K6-78
D. R. Fisher K3-53
L. G. Florek K4-16
M. E. Foreman P7-56
W. C. Forsythe K4-16
K. M. Gideon K4-10
R. A. Gies K4-13
A. W. Gieschen K4-16
E. S. Gilbert P7-82
M. F. Gillis K1-50
W. A. Glass K4-13
B. J. Greenspan K4-16
D. K. Hammerberg K4-16
B. K. Hayden K4-16
L. A. Holmes K1-29
M. G. Horstman K4-10
V. G. Horstman P7-58
J. R. Houston A3-60
J. E. Hulla P7-56
A. C. James K3-51
A. E. Jarrell K4-10
J. R. Johnson K3-53
R. F. Jostes K4-13
D. R. Kalkwarf P7-50
M. T. Karagianes P7-57
R. M. Kitchin P7-56
M. Knotek K1-48
S. A. Kreml (2) P7-58
E. G. Kuffel K4-16
W. W. Laity K2-15
K. E. Lauhala P7-58
C. L. Leach K4-10
F. C. Leung K4-13
M. K. Lien P8-47
J. A. Mahaffey P7-82
E. M. Maloney K4-13
D. B. Mann P7-53
T. J. Mast K4-10
K. E. McDonald P7-56
P. W. Mellick K4-10
M. E. Mericka K4-10
H. K. Meznarich P7-53
D. L. Miller P7-53
J. H. Miller P8-47
M. C. Miller P7-44
R. A. Miller K4-10
T. L. Morgan P8-47
J. E. Morris P7-56
D. A. Mueller P7-50
D. A. Nelson K2-44
J. M. Nelson P8-47
J. F. Park (50) P7-58
R. W. Perkins P7-35
J. T. Pierce K4-10
C. A. Poindexter K4-16
G. J. Powers P7-53
H. A. Ragan K4-13
R. A. Renne K4-10
D. N. Rommereim K4-28
R. L. Rommereim K4-10
C. O. Romsos K4-10
E. J. Rossignol K4-16
S. E. Rowe K4-10
P. S. Ruemmler K4-10
J. L. Ryan P7-25
C. L. Sanders P7-56
L. B. Sasser P7-53
G. F. Schiefelbein K2-03
J. E. Schmaltz K1-86
L. C. Schmid K1-34
R. P. Schneider P7-56
L. E. Sever P7-82
B. D. Shipp K1-73
M. R. Sikov P7-53
J. C. Simpson K1-86
E. C. Sisk P7-56
L. G. Smith P7-58
D. L. Springer P7-53
J. G. Stephan K3-56
R. G. Stevens P7-82
D. L. Stewart K6-91
G. L. Stiegler P7-56
L. C. Stillwell P7-56
G. M. Stokes K1-74
K. H. Stoney K4-16
K. L. Swinth K3-55
W. L. Templeton K1-30
T. S. Tenforde (10) K1-50
R. M. Thomas P7-53
R. C. Thompson P7-58
B. D. Thrall P7-50
L. H. Toburen P8-47
R. J. Traub K3-57
V. D. Tyler K4-13
H. R. Udseth P8-19
B. E. Vaughan K1-66
M. B. Walter K6-96
C. R. Watson P7-82
R. J. Weigel K4-16
R. E. Weller P7-52
R. B. Westerberg K4-16
T. J. Whitaker K2-21
E. L. Wierman (2) P7-52
R. E. Wildung P7-54
L. D. Williams K1-41
W. E. Wilson P8-47
J. D. Zimbrick (10) P7-58
Health Physics Department Library
Life Sciences Library (2)
Publishing Coordination
Technical Report Files (5)